237
8/11/68 by

DR-390

AGN-8258
AEC RESEARCH AND
DEVELOPMENT REPORT
UC-23, Isotopes-Industrial
Technology
TID-4500 (52nd Ed.)

NEMO

CONCEPTUAL DESIGN OF AN IMPLANTABLE RADIOISOTOPE POWER SOURCE FOR CIRCULATORY SUPPORT SYSTEMS

FINAL TECHNICAL REPORT

26 January 1968

Prepared Under
Contract AT(04-3)-368, P.A. No. 7
Division of Isotopes Development
U.S. Atomic Energy Commission

NUCLEAR ENGINEERING AND MANUFACTURING OPERATIONS
NUCLEAR DIVISION AEROJET-GENERAL CORPORATION
SAN RAMON, CALIFORNIA

DISCLAIMER

AGN-8258
AEC RESEARCH AND
DEVELOPMENT REPORT
UC-23, Isotopes-Industrial
Technology
TID-4500 (52nd Ed.)

CONCEPTUAL DESIGN OF AN IMPLANTABLE RADIOISOTOPE POWER SOURCE FOR CIRCULATORY SUPPORT SYSTEMS

FINAL TECHNICAL REPORT

Published
26 January 1968

Prepared Under
Contract AT(04-3)-368, Project Agreement No. 7
for the
Division of Isotopes Development
U.S. Atomic Energy Commission

Approved: R H Chesworth
R. H. Chesworth, Manager
Nuclear Engineering and
Manufacturing Operations

Printed in the United States of America

Available From
Clearinghouse for Federal Scientific and Technical Information
National Bureau of Standards, U.S. Department of Commerce
Springfield, Virginia 22151
Price: Printed Copy $3.00; Microfiche $0.65

NUCLEAR DIVISION
AEROJET-GENERAL CORPORATION
San Ramon, California

LEGAL NOTICE

The information herein is regarded as preliminary and subject to further checking, verification, and analysis.

CONCEPTUAL DESIGN OF AN IMPLANTABLE RADIOISOTOPE POWER SOURCE FOR CIRCULATORY SUPPORT SYSTEMS

FINAL TECHNICAL REPORT

TABLE OF CONTENTS

CONTENTS - Continued

CONTENTS - Continued

LIST OF FIGURES

(Continued)

FIGURES - Continued

(Continued)

FIGURES - Continued

LIST OF TABLES

BLANK

CONCEPTUAL DESIGN OF AN IMPLANTABLE RADIOISOTOPE POWER SOURCE FOR CIRCULATORY SUPPORT SYSTEMS

FINAL TECHNICAL REPORT

ABSTRACT

This document describes the development of a conceptual design for a radioisotope power source suitable for implantation in the human body. The output power (7 watts) from the device is to be used for circulatory support, either to assist a damaged heart or to drive an artificial heart. The engine studied is based on the Stirling cycle but differs from the conventional Stirling engine. The piston and crank mechanism of the conventional engine are replaced by a free piston arrangement to eliminate the requirement for high performance seals and bearings and to increase the potential engine life. Power is extracted from the engine in the form of pressurized gas rather than mechanical work; this permits the use of a simple intermediate fluid and bellows arrangement to couple the engine output to the circulatory support system. The engine is fueled with about 35 watts of Plutonium-238 which is encapsulated in and shielded by a tungsten alloy. An outer shield of polyethylene is provided to reduce the surface neutron dose. Waste heat from the engine is transfered to the blood stream under conditions which limit the maximum blood temperature to prevent damage to the blood. A summary of power source characteristics is presented on page xii.

SUMMARY OF POWER SOURCE CHARACTERISTICS

Net power output, watts	7
Gross power input, watts (end of life)	33.7
Overall efficiency, %	20.7
Overall volume, cm^3	1800
Overall weight, gm	1780
Maximum fuel temperature, ^oF	1350
Maximum engine gas temperature, ^oF	~1200
Minimum engine gas temperature, ^oF	~ 250
Maximum engine pressure, psia	74
Minimum engine pressure, psia	60
Engine speed, cycles/min	1000
Engine displacement, in^3	1.32
Fuel	Pu-238
Fuel form	PuN
Surface dose rate, mrem/hr	50

CONCEPTUAL DESIGN OF AN IMPLANTABLE RADIOISOTOPE POWER SOURCE FOR CIRCULATORY SUPPORT SYSTEMS

FINAL TECHNICAL REPORT

1.0 INTRODUCTION

Aerojet-General, under contract to the Atomic Energy Commission*, has completed a conceptual design study of an implantable power source for circulatory support that incorporates a modified Stirling cycle power conversion system.

The conceptual design included evaluation of alternate overall engine configurations and component concepts. The performance of each component was analyzed in detail and the effect of component performance on the overall engine performance was determined. Analytical models of the overall engine were also developed.

Major emphasis was placed on the power conversion system. This system has two major areas of interface, on one side with the radioisotope fuel and on the other with the heart pump and physiological requirements. These two interface areas were considered during the conceptual design only to the extent that they affect the engine. The fuel investigation consisted primarily of a study of the heat source and shield size and configuration. The physiological considerations were concerned primarily with the form in which power is required at the heart, the heat rejection concepts and the requirements associated with the control of the delivered power. Since firm criteria were not available in some areas, the engine concept was made as flexible as possible to accommodate possible change in requirements.

The basic objective of the study was to develop an engine design with maximum efficiency and reliability and minimum size using the concept described in the Aerojet proposal to the AEC**. The attractive features attributed to the engine by the brief analysis presented in that proposal have been

* Contract AT(04-3)368, Project Agreement, No. 7 with the San Francisco Operations Office, U. S. Atomic Energy Commission.

**ANU 67-11, "Proposal for a Conceptual Design Study of Implantable Power Sources for Circulatory Support", February 13, 1967.

verified. The size of the engine has been reduced from 1982 cm^3 to 1800 cm^3. A more accurate analysis of the thermodynamic performance of the engine shows that an overall efficiency of about 20% can be achieved; this value is not significantly different from the 23.9% originally estimated. Several design changes that should significantly improve engine reliability have also been made.

Aerojet-General has committed significant resources to improve the Corporate capabilities in the areas of the application of radioisotopes, Stirling engine technology and medical engineering. Specifically, in support of the contract work reported herein, Aerojet has independently undertaken experimental work to demonstrate the operation and measure the performance of the modified Stirling engine; the results of those activities will be documented in a separate report but are summarized in Appendix R.

2.0 PRINCIPLES OF ENGINE OPERATION

2.1 REQUIREMENTS AND CRITERIA

The general requirements that must be satisfied by an implantable power supply are:

- Reliability
- Long Operating Life
- High Thermodynamic Efficiency
- Minimum Size
- Minimum Weight
- Attitude Insensitivity
- Resistance to Shock and Vibration

The standard Stirling engine has the highest thermodynamic efficiency of available closed cycle engines and satisfies all of the requirements cited above except long operating life. If the operating life of Stirling engines can be improved, they will be well suited for many potential radioisotope applications and particularly for implantable power sources for circulatory support.

In the Aerojet concept, the standard Stirling engine is modified to improve the operating life. These modifications involve, primarily, the elimination of engine bearings that must withstand high oscillating loads and the provision of a direct coupling between the thermodynamic converter and the circulatory support system. Two changes have been made in the engine concept: the piston and crank mechanism of the conventional Stirling engine are replaced by a free piston to eliminate the requirement for high performance seals and bearings and to increase the potential engine life dramatically; and power is extracted from the engine in the form of pressurized gas rather than mechanical work, which permits the use of a simple intermediate fluid and bellows arrangement to couple the engine output to the circulatory support system.

2.2 MODIFIED STIRLING CYCLE

2.2.1 Fundamentals of Compressor Operation

The Aerojet modified Stirling engine can be thought of as one in which heat is converted to mechanical work by alternately heating and cooling a gas. Consider an enclosed volume of gas as shown in Part A of Figure 1 and, for a moment, neglect the check valves. As the piston moves down, cold gas is displaced from the cold chamber through the regenerator, in which it is heated, to the hot chamber. The pressures in both hot and cold chambers are always virtually equal. However, the pressure level in the engine as a whole has increased since the average gas temperature in the enclosed volume has increased. The pressure increases by the ratio $P_2/P_1 = T_2/T_1$, typical of a constant volume process. The pressure profile resulting from alternating piston motion, again neglecting the check valves, is shown in Part B of Figure 1.

Now consider the system with check valves. The outward flowing check valve is connected to a gas reservoir at a pressure equal to the mean pressure of the previous case. The inward flowing check valve is connected to a reservoir at the minimum pressure. As the piston starts down, both valves are closed and the pressure increases as before, but only until it reaches the pressure of the high pressure reservoir. At this point the check valve opens and gas is forced into the high pressure reservoir until the end of the stroke is reached. As the piston starts back up, the pressure in the engine starts to decrease (because the average temperature is decreasing) and the check valve closes. The pressure continues to decrease until it equals that in the low pressure reservoir, at which time the inward flowing check valve opens and gas is drawn into the engine. The pressure profile for this simplified model is shown in Part C of Figure 1. Thus, in a complete cycle, gas is pumped from the low pressure reservoir to the high pressure reservoir. The loop is closed through the pumping chamber, in which the high pressure gas delivers work while expanding to the low pressure. If the gas is expanded adiabatically,the ideal modified Stirling cycle efficiency is equal to the efficiency of the ideal Carnot cycle.

2.2.2 Linear Engine Concept

Elimination of the crank mechanism normally used in Stirling engines is an important feature of the Aerojet engine concept. The alternate drive mechanism for the displacer piston must accomplish two functions previously provided by the crank mechanism: It must reverse the direction of motion as the piston reaches the end of stroke; and it must provide a means of making up mechanical energy lost from the piston due to fluid and mechanical friction.

Oscillating linear motion can be obtained in a number of ways. The spring-mass approach is attractive because the kinetic energy of piston motion is conserved in such a concept. The spring can, of course, be mechanical, pneumatic or magnetic. A pneumatic spring system was selected for the Aerojet engine concept because this approach simplifies the accomplishment of the energy addition function (Figure 2).

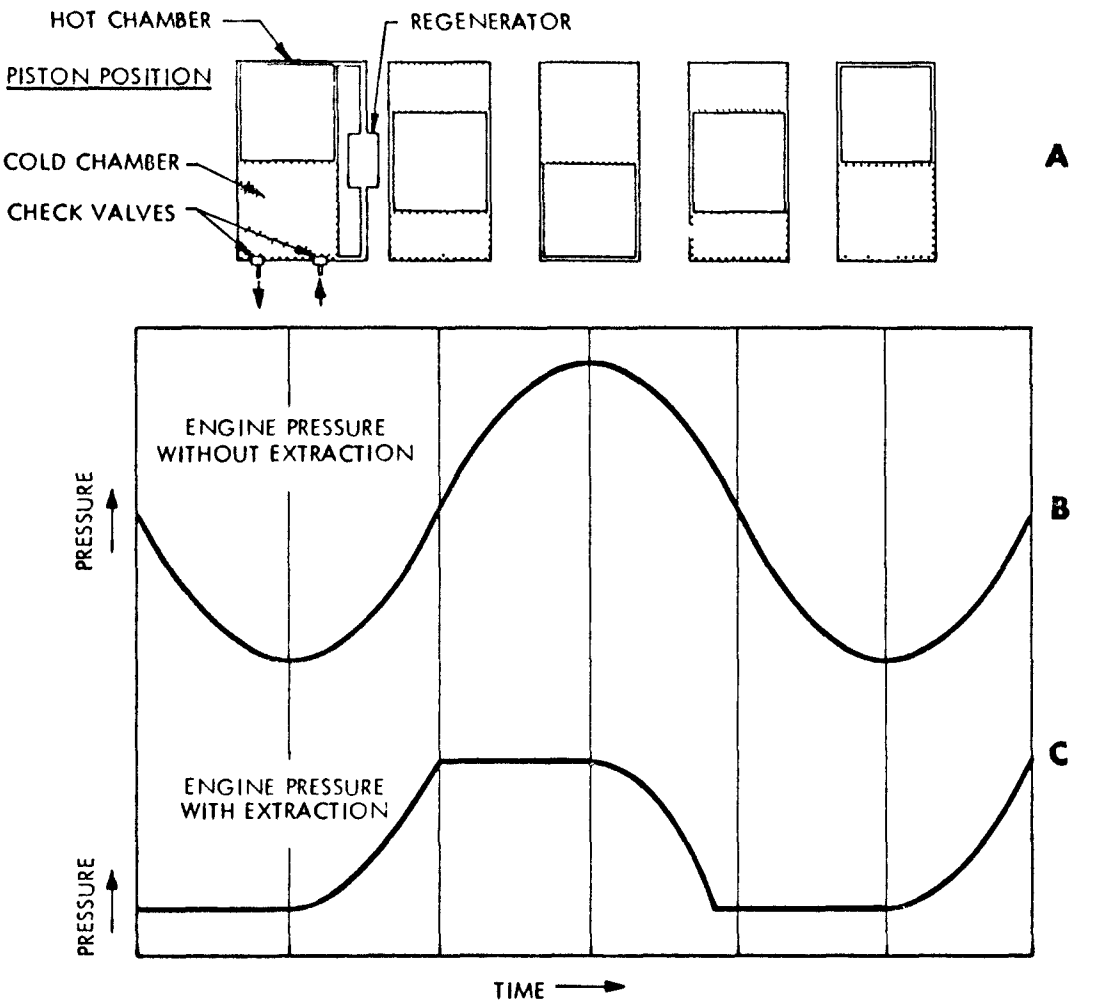

FIGURE 1. MODIFIED STIRLING ENGINE COMPRESSOR OPERATION

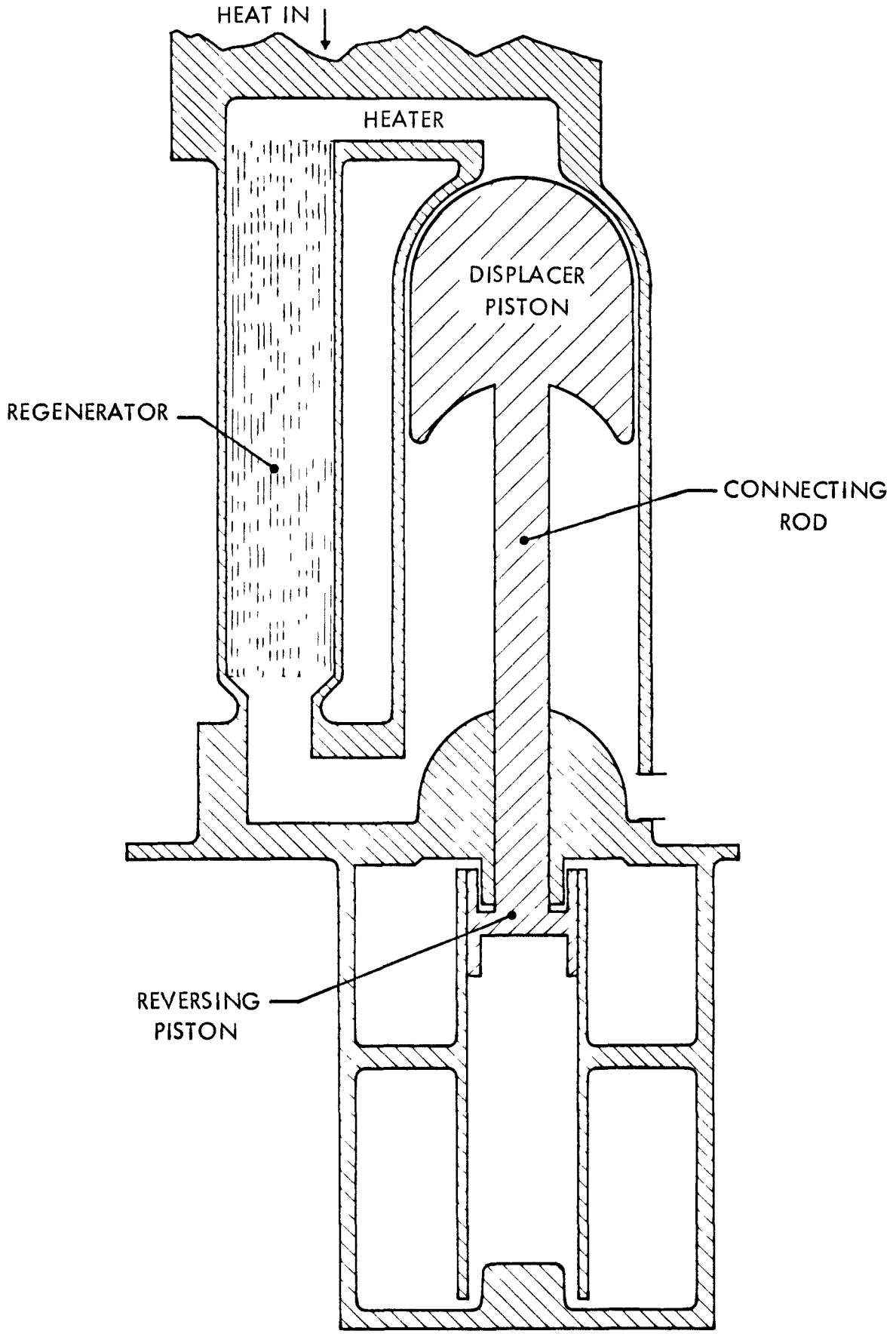

FIGURE 2. LINEAR STIRLING CYCLE ENGINE CONCEPT

With a penumatic reversing piston, energy addition to the oscillating system occurs directly from the displacer piston as a result of the non-symmetrical nature of the pressure profile in the displacer cylinder. As the piston assembly moves downward, the pressure in the displacer cylinder (which is acting on the area of the connecting shaft) is higher than when the piston is moving upward. The net effect is the addition of energy to the oscillating system.

2.3 APPLICATION TO CIRCULATORY SUPPORT

The manner in which the modified Stirling engine can be used to provide power for a circulatory support system is shown in Figure 3. The interface between the engine and the circulatory support pump is, primarily, the pumping chamber.

2.3.1 Pumping Chamber

The configuration and operation of the pumping chamber is basically as follows. The chamber contains a movable plate to which three sets of bellows are attached. One set of bellows contains the pumping fluid that operates directly on the pumping membrane of the blood pump. A second set, located on the opposite side of the movable plate, contains a fluid at atmospheric pressure. The third set is located on both sides of the plate and contains the engine gas. By alternately valving high pressure and low pressure gas to the two sides of the plate, pulsating power is delivered to the pumping fluid and, consequently, to the blood pump.

The purpose of the fluid at atmospheric pressure is to compensate for gross changes in atmospheric pressure so that atrial pressure can be held to within a few mm Hg of atmospheric. The fluid is supplied from a flexible sack in the pleural cavity. The area ratio between the atmospheric pressure bellows and the pumping fluid bellows in the pumping chamber serving the left ventricle is selected to result in an equilibrium pressure in the pumping fluid of about 90 mm Hg. During systole, the pressure in the gas bellows increases the pumping fluid pressure to about 190 mm Hg and during diastole the pressure is reduced to about atmospheric pressure.

2.3.2 Heat Rejection

A system of the type shown in Figure 3 offers many alternate methods of transferring waste heat from the engine to the blood. Waste heat can be extracted from the engine either by cooling the cold chamber or by cooling the low pressure gas that is drawn into the cold chamber; the second approach has been selected for the conceptual design.

The low pressure gas could be cooled directly in a blood heat exchanger but the heat exchanger design problems would be severe. The difference in temperature between inlet and outlet gas is $> 100^{\circ}F$ so that great care would be required to avoid overheating the blood. A more attractive technique is to first transfer the heat to a liquid, such as the pumping fluid or the atmospheric pressure reference fluid. The heat capacities and mass flow rates of these liquids are much higher than those of the gas so that a temperature rise of only a fraction of a degree results from the transfer of the engine waste

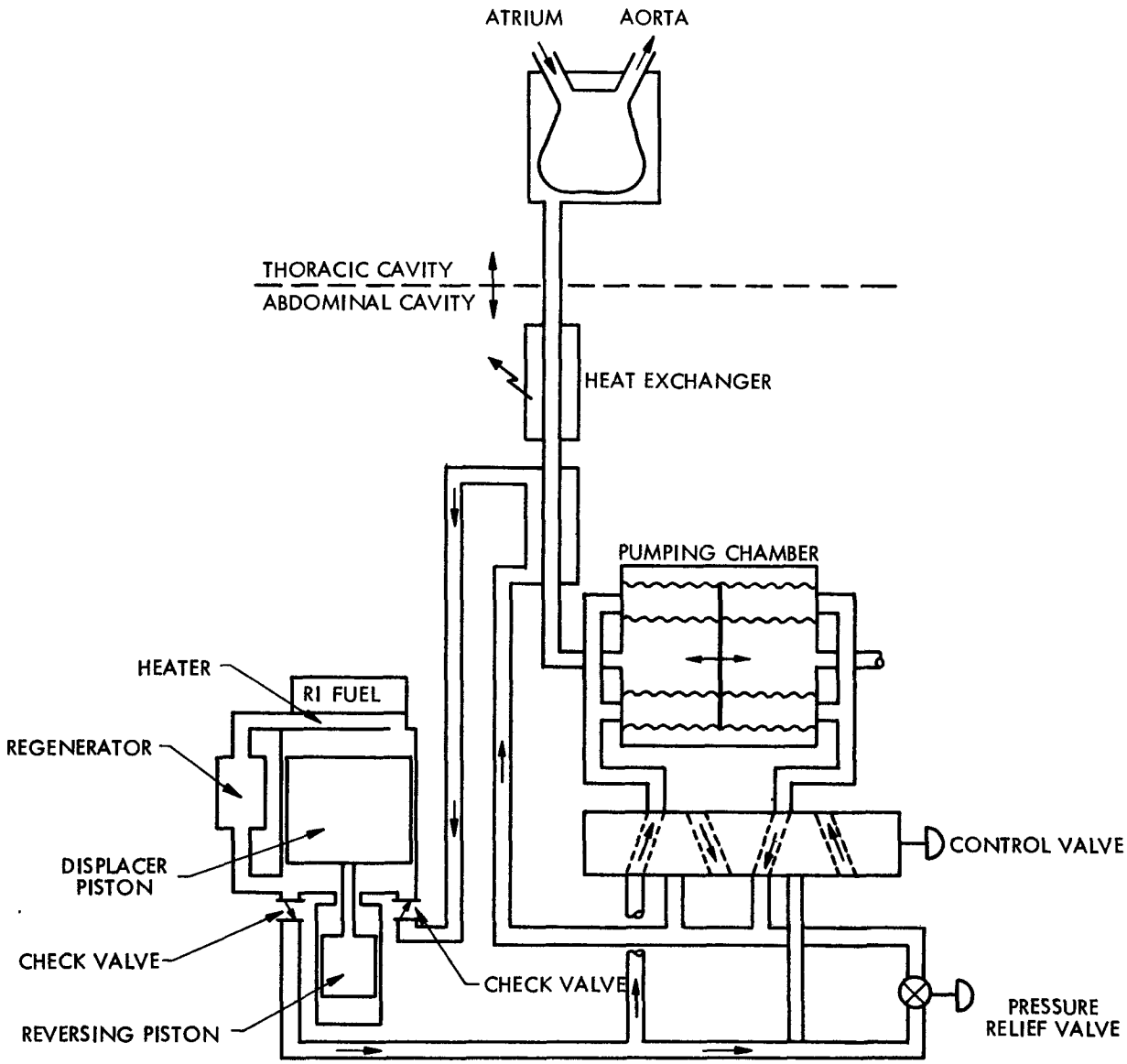

FIGURE 3. APPLICATION OF MODIFIED STIRLING CYCLE ENGINE TO CIRCULATORY SUPPORT SYSTEM

3.01-67-987

heat. If the pumping fluid is used, the heat may be transfered to blood either in a separate heat exchanger or through the pumping membrane in the blood pump. The system shown in Figure 3 uses a separate heat exchanger although some of the waste heat will be transfered to the blood in the blood pump.

BLANK

3.0 DESCRIPTION OF ENGINE

The modified Stirling cycle engine and its major components are briefly described in this section. A more detailed description of each component, a discussion of the design considerations involved in the selection of system configuration and operating conditions, and a description of the analytical techniques used are presented in Section 5.0.

3.1 CONFIGURATION

The manner in which the major components of the power source are combined into an integrated system is shown in Figure 4. This drawing shows all components except the flexible sack (containing the fluid used as an atmospheric pressure reference) and the waste heat exchanger.

A linear arrangement of the heat source, displacer and reversing system results in the simplest layout and minimizes the parasitic heat loss from the heat source. Since the location of the pumping chamber with respect to the other components is not critical, a configuration which results in a fairly regular external envelope was selected.

3.2 THERMODYNAMIC PERFORMANCE

The overall efficiency of the modified Stirling engine in terms of the ratio of power delivered to the artificial heart to the total thermal power required is 20.7% The major factors that effect efficiency are:

Net power output, watts	7.0
Power to reversing piston, watts	0.9
Control power, watts	1.0
Pumping chamber and line losses, watts	0.5
Check valve loss, watts	0.3
Gross output power required, watts	9.7

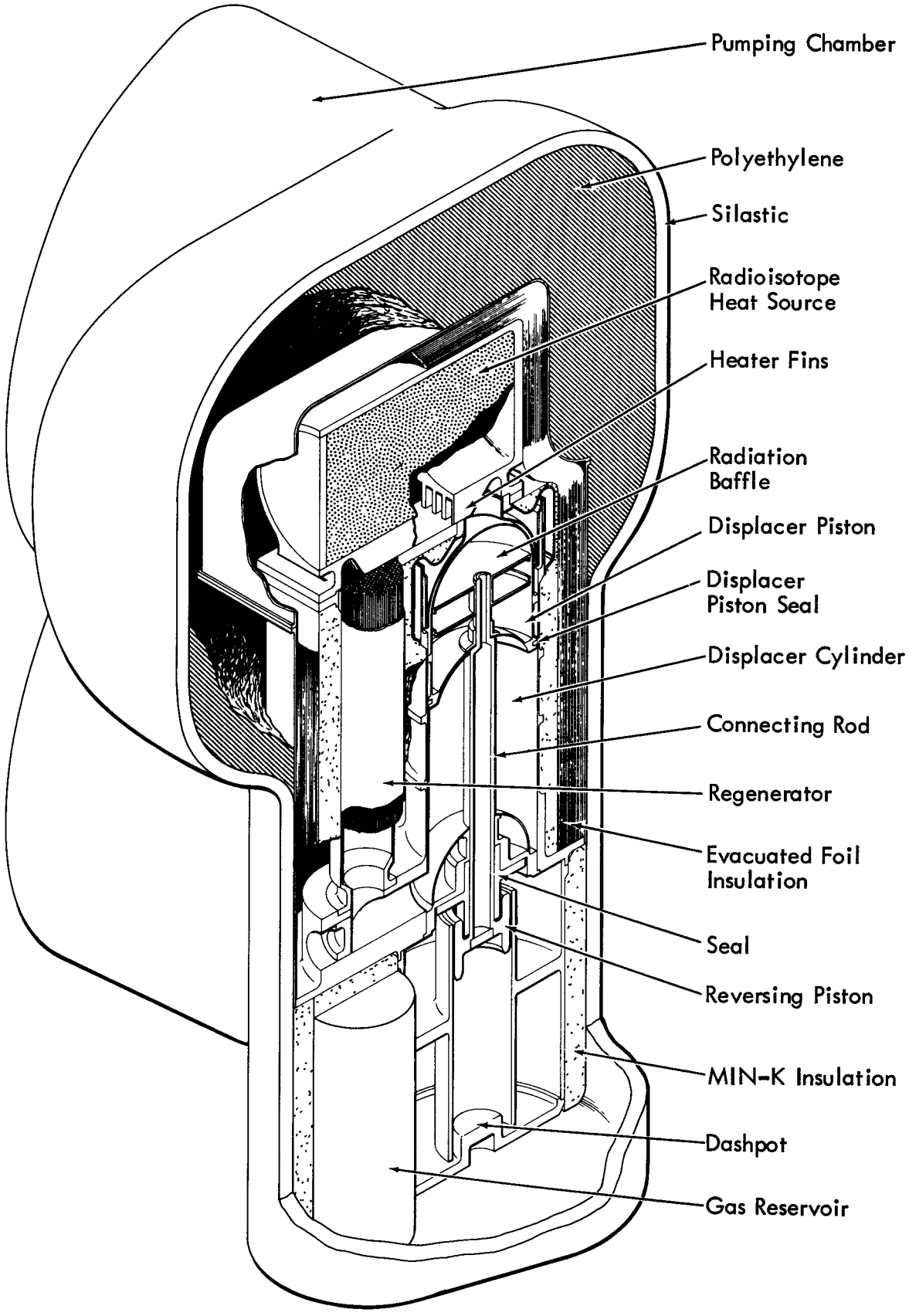

3.01-67-1001

FIGURE 4. IMPLANTABLE POWER SOURCE

Gross thermodynamic efficiency*	41%
Thermal power input to gas, watts	23.7
Total parasitic thermal loss, watts	10.0
Total thermal power required, watts	33.7
Overall efficiency, %	20.7

*(includes regenerator ineffectiveness and heat transfer from gas to cylinder wall).

3.3 HEATER

All of the thermal power needed to sustain engine operation is transfered from the heat source (by conduction) to the heater which, in turn, heats the working gas. This transfer must be accomplished with a minimum temperature drop to minimize the parasitic losses, which affect the system efficiency and have physiological implications. The pressure drop sustained by the gas in passing through the heater must also be minimized since power lost in this manner must be made up in the reversing system. Finally, the volume of gas contained in the heater and its connecting plenums must be minimized since such volume is part of the unswept volume of the engine which influences engine pressure ratio and power density.

The heater temperature drop, pressure drop and volume are interrelated and affect overall engine performance in a complex way. The optimum conditions were identified by the parametric studies described in Section 6.0. Characteristics of the heater resulting from these studies are as follows:

Length, in.	1.25
Channel width, in.	0.0645
Channel height, in.	0.1972
Hydraulic diameter, in.	0.0977
Total volume, $in.^3$	0.1275
Heat transfer ΔT, ^oF	50
Energy loss from ΔP, watts	0.047

The general configuration of the heater is shown in Figure 5.

3.4 DISPLACER CYLINDER AND PISTON

The displacer cylinder is essentially a constant volume chamber, one end of which is hot while the other end is cold. The function of the displacer piston is to transfer the engine working gas back and forth between the hot and cold ends through the regenerator and heater.

The major displacer cylinder design criterion is that the parasitic heat loss from hot to cold end should be minimal. The piston and cylinder walls must be fabricated of light gauge material with a low thermal conductivity to limit heat loss by conduction through these components. The cylinder is also made long and the diameter is minimized to reduce the

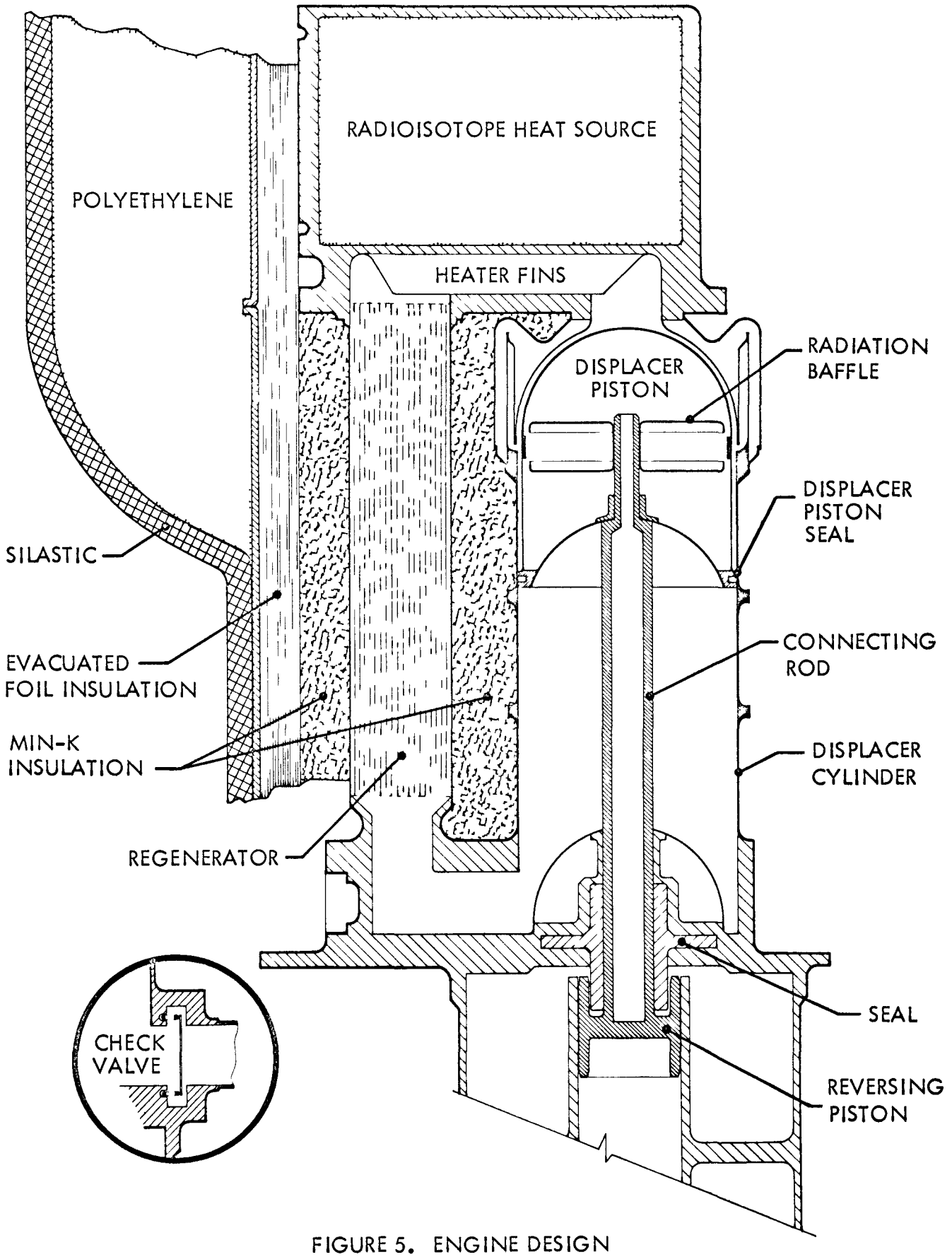

3.01-67-1002

FIGURE 5. ENGINE DESIGN

conduction loss. Thermal radiation through the piston is limited by radiation baffles. In addition to the loss due to thermal conduction, mechanical transport of heat by the moving piston also contributes to the axial heat loss. Heat is transfered from the hot portion of the cylinder to the piston at the upper portion of the stroke and, subsequently, transfered to the low temperature portion of the cylinder wall when the piston is in the lower portion of the stroke.

The upper portion of the cylinder is designed to limit this mechanical transport in two ways: the extended heat path from the heater to the cylinder wall reduces the wall temperature in the upper portion of the cylinder; and the hemispherical shape of the piston end limits the piston area in close contact with the cylinder wall.

The displacer piston and cylinder are to be made from Hastelloy C, a solid solution strengthened nickel alloy. This material has good high temperature strength, can be fabricated using most standard techniques, and has a low thermal conductivity.

3.5 REGENERATOR

The function of the regenerator is to maintain the temperature difference between the gas in the hot and cold chambers with minimum heat addition from an external source. This is accomplished by absorbing heat in the regenerator as the gas passes from the hot chamber to the cold chamber and, subsequently, reheating the gas when it returns to the hot chamber.

The volume of the regenerator should be small since it is a portion of the unswept volume of the engine. The effectiveness of the heat exchange between the regenerator and the gas must be maximum, which implies a large surface area and small hydraulic diameter. Axial conduction through the regenerator must be minimized to control the parasitic heat losses and the gas pressure drop must also be minimized. Since all of these parameters are interrelated, the final configuration was selected on the basis of maximum overall engine efficiency (see Section 5.3.2).

The selected regenerator core geometry consists of many small hexagonal gas passages. The metal webs that form the wall of the gas passages are one mil thick, except for one third of the walls which are double thickness. Other characteristics of the regenerator are as follows:

Flow length, in.	2.5
Core diameter, in.	0.625
Hydraulic diameter, in.	0.0255
Effectiveness	0.98
Average pressure drop, psi	0.1
Energy loss due to ΔP, watts	0.4
Axial heat loss, watts	2.28

3.6 HIGH TEMPERATURE INSULATION

The function of the high temperature insulation is to minimize the parasitic heat loss from the heat source and high temperature portions of the engine. The insulation should be as close to the engine and heat source as possible to minimize the total volume and the weight of the neutron shield (which is outside the thermal insulation). The insulation need not have high compressive or shear strength but should have insulating properties which do not degrade with time. The thermal insulation should also contribute as little as possible to the axial heat loss down the regenerator and displacer cylinder.

Although evacuated foil insulation has the lowest conductivity of available insulating materials, its insulating properties are not isotropic; the conductivity along the foils is much greater than that normal to the foils. An isotropic insulator must be used at least in the area of the displacer cylinder and regenerator to avoid excessive axial heat loss.

The selected configuration provides a layer of Min-K-1301 immediately surrounding the displacer piston and regenerator and a layer of evacuated foil insulation covering the heat source and the Min-K. (Fig. 4) The characteristics of the insulation are as follows:

	Min-K	Evacuated Foil
Thickness, in.	0.2	0.25
Approximate conductivity, Btu/hr-ft-^{o}F	0.02	0.3×10^{-3}
Heat loss, watts	1.7	

3.7 CHECK VALVES

The check valves regulate the flow of gas into and out of the displacer cylinder. The inlet check valve opens when the engine pressure is less than that at the low pressure inlet. The exhaust check valve opens when engine pressure is greater than the pressure in the high pressure outlet line.

The design criteria for the check valves include high reliability, and minimum opening resistance, flow resistance and backflow on closing.

A simple disk valve appears to satisfy these criteria very well. Movement of the disk is controlled automatically by gas pressure. By proper selection of the geometry and dimensions, the pressure loss and back flow can be kept very low and low rate springs are used to further reduce the back flow.

Valves of this type were tested in the experimental investigation and the anticipated performance was verified (see Appendix R).

3.8 REVERSING SYSTEM

The general purpose of the reversing system and the way in which it accomplishes its function was described in Section 2.2.2. The configuration of the reversing system is shown in the lower portion of Figure 2.

The purpose of the gas chamber surrounding the reversing piston is to provide sufficient compression and expansion volume so that the pressure ratio in the reversing cylinder is about the same as in the displacer cylinder. This results in a nearly continuous transfer of energy from the displacer piston to the reversing piston, although not at a constant rate. The amount of energy transfered is porportional to the area of the connecting shaft. The shaft area used is about 10% larger than needed; this tends to make the piston operate with a stroke slightly longer than the design stroke. Excess energy is dissipated by the dashpots at the ends of the reversing cylinder.

3.9 SEALS AND BEARINGS

A major advantage of the linear engine concept is that all bearing loads are low. Bearing surfaces are required only for alignment and to sustain the acceleration loads imposed by gravity and external movement. As a consequence, the surfaces provided for seals on the piston can also be used as bearings.

Three seals are required in the engine: one on the displacer piston; one on the reversing piston; and one between the displacer cylinder and the reversing cylinder. None of these need to be an absolute seal but leakage must be held to a small fraction of the gas volumes involved; the most stringent seal requirements are on the reversing piston. Both the piston and shaft seals must withstand the full engine pressure ratio of 1.25. The sealing requirement on the displacer piston is much less severe since the pressure difference across the displacer piston is very low.

Since the operating temperature of the reversing piston is less than 250^{o}F, a wide variety of materials are suitable for use as seals, including many of the filled and impregnated forms of Teflon. The main selection criteria are low coefficient of friction and a low wear rate. More severe requirements are imposed on the displacer piston seal since it may be exposed to a temperature of 600 to 800^{o}F; several of the solid bearing materials based on mixtures of silver, boron nitride, graphite and MoS_2 with binders or in porous metal matrices appear to have the properties required for this application.

3.10 PUMPING CHAMBERS

The pumping chambers form the interface between the engine gas and the pumping fluid used to transmit power to the blood pump. These chambers convert the pressure level and pressure ratio most advantageous for engine operation to those required by the blood pump and also automatically adjust the output pressure for changes in atmospheric pressure. The principle of operation of the pumping chambers was described briefly in Section 2.3.1.

The pumping chambers must prevent leakage or diffusion of the engine working gas into the pumping fluid and, as a consequence, metallic, rather than a plastic, seal material must be used. Other pumping chamber requirements are maximum reliability and minimum volume.

The general configuration of pumping chamber is shown in Figure 6. Welded metal bellows are used because of their long cyclic life; this type of bellows has very good fatigue life if the stress level is maintained at a sufficiently low value. The various bellows are arranged so that the pressures outside the bellows are always higher than the internal pressures; this prevents a phenomenon known as bellows squirm, a mechanical instability analogous to column buckling.

The size of a pumping chamber is fixed by the size of the required blood stroke volume. Separate left and right pumping chambers are provided in the conceptual design; this permits synchronous pumping of left and right heart chambers and independent control of both sides.

3.11 HEAT REJECTION

Waste heat is removed from the engine by cooling the extracted working gas before it is returned to the engine. Heat from the gas stream is transfered to the pumping fluid before it is transferred to the blood for the reasons discussed in Section 2.3. A number of techniques can be used in transferring heat from the pumping fluid to the blood; the method chosen is to incorporate the heat exchanger into the abdominal aorta since this location is close to the engine and since the blood flow rate at this location is suitably high. The heat exchanger is a simple tubular exchanger with the blood flowing in the central tube in a geometry nearly identical with that in a normal artery. The pumping fluid flows in an annular chamber around the tube carrying the blood. An inner diameter of about an inch and a length of about six inches result in heat transfer conditions which prevent damage to the blood (due to overheating), even at the lowest blood flow rates.

3.12 RADIOISOTOPE FUEL AND SHIELD

Plutonium 238 was selected as the thermal power source for the implantable power system primarily because of its long half life; it is the only radioisotope fuel capable of producing power for 10 years without refueling. The major problems associated with the use of Pu-238 are the neutrons emitted as a result of spontaneous fission and the possible release of helium resulting from alpha particle emission.

The chemical form of plutonium used is the nitride. This compound is stable at temperatures much higher than those expected in the implantable power source and it has some advantages over the oxide (a slightly higher plutonium density, a higher thermal conductivity and complete absence of neutrons from α, n reactions, although these can also be eliminated in the oxide by the use of isotopically separated oxygen).

The fuel is pressed into cylindrical pellets and encapsulated in a tungsten-rhenium alloy vessel. The wall thickness of the tungsten alloy vessel is based on gamma shielding requirements since this thickness is greater than that required to contain the pressure buildup. Although the tungsten alloy has the required strength, it is encapsulated in a thin can of Hastelloy C for atmospheric corrosion protection. Polyethylene is

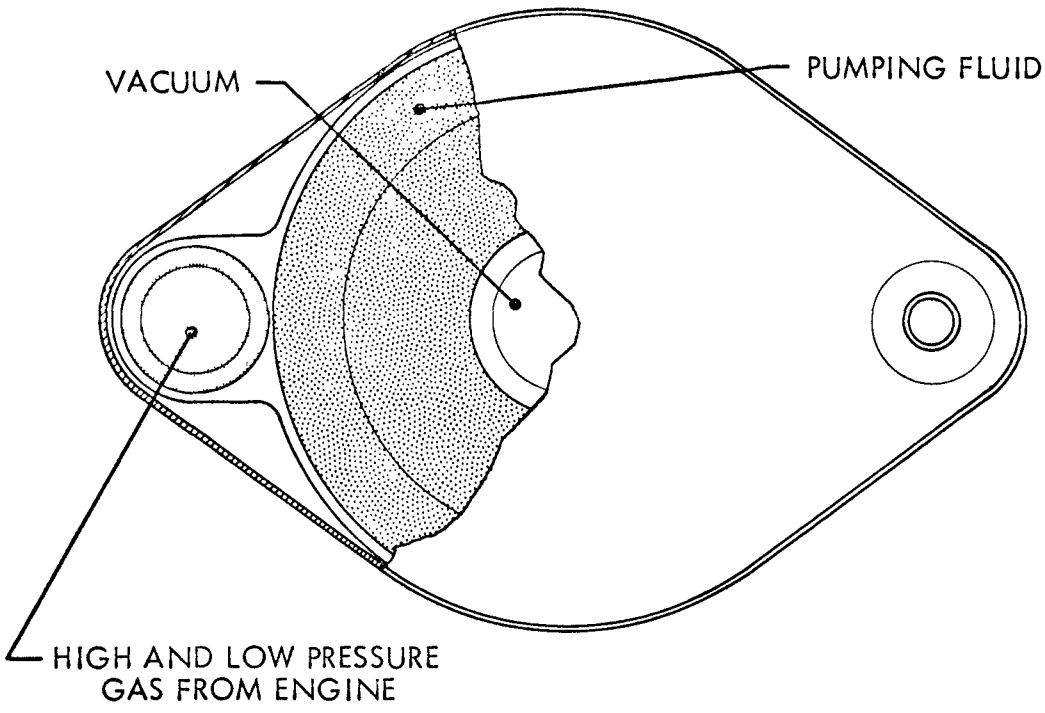

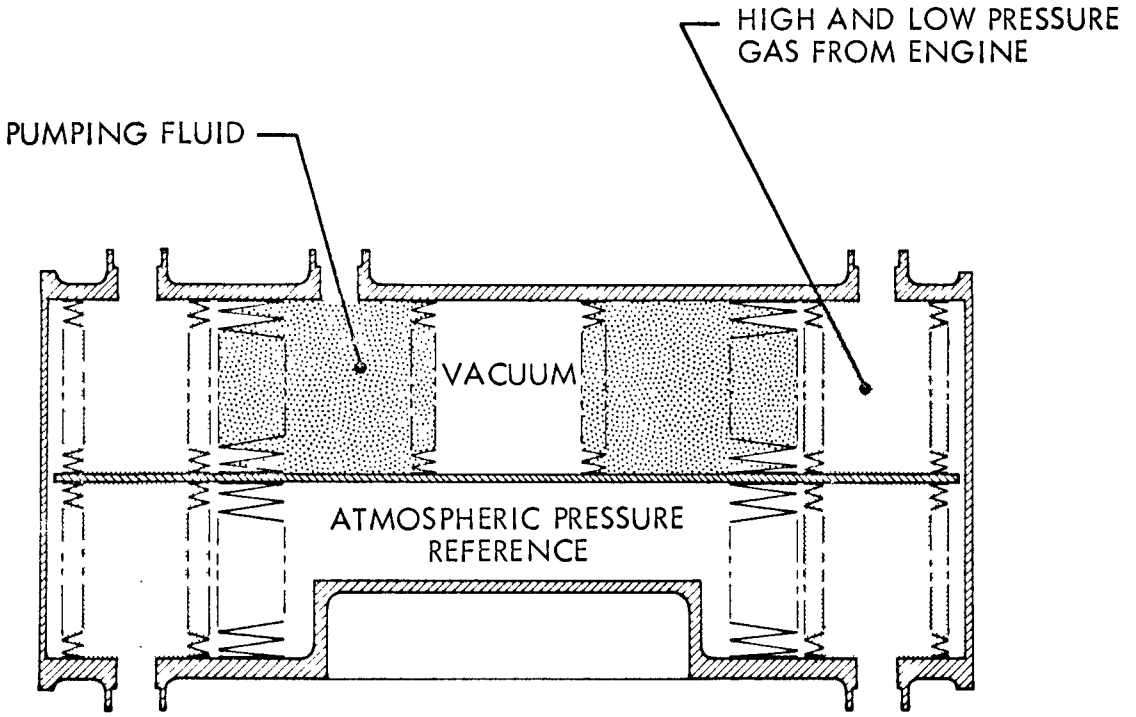

FIGURE 6. PUMPING CHAMBER

provided outside the thermal insulation to reduce the neutron flux at the surface of the shield. About one inch of polyethylene is required.

3.13 PUMPING CHAMBER CONTROL

Largely because of autoregulatory regional circulatory controls, the heart, as a pump, probably fulfills its life-sustaining functions if it satisfies the following basic criteria:

1) It must maintain sufficient cardiac output (blood volumetric flow rate and systemic pressure) to satisfy all the needs of the body.

2) It must provide for flow balance between the right and left heart circuits, and between cardiac output and venous return.

These same criteria describe the characteristics of an artificial heart pump which, in addition, should have a stroke profile and pulse rate similar to those of the natural heart, to accommodate the dynamic changes in vascular impedance.

Cardiac output is the product of stroke volume and heart rate. For a system in which systole and diastole are synchronized for both sides of the heart, flow balance can only be adjusted by varying the stroke volume. Atrial pressure is the most sensitive control signal for flow balance compensation. Until further clinical evaluations are completed, heart pump operation should correspond closely to normal physiological behavior. It is therefore assumed that pulsatile flow, and a capability for varying the relative duration of systole and diastole, as well as heart rate and stroke volume, are required.

A schematic diagram of the control system designed to vary the implantable heart pump operating parameters is shown in Figure 7. A load sensitive bistable fluidic amplifier (FA-1) is used as the primary switching element which directs the high pressure gas stream to the right ventricular pump during systole and diastole. Operation is based on the principle of "wall attachment"---the Coanda Effect. The fluidic device also provides pressure to actuate the spool valve (SV-1), which cyclically vents the opposite side of the right ventricular pumping chamber; and provides pressure to actuate the spool valve (SV-2) which directs the high pressure supply stream to the left ventricular pumping chamber and vents the opposite side of the chamber. The left ventricle is not directly driven by a bistable fluidic amplifier, as the output of such a device is only 40 to 50 percent of the supply pressure.

The load sensitive bistable fluidic amplifier automatically switches at the end of systole and diastole, when the pumping chamber reaches its maximum displacement. The pumping chamber vent line is connected directly to the low pressure reservoir during systole so that the full available pressure differential is always applied for a firm systolic pulse. The duration of systole is therefore determined by the body autoregulatory mechanisms which control peripheral impedance. Control valve V-1, located in the right ventricle pumping chamber diastole vent line, determines the

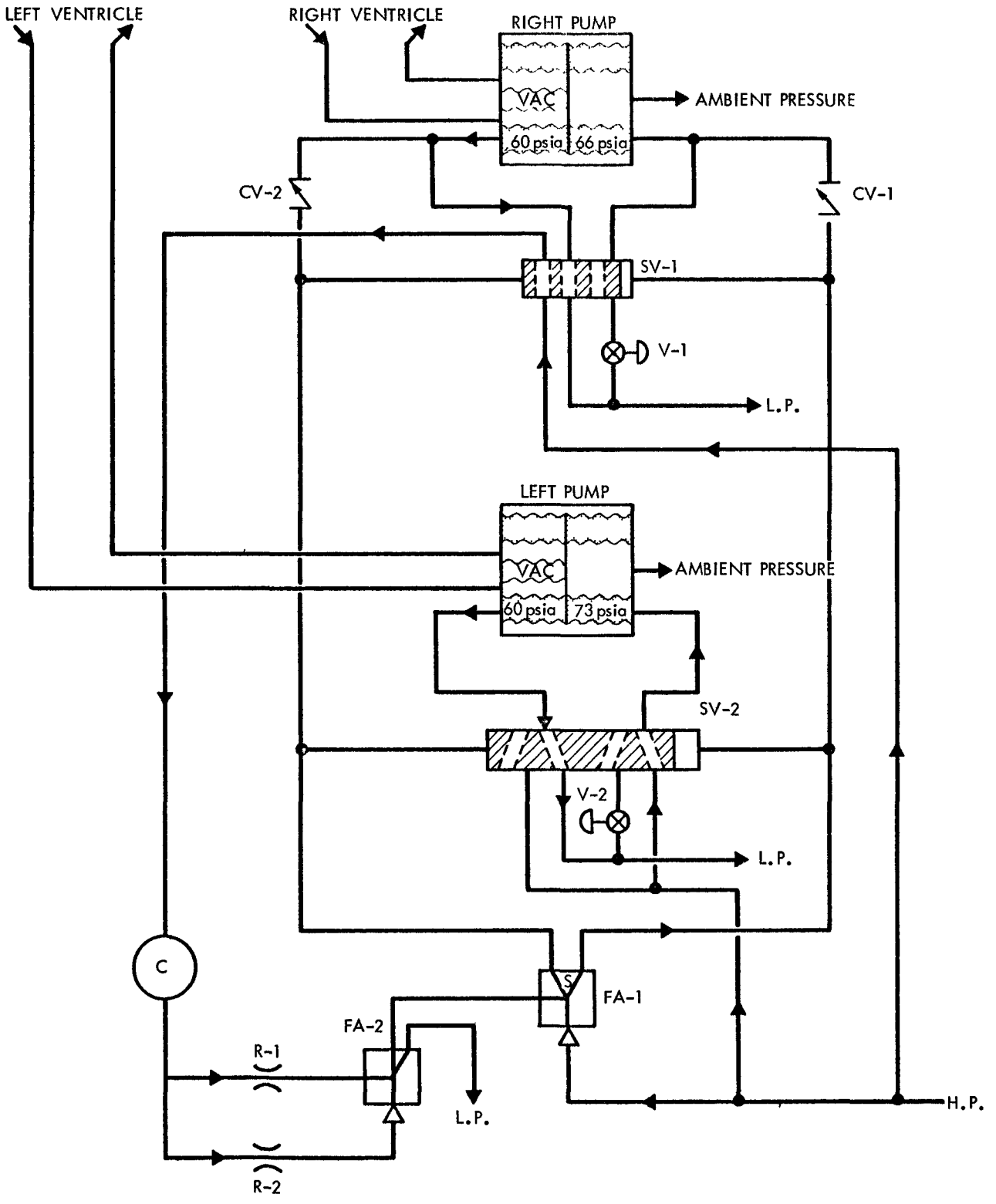

FIGURE 7. CONTROL SYSTEM SCHEMATIC DIAGRAM

3.01-67-989

duration of diastole and the pulse rate. Control valve V-2, located in the left ventricle diastole vent line, is required to adjust the left ventricular stroke displacement and maintain flow balance between the left and right ventricles. Two atrial pressure sensors are required to provide the control signals for V-1 and V-2.

A timing circuit is provided to limit the pulse rate to a minimum permissible value consistent with normal physiological requirements, i.e., 60 to 65 beats per minute. During systole, a capacitive element, C, is fully charged to line pressure by the actuation of spool valve SV-1. Restrictors R-1 and R-2 control a fixed leakage flow rate to the fluidic amplifier device, FA-2. This leakage is normally vented to the low pressure reservoir. If the pulse rate is too low (less than the minimum allowable rate of 60 to 65 beats per minute), the pressure in the capacitive element will be reduced by the controlled leakage to the point at which FA-2 will switch and direct an input signal to FA-1. This signal will automatically terminate the diastolic period and initiate systole.

3.14 ENGINE OUTPUT CONTROL

The engine described in this document was designed for a sustained power output of seven watts. The radioisotope heat source must therefore be sized on the basis of this continuous seven watt output. Under these conditions, there is little to be gained by reducing engine output since the surplus radioisotope heat output would have to be rejected in any case. It is much easier to generate full power at all times and to dissipate any surplus power generated, as is the case in the concept described in the preceeding sections.

However, if the seven watt output is required only occasionally and for short periods, other options are available which offer some advantages. The engine may be designed for a maximum seven watt output but operated at a lower power level except when the maximum output is required. Under this concept, the radioisotope heat source may be sized for the thermal power required at the average power level provided a thermal storage system is incorporated to deliver supplemental heat during periods of high power demand. An attractive thermal storage concept involves the use of lithium hydride as a combined radioisotope shield and thermal storage material. Lithium hydride melts at a temperature slightly above that required by the modified Stirling engine and is an excellent neutron shielding material. The latent heat of fusion is high, so that relatively long periods of high power demand can be sustained.

The combined radioisotope/thermal storage approach is practical only if the thermal power required by the engine is reduced at low output power levels. The decrease in thermal power required is never porportional to the decrease in power output, particularly in small engines, because parasitic losses account for a large fraction of the total power required. The device used to control power output should therefore provide a maximum decrease in thermal power requirement with decreasing power output.

The best technique for the modified Stirling engine is simply to reduce the engine speed to reduce power output. This results in the maximum reduction of both mechanical and thermal losses as power is decreased. Engine speed control can be accomplished in the reversing piston by varying the energy absorbing characteristics of the dashpots. Maximum speed corresponds to completely elastic dashpots while minimum speed results from maximum kinetic energy absorption.

BLANK

4.0 EVALUATION OF CONCEPT

An implantable power source must perform with high thermodynamic efficiency to minimize the size and weight of the radioisotope heat source and the heat load on the body. High efficiency is always difficult to achieve in small engines since it is difficult to reduce parasitic heat losses to values that are small compared with output power. One of the advantages of the Stirling cycle is high cycle efficiency; a Stirling engine can operate with an overall efficiency of about 20% including consideration of parasitic heat losses.

The minimization of parasitic heat losses was a major criterion in the conceptual design effort. High power density, achieved by high speed operation and relatively high pressure, reduces the size and consequently the heat loss from engine components. The configuration of the engine was optimized for maximum overall efficiency by a proper balance between size, mechanical and thermal losses.

Long operating life and reliability are vital engine characteristics for the proposed application. Long engine life is assured by the elimination of crank mechanisms, zero leakage seals and high bearing loads. Flexing elements, such as the pumping chamber bellows, operate at the heart frequency rather than the engine frequency to reduce the number of cycles experienced. The design stress in these flexing elements was established at a level significantly below that required to assure a 10 year life. The use of an inert gas working fluid eliminates corrosion and assures that the heat transfer and flow characteristics of the engine will remain constant.

The reference concept of peumatic transmission of energy from the engine to the artificial heart is simple and permits wide flexibility in the selection of the specific design of the heart pump. The control system is also pneumatic eliminating the problems associated with the generation of electrical energy and the interface between electrical and pneumatic equipment. The reference control system is also quite flexible and can accommodate changes in control philosophy and criteria without major redesign.

The implantable power source must be insensitive to gravitational orientation to permit full patient mobility. The use of a single-phase gas working fluid, as opposed to a two-phase steam/water working fluid, simplifies the

problems of satisfying this criterion. None of the engine components depend on orientation for proper functioning and all are designed to withstand accelerations of 3g. The effect of externally imposed acceleration on the free piston is small because it is normally subjected to forces many times larger than gravity. The control system has been designed so that no valves or other control elements can be moved by external forces, including a sustained acceleration of three times gravity. These same characteristics make the power source insensitive to shock and vibration.

A reduction must be made in engine size before the system can be considered completely satisfactory. The reference engine size, while within the specified 2000 ml limit for an abdominal implant, is larger than desirable. The major part of the volume is the neutron shield for the radioisotope heat source. The reduction in the size of this shield is a problem not related to the engine type selected but one that must be solved before a practical system can be evolved. The pumping chambers are also quite large; some reduction in size can be made if the pulse size can be reduced by using a higher pulse rate to achieve the desired cardiac output. A sizeable reduction could also be made if non-synchronous pumping of left and right ventricle is acceptable. Some size reduction may be achieved by integrating the pumping chamber with the artificial heart if such a concept is feasible.

It is submitted that the preferred cycle for use in an implantable power source is the Stirling cycle and that the Aerojet linear engine concept represents the most attractive utilization of the Stirling cycle for this application.

5.0 CONCEPTUAL DESIGN

A discussion of the design considerations that were involved in the selection of component configurations and operating conditions for the reference conceptual design is presented in this Section. The functions and operating requirements for each component are given and final reference component designs are described.

Alternate component concepts that were considered are described along with reasons for rejection. Descriptions of the methods used to analyze component performance are also presented; analysis of the operation of the overall system is described in Section 6.0 and details of the calculational procedures are presented in appendices which are referenced in this Section where appropriate.

5.1 DISPLACER CYLINDER AND PISTON

5.1.1 Function

The functions of the displacer cylinder and piston are to provide hot and cold chambers for the working fluid and a means of transfering the working fluid between the two chambers via the heater and regenerator.

5.1.2 Requirements

- Provide for reliable operation for 5×10^9 cycles
- Provide minimum practical parasitic thermal losses
- Provide minimum practical friction loss
- Limit bypass leakage to less than 4% of regenerator flow
- Provide a minimum practical unswept volume
- In conjunction with reversing piston, provide for making up power loss in the reciprocating mass resulting from aerodynamic and frictional losses

5.1.3 Reference Design

The reference design of the displacer piston and cylinder is shown in the engine layout, Figure 8.

The piston consists of a right cylindrical section with hemispherical ends. The upper hemisphere is convex and the lower is concave. The ends and side walls are fabricated from 0.005 in.-thick Hastelloy C. Two circumferential webs and a backing ring at the upper joint are provided to facilitate fabrication and to improve the strength and shape stability of the piston. Internal baffling is provided to reduce radiative heat transfer between the relatively hot upper dome and the cooler side walls and lower dome. The displacer piston has a diameter of 1.08 in. and is connected to the reversing piston by a hollow Hastelloy C rod approximately 0.215 in.in diameter. A grooved ring is provided at the lower end of the piston to accommodate the split ring seal.

The piston assembly will be electron beam welded to assure high reliability of the joints. After welding, the piston will be filled with helium gas to a pressure of approximately 24 psia through the hollow rod; this pressurization results in low pressure differentials across the piston walls at operating temperatures and pressures.

The displacer cylinder is fabricated from 0.010 in.-thick Hastelloy C in the form of a right cylinder with hemispherical ends to match the displacer piston. Two integral, 0.030 in.-thick peripheral reinforcing rings are provided to facilitate fabrication and to increase the strength and shape stability of the cylinder.

The upper end of the displacer cylinder is designed to support the heater and fuel assembly while providing a relatively torturous heat leakage path. The internal upper dome structure is in intimate contact with the working fluid and operates relatively close to the average hot chamber gas temperature. The double cylindrical structure is designed to provide high thermal impedance between the dome and the relatively cool lower cylinder.

A base plate, which serves as an interconnection between the cylinder, regenerator, and reversing piston, is located at the base of the cylinder. The rod seal assembly is located in this base plate, and the lower dome is attached to the seal assembly. The two check valves are located on the periphery of the cylinder just above the base plate.

The major factors which affect the design of the displacer piston and cylinder are the minimization of thermal leakage from the hot end to the cold end and the limit on the desirable overall length of the engine. The reciprocating motion of the piston increases the heat leakage through the cylinder several fold over that observed in a static condition because of a mechanical heat pumping phenomenon. The effect can be explained by considering the piston at top and bottom dead center positions. At top dead center, heat from the cylinder upper side wall and dome is transferred across the gas gap to the displacer piston. At bottom dead center, thermal energy is transferred from the piston across the gas gap to the lower cylinder wall and dome. The net effect is to thermally "short-circuit" the cylinder wall. Analytical studies

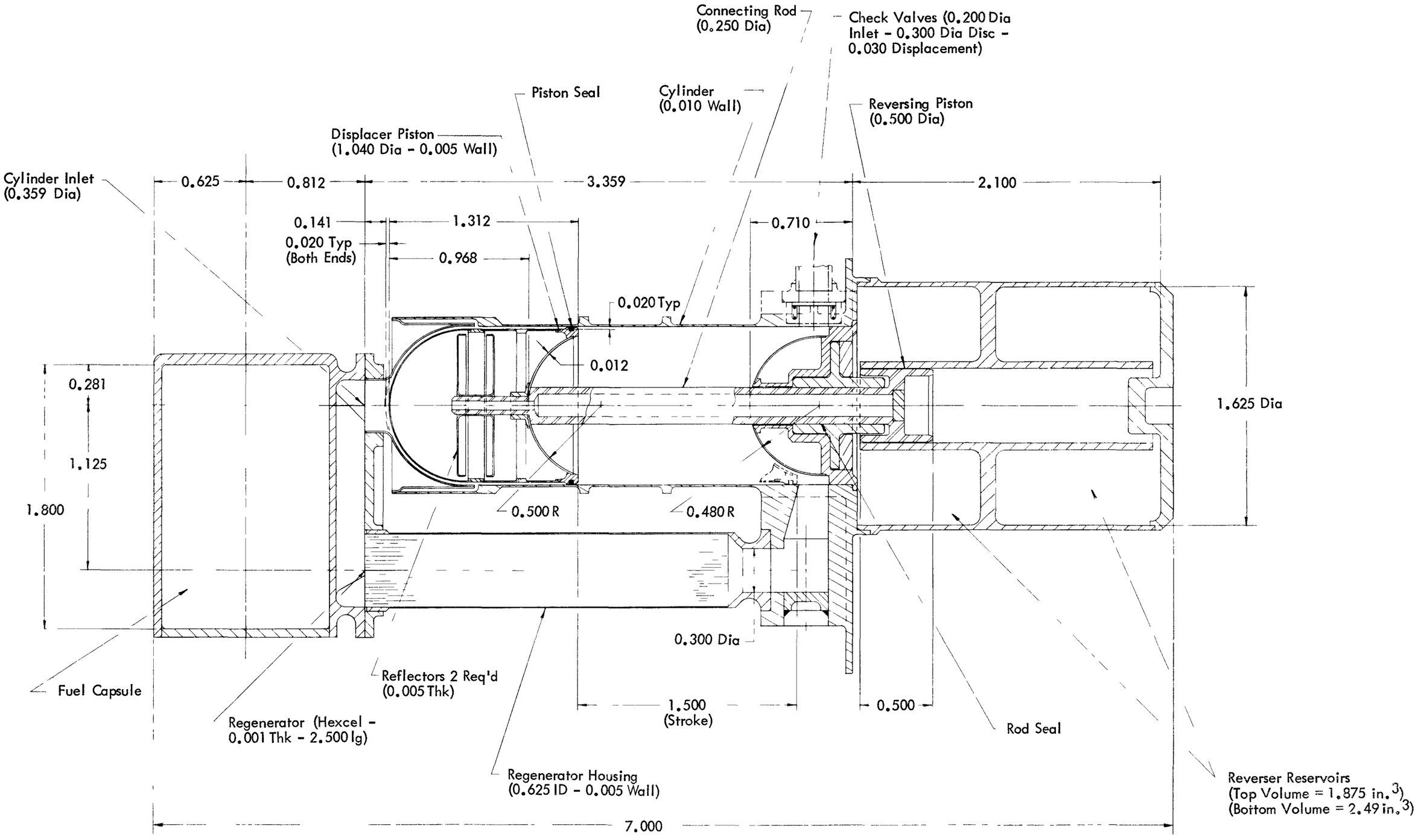

FIGURE 8. IMPLANTABLE POWER SOURCE ENGINE LAYOUT

301-68-065

BLANK

show that the mechanical pumping decreases rapidly as the gap width is increased until a gap of approximately 0.020 in. between the piston and cylinder is reached. Larger gaps do not decrease the parasitic heat losses significantly. Therefore, the reference design incorporates a 0.020 in. radial gap around the piston except in the seal area where a nominal 0.001 in. gap is provided.

For constant piston and cylinder wall thicknesses, both the conductive and mechanical heat pumping decrease as the stroke length increases. Any incremental increase in stroke length increases the length of the implantable package by twice the stroke length increase since both the displacer and reversing cylinder lengths must be increased by the incremental value. The reference design specifies a stroke length of 1.5 in., which results in an overall engine length near the practical maximum.

The working fluids in both the hot and cold chamber are not at a constant temperature as in the ideal Stirling cycle but undergo temperature cycles due to compression and expansion. This temperature cycling causes heat transfer in and out of the upper and lower piston domes. The wall thickness of these domes is made as small as possible to limit the undesirable heat transfer to or from the relatively cool piston side walls.

The bottom piston dome is concave to provide room for the shaft seal assembly, otherwise this shaft seal would require a longer overall engine.

The end effect of all the complicated heat transfer mechanisms is illustrated in Figure 9. The temperature profile between the upper and lower cylinder positions would be more or less linear for the static piston case, but the actual temperature profile is not linear. The parasitic heat loss for the static case is approximately 2 watts while that for the dynamic case is approximately 6 watts.

5.1.4 Alternates Considered

The fundamental function of the displacer piston and cylinder is to transfer the working fluid from the hot to the cold regions and from the cold to the hot regions. This basic function could be accomplished by a variety of methods and mechanisms. The function of the displacer piston could be combined with that of the regenerator by mounting the regenerator heat transfer surfaces inside or around the periphery of the displacer piston. This alternate was subjected to a preliminary evaluation but discarded, primarily becasue of the difficulty of integrating an effective heater into the system.

The bypass leakage could be eliminated by the use of one or more bellows to perform the displacing function. A variety of geometrical configurations could be used, ranging from installing a bellows in the existing design to the replacement of the piston and cylinders with a single large bellows with a centrally-located bulkhead. These bellows concepts were rejected because of the unacceptably high fatigue which would be encountered in the bellows operation. The added complication of mounting the heat source for the complete bellows concept was also a factor.

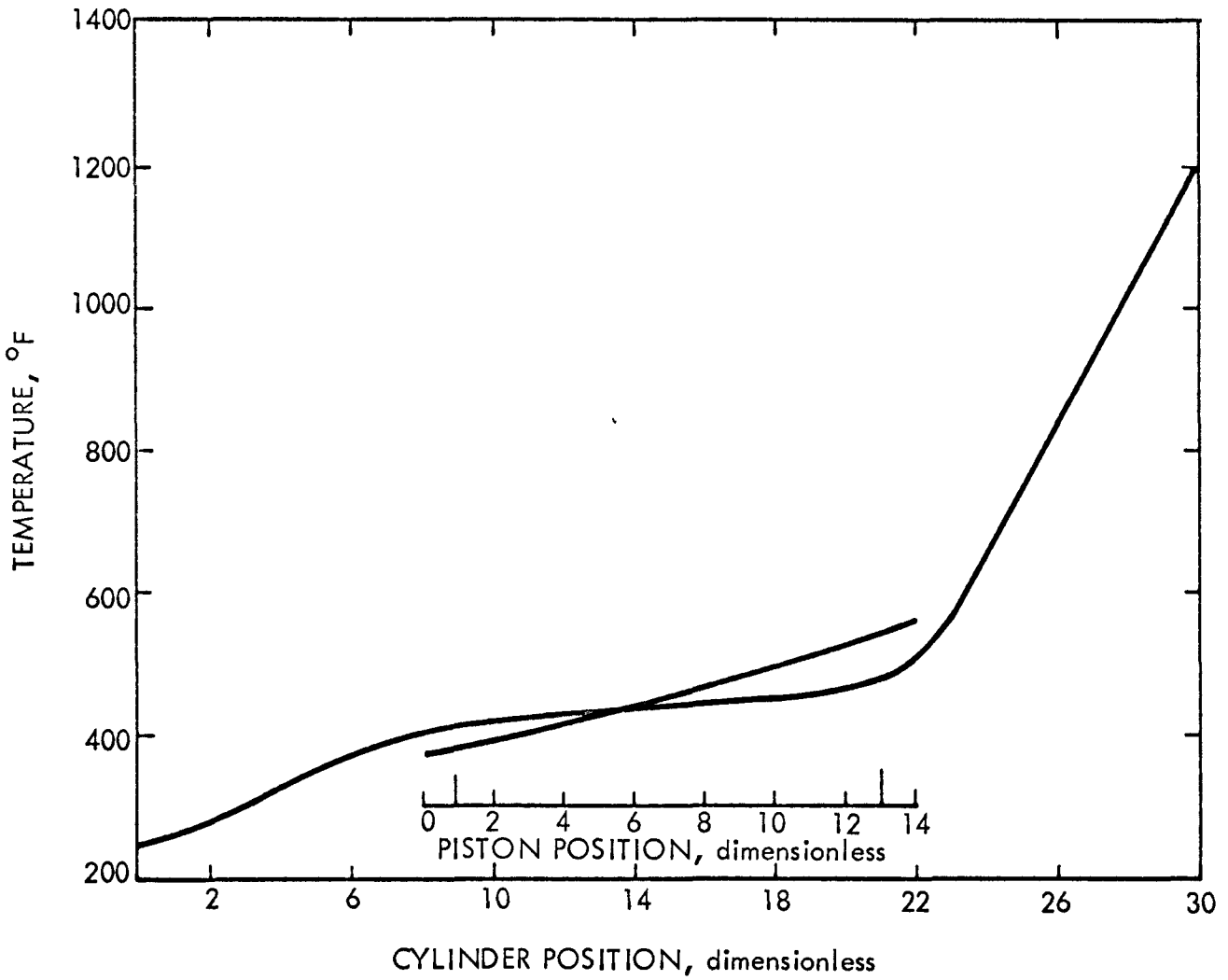

FIGURE 9. DISPLACER CYLINDER AND PISTON TEMPERATURE PROFILE

3.01-68-066

Even with the conventional piston-cylinder configuration such as that used in the reference design, numerous design alternates are possible. One of the more obvious alternates is to use a much larger diameter system with a shorter stroke. As discussed in the preceding section, the shorter stroke results in an unacceptably large parasitic heat loss through the piston-cylinder assembly due to increased thermal conduction and mechanical pumping. A similar alternate involves an increase in the swept volume with a corresponding decrease in the reciprocating speed. In this case also, a preliminary evaluation of the parasitic heat losses indicated that this method was unacceptable.

A variety of piston configurations were considered. The experimental engine, which is described in Appendix R, used a right cylindrical piston with flat ends. In this case, the end plates were made relatively thick to satisfy the structural requirements imposed by the anticipated pressure differences between the internal and external piston pressures. These thick end plates resulted in high thermal losses. The structurally-strong hemispherical ends in the reference design operate near the average gas temperature, primarily as a result of the high thermal impedance to the piston side walls attainable with the thin wall sections. A completely spherical piston would decrease the mechanical thermal pumping but the heat transfer from upper to lower surfaces would be unacceptably high.

A significant reduction in the parasitic heat losses could be accomplished by the use of a high efficiency insulation material over the end plates of the piston or the cylinder end plates, or both. This method of heat loss reduction would be particularly effective for the piston design incorporating flat end plates. This design concept has not been eliminated, but was not used in the reference design because a material with acceptable long term reliability was not identified. Several alternate materials for fabrication of the piston and cylinder were evaluated. The most important properties for this material are low thermal conductivity and high strength at operating temperatures. The two most attractive materials are Hastelloy C and titanium alloy. Hastelloy C was chosen despite of its slightly higher thermal conductivity since its significantly superior high temperature strength, would permit the use of a thinner wall section to improve overall engine performance.

5.1.5 Method of Analysis

The analysis of the displacer piston and cylinder can be subdivided into three distinct categories: structural; bypass leakage and friction; and thermal. The structural analyses were performed by conventional methods and do not warrant a detailed discussion. The bypass leakage is covered in Section 5.7 and Appendix E.

The thermal analysis was performed with the aid of a computer program which was written specifically to analyze the oscillating piston heat transfer. The analytical model was constructed by subdividing the piston and cylinder into a specified number of axial nodes. The material thickness for each node can be specified by the operator and the gap between any particular piston node and the adjacent cylinder node can also be specified. The axial length of all piston and cylinder nodes was equal.

At any particular piston position, the computer code calculated the heat transfer between the adjacent piston and cylinder nodes and between the piston and domes and the adjacent gas or cylinder end plates. Then, the conductive heat transfer between adjacent nodes on the cylinder and then on the piston were calculated and the temperatures of the two nodes involved were adjusted to account for the quantity of heat transfered. At the end of the calculation described above, the piston was moved up (or down) one node relative to the cylinder and the calculation was repeated at the new piston position. This process was continued until the piston completed a full cycle. Actually, the dwell time at each position was varied so that the motion was approximately sinusoidal.

The boundary conditions imposed on the problem were: the upper and lower cylinder temperatures were specified and maintained constant; and the hot and cold chamber gas temperatures were input from those predicted by the intermediate analytical technique (see Section 6.4). After the first cycle, the temperatures of the various nodes varied from those assumed by a small amount. The problem could be solved by continuing to cycle the piston until equilibrium was achieved; however, this method was very slow since it required thousands of cycles to achieve equilibrium and a prohibitive amount of computer time was involved. As a consequence, the computer program was modified to provide for the relatively expeditious achievement of equilibrium.

5.2 HEATER

5.2.1 Function

The function of the heater is to transfer the input heat from the radioactive source to the working fluid of the modified Stirling engine in a manner which maximizes the efficiency of the engine.

5.2.2 Requirements

- Provide heat transfer capability for up to 35 watts (thermal).
- Provide for transport of the working fluid to and from the regenerator and the hot chamber with minimum practical inlet, exhaust, friction and other fluid dynamic losses.
- Provide for transport of thermal energy from the source to the engine working gas with minimum practical temperature drop.
- Incorporate minimum practical fluid volume.

5.2.3 Reference Design

The reference design of the heater consists of eight rectangular passages between the regenerator outlet and the hot chamber inlet.

For the reference design engine, the working fluid velocities at the exit from the regenerator and at the inlet to the heater are sufficiently small so that abrupt changes in flow area do not result in significant pressure drop. Accordingly, no effort has been made to provide smooth transitions at the inlet and outlet of the heater.

The design parameters for the heater are listed in Table 1. The dimensions of the flow passages were selected to provide the necessary heat transfer and fluid flow characteristics. The thermal energy is transfered by thermal conduction from the radioisotope source to both the upper and lower surfaces of the heater. The heater walls between the flow passages are sufficiently thick to limit the maximum thermal conduction temperature drops to approximately $10^{o}F$.

TABLE 1 – REFERENCE HEATER PARAMETERS

Length of flow, in.	1.25
No. of passages	8
No. of fins	7
Height of passage, in.	0.1972
Width of passage, in.	0.064
Fin thickness, in.	0.042
Total heater width, in.	0.808
Heater volume, $in.^3$	0.127

The heater will be fabricated from Hastelloy C to avoid interface problems with the heater capsule and to facilitate attachment to the regenerator and displacer cylinder.

As discussed in the following section, a shorter heater with the same flow volume would, theoretically, have performance superior to that of the reference design. However, the reference design has the advantage of requiring only small volumes for the inlet and exhaust plenums. The loss in performance of the longer heater is compensated for by smaller plenum volumes than are required for the shorter heater.

5.2.4 Alternates Considered

5.2.4.1 Disc Heater

For a fixed heat transfer capability, log mean temperature difference, fluid flow rate, and internal volume, the pressure drop and flow power loss are both proportional to the square of the heater length. Ideally, the shorter the heater the better performance. As the heater length is decreased the cross section area increases. Neglecting some physical limitations, the ideal heater is an infinitely thin, infinitely large disc. The limitation may be one of the following: the size which can be mated with the engine; the size which can be insulated efficiently; the size which permits good thermal transfer from the heat source to all parts of the disc; or, the size which can be effectively mated to both the heater and regenerator.

A disc heater of the type shown in Figure 10 with a 0.300 in.-thick disc was analyzed. This thickness was selected on the basis that it was at or near the shortest practical length, and resulted in a disc diameter about 1/4 of

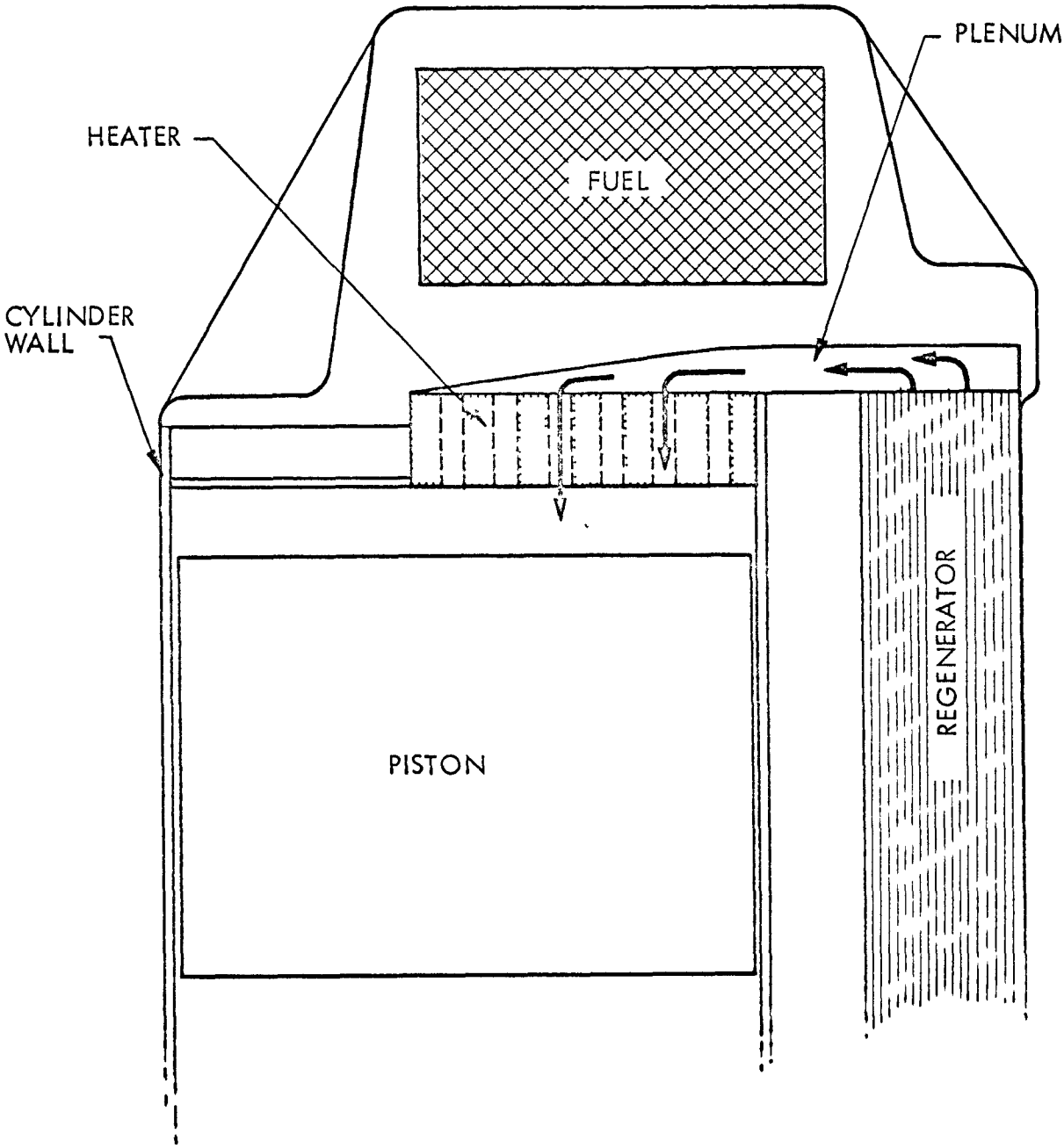

FIGURE 10. DISC HEATER

301-68-067

that of the displacer piston. In this concept, the heater consisted of 61 holes in a fan pattern. The engine working fluid was routed from the hot end of the regenerator through a short connecting tube into the heater inlet plenum. The inlet plenum connected all 61 holes and was tapered from the inlet to outlet to maintain an approximately constant flow/unit area. The working fluid passed from the plenum through the sixty-one holes directly into the hot chamber.

The area of the disc heater was too large for efficient thermal conductivity from the periphery. Accordingly, thermal conduction fins were provided which extended through the plenum and were attached to the heater disc.

The inherent advantages of this heater configuration are low pressure drop and low fluid flow losses. The obvious disadvantage is the relatively large plenum volumes required. A comparative study was made using a computer code; the results of this work revealed that the decrease in pressure drop across the heater results in a smaller increase in engine efficiency than the loss of engine efficiency associated with the relatively large plenum volume. The reference design was selected as being superior to the disc concept in view of the higher inherent efficiency associated with the former.

5.2.4.2 Short Heater

This concept is similar to the reference design but is slightly shorter. Since the minimum distance between the regenerator and the displacer piston cylinder is determined by heat transfer considerations, the shorter heater junction with the hot chamber was near the periphery of the latter. Figure 11 shows that the shorter (1 in.) heater results in a slight efficiency improvement for the ideal engine. However, the use of the shorter heater required a more complicated joint with the hot chamber and interfered with the long thermal path provided in the reference design. The reference design was selected because of the simpler hot junction joint.

5.2.5 Method of Analysis

Certain basic assumptions were made in the design analysis of the heater. These assumptions simplified the design process with only a moderate reduction in accuracy. Detailed analysis of the performance of the resulting heater was undertaken in the parametric analysis task.

The most important of the basic assumptions made for the design analysis was that the continuously transient flow through the heater can be analyzed by conventional steady state heat transfer and pressure drop correlations. The second assumption was that steady state temperatures exist (that is, the gas from the regenerator to the heater is at a constant temperature and the gas leaving the heater is at a constant temperature) and that heat is transfered to the gas only for half of the cycle. (This is a very good assumption if the regenerator performance is high). The third assumption was that the average flow rate can be used in the pressure drop and heat transfer correlations although the true flow rate is nearly sinusoidal with maximum flow occurring near mid-stroke and zero flow occurring at top and bottom dead center.

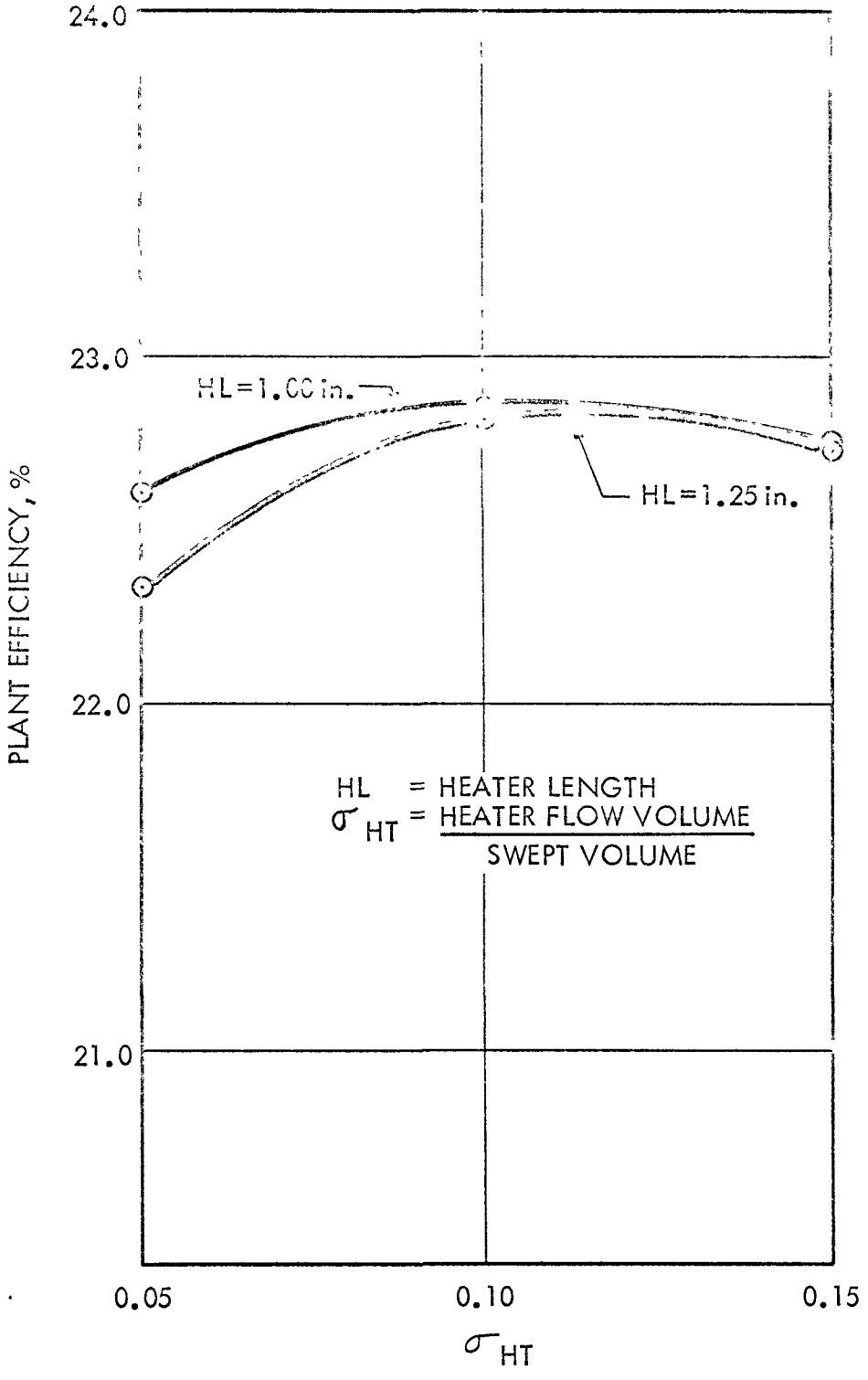

FIGURE 11. EFFECT OF HEATER LENGTH ON PLANT EFFICIENCY

301-68-065

The approximate effect on heat transfer can be shown by the following:

$$\frac{hD}{k} = 1.75 \left(\frac{\pi}{2}\right)^{1/3} \frac{1}{\pi} \left(\frac{C_p \bar{W}}{KL}\right) \int_0^{\pi} \sin\theta \, d\theta$$

The value for h is,

$$h = 0.95 \left[1.75 \frac{k}{D} \left(\frac{\bar{W} C_p}{KL}\right)^{1/3}\right]$$

where:

- h = heat transfer coefficient
- D = effective diameter
- k = thermal conductivity of the gas
- C_p = heat capacity of the gas
- $\bar{W}$ = average flow rate
- L = flow length
- θ = angular position of the piston

The error associated with the use of the average flow is about 5%.

The analysis of the effect of the heater on system performance was based on the Schmidt equation and is discussed in Appendix M. The computer code that was written for the Schmidt analysis is also presented in this Appendix.

The parameters that define the heater design are the volume, the flow length and the temperature drop between the heater and the gas. In order to optimize engine efficiency, each of these parameters was varied over a range until the peak performance was bracketed. The code output yielded information on the hydraulic diameter of the flow passage and the friction pressure drop. The shape of the passage was determined by physical limitations and by the conductive heat transfer from heat source to heater surface. When the shape of the passage was established, it was possible to define the flow area and number of passages. The physical design was then based on these optimized parameters although some modifications were required for practical reasons.

5.3 REGENERATOR

5.3.1 Function

The function of the regenerator is to increase the thermal efficiency of the Stirling engine by storing thermal energy from the working fluid during transport from the hot to cold chamber and returning the energy to the cold working fluid during the return to the hot chamber.

5.3.2 Requirements

There are four major regenerator parameters which grossly affect the Stirling engine performance. These parameters are all interrelated and must be balanced for maximum engine efficiency. The descriptive adjectives, high and low, used in the below listing of parameters are in the context of maximizing the engine efficiency:

- High heat transfer effectiveness
- Low flow power consumption
- Low gas volume
- Low thermal loss by axial conduction

5.3.3 Reference Design

The reference design of the regenerator consists of a honeycomb matrix constructed from one mil-thick titanium foil. The matrix will be brazed into a nominal 0.5 inch diameter case to provide a stable structural design. This design is shown in Figure 8.

The honeycomb matrix will be fabricated by resistance welding one mil-thick titanium sheets, expanding the hexagonal structure, machining to the proper size and furnace brazing into the regenerator outer housing.

The detailed design values for various parameters are listed in Table 2.

TABLE 2 – REFERENCE REGENERATOR PARAMETERS

Effectiveness	0.98
Web thickness, in.	0.001
Length, in.	2.5
No. of passages	567
Hydraulic diameter, in.	0.0255
Hexagon side, in.	0.0146
Assembly diameter, in.	0.625
Gas volume, $in.^3$	0.763
Pressure drop, average, psi	0.104
Flow energy losses, watts	0.40
Axial thermal conduction, watts	1.78
Case conduction, watts	0.5

5.3.4 Alternate Configurations

Stacked wire screens and randomly packed wire (similar to steel wool) have been used for regenerators in conventional Stirling engines and both concepts were considered for use with the modified engine. The major advantage of the screen and wire concepts over the concept selected is lower conductive heat transfer in the axial direction; the major disadvantage appears to be a higher pressure drop for given heat transfer conditions.

Gas flow in the regenerator is laminar and, as a consequence, heat transfer to and from the gas is essentially by conduction through the gas stream. Heat transfer is improved by lowering the heat flux and decreasing the distance the heat must be transfered into the gas, which is equivalent to increasing the heat transfer surface area and decreasing the hydraulic diameter. Once these two parameters are fixed, the heat transfer is not improved as much as the pressure drop is increased by forcing the gas to follow a tortous path (such as through the stacked screens or random wire). Empirical data* indicate that, for the same hydraulic diameter and Reynolds number, the heat transfer to gas flowing through screens is 7 times that transferred to gas flowing in smooth tubes while the pressure drop per unit length is 14 times as great.

The major advantage of the screen and wire concepts (lower axial heat conduction) results in a smaller regenerator length which could, theoretically, compensate for the higher pressure drop per unit length. However, the axial conduction through the outer housing of the regenerator limits the extent to which the length can be reduced. Tubing must also be provided to connect the short regenerator to hot and cold chambers, so that the potential reduction in unswept volume cannot be fully realized.

5.3.5 Method of Analysis

The computer code described in Appendix M was used to define the optimum configuration for the basic type of regenerator specified in the reference design. The variables that effected the regenerator performance were the flow length, the volume, and the thermal effectiveness.

The optimization was performed by holding a selected length and effectiveness constant while the volume was changed over a sufficient range to identify a peak engine efficiency. The new length was selected and the above process repeated until an ideal length was identified. Figure 12 shows these results of this work.

The thermal effectiveness was found to have a small effect over the range considered (0.96 to 0.99); the optimum effectiveness was found to be about 0.98.

As in the case for the heater (Section 5.2.5), the assumptions were made that fully developed parabolic flow existed throughout the regenerator and that some average flow rate existed over the whole cycle. Use of the simplified analytical technique to determine the effect of regenerator performance on overall engine performance also required the assumption that incoming flow from both the hot and cold chambers be at a constant temperature through the cycle.

*Kays, William and London, A.L., "Compact Heat Exchangers", 2nd Ed. McGraw-Hill 1964, p. 182, 228 - 230

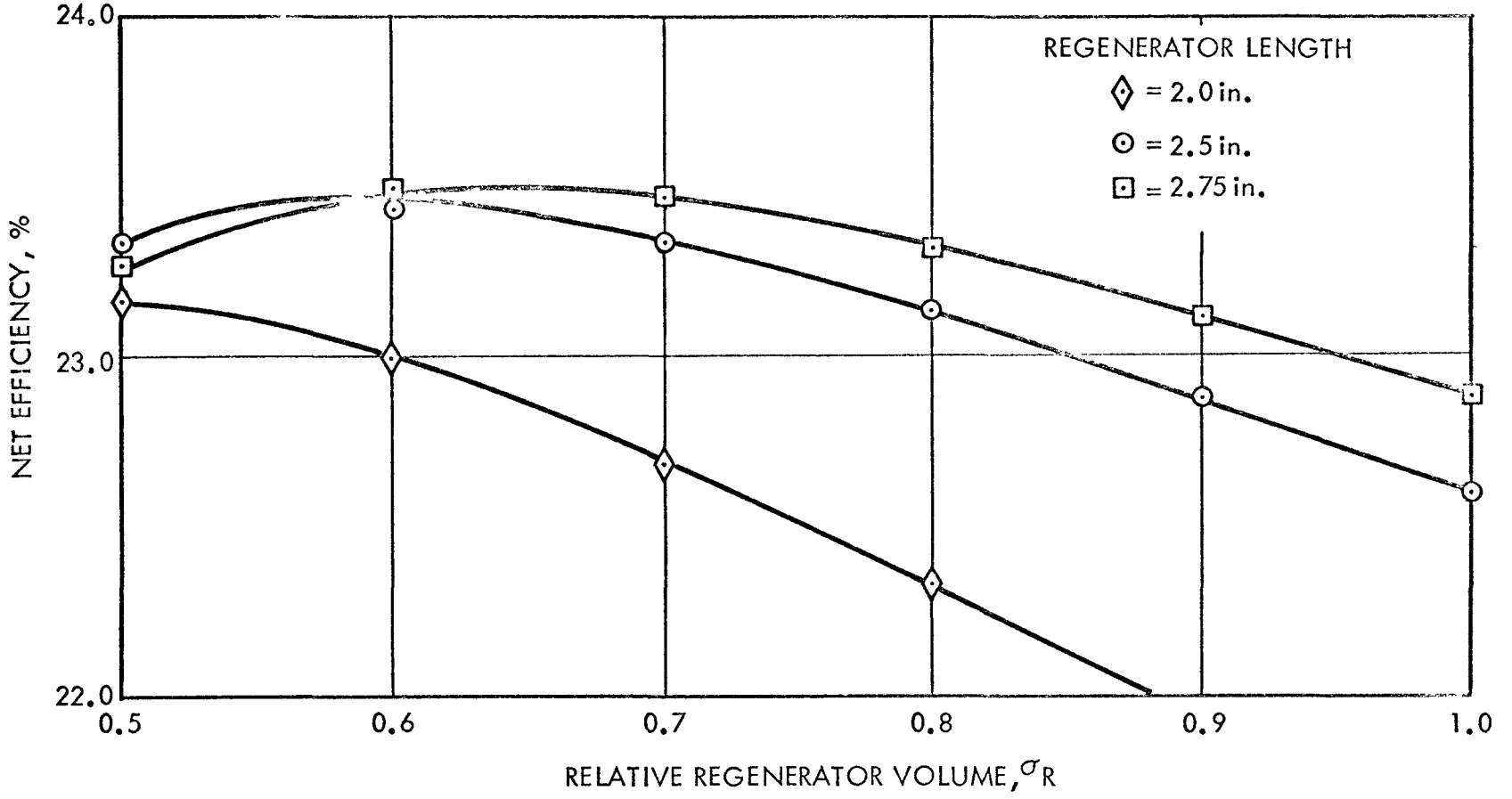

FIGURE 12. REGENERATOR TRADE-OFF STUDY

5.4 THERMAL INSULATION

5.4.1 Functions

High temperature insulation is provided to limit parasitic thermal losses from the high temperature regions of the engine and to limit the temperatures and heat fluxes at the outer surface of the power source to acceptable (physiological) levels.

5.4.2 Requirements

- Parasitic thermal losses* less than 2 watts.
- Operating life of up to 10 years without unacceptable degradation.
- Minimum practical volume.

5.4.3 Reference Design

The insulation was designed to satisfy the varying requirements imposed by: the radioisotope source and heater; the displacer cylinder walls; the regenerator walls; and the low temperature regions of the engine.

The surface area surrounding the source and heater is almost isothermal and the principal heat loss is outward. This area is covered with evacuated foil-type insulation which has the lowest effective thermal conductivity.

A significant axial thermal gradient will exist around the cylinder and regenerator walls. In this case, it is desirable not only to minimize thermal losses from the engine, but also to minimize the axial thermal heat flow. A radiation barrier-type insulation cannot be used in this area practically because this insulation has a relatively large effective thermal conductivity parallel to the barrier. The reference design, therefore, consists of a layer of isotropic insulation covered with a layer of evacuated foil-type of insulation. This combination prevents axial "short-circuiting" of thermal energy but provides for very low thermal losses to the environment. Separate cavities are provided at the top and bottom of the chamber to restrict direct heat flow down the displacer cylinder walls.

Surface temperatures at low temperature regions of the engine range from 100 to 250°F. Thermodynamic and physiological considerations make it undesirable to dissipate a large amount of heat from these surfaces to the body. Where appropriate, MIN-K or fibrous insulation is extended from adjacent areas to cover the low temperature regions of the engine. For some areas, however, a simple silastic covering provides sufficient insulation.

The insulation used to restrict axial heat flow will be MIN-K 1301 or a similar isotropic material. The reference insulation configuration involves a layer of MIN-K 1301 immediately surrounding the displacer piston and regenerator, with a layer of evacuated foil insulation covering both the heat source and the MIN-K. The characteristics of the insulation are as follows:

*Exclusive of thermal losses due to axial thermal conduction in the piston, cylinder and regenerator.

	MIN-K	Evacuated Foil
Thickness, in.	0.2	0.25
Approximate conductivity, Btu/hr-ft-°F	0.02	0.3×10^{-3}
Heat loss, watts	1.7	

5.4.4 Alternates Considered

An all MIN-K system was evaluated, but because of the high thermal conductivity (0.02 Btu/hr-ft-°F) of this material, the system volume was unacceptably large.

The disadvantage of evacuated foil insulation is the high thermal conductivity in the direction parallel to the foils. This is a serious limitation in insulation to be used around the displacer cylinder and regenerator where an axial temperature gradient exists. The optimum solution, from the standpoint of minimum heat loss, would be to arrange each foil to follow an isotherm. However, this alternate was not adopted because it appeared to involve extremely difficult fabrication and assembly problems.

Another method of limiting axial heat loss along the evacuated foil insulation is to assemble the insulation in a tapered configuration with each individual foil cylindrical in shape but of a different length (the inner foils are shortest and the outer foils are full length). In this way, axial conduction is restricted since foils that extend to the lower (cooler) portion of the cylinder are located in the outer (cooler) portion of the insulation at the upper end. The high temperature foils are shortest and do not contribute much to axial heat loss. The volume between the cylinder wall and the foils would be filled with an isotropic insulating material.

While the above thermal insulation scheme appears to have certain advantages over the type selected, it was conceived late in the design effort and therefore could not be fully analyzed.

5.4.5 Method of Analysis

As described in Section 5.4, the insulation system is comprised of two basic types of insulation. The basic type of insulation used in the high temperature region is a radiation barrier-type. The method used to determine the thickness of this type insulation required was the usual heat transfer analysis technique based on the relationship:

$$Q = KA\Delta T/L$$

The radiation barrier-type insulation has very low effective thermal conductivity in a direction perpendicular to the radiation shields but relatively high effective thermal conductivity in the direction parallel to the radiation barrier. In applications where thermal gradients exist in the surface of the insulated device, the radiation barrier-type of insulation performs relatively poorly. In such cases, it is desirable to utilize a material which has isotropic properties, even though the thermal conductivity may be significantly greater

than that of the radiation barrier-type. Since the displacer cylinder and regenerator in the reference design constitute an area with an axial surface temperature gradient, it is desirable to use an isotropic insulation.

The analysis performed to define the required thickness of isotropic insulation included the following assumptions:

- The radial heat flow is negligible
- The axial conduction of the radiation barrier insulation can be represented by effective thermal conductivity and thickness, and
- The radial and axial heat flow through the isotropic insulation can be treated separately.

A mathematical model for the radial heat flow through the isotropic insulation is derived in Appendix K. The heat flow through the isotropic insulation was determined as a function of thickness; Figure 13 shows the results of this analysis. As noted, the minimum heat transfer occurs for the isotropic insulation (MIN-K-1301) thickness of 1.1 inches but, since this thickness was not acceptable in consideration of other system parameters, a reference design value of 0.2 in. was selected.

5.5 CHECK VALVES

5.5.1 Functions

The check valves control the flow between the cold chamber and the high and low pressure reservoirs as required for efficient operation of the engine.

5.5.2 Requirements

- Reliable operation for 5×10^9 cycles
- Low flow energy dissipation
- Low accumulated back flow loss
- Synchronous operation with engine
- Small volume on engine side of valve
- Operation in 3 g field in any attitude.

5.5.3 Reference Design

The check valve design is illustrated in Figure 14. The same design is used for both the suction and exhaust valves. The check valve consists of a 3 mil-thick, flat aluminum disc which is operated, primarily, by the aerodynamic forces developed by the working fluid flowing in and out of the engine. In addition to the aerodynamic forces, a light (low spring constant) spring is provided to assist in valve closure and reduce the back flow to an acceptable level.

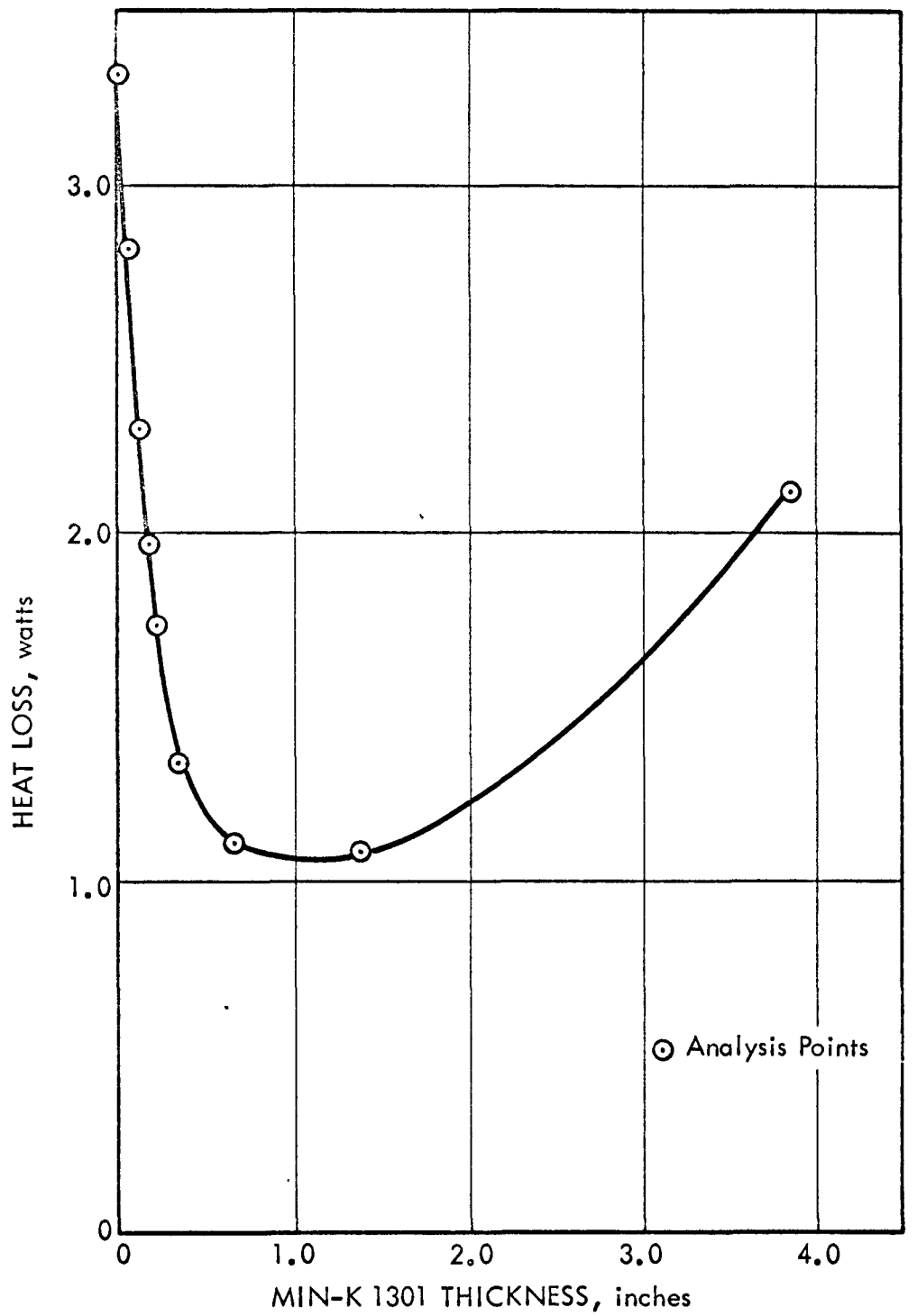

FIGURE 13. HEAT LOSS DOWN ISOTROPIC INSULATION

3.01-68-020

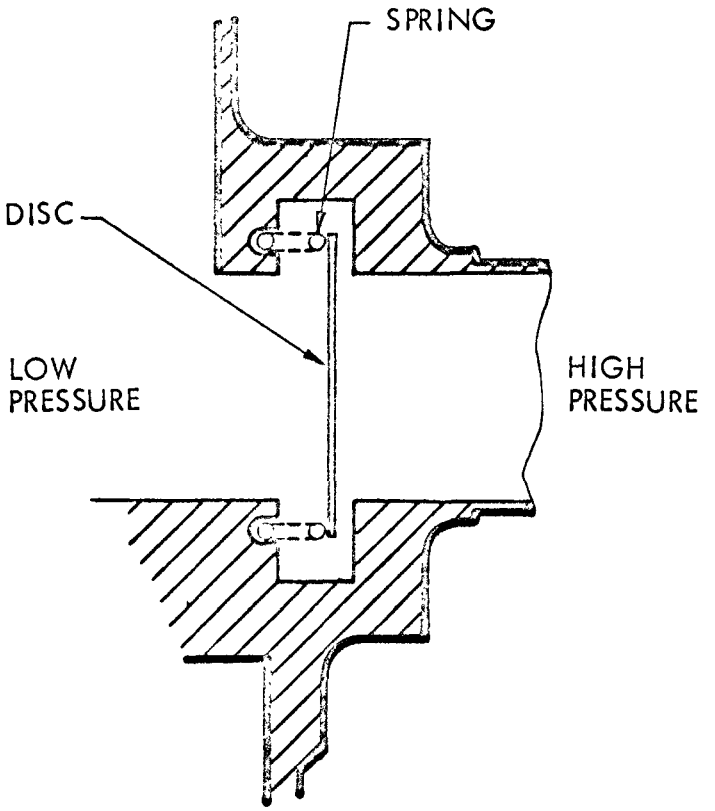

Note: Shown in open position

FIGURE 14. CHECK VALVE DESIGN

3.01-68-071

The operation of the valve can be described by following a cycle of the exhaust valve. As the working fluid pressure in the cold chamber reaches and exceeds that of the high pressure reservoir, first the static pressure and then the fluid dynamic forces act to open the valve. The flat disc first impacts on the closing spring and then on the opening stop, the latter being an inelastic collision. The valve disc continues to oscillate until all of the opening energy is dissipated.

As the displacer piston reaches bottom dead center, the engine is no longer able to support an outward flow of working fluid. As the flow approaches zero, the spring starts the valve disc moving towards the closed position. As the flow actually reaches zero and starts to reverse, fluid dynamic forces accelerate the closing of the valve.

A plot of the valve opening and flow rate for an operating cycle is shown in Figure 15. A 0.164 watt power loss due to flow pressure losses and a back flow of 0.012% were calculated for the reference design. Assuming 0.092 watts per percent back flow, each valve requires a total power of 0.164 watts.

Aluminum was selected as the disc material to minimize the weight and maximize the speed of operation; this material has sufficient strength for long term operation. The valve spring will be made of AM350 and will be lightly stressed to insure long lifetime. The valve body will be constructed of Hastelloy C, the same material as the displacer cylinder base into which the valves are integrated.

5.5.4 Alternates Considered

5.5.4.1 Disc Valve Without Spring

A valve design was considered which was essentially identical with the reference conceptual design except that no closing spring was provided. In this case, there was a clearly defined trade-off between the total valve opening and the back flow. The fluid losses decreased with increasing valve openings but the back flow also increased and soon became excessive. The back flow decreased to acceptable levels with decreasing valve opening but the fluid friction losses became excessive.

The valve without springs results in a system with less oscillation tendencies, as shown in Figure 16. The net overall power required for the springless valve is greater than that for a system including a spring because the back flow is considerably higher in the former. The premium placed on overall efficiency for this application resulted in the selection of the more complex but more efficient spring valve.

5.5.4.2 Mechanically Operated Valves

The basic engine cycle requires that both the inlet and exhaust valves open at mid-stroke and close at one (or the other) end-of-stroke positions. This assymetry eliminates consideration of a conventional mechanically-operated valve system. In addition, the optimum positions for valve opening will change slightly during the life of the engine and, as a consequence, even a highly sophisticated valve operating mechanism could not compete with the basic effectiveness of a pressure-operated valve.

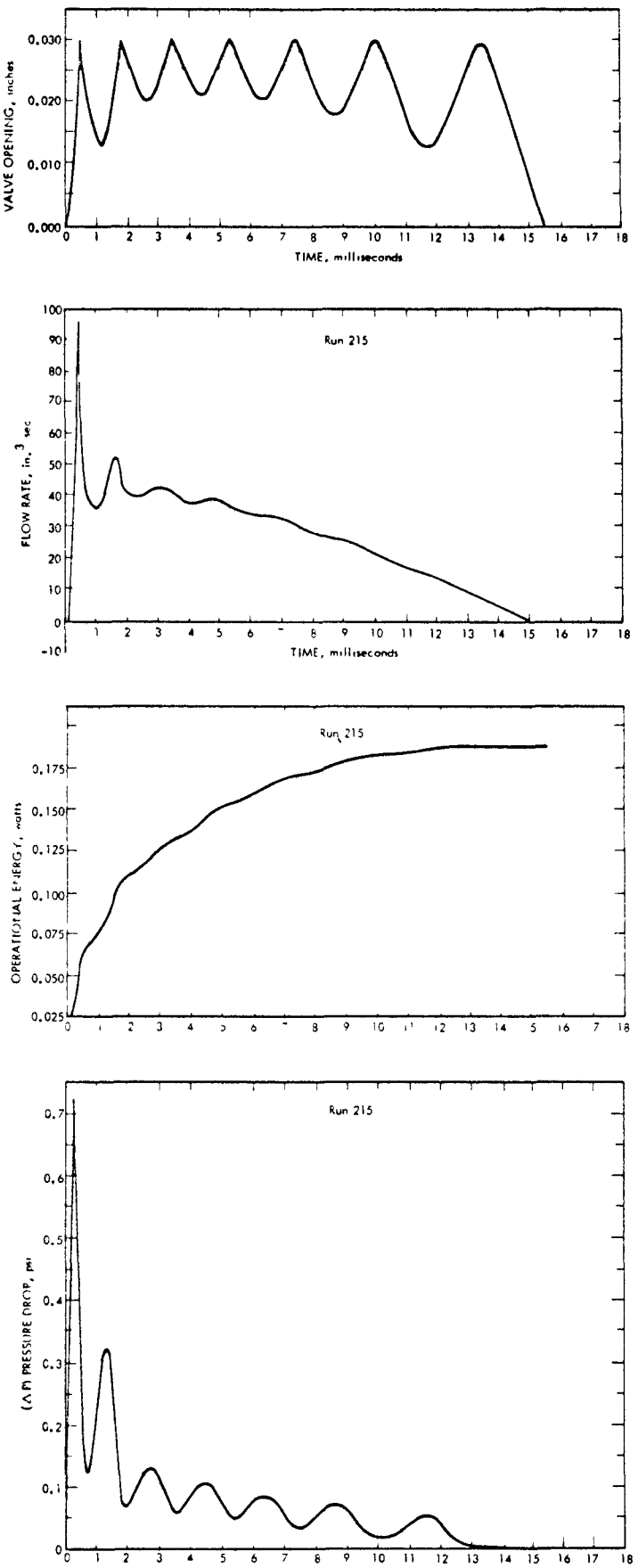

FIGURE 15. REFERENCE CHECK VALVE PERFORMANCE

301-68-072

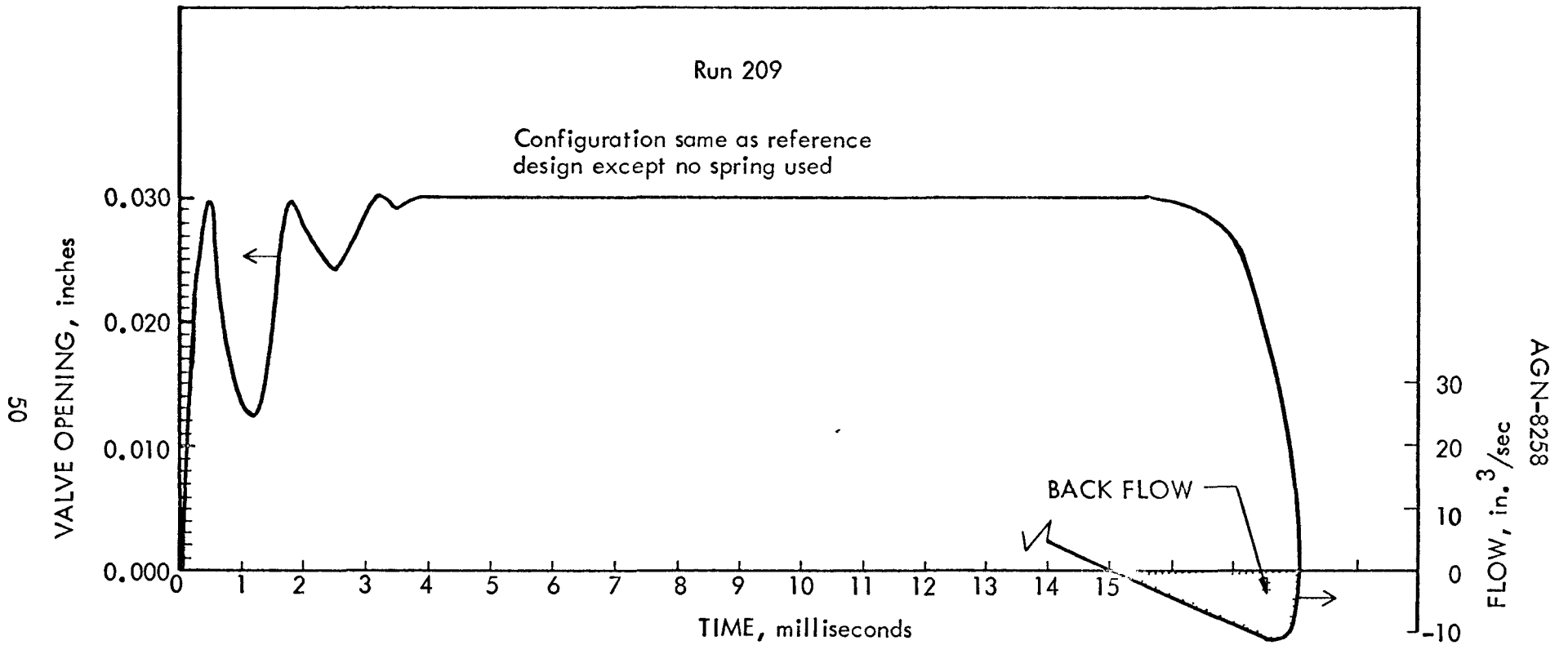

FIGURE 16. ALTERNATE CHECK VALVE DESIGN PERFORMANCE

In spite of these inherent difficulties, a type of mechanically operated valve was considered in some detail. This valve was designed to take advantage of both the positive closing action of the pure mechanically-operated valve and the performance advantage of the pressure-operated valve. The configuration of this valve is shown schematically in Figure 17. The valve opens in the same manner as the springless disc valve discussed above. As the displacer piston approaches bottom dead center, which is the desired valve closing position, it impacts with the sliding cup. Simultaneously,the cup is driven towards the disc and the disc is driven towards the seat on the cup. The result is minimum back flow and very efficient performance. The springs return the sliding cup to the full up position after the displacer piston has moved beyond bottom dead center. This design was not selected because of the inherent unreliability of the sliding seals required at the upper end of the sliding cup.

5.5.4.3 Alternate Configuration

Alternates to the flat disc were considered. A cup disc was considered to provide a flow pattern with better centering capability. A hollow sphere and tapered cup were considered but not selected because of their inherently higher weight. The experimental program (Appendix R) demonstrated that the flat disc performed satisfactorily and no further effort was expended on the evaluation of alternate disc configurations.

5.5.4.4 "Goose Caller"

A check valve with a configuration resembling that of a goose caller could be used in the engine. This type of valve is shown schematically in Figure 18. The valve is constructed of some type of resilient material which is opened by flow in one direction and closed by reverse pressure. The complex mechanisms involved in the operation of this type of valve prohibit even a rough evaluation of its operational characteristics, and its use would require an experimental development. Since the operating characteristics of this type valve were not determinable within the scope of the conceptual design effort, it was not selected for the reference design.

The performance of such a valve might be inferred from some of the analyses made on the reference design valve. Any of the disc valves which had large oscillations were found to have relatively large fluid losses. Since the goose caller may be in a continual state of oscillation during operation, large fluid flow losses are possible. However, the small back flow capability of this type of valve make an experimental evaluation desirable in future development efforts.

5.5.5 Method of Analysis

The relatively complex operational characteristics of the disc-type check valve, including the interaction with the Stirling engine, made the use of a computer highly desirable. Accordingly a computer program was written and the theoretical development is included in Appendix C.

The operation of the check valve is highly dependent on the operational characteristics of the Stirling engine and the reservoirs. For the purposes of the check valve evaluation, the engine was assumed to be ideal and the reservoirs were assumed to be constant pressure

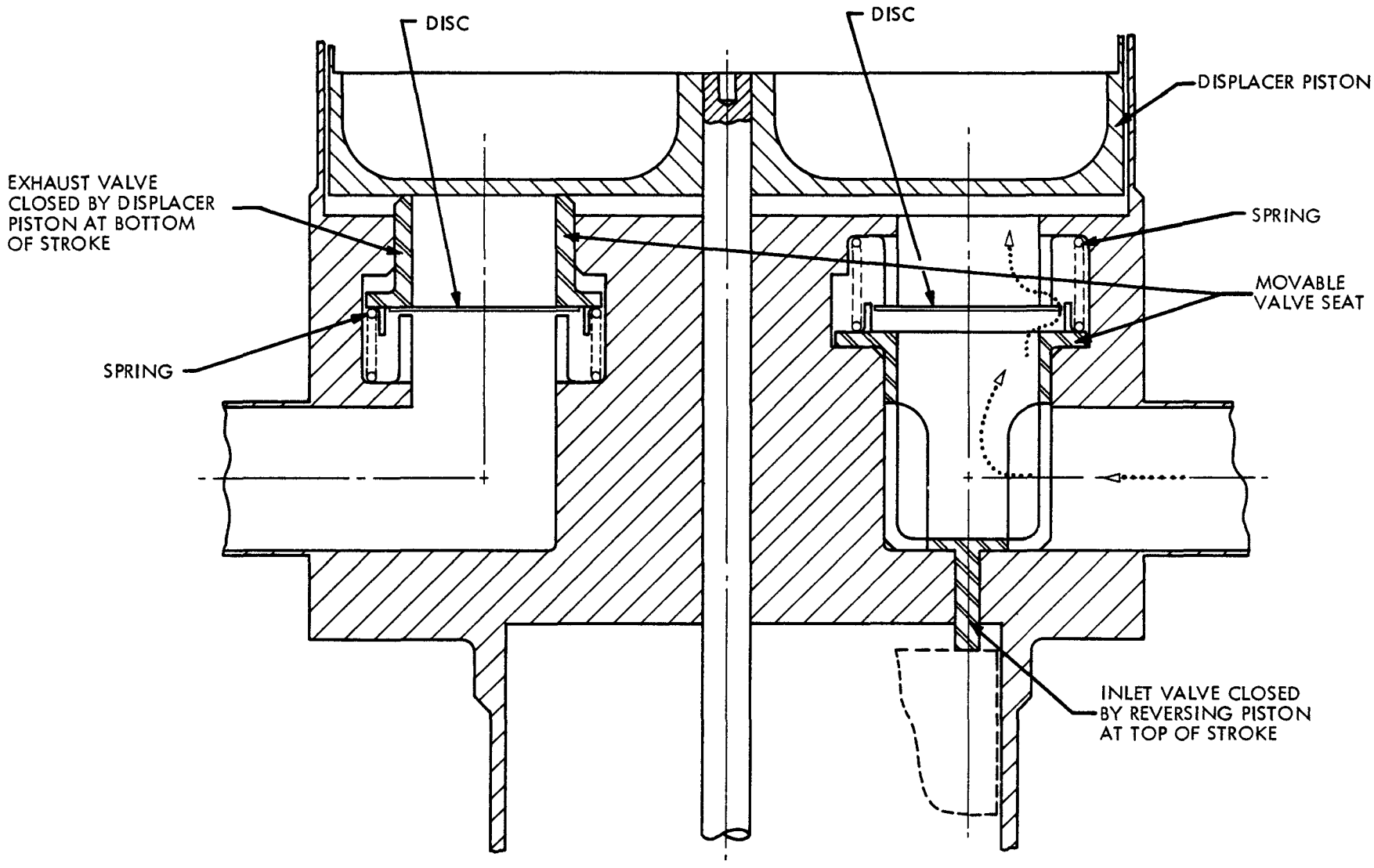

FIGURE 17. MECHANICALLY OPERATED CHECK VALVES

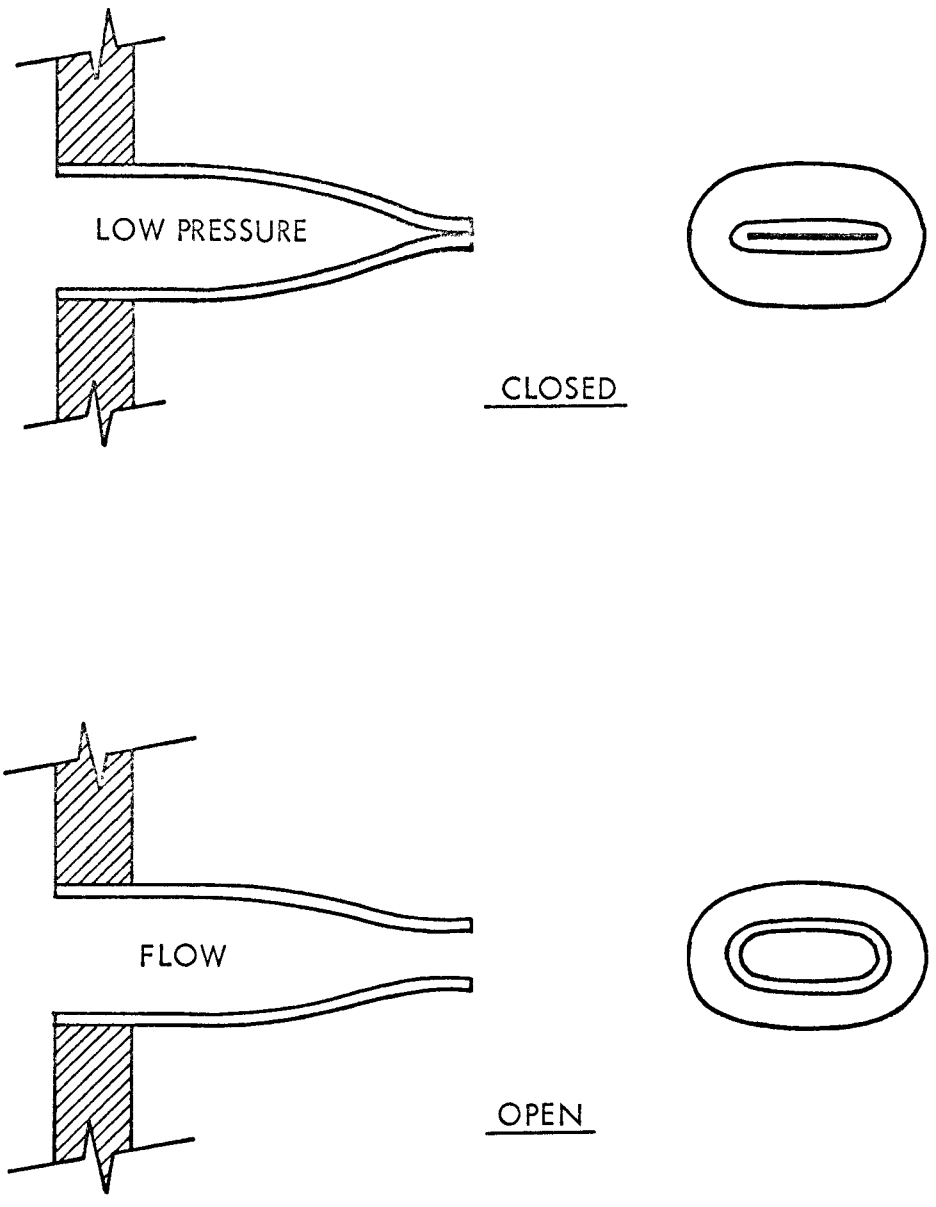

FIGURE 18. "GOOSE CALLER" - TYPE CHECK VALVE

3.01-68-025

devices. Flow equations were derived for conditions on the upstream side of the disc. Friction losses and a velocity head loss at the periphery of the disc were formulated for flow in the forward direction. Friction losses and a velocity head at the center of the disc were formulated for flow in the reverse direction. The resulting pressure distributions were converted into forces on the disc and the additional force due to spring action, if any, was added. A stepwise calculation of the motion of the disc was performed and the elapsed time, disc position, flow rate, accumulated flow pressure drop, and accumulated energy loss were calculated at each iteration. Impact at the end of each stroke was assumed to be inelastic with a specified fractional energy loss. Input data included the size of the inlet port, the disc size and density, the spring constant, the position at which the spring was engaged, the maximum opening, and the engine parameters.

The results of this calculation for the reference design are included in Appendix C. The final selection of a check valve was based on the consideration of both flow losses and back flow. The flow losses are printed out directly in watts and the back flow in cubic inches per cycle. The rational evaluation of valve performance requires the conversion of the back flow into effective power loss.

The gross effect of back flow on output power was not expected to be linear; therefore it was necessary to use the Schmidt-type analysis to evaluate this parameter. The computer code was modified slightly to obtain the desired influence coefficient for back flow.

5.6 REVERSING PISTON

5.6.1 Function

The reversing piston controls the reciprocating motion of the displacer piston, establishes the oscillatory frequency, and provides a method of energy addition to compensate for frictional and aerodynamic losses in the engine.

5.6.2 Requirements

- Provide the force necessary to reverse the direction of motion of the reciprocating mass consisting of the displacer and reversing pistons and the hollow connecting rod (45 grams).
- Establish reciprocating motion of the system.
- Establish the speed of the engine.
- Involve minimum energy loss to the system.
- Provide a stroke limiting action.
- Provide one surface for alignment for the reciprocating system. (The second surface is at the lower edge of the displacer piston.)
- Involve minimum practical weight and volume.

5.6.3 Reference Design

The reversing system consists of a piston, cylinder, two gas volume enclosures, and two pneumatic dash pots. The system is, essentially, a pneumatic spring which causes the reciprocating assembly to oscillate at the natural frequency of the combination. In addition, the reversing system, when combined with the displacer piston, provides a method for adding energy to the reciprocating mass to compensate for the frictional and aerodynamic losses of the Stirling engine.

The reversing piston and connecting rod assembly are fabricated from Hastelloy C. The outer sliding surfaces are coated with solid state lubricant to minimize friction and wear. The reversing piston has a nominal diameter and length of 0.5 in. It is hollow, with an "H" cross section to reduce weight and to serve as the female part of the two dash pots. The rod connecting the reversing piston to the displacer piston is an integral assembly with the reversing piston.

The reversing cylinder and gas enclosure are also fabricated as an integral assembly from Hastelloy C and mounted directly to the displacer piston end plate. The cylinder has a nominal diameter of 0.5 in. and is 2 in. long with a wall thickness of 0.030 in. The cylinder volume and enclosure volume establish the reversing piston pressure ratio and the natural frequency of the system.

For the reference design, the pressure ratio selected for the reversing system is identical with that of the displacer system. This pressure ratio was selected so that the leakage across the shaft seal from the reversing cylinder to the displacer cold chamber is minimized and the energy addition requirement is always positive. The volumes of the upper and lower gas enclosures are 1.875 and 2.49 $in.^3$, respectively. The side walls of the enclosure are 0.030 in.-thick and the web and bottom plate are 0.050 in.-thick.

The energy input is directly dependent on the cyclic pressure profile of the Stirling engine and the diameter of the rod connecting the displacer and reversing pistons. The reference design incorporates a 0.215 in. diameter rod, which results in a 0.9 watt input energy. This energy input is sufficient to accommodate expected frictional and aerodynamic losses to assure operation at full stroke. The excess energy will be absorbed by the dash pots at either end of the reversing system. The upper male portion of the dash pot is combined with the reversing system-to-cold chamber shaft seal and the lower male portion is an integral part of the bottom enclosure end cap.

5.6.4 Alternates Considered

5.6.4.1 Discussion

Rather late in the conceptual design effort, the refined calculations revealed that energy is "automatically" added to the system because of the configuration of the shaft connecting the displacer and reversing piston. Prior to this time, some effort had been devoted to the development of other techniques for adding energy to the reversing piston to compensate for the

frictional and aerodynamic losses. Although the current evaluation indicates that pneumatic energy addition to the reversing piston will not be necessary, a description of the results of the work on energy addition is included to complete the documentation of contract activity.

The first two functions specified for the reversing piston (establishing the reciprocating motion and speed of the system) could be satisfied by a variety of concepts, including the use of a simple mechanical spring mass system. In fact, if a simple, practical method of energy addition could be developed, mechanical spring oscillation would probably result in a more compact engine configuration than the reference design.

Since it is undesirable to use other than the pneumatic power generated by the engine for make-up power for the reciprocating system, the combination of the reversing and energy addition functions is a natural approach. All of the alternates presented in this section except the last reflect the desirability of combining these functions and the energy addition function is fulfilled by utilizing a portion of the pneumatic output of the engine.

5.6.4.2 Pneumatic Piston with External Energy Addition

The reference design consists of a pneumatic reversing system and an energy addition system to make up for mechanical and fluid friction losses that acts directly through the piston connecting rod. An alternate which was considered incorporated the reference concept for the reversing mechanism along with an external means of adding energy. The required energy was added through a porting system which transferred pneumatic energy from the low and high pressure reservoirs. A schematic diagram of a reversing piston with this sort of porting is shown in Figure 19 along with a pressure-volume diagram for one of the two chambers. As the reversing piston oscillates, each of the two chambers is ported to the appropriate reservoir. The result is that, in addition to the regular oscillatory motion, a small amount of work, as indicated by the shaded area of the pressure-volume diagram, is added during each cycle.

The location of the ports is variable; in fact, it is desirable to locate them about a quarter-stroke from the mid-point so that a small decrease in stroke would not cause an engine failure. The vertical lines on the pressure-volume diagram indicate the irreversible mixing of reversing piston gas and reservoir gas and,hence,are a measure of inefficiency. Figure 20 shows the relationship between port location, efficiency, and work per cycle. As in the reference design, there is a relationship between the various parameters such as piston area,enclosed volume,stroke, etc. which must be maintained to provide the desired speed.

5.6.4.3 Low Pressure Reversing Piston

This alternate design is similar to that described in the preceeding section. The primary operational difference is that the porting is arranged so that the reversing piston volumes are opened to one or the other reservoir for a large portion of the stroke. Starting down from mid-stroke, the gas in the lower chamber is adiabatically compressed until the port is opened to the high pressure reservoir. From this point to the end of stroke and return, the

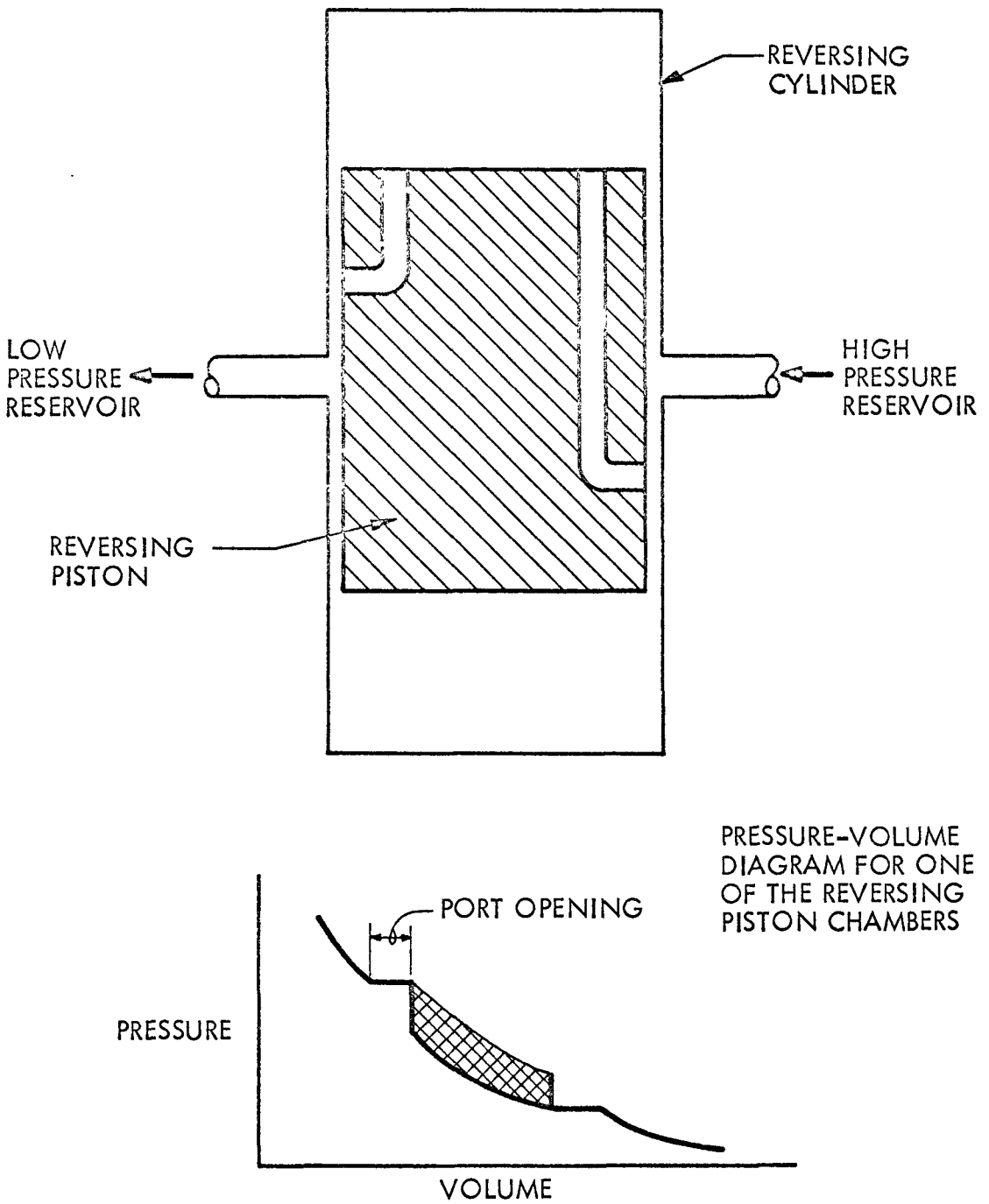

3.01-63-026

FIGURE 19. REVERSING PISTON WITH EXTERNAL ENERGY ADDITION

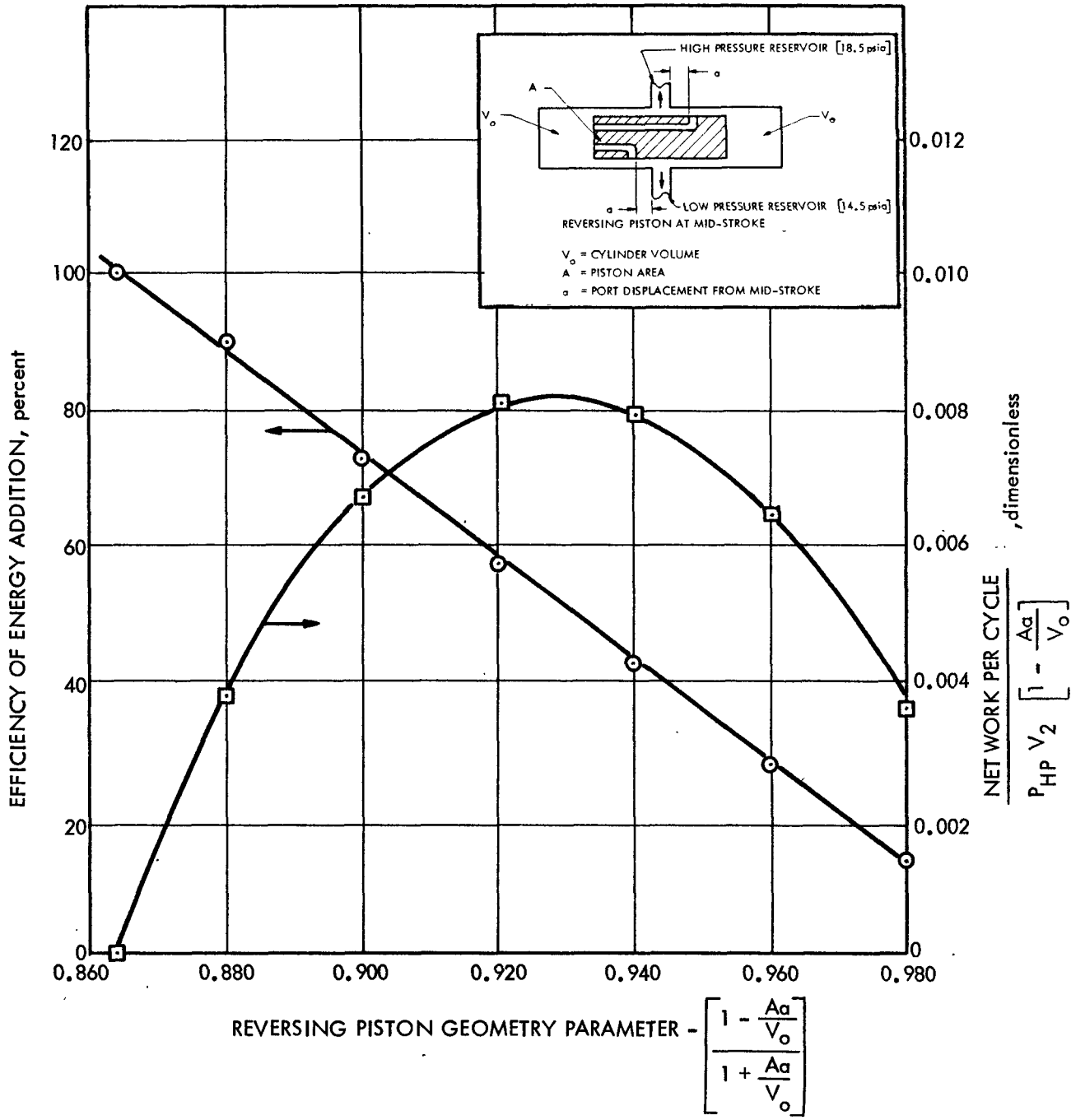

FIGURE 20. REVERSING PISTON PERFORMANCE

16.1-67-683

lower volume is ported to the high pressure reservoir. The gas is then adiabatically expanded until the low pressure reservoir port opens. The port remains open to the low pressure reservoir until the reciprocating mass reaches the end of stroke and returns. Thermodynamically, the difference between this system and that described earlier is that the reversing piston works against the reservoir gas pressure rather than the adiabatic compression (or expansion) of the gas contained within the reversing cylinder. As before, the porting can be arranged to add an incremental amount of work per cycle.

In general, the piston areas required for this concept are larger than with adiabatic compression because of the lower pressure involved. However, no residual volume other than the swept volume is required. The pressure difference between the upper reversing chamber and cold chamber is minimized, thereby decreasing the flow across the interconnecting shaft seal.

One disadvantage is that the reservoirs must be designed to accept the relatively large volumes of gas from the reversing piston volumes without significant pressure variations.

5.6.4.4 Spring Driven System

The realization that an increment of energy was added to the reciprocating mass during each cycle when a shaft is installed between the displacer and reversing piston led to the consideration of some interesting variations. It can be easily determined that the same energy addition is obtained if a single-sided reversing piston is used (that is, the reversing piston is a simple shaft extending down from the displacer piston). Accordingly, a workable driving system could consist of a spring system to provide the basic oscillatory motion and a shaft extending down into a small volume connected to one of the reservoirs. This system is shown schematically in Figure 21.

The possible advantage of such a concept is that the overall length of the engine might be reduced although no layout was made of this concept. The disadvantage is the unreliability of the springs, which must operate approximately 5×10^9 cycles at relatively high loads if the 10 year life objective is to be attained.

5.6.5 Method of Analysis

The motion of the piston assembly was calculated from a force balance on the system. Reversing forces result from compression and expansion of gas in the reversing system, which occurs nearly adiabatically. The total mass of the reciprocating system, reversing piston area, reversing cylinder volumes and the average pressure in the reversing cylinder define the natural frequency at which the pistons oscillate. The derivation of this relationship, given in Appendix D, shows that piston motion is very nearly sinusoidal.

The total amount of energy transfered to the reciprocating pistons over a full cycle is independent of the pressures in the reversing cylinder since these are symmetrical over the complete cycle. The energy transfered is a function only of the pressure profile in the displacer cylinder and the connecting shaft area. A simplified method of calculating the power input, based on a linearized pressure profile, is also described in Appendix D. The use of this mechanism to drive the reversing system was verified using the analog techniques described in Section 6.4.

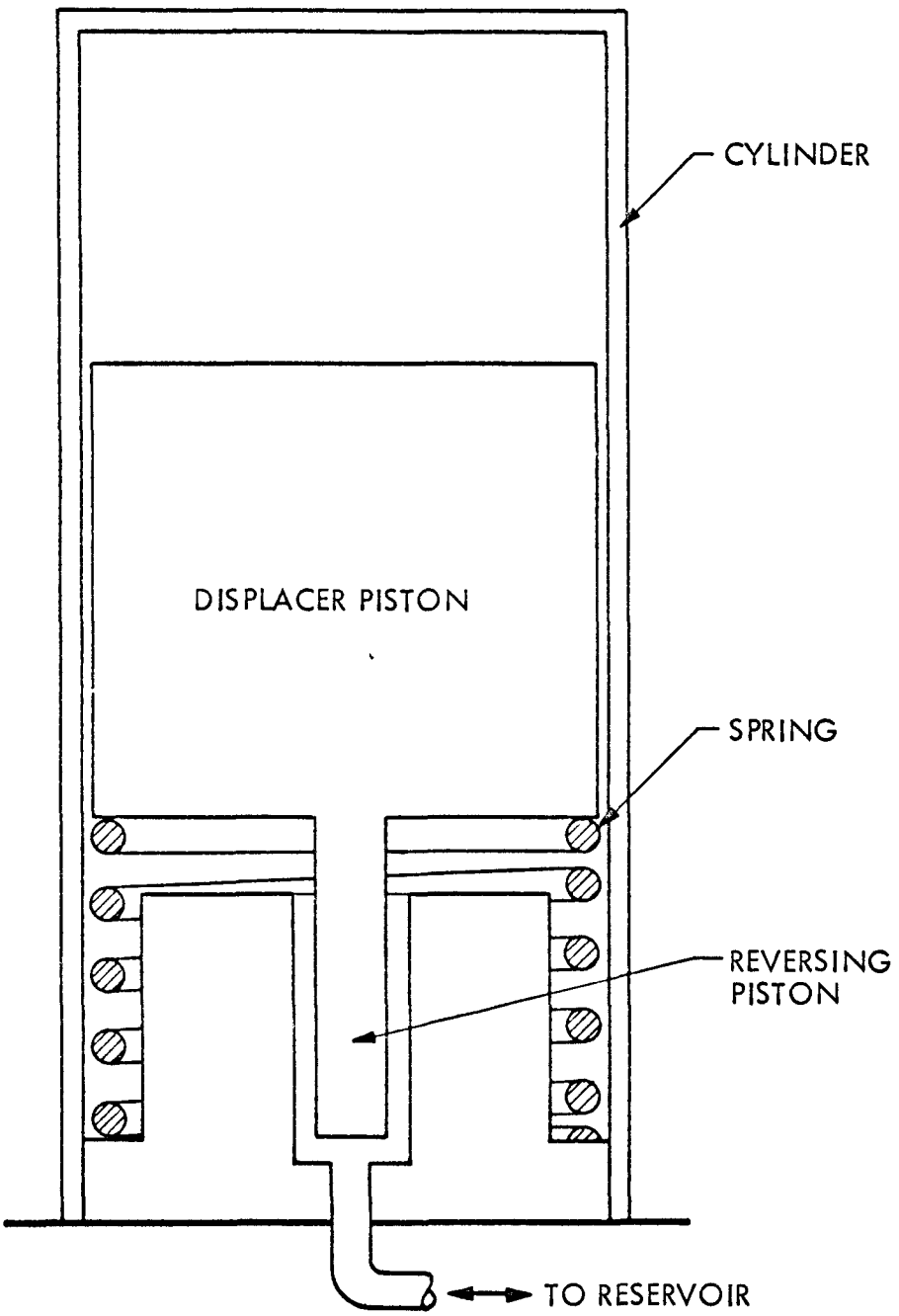

FIGURE 21. SPRING-DRIVEN REVERSING SYSTEM

301-68-027

5.7 SEALS AND BEARINGS

5.7.1 Function

The function of the seals and bearings is to limit the gas flow past displacer and reversing pistons and through the port where the piston rod penetrates the displacer cylinder bottom end plate, to provide low-friction sliding surfaces, and to maintain the alignment of the reciprocating system.

5.7.2 Requirements

- Reduce friction on all sliding surfaces to less than 0.1 lb.
- Control leakage past the displacer piston to less than 4% of the displaced volume.
- Control leakage past the reversing piston and shaft seal to the minimum practical amount.
- Operate satisfactorily for 10 years (1.5×10^{10} in. of reciprocating system travel).
- Maintain alignment of the oscillating system.

5.7.3 Reference Design

The reference design incorporates a split ring expansion seal (piston ring) at the bottom edge of the displacer piston. This ring will limit gas leakage past the piston and will also serve as one of two alignment points for the reciprocating system. The inside surface of the displacer cylinder will be coated with a mixture of MoS_2-graphite-silver-boron nitride in a sodium silicate binder. Care will be exercised to assure that proper clearances are maintained at operating (steady-state) temperatures.

The seal on the connecting shaft is long to minimize the leakage between the displacer and reversing piston chamber. The wear must be limited to approximately 0.5 to 1.0 mil to minimize power lost due to gas leakage. This seal is designed to float in the plane perpendicular to the axis of the shaft and is not involved in the maintenance of the alignment of the reciprocating system. The alignment is controlled by the physical relationship between the displacer piston ring and the reversing piston.

A review of the literature (see Bibliography in Appendix E) was performed to identify data which would be helpful in developing an estimate of wear on the seals. No data were available in the literature reviewed except for some information concerning internal combustion engines used in automobiles. These data, along with comparative data for the modified Stirling cycle engine, are presented in Table 3.

TABLE 3 – COMPARISON OF MODIFIED STIRLING ENGINE AND INTERNAL COMBUSTION ENGINE

	Stirling Engine	Internal Combustion Engine (200 hp)
Lifetime	10 years	100,000 miles
Distance traveled per cycle, in.	3	12
Total lifetime distance, in.	1.50×10^{10}	0.36×10^{10}
Maximum side loads, lb	0-2.6	0-800
Lubrication	Solid bonded	Oil splash
Temperature, ^{o}F	100-600	1000-1500
Dynamic mass, lb	0.1	5
Piston velocity, ft/min	250	2600
Expected wear, mils	1/2-1	15-20

As indicated in the Table, the lifetime distance of the linear engine is only 4.5 times greater than that of the internal combustion engine while the load is at least 400 times smaller, the dynamic mass is 50 times smaller, the temperature is from 3 to 10 times lower, and the velocity is 10 times smaller. In consideration of these factors,it seems reasonable that wear during the 10 year lifetime of the modified Stirling engine can be held to 1/2 to 1 mils by careful engineering.

5.7.4 Alternates Considered

Bonded solid-film lubrication is a relatively new area of technology. The literature (see Bibliography in Appendix E) discusses many apparently acceptable approaches to the application of this concept to the modified Stirling engine but the final selection of the optimum solid-film lubricant can be made only after experimental testing at operating conditions. Several experimental techniques are discussed in the literature which appear to be adaptable for use in this testing program.

A labyrinth seal was investigated as an alternate to the reference shaft seal. However, the optimum established by the limit of the analysis was a smooth long bearing as shown in Figure 8.

A relatively long, small annulus gap was considered as an alternate to the split ring expansion seal on the displacer piston. The most serious disadvantage of this concept was the mechanical pumping of heat energy. During the cycle, the piston absorbs heat at the top dead center (TDC) position and then discharges it by conduction through the gas directly to the cylinder wall at the bottom dead center (BDC) position. The amount of heat lost in this manner is excessive with the "long gap" seal concept. In addition, the nonlinear differential expansion between the piston and cylinder wall would result in difficult design problems.

A two-point suspension system involving the reversing piston and shaft seal (with the displacer piston floating) was considered as an alternate alignment system. This concept was not selected because the bearing loads on the shaft seal were excessive because of the short distance between the alignment surfaces when the reversing piston is TDC. Potential binding of the displacer piston is another disadvantage of this concept.

5.7.5 Method of Analysis

An analysis was performed to estimate the maximum frictional load possible and to consider possible non-standard conditions (See Appendix E). This analysis indicated that:

- If the center of gravity were eccentric to the central axis by as much as 0.010 inch, the normal force necessary to counteract this moment is 0.0091 lb.
- If the reversing piston were cocked at T.D.C. or B.D.C, the calculated maximum normal force is 2.6 lb.
- A total radial wear of 1 mil can be tolerated in the displacer piston area and 1/2 mil in the reversing piston area.

5.8 PUMPING CHAMBERS AND RESERVOIRS

5.8.1 Function

The pumping chambers form the interface between the engine gas and the pumping fluid used to transmit power to the blood pump. These chambers convert the pressure level and pressure ratio most advantageous for engine operation to those required by the blood pump and also automatically adjust the output pressure for changes in atmospheric pressure. An additional function of the reservoirs in the reference design is to reduce the pressure variations seen by the pumping fluid to acceptable levels.

5.8.2 Requirements

- Reliable operation for 5×10^8 cycles.
- Fluid volume pumping capacity up to 4.6 cubic in. per stroke.
- Provide average systole pressures of 3.8 psi (left ventricle) and 1.25 psi (right ventricle) and the capability, with proper control valves, for diastole pressures in the range from 0 - 0.2 psi.
- Provide compensation for changes in atmospheric pressure.
- Provide an impermeable barrier between the engine working fluid and pumping fluid.
- Reduction of pressure pertubations and variations to acceptable levels.

5.8.3 Reference Design

5.8.3.1 Left Ventricle Pumping Chamber

The design of the left ventricle pumping chamber is shown in Figure 6.

The configuration and operation of the pumping chamber is basically as follows. The chamber contains a movable plate to which three sets of bellows are attached. One set of bellows contains the pumping fluid that operates directly on the pumping membrane of the blood pump. A second set, located on the opposite side of the movable plate, contains a fluid at atmospheric pressure. The third set is located on both sides of the plate and contains the engine gas. By alternately valving high pressure and low pressure gas to the two sides of the plate, pulsating power is delivered to the pumping fluid and, consequently, to the blood pump.

The purpose of the fluid at atmospheric pressure is to compensate for gross changes in atmospheric pressure so that atrial pressure can be held to within a few mm Hg of atmospheric. The fluid is supplied from a flexible sack in either the thoracic or abdominal cavity. The effective area of the pumping fluid bellows is reduced by the area of the small internal bellows, which is evacuated. The area ratio between the atmospheric pressure bellows and the pumping fluid bellows in the pumping chamber serving the left ventricle is selected to result in an equilibrium pressure in the pumping fluid of about 90 mm Hg. During systole, the pressure in the gas bellows increases the pumping fluid pressure to about 190 mm Hg and during diastole the pressure is reduced to about atmospheric pressure.

The gas bellows are all identical. The volume external to the bellows but inside the pumping chamber is utilized as part of the high pressure reservoir system. Since all of the bellows are of the identical type and size, the pressure external on the bellows does not effect the force balance on the pressure plate.

The configuration selected for the pumping chamber was influenced by the characteristics of the bellows. Bellows subjected to high internal pressures are subject to a phenomenon known as bellows squirm. This squirm phenomenon is roughly equivalent to that encountered in compressively loaded columns. Theoretically, the critical pressure above which squirm may occur can be determined by the following relationship:

$$P_{crit} = \frac{2\pi K_a}{L}$$

where:

P_{crit} = maximum critical pressure
K_a = axial spring constant
L = bellows length

One of the leading manufacturers of bellows recommends that the operating internal pressure be less than 30% that of the theoretical critical pressure. Since a stringent limitation is imposed on the bellows spring constant, it is necessary to avoid any situation where a net internal pressure exists. On the other hand, it is necessary that the bellows withstand a large number of

operating and pressure cycles and yet have a relatively low spring constant. (A large spring constant would cause a large pressure change in the pumping fluid as the amount of fluid in the chamber changed, even though the reservoir pressures were held constant).

A computer code was written to predict the performance of the pumping chamber when connected to an ideal Stirling engine and, especially, to evaluate the effect of bellows spring constant. It was necessary to simulate the action of an artificial heart to provide a reasonably accurate prediction of the performance of the pumping chamber. Since the effects of pressure oscillations and non-uniform pressure profile are not known, the interpretation of the results of the computer program are somewhat subjective; however, the computer studies did indicate that the maximum allowable combined spring constant of all bellows was approximately 15 lb/in. As a consequence, it was necessary to select a bellows material with a high strength-to-modulus of elasticity ratio and with a good fatigue strength. Several titanium alloys were identified which satisfy these criteria; two which were evaluated were Ti-6Al-4V and Ti-5Al-2.5Sn. The former was selected for the reference design, primarily because of its higher tensile strength (165 kpsi as compared to 116 kpsi for the latter) even though its fatigue strength was slightly lower (68 kpsi as compared with 74 kpsi). A total spring constant of less than 15 lb/in was achieved with the titanium bellows.

The chamber walls and pressure plate will be fabricated from titanium to minimize welding problems and weight.

5.8.3.2 Right Ventricle Pumping Chamber

The design of right ventricle pumping chamber is essentially identical with that of the left ventricle chamber except for the changes required by the different systole pressure and the different supplied gas pressure (see Section 5.12). For a fixed working fluid bellows size, the gas bellows effective area is proportional to the gas pressure. The pumping pressure for the right ventricle chamber is approximately 1/3 and the gas pressure is approximately 1/2 that of the left ventricle pumping chamber. Consequently, the bellows have an effective area approximately 2/3 that used in the left ventricle pumping chamber.

5.8.3.3 Gas Reservoirs

The engine cycle requires that high pressure gas be exhausted during approximately 1/4 of the cycle, that low pressure gas be admitted during approximately 1/4 of the cycle, and that the engine be passive (as far as gas movement is concerned) for approximately 1/2 of the cycle. The pulsating gas movement associated with the cycle will result in undesirabily large pressure pulsations unless gas reservoirs are provided in both the high- and low-pressure systems. In addition, the operation of the control valve at the termination of systole and diastole will also result in undersirably large pressure surges if reservoirs are not provided.

The selection of the reservoir sizes is only subjective at this time because the magnitude of acceptable pressure pertubations and lags have not been determined or specified. An evaluation of the magnitude of the pressure surges

was performed with a computer code; the results of this study indicate that the minimum reservoir size in both the high and low pressure system is approximately 2 cubic inches (the capacity of the lines between the engine and the reservoirs can be considered as part of the reservoir volume).

As discussed in Section 5.8.3.1, a high pressure is required external to all bellows in the pumping chambers. The volume provided in the chamber to satisfy this requirement will serve as the high pressure reservoir. The volume available in both the left and right pumping chambers exceeds the required 2 $in.^3$. A low pressure reservoir of approximately 1-1/4 $in.^3$ is required to supplement the 0.75 $in.^3$ volume of the various gas lines; this reservoir will be fabricated from titanium and will be a right cylinder, 0.815 in. in diameter and 2.2 in. long.

5.8.4 Alternate Configurations Considered

5.8.4.1 Concentric Bellows Pumping Chamber

In this concept, the four gas bellows in the reference design are replaced with two bellows which are located concentrically around both the pumping fluid bellows and the reference pressure bellows. The average diameter required for this bellows exceeds that of the large pumping bellows by only 7%; hence small bellows spans (the radial distance from bellows inner to outer radius) are required for both of these bellows. This relatively small span requires a considerably larger number of convolutions and a correspondingly greater compressed height to provide the relatively low spring constants desired for this application. While the resulting right cylindrical shape is desirable, the additional volume resulting from the larger bellows nesting height was undesirably large.

5.8.4.2 Combined Pumping Chamber

The combination of the right and left ventricle pumping functions into a single assembly was considered. The resulting design, shown schematically in Figure 22, is quite similar to the reference design. As indicated in this Figure both pumping fluid bellows are centrally located within the pumping chamber and the gas bellows and the reference pressure bellows are located around the periphery of the pumping fluid bellows.

The problems associated with this concept are: the left and right ventricles have to be pumped asynchronously; systole and diastole have to be of equal length; and, additional control is required to regulate the pressure in each ventricle. The latter would probably consist of two lines interconnecting the right and left ventricle pumping fluid systems. These lines would contain check valves which would open at predetermined pressures. A closer examination of the actual requirements may necessitate the use of a more complicated control system.

The use of a combined pumping chamber may prove desirable for the ultimate system; however, it was not selected for the reference design because of the many unknowns involved with the acceptability of asynchronous pumping and equal systole and diastole durations, and with the basic requirements of the associated control system.

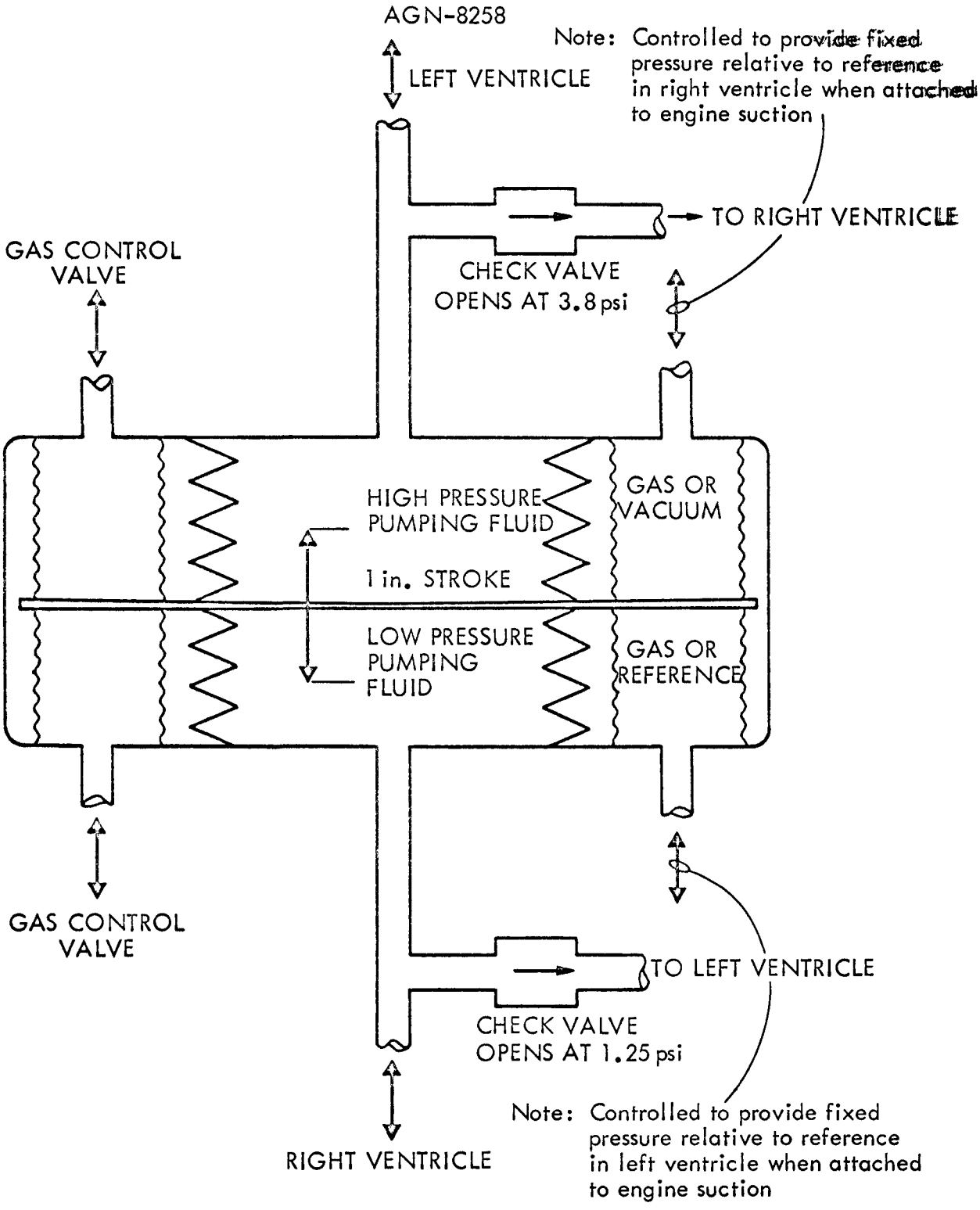

3.01-68-078

FIGURE 22. DUAL ACTING PUMPING CHAMBER

5.8.4.3 Differential Pumping Chamber

The application of the pneumatic power output of the engine to the pressurization of the pumping fluid could be accomplished by a simple differential bellows. However, other means for compensating for atmospheric pressure changes and a more elaborate gas reservoir system would be required for use with such a concept.

In this concept, the pumping chamber consists of two bellows; one containing the pumping fluid and a second containing the engine working fluid. As shown in Figure 23, both bellows are encased in an outer, pressurized housing. A separate pumping chamber is required for the systemic and pulmonary circulation systems. The area ratio between the two bellows in each pumping chamber must be adjusted to the pressure output of the engine. In addition, the Stirling engine must be designed to provide a pressure ratio nearly equal to that required by the systemic system. As in the reference design, the spring constant of the bellows is relatively critical if significant pressure drops are to be avoided in the pumping fluid profile.

The main advantages of this concept are its basic simplicity and reliability. The overriding disadvantages are: the restrictions imposed on engine pressure ratio; the inefficiency of pulmonary system pumping due to the high pressure ratio required by the systemic system; the more elaborate reservoir support system required; and, the requirement for compensating for atmospheric pressure changes by other, more complex techniques.

5.8.4.4 Dual Piston Pumping Chamber

This concept, shown in Figure 24, eliminates the requirement for bellows in the pumping chamber. In this design, the pumping chamber consists of two pistons joined by a connecting rod. The lower piston is driven up and down by alternately connecting the high pressure reservoir to the upper and lower chamber. The pumping fluid is located above the upper piston and a reference atmospheric pressure is maintained below the upper piston. Relatively good seals are required on the upper piston and the connecting rod.

In this concept, the same fluid would be used as the pumping fluid and as the atmospheric reference pressure fluid to eliminate undesirable effects of the leakage past the upper piston. A shaft seal is provided between the two pistons on the interconnecting shaft. It is assumed that the small amount of helium leakage past this seal would be diffused through either the atmospheric pressure bladder or the heart membrane and dissipated by the body. In the event further evaluation showed that the helium leakage was unacceptable, a bellows seal would be provided to replace the shaft seal. Since different pressures are required for the systemic and pulmonary systems, it is desirable to use individual pumping chambers for each.

The main feature of this system is that it has, at most, one bellows and could probably be designed without any. The main disadvantages are that it requires additional sliding seals and, because of this, the entire configuration involving the two pistons would be difficult to integrate into the engine package.

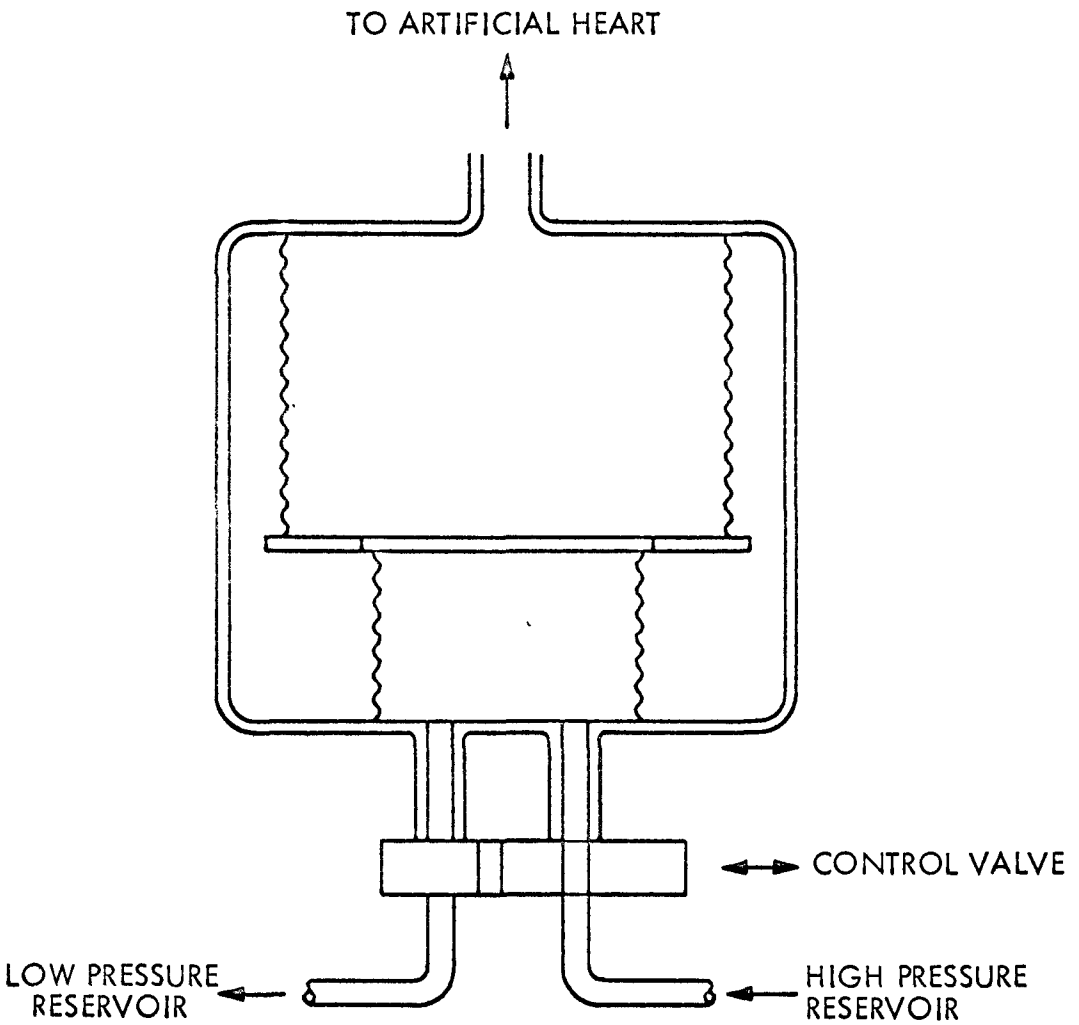

FIGURE 23. DIFFERENTIAL PUMPING CHAMBER

301-68-079

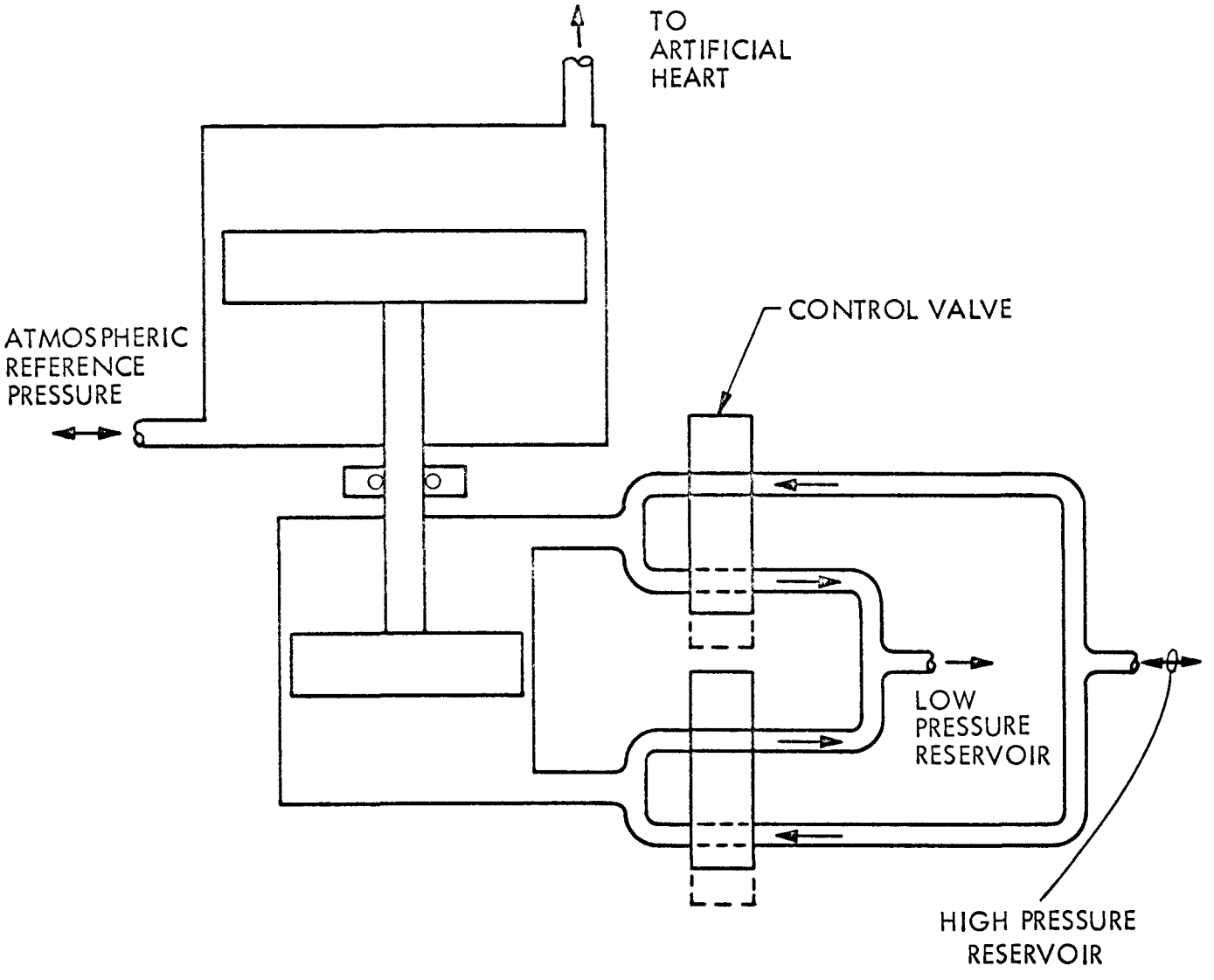

FIGURE 24. DUAL PISTON PUMPING CHAMBER

3.01-68-080

5.8.4.5 Alternate Reservoirs

The reference design for the modified Stirling engine for circulatory support presented herein does not require elaborate pneumatic reservoirs. However, for a considerable portion of the evolution of the design, more elaborate pressure reservoirs were required to support both the pumping chamber and reversing piston operations. Accordingly, design effort was expended on "constant pressure" reservoirs. Though unlikely, continued development of the engine could create a demand for more elaborate reservoirs; hence the results of the work will be retained in the files for possible future use.

5.8.5 Method of Analysis

5.8.5.1 Engine - Pumping Chamber Coupling Code

The main area ratio for the reference pumping chambers can be established by a relatively simple static balance on the pressure plate. Beyond this elementry static balance, it was desirable to determine both the dynamic interaction between the pressure chamber and an idealized Schmidt engine and the effect of the combined spring constants of the bellows. A computer code was written to accomplish these objectives.

The computer code assumes a frictionless Schmidt Stirling engine with a fixed swept volume ratio. Further assumptions include perfect check valves, infinitely fast acting control valves, and constant temperature in all parts of the system except the engine. The flow rate of pumping fluid in and out of the pumping chamber was assumed to follow the following relationships:

$$\text{Flow Out} = C_{out} (P_{FF} - P_o)$$
$$\text{Flow in} = C_{in} (P_{oo} - P_{FF})$$

where P_{FF} is the pressure of the pumping fluid. C_{out}, C_{in}, P_o, and P_{oo} were specified constants for each computer run.

The heart beat was subdivided into 156 intervals. In addition to those indicated above, the following input variables were provided: maximum temperature, minimum temperature, average pressure, area ratios, mean pumping fluid pressure, engine displacement, low and high pressure reservoir volumes, spring constants, stroke, and relative length of systole and diastole. The output information included pumping chamber gas pressure, pumping fluid pressure, reservoir pressures, and volume of pumping fluid pumped to the heart.

Figure 25 shows a plot of a typical run using the computer code.

5.8.5.2 Pumping Chamber Bellows

The analytical method used to evaluate bellows was essentially that presented in "Nomograms and Charts for Welded Diaphragm Metal Bellows Design", by S. T. Zierak and P. Juderslehen,Design News, October 26, 1966.

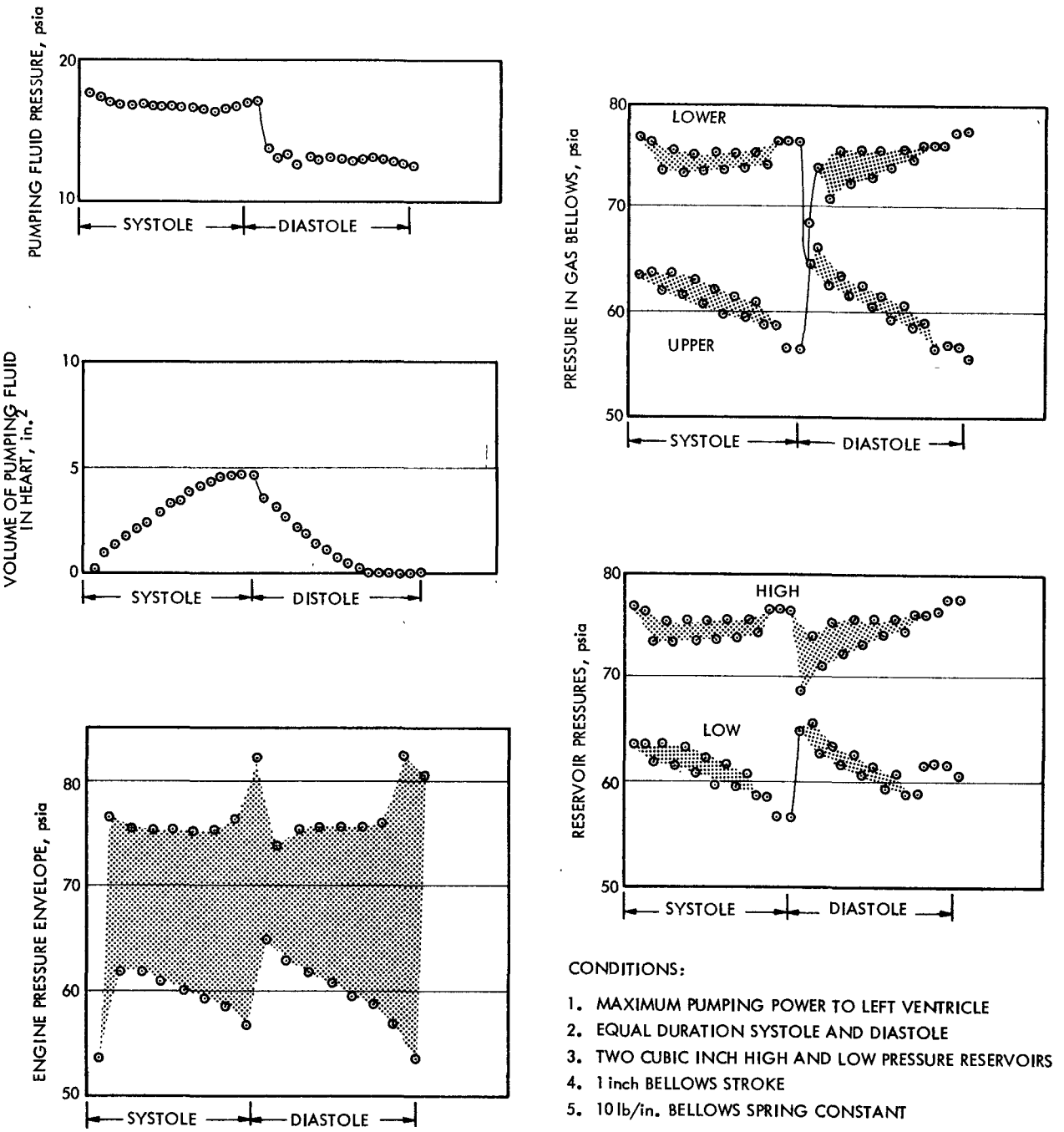

CONDITIONS:

1. MAXIMUM PUMPING POWER TO LEFT VENTRICLE
2. EQUAL DURATION SYSTOLE AND DIASTOLE
3. TWO CUBIC INCH HIGH AND LOW PRESSURE RESERVOIRS
4. 1 inch BELLOWS STROKE
5. 10 lb/in. BELLOWS SPRING CONSTANT

FIGURE 25. INTERACTION BETWEEN ENGINE AND PUMPING CHAMBER

301-68-081

The limitations imposed to prevent bellows squirm were developed from a theoretical derivation and catalog data. The theoretical derivation was taken from "Analyses of Stresses in Bellows, Part I, Design Criteria and Test Results Appendix A", NAA-SR-4527, October 1964. Applying the derived theoretical limits to the catalog data of the "Metal Bellows Corporation", it was found that the theoretical limitation should be reduced by a factor of approximately 3.5, or:

$$P_{critical} = \frac{1}{3.5}\left[\frac{2\pi K_a}{L}\right]$$

where:

K_a = axial spring constant

L = length

$P_{critical}$ = critical internal pressure

Since the spring constant is of such importance in the design of the pumping chamber, it is desirable to determine the minimum spring constant as a function of the critical stress parameter. Figure 26 shows the value of spring constant as a function of span for a fixed maximum pressure stress. In general, the design point for the bellows used in the reference pumping chamber was at the minimum of this curve.

Externally pressurized bellows result in a tensile stress on the ID of each convolution. If this tensile stress is not accommodated by the compressive deflection strength, a stress concentration factor of two must be applied. In the reference pumping chamber design, all of the bellows except the vacuum bellows are compressed during assembly to eliminate the tensile stress on the ID.

5.9 HEAT REJECTION SYSTEM

5.9.1 Function

The function of the heat rejection system is to transport the waste heat from the engine working fluid to the blood stream.

5.9.2 Requirements

- Dissipation of the waste heat under the parameters listed in Table 4.
- Maximum blood temperature, 43°C
- Maximum working fluid return temperature, 115°F
- Maximum heat flux to tissue, 0.1 watts/cm^2

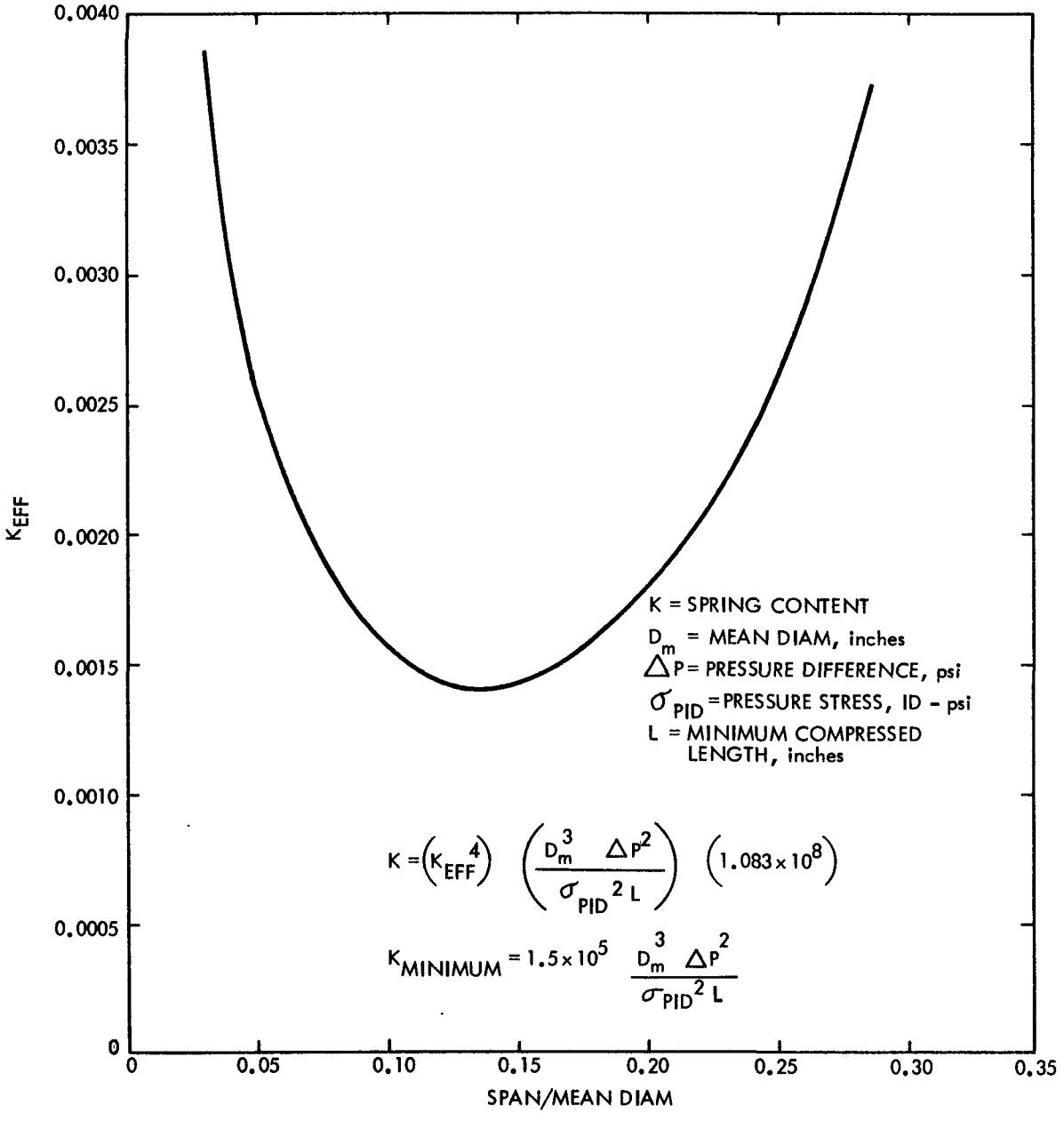

FIGURE 26. SPRING CONSTANT FOR INTERNALLY PRESSURIZED BELLOWS

TABLE 4 – ASSUMED PARAMETERS - HEAT REJECTION SYSTEM

		Condition I	Condition II
1.	Heat rejection, watts(t)	25	30
2.	Pumping fluid flow rate, 1/min	24	12 systole 6 diastole
3.	Average blood flow rate*, 1/min	7.2	2.4
4.	Inlet blood temperature, °C	39	39
5.	Systole/diastole duration	1:1	1:2
6.	Relative blood flow during systole	1	1
7.	Relative blood flow during 70% diastole (forward and reverse - average)	0.2	0.2
8.	Relative blood flow during 30% diastole	0	0
9.	Aorta diameter, cm	2.5	2.5
10.	Maximum fluid-to-blood heat exchanger length, cm	17	17

*The aorta section passing through the abdominal cavity which is assumed to carry 60% of the heart volumetric output.

5.9.3 Reference Design

The establishment of firm design criteria for the heat rejection system is dependent on many physiological limitations. While, to a large extent, the whole artificial heart engine is affected by the physiological interfaces, the design of the heat rejection system is more dependent on the final selection of these interface parameters. Since these parameters are not well established, it was necessary to assume a range of values (see Table 4). The design of the heat rejection system is wholly dependent on these assumed values; accordingly, the design will be modified to the extent necessary as the physiological interfaces become better established.

The reference heat rejection system consists of two heat exchangers. One heat exchanger provides for the removal of the waste heat from the low pressure engine working fluid by transfer to the left ventricle pumping fluid. A large portion of this waste heat is transfered directly to the blood stream in the second heat exchanger; the remaining portion is dissipated to the blood through the flexible membrane of the artificial heart. This heat exchanger is a one inch long, gas-to-liquid heat exchanger which is located within the engine assembly. The exchanger is a concentric tube-type with the pumping fluid passing through a 3/4 in. diameter central tube and the helium engine

working fluid passing through a 0.010 in. annulus. The normal working fluid inlet and outlet temperatures are 250°F and 115°F, respectively; the nominal pumping fluid temperature is 110°F. The gas-to-liquid heat exchanger will be fabricated from the same titanium alloy as the pumping chambers.

The second heat exchanger is a 6.6 in.-long, concentric tube, liquid-to-blood heat exchanger. The main criteria for the design of this heat exchanger are: the blood temperature shall not exceed 43°C; and, that portion of the heat exchanger through which the blood passes shall be easily integrated and connected into the aorta and shall not result in any undue turbulence or contain any stagnant volumes. The design selected to satisfy these criteria is a concentric tube heat exchanger. The central tube is a straight stainless steel tube, of the same size as the aorta, which will replace a section of the aorta and be attached to the lower aorta in accordance with the best existing technique. The pumping fluid will be routed through a 0.15 inch annulus surrounding the tube. The critical parameter determining the size of this liquid-to-blood heat exchanger is the film temperature rise when the blood is flowing at the lowest rate. In this case, the quantity of waste heat to be dissipated is greatest and the heat transfer coefficient is the lowest.

At the low blood flow rate, the bulk of the flow occurs during systole; however, the flow is never stagnant for any significant period of time since the pulsating nature of the heart causes small forward and backward secondary pulses, even during diastole. For purposes of sizing the pumping fluid-to-blood heat exchanger, a blood flow rate profile equivalent to that indicated in Table 4 was assumed. It should be emphasized that because the bulk temperature rise in the blood is small compared to the film drops, it is immaterial which way the blood flows.

In order to develop a complete analysis of this heat exchanger, it is necessary to include the transport and thermal properties of blood. While viscosity and density data for whole blood are readily available, no appropriate data on the values of heat capacity and thermal conductivity could be found. Accordingly, blood was assumed to be water-like, except for the viscosity. The blood flow through a 1 in. tube at the low flow rates was found to be laminar. Using established laminar dimensionless relationships, a heat transfer coefficient of approximately 75 Btu/hr-ft^2-°F was obtained. This value is based on the assumption of established flow; however, since the blood flow rate is varying continuously, the estimated heat transfer coefficient is probably lower than will actually be experienced. The controlling criterion on the fluid side is the pressure drop; an annulus with a radial gap of 0.15 in. is specified to maintain the pressure drop at less than 0.1 psi at the high flow rate. In addition to the heat transfer occurring in the pumping fluid-to-blood heat exchanger, a fraction of the waste heat will be transfered to the blood in the artificial heart. The extent of this heat dissipation will depend on the detailed design of the artificial heart. For purposes of the reference design, it was assumed that the heart was constructed of a 30 mil silicone rubber sheet and had total area of 18 square inches. In addition, it was assumed that the geometry was such that the heat transfer coefficient was approximately that achieved in the pumping fluid-to-blood heat exchanger. Approximately 25% of the waste heat is dissipated in the heart at the low flow conditions.

5.9.4 Alternates Considered

5.9.4.1 Total Heat Rejection to the Artificial Heart

This concept is similar to the reference design except that the pumping fluid-to-blood heat exchanger in the abdominal aorta is eliminated and the total heat dissipation occurs in the artificial heart. The acceptability of this alternate is dependent on the final detailed design of the artificial heart to be used. This concept is attractive from the standpoint of minimizing the surgical implant procedures but a coordinated effort between the engine and artificial heart developers will be required to assure adequate heat transfer capability across the pumping membrane. Providing this capability could affect the basic design of the artificial heart and could increase its size.

For purpose of this study, it was desirable to make the engine compatible with a variety of pneumatically-actuated artificial hearts and to minimize the number of interfaces; hence, this alternate was not selected. For the final design, this alternate should be reconsidered because of the associated potentially simpler implant procedures.

5.9.4.2 Separate Fluid to Abdominal Aorta

This concept requires the incorporation of an additional fluid system into the pumping chamber. The regular pumping fluid lines to the heart would no longer contain the gas-to-pumping fluid and the pumping fluid-to-blood heat exchangers, but would be routed directly to the heart. The new fluid system would require additional bellows on both sides of the pressure plate, and would contain the two heat exchangers used in the reference design. The new heat transfer fluid would be pumped in one direction during systole and the reverse direction during diastole. The waste heat would be transfered from the engine working fluid to this fluid and then to the blood in a manner similar to that used in the reference system. Lower flow rates would be used so that some modification of the heat exchanger design would be required.

This alternate has the advantages of separating the thermal heat dissipation function from the pumping fluid and permits a lower pumping fluid operating temperature. The disadvantage is that a more complex and larger left ventricle pumping chamber is required. In addition, the length of the pumping fluid-to-blood heat exchanger capable of handling the whole heat load under all conditions could exceed the length available in the abdominal aorta. Accordingly, it is likely that additional heat dissipation equipment would have to be provided to dissipate all of the waste heat.

5.9.4.3 Heat Dissipation by Reference Pressure Fluid

This concept utilizes the reference pressure fluid to dissipate the waste heat. Since this system already exists for other reasons, it could be utilized in a manner similar to that described in the preceding section. The advantages and disadvantages are essentially identical with those given for "separate fluid to abdominal aorta" system.

5.9.5 Method of Analysis

The heat rejection system consists of two conventional heat exchangers and interconnecting tubing. The only unusual feature of the system is that the pumping fluid-to-blood heat exchanger must have a blood transport system of the straight-through design of a fixed size and that strict limitations are placed on the maximum blood temperature.

Conventional analyses were used since the system is composed of conventional heat exchange equipment; detailed analyses are presented in Appendix H. Several assumptions were made in the analyses:

- The thermal properties of average whole blood were not available and, for this analysis, blood was assumed to have the properties of water at the same temperature except for density and viscosity (which data were available in the literature).

- The pumping fluid was assumed to have properties similar to water; since the pumping fluid will affect both the engine and artificial heart, it is desirable to delay the final selection until the artificial heart is more clearly defined. (The selection of a particular fluid may require slight modification in the heat exchanger design, but any changes are expected to be minor.)

5.10 RADIOISOTOPE FUEL AND SHIELD

5.10.1 Function

The function of the radioisotope is to provide the heat energy to the engine. The radiation shield is provided to reduce the dose rate to a maximum of 50 mrem/hr on the outside surface of the packaged system.

5.10.2 Requirements

Source

- 10 year operating life at high temperature without excessive power decay.
- 35 watts of thermal power.
- Minimum practical size.
- Minimum biological shield volumes and weights.

Shield

- Sufficient mass and density for the absorption of γ radiation.
- Sufficient neutron absorption.
- Sufficient mechanical strength to contain helium released during life of the fuel.

5.10.3 Reference Fuel System

The reference fuel system for this application is 238-PuN (plutonium nitride), pressed into ring-type pellets (approximately 88% of theoretical density) and double-encapsulated in a weldable tungsten-base alloy and Hastelloy C.

Because of the similarity of chemistry and metallurgy, the nitride of plutonium, PuN, is assumed to be similar to UN and to have the following properties:

- Good thermal stability at temperatures well above those of this appplication
- Power density slightly higher than PuO_2
- Thermal conductivity considerably better than PuO_2
- Compatibility with iron, stainless steel, refractory metals and alloys of tungsten, tantalum and molybdenum, but questionable compatibility with nickel and chromium

- More pyrophoric than PuO_2

These assumptions conform with the BMI data available from the literature (see bibliography in Appendix I).

The reference conceptual fuel system for the implantable power source is described in Table 5. The dimensions selected are near-optimum for the minimum dose rate at the power system surface, minimum power system weight and minimum power system size (see Appendix J).

TABLE 5 — REFERENCE CONCEPTUAL FUEL SYSTEM CHARACTERISTICS

Thermal power, BOL, watts	35
Radioisotope	Pu-238
Isotopic purity, %	> 99
Other radioactive contaminants	nil
Fuel compound	PuN
Chemical purity, %	> 99
Fuel form	hollow-core cylindrical pellets
Fuel density, % of theoretical	88
Pellet height, in.	0.350
Pellet diameter, outside, in.	0.742
Pellet diameter, inside, in.	0.500
Number of pellets	4
Number of fueled containers	1
Encapsulation:	
Inner (primary) pressure resistant container	W-26 Re
Closure technique	TIG weld
Wall thickness, in.	0.170
End-cap thickness, in.	0.170
Outer (atmospheric) protection container	Hastelloy C
Closure technique	electron beam weld
Wall thickness, in.	0.030
End-cap thickness, in.	0.030

The fuel capsule has an internal volume of 0.605 $in.^3$; the crystalline fuel volume is 0.288 $in.^3$, leaving a void volume of 0.317 $in.^3$. The capsule is designed to contain an internal pressure that corresponds to 25% helium gas release during the life of the fuel.

The specified source material is not available today, but will be available in the future. The production of 238-PuN from Am-241 results in a material with effectively no low-Z material impurities and, primarily, only low energy gammas (the only neutrons produced are by spontaneous fission as explained in Appendix I). Use of the PuN fuel results in the system with minimum weight and volume.

The reference design provides for a 0.170 in. thickness of W-25% Re material to attenuate the gammas and to serve as a pressure vessel to contain the released helium. The neutron shield is a 1-1/8 in.-thick layer of borated polyethylene to minimize the weight (See Appendix J).

5.10.4 Alternate Fuels Considered

The three radioisotopes that were suggested by the AEC as potential fuels for implantable power supplies were considered as alternates. General characteristics of these fuels are listed in Table 6.

TABLE 6 — CANDIDATE RADIOISOTOPES FOR IMPLANTABLE POWER SOURCE FUEL

Radioisotope	$T_{\frac{1}{2}}$, yr	Radiations/Energy, Mev	Comments
Pm-147	2.62	β^-/0.225 max.	Pm-146 impurity
Tm-171	1.9	β^-/0.097 max.	Tm-170 impurity
Pu-238	89.6	α/5.5	SF and (α,n) neutrons

An evaluation of each of the candidate radioisotopes is presented in the following sections; a summary of the evaluation is shown in Table 7.

5.10.4.1 Promethium-147

The Promethium-147 currently available (separated from fission product wastes) contains approximately 0.25 ppm of Pm-146. This impurity results in a dose rate of about 1000 mr/hr at the power system surface for a shield-encapsulated fuel system weighing 2000 gms. If re-irradiation in a highly thermalized flux can be used to selectively burn out the Pm-146 and reduce the abundance of this isotope by a factor of ten, the dose rate could be reduced to about 100 mr/hr for the same system weight. This still represents a dangerously high dose rate. Thus, consideration of the high dose rate and the relatively short half-life of Pm-147 fuel resulted in the elimination of this radioisotope from consideration for this application. However, if it becomes possible to reduce the Pm-146 abundance by much more than a factor of 10, with an acceptable increase in fuel cost, Pm-147 should be reconsidered.

5.10.4.2 Thulium-171

Thulium-171 can be produced by:

- Irradiation of natural erbium, followed by chemical separation of thulium, or by,
- Irradiation of enriched erbium, followed by chemical separation of thulium, or by,
- Irradiation of natural thulium (Tm-169) in a high flux to obtain a high ratio of Tm-171-to-Tm-170.

It has been estimated that thulium irradiation would yield the highest Tm-171-to-Tm-170 ratio, but that this product would contain about 2% Tm-170, and cost $1300 per watt. Radiation data in ORNL-3576 show that the Tm-170 content must be reduced to about 1 ppm to reduce the dose rate to acceptable levels. This is not possible with any published production method.

The half-life of Tm-171 is so short that a refueling operation would be necessary every year, even if the fuel power at the beginning of each fuel implant were the maximum allowable. Any additional heat from Tm-170 (which produces over 6 times as much power per unit weight of fuel as Tm-171) would thus be unacceptable, even if the dose rate were not a serious problem.

In consideration of the above, Tm-171 was eliminated from consideration in this application until a reasonable cost production method is developed by which the Tm-171-to-Tm-170 ratio is increased to about 10^6 at the time of implant. Even then, the relatively short half-life of Tm-171 would place it in an unfavorable position, unless the supply of longer-lived candidates was insufficient to meet demand.

5.10.4.3 Plutonium-238

Pu-238 is the only potential candidate that could be implanted for 10 yr without refueling.

5.10.4.4 Alternate Shields Investigated

Alternate neutron shielding materials considered were, boron nitride, lithium hydride and unborated polyethylene. The boron nitride results in a very heavy system and lithium hydride involves many materials handling problems and only a 10% volume reduction. Small gains are achievable from the use of borated polyethylene compared with normal polyethylene and the former was selected as the reference neutron shielding material.

Gamma shield configurations investigated included right cylindrical arrangements with various length-to-diameter ratios. The length was selected to best fit the regenerator and engine configuration.

A spherical fuel cavity would result in the minimum weight but would involve an undesirable extension of the length of the engine assembly. However,

this configuration does produce the most efficient fuel/gamma/neutron shield arrangement and re-examination will probably be warranted as more information becomes available on the permissible shapes to fit the body cavity.

TABLE 7 — EVALUATION OF CANDIDATE RADIOISOTOPES FOR IMPLANTABLE POWER SOURCE FUEL

Radioisotope	Fuel Form	Production Method	Comments
Pu-238*	PuN or PuO_2^+	Am-241 irradiation, decay and two chemical separations	10-yr capability; low dose rate.
Pu-238**	PuN or PuO_2^+	Np-237 irradiation, two chemical separations (one after 5 yr of use)	10-yr capability; moderate dose rate.
Pm-147	Pm_2O_3	Fission product separation, thermal flux irradiation	Required $\frac{\text{Pm-146}}{\text{Pm-147}} < 10^{-8}$
Tm-171	Tm_2O_3	Isotopic separation, high flux irradiation	Production technique required to yield $\frac{\text{Tm-170}}{\text{Tm-171}} < 10^{-6}$

* Reference design
** Back-up design
\+ Using isotopically separated 0-16

5.10.5 Method of Evaluation

The fuel was sized to produce 35 watts (thermal). The encapsulation was designed to withstand the internal helium pressure resulting from a 25% helium release. Detailed capsule calculations are presented in Appendix I.

The tungsten alloy and polyethylene shield was designed to reduce the combined photon and neutron dose to 50 mr/hr as calculated using a neutron RBE of 8. The calculations are presented in Appendix J.

5.11 ENGINE OUTPUT CONTROL

5.11.1 Function

The primary function of the engine output control is to assure that the engine output is compatible with the artificial heart within the criteria specified for the engine.

A second, non-mandatory, function is to reduce the thermal input during periods of extended low power output.

5.11.2 Requirements

5.11.2.1 Mandatory Requirements

- Protection against over-pressurization of the artificial heart.
- Reliable control for 10 years.
- Lowest practical losses during full power operation of artificial heart.

5.11.2.2 Non-Mandatory Requirements

- Provide a maximum practical reduction of thermal energy requirements for power output reductions up to 50%.

5.11.3 Reference Design

The reference design does not fulfill the non-mandatory requirement. The engine output control selected provides for essentially constant engine power and the dissipation of excess power through a throttling valve. The alternate and more complex, control system provides for a variable power output and sizeable reduction in average heat input. This concept may be used in the final implantable engine; however, because the emphasis during the current program was to show a basic feasibility, the simpler, constant power system was selected.

The reference engine is essentially a constant frequency device. The engine speed is primarily determined by the natural frequency of the "spring"-mass system of the reciprocating weight and the reversing piston system. If no engine controls were provided, the pressure ratio output of the engine would increase during periods of low heart demand. The reference design of the pumping chamber would transmit this higher pressure ratio as an undesirable overpressure in the pumping fluid. To avoid this overpressure, a valve is provided to limit the pressure difference between the low and high pressure reservoir to a preselected value. A schematic diagram of the pressure control valve is shown in Figure 27. This valve has the same basic design as the conventional spring loaded pressure relief valve. The operation of the valve is as follows: The ball is maintained against a seat by a preloaded spring. When the pressure forces (the pressure differential across the valve) exceed the spring preload, the ball will be lifted off the seat. The preload on the spring will be adjusted with the hollow adjusting screw to provide the desired opening pressure differential.

The valve will be fabricated from the titanium alloy used for the pumping chamber to minimize assembly problems.

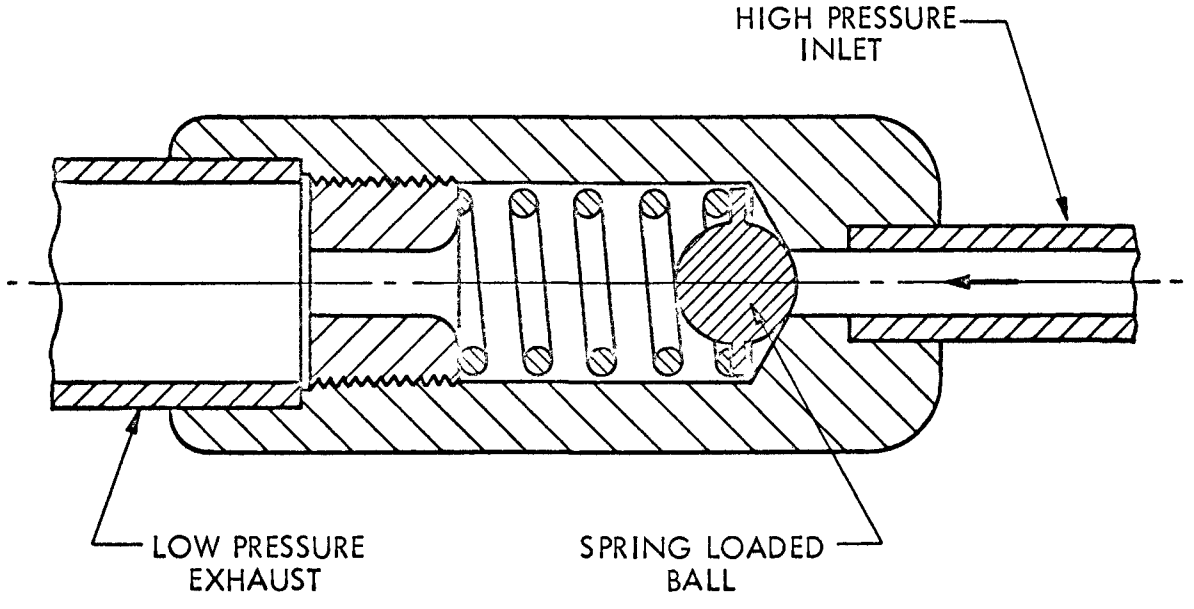

FIGURE 27. SPRING-LOADED PRESSURE RELIEF VALVE

3.01-68-083

5.11.4 Alternate Configurations Considered

5.11.4.1 Variable Speed - Constant Stroke

This alternate concept requires a control system to adjust the engine speed and reduce the required input heat during periods of low power demand by the artificial heart. One possible method of changing the frequency of the reciprocating mass while maintaining a fixed stroke is to modify the unswept volume in the reversing piston. By decreasing the ratio of swept-to-total volume in the reversing piston, the frequency is decreased but not in a linear manner. Engine speed control can also be accomplished by varying the energy absorbing characteristics of the dash pots; maximum speed results from completely elastic dashpots while minimum speed results from maximum energy absorption.

The reduction in input power as a function of output power is shown in Figure 28. This concept reduces the heat input to 56% of reference for a power output demand of 30% of the maximum by reducing the speed to approximately 40% that used at full power.

5.11.4.2 Variable Stroke

A second alternate method of varying engine output is to vary the reciprocating mass stroke. In order to avoid excessive loss of engine efficiency, it is necessary to accomplish the reduction in stroke without increasing the absolute value of the engine unswept volume. This could be achieved by driving both ends of the hot and cold chambers in an axial direction to match the increase or decrease in stroke. Actually the dash pots could be moved from the reversing piston assembly to the displacer piston assembly so that the adjustable end positions automatically set the stroke.

Figure 29 shows the control provided by this concept. For the plot shown, it is assumed that the reversing piston geometry is unchanged; hence the speed actually increases for the shorter strokes. By comparing Figures 28 and 29, it is easily determined that the variable speed control system described in preceding section is superior. For example, the variable speed control system provides 30% of full power output with a heat input 56% that of the full power input. The variable stroke requires approximately 67% of the full power heat input for the 30% output.

5.11.4.3 Dual Engine

This concept assumes that the cardiac demand can be divided into two distinct regions; a region of approximately seven watts total demand and a region where the demand is in the 1 to 3 watt range. The concept consists of an engine with two displacer pistons and a single reversing piston (which operates both displacer pistons). The geometrical configuration could be an inline design or, alternately, the two displacer pistons could be located adjacent to each other with an appropriate tie-bar. Each displacer piston would have its own regenerator-heater circuit. One of the two displacer pistons would be sized to provide the 1-3 watts of pneumatic power on a continuous basis and would operate in a manner similar to the reference design. The second displacer piston would be designed to deliver about 4

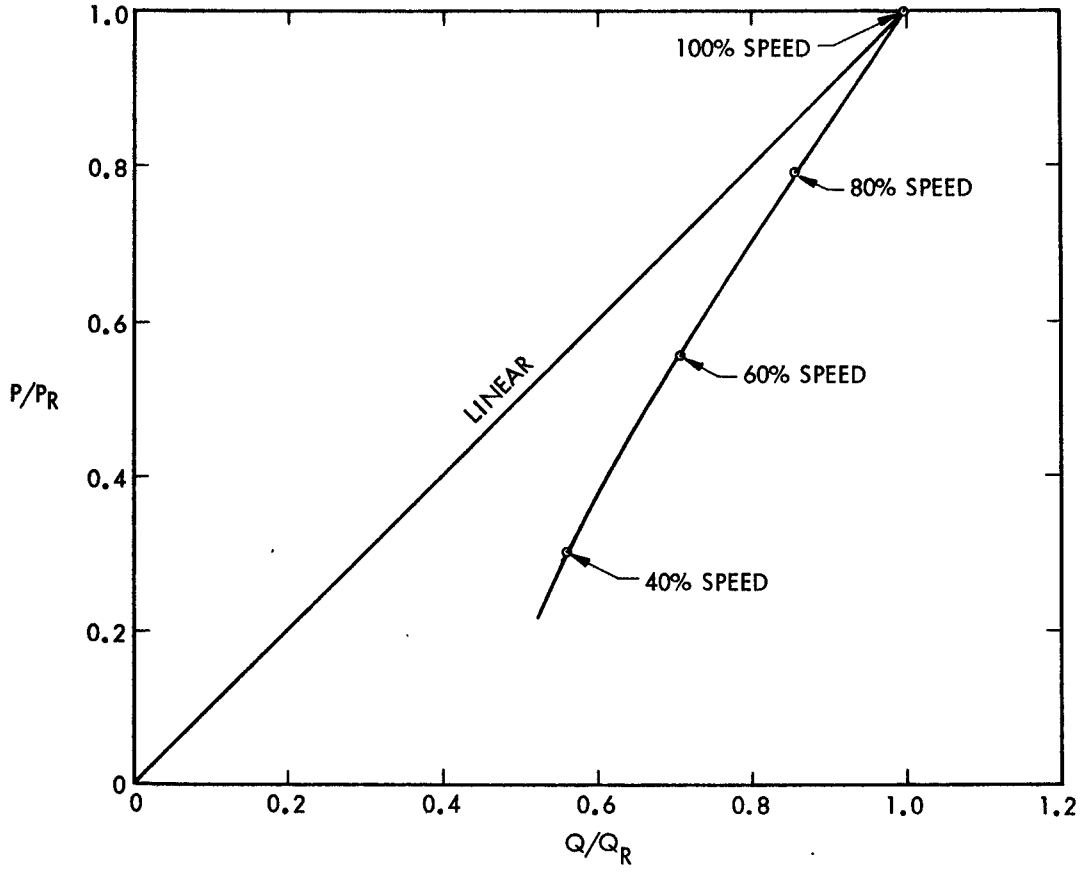

P = POWER OUTPUT
Q = HEAT INPUT
SUBSCRIPT R = 100% SPEED

FIGURE 28. POWER OUTPUT AND HEAT INPUT AS A FUNCTION OF ENGINE SPEED

3.01-68-084

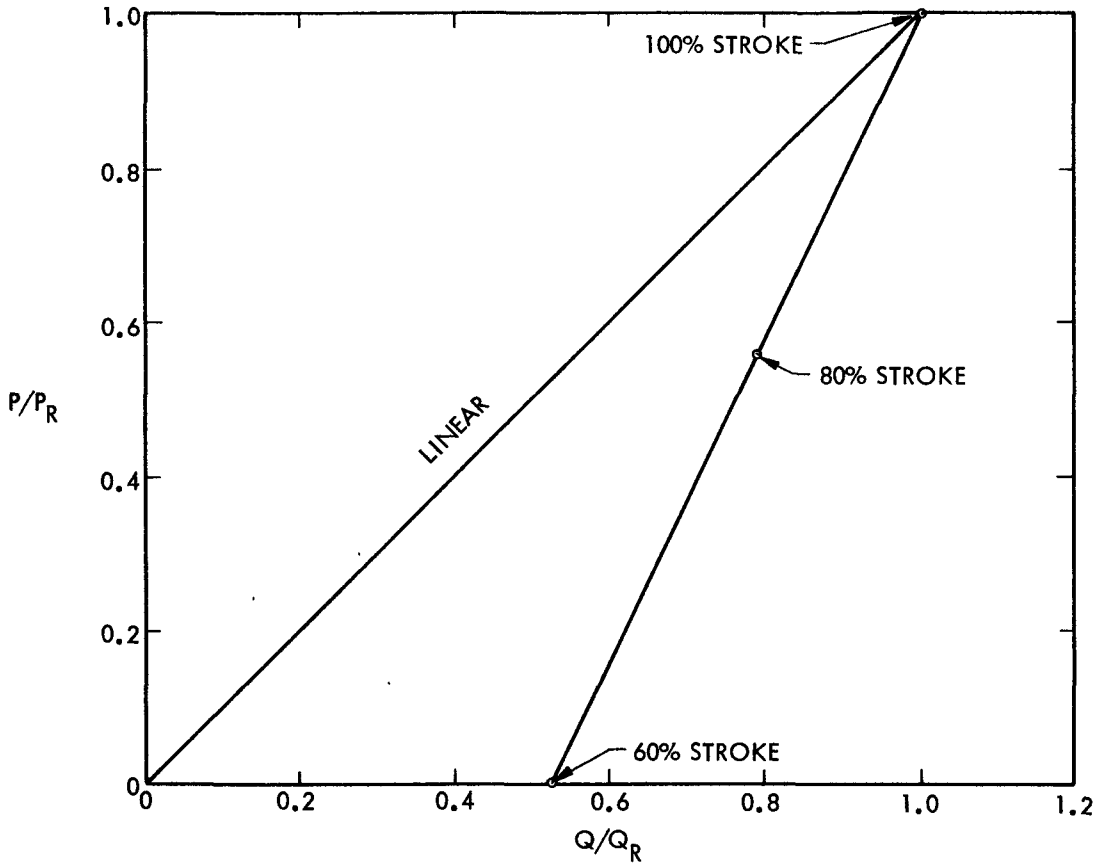

P = POWER OUTPUT
Q = HEAT INPUT
SUBSCRIPT R = 100% STROKE

FIGURE 29. POWER OUTPUT AND HEAT INPUT AS A FUNCTION OF STROKE

3.01-68-085

watts of power and would be fitted with a bypass line in parallel with the regenerator-heater loop. The bypass would either be full open (in case the heart demand was below 3 watts) or full closed (for the larger power demands). The flow impedence of the bypass loop would be small compared to the regenerator-heater loop so that when it was open almost all of the flow would be carried by this line and relatively little by the regenerator-heater line. The net result will be that, when the bypass opens, the displacer piston will produce no power and absorb relatively little heater power but when closed, the displacer piston will produce approximately 4 watts. This arrangement would permit operation of the engine at low power for long periods of time and absorb correspondingly less heat from the thermal supply system.

This dual engine was investigated only qualitatively; the parasitic thermal losses would be greater than the reference design because of the two cylinders, two regenerators, etc.

5.11.4.4 Variable High Pressure Pumping Chamber

In this concept, the pumping chamber is redesigned to accommodate a variable high pressure. When operated in conjunction with an appropriate control system, the redesigned pumping chamber would provide a pumping output power which is a function of the high pressure level. The output power could be controlled by controlling the pressure level; the exhaust valve will open at different positions in the displacer piston cycle and provide a variable engine power output. Figure 30 shows the engine power output, heat input, high pressure level, and exhaust valve opening position for this concept.

No redesign of the basic engine is required under this concept; all components, including the check valves, operate in the same manner as the reference design for all conditions. The design of the pumping chamber and control system would require modification to the extent necessary to provide acceptable cardiac pumping.

5.11.5 Method of Analysis

The method of analyses for the studies summarized in the preceding sections was to utilize the Schmidt analysis computer code discussed in Appendix M. This computer program yielded only approximate answers because the computer code selects the heater and regenerator hydraulic diameters and the high pressure as a function of the other input variables.

5.12 PUMPING CHAMBER CONTROL

The circulatory system is equipped with an intricate control system which is designed to satisfy the metabolic needs to maintain hemodynamic equilibrium. At least three known groups of factors -- mechanical, nervous, and chemical -- operate to regulate the action of the heart and blood vessels. Pressure and flow transducers and pH and blood chemistry sensors constantly monitor blood system parameters, and the output data are processed in real time by an intricate neural computer. Higher cortical levels influence these automatic controls; for example, blood distribution to upper parts of

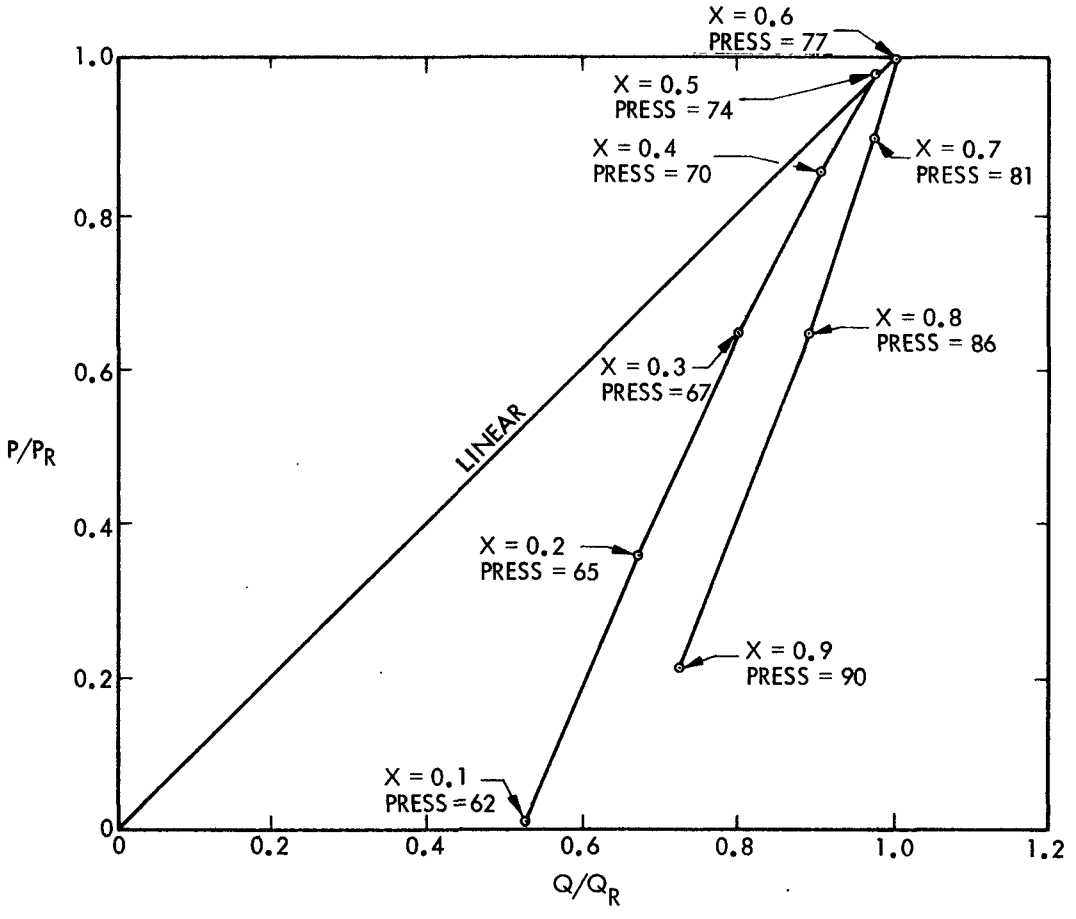

P = POWER OUTPUT

Q = HEAT INPUT

SUBSCRIPT R = REFERENCE

X = FRACTION OF STROKE FROM TDC THAT EXHAUST VALVE OPENS

PRESS = HIGH PRESSURE, psi

FIGURE 30. POWER OUTPUT AND HEAT INPUT AS A FUNCTION OF EXHAUST VALVE OPENING POSITION

3.01-68-086

of the body is stimulated in anticipation of arising from a supine to an erect position. Hormonal regulators released into the blood stream also exert dramatic influences on circulatory dynamics. In addition to these gross controls, all vital regions of the body -- brain, kidney, gut, and others -- possess autoregulatory mechanisms which stimulate or retard regional blood flow in accordance with local requirements.

5.12.1 Control Requirements

Largely because of autoregulatory regional circulatory controls, the heart, as a pump, probably fulfills its life-sustaining functions if it satisfies the following basic criteria:

1) It must maintain sufficient cardiac output (blood volumetric flow rate and systemic pressure) to satisfy all the needs of the body.

2) It must provide for flow balance between the right and left heart circuits, and between cardiac output and venous return.

These same criteria describe the characteristics of an artificial heart pump which, in addition, should have a stroke profile and pulse rate similar to those of the natural heart, to accommodate the dynamic changes in vascular impedance. Cardiac output is the product of stroke volume and heart rate. For a system in which systole and diastole are synchronized for both sides of the heart, some variability of stroke volume is necessary to provide an independent means for individually regulating flow between left and right circulations to maintain prescribed pressure limits. Adjustments to maintain flow balance and obtain required cardiac output must be guided by prescribed variations in atrial pressure since excessive pressure increases the impedance to venous return and the risk of producing pulmonary edema. Until further clinical evaluations are complete, heart pump operation should correspond closely to normal physiological behavior. It is therefore assumed that pulsatile flow, and a capability for varying the relative duration of systole and diastole, as well as heart rate and stroke volume, are required. Typical variations in these parameters which occur in the natural heart are:

	Pulse Rate, bpm	
	60	160
Duration of Systole, sec	.32	.17
Duration of Diastole, sec	.68	.21
Stroke Volume, ml	66.5	75
Output, l/min	4	12

The change in stroke volume is relatively small for a large change in pulse rate and cardiac output; and the duration of diastole undergoes a larger relative change than for systole. The duration of systole is about one-half that for diastole at low pulse rates, and the two are approximately equal at high pulse rates. Normal venous pressures range from 2 to 12 mm Hg for

the left atrium and 1 to 6 mm Hg for the right.

In addition to these control parameters and operating characteristics, the control system must have a high reliability, so as not to restrict the lifetime of the basic heart pump system, and must not consume a large fraction of the output power. The number of input control signals must be minimized by maximum use of the normal autoregulatory control mechanisms. For example, changes in load might particpate in the regulation; i.e., vasoconstriction could provide an automatic feedback which instructs the heart to pump less blood, while vasodilation would cause an increased flow. In the limit, sensing atrial pressure to maintain flow balance coupled with the normal autoregulatory body functions may be sufficient to achieve adequate control of an artificial heart if the control system and pump are sensitive to load fluctuations.

5.12.2 Examples of Operational Control Devices

Several artificial heart systems have been evaluated by the Cleveland Clinic Foundation*, e.g. the Detroit Coil Timer, fluid amplifier, and computerized NASA systems. In the Detroit Coil Timer system**, the silastic twin-sac heart is driven by alternate pressure and vacuum delivered through a three-way solenoid valve. The control of the valve allows variations in pulse rate (60 to 100) and duration of systole (15 to 50%). Manual regulators vary the pressure (0 to 5 psi) and vacuum (0 to -5 in. Hg). The systolic pressure is normally set for higher than systemic blood pressure, which will empty the ventricle during each stroke. Thus, the cardiac output is strictly a function of diastolic filling for fixed control settings.

In the fluid amplifier artificial heart***, pressure and vacuum are alternately supplied to the heart by the switching action of a bistable fluidic amplifier (see Figure 31). The vacuum is self-generated by entrainment at the power jet within the amplifier and a manual pressure regulator controls stroke amplitude. Systole is initiated automatically upon filling of the ventricle. This system regulates cardiac output by changing the pulse rate automatically as a function of ventricular filling rate but the stroke volume remains relatively constant. Two fluid amplifier systems are required to drive both sides of the heart. Since the stroke volume cannot be varied by a significant amount, flow balance must be maintained by adjusting the individual pulse rates of each system, and, consequently, the pulse rates are not synchronized.

---

* Y. Nose' et al., "Respect the Integrity of the Large Veins and Starling's Law", Trans. Amer. Soc. Artificial Internal Organs, Vol. XIII, 1967.

** Y. Nose' et al., "Artificial Hearts Inside the Pericardial Sac in Calves", Trans. Amer. Soc. Artificial Internal Organs, Vol. XI, 1965, and Y. Nose' and W. J. Kolff, "The Intracorporeal Mechanical Heart", Vascular Diseases, Vol. 3, Feb. 1966.

*** K. E. Woodward, et al., "An Intrathoracic Artificial Heart Controlled by Fluid Amplifiers", Trans. Amer. Soc. Artificial Internal Organs, Vol. XII, 1966.

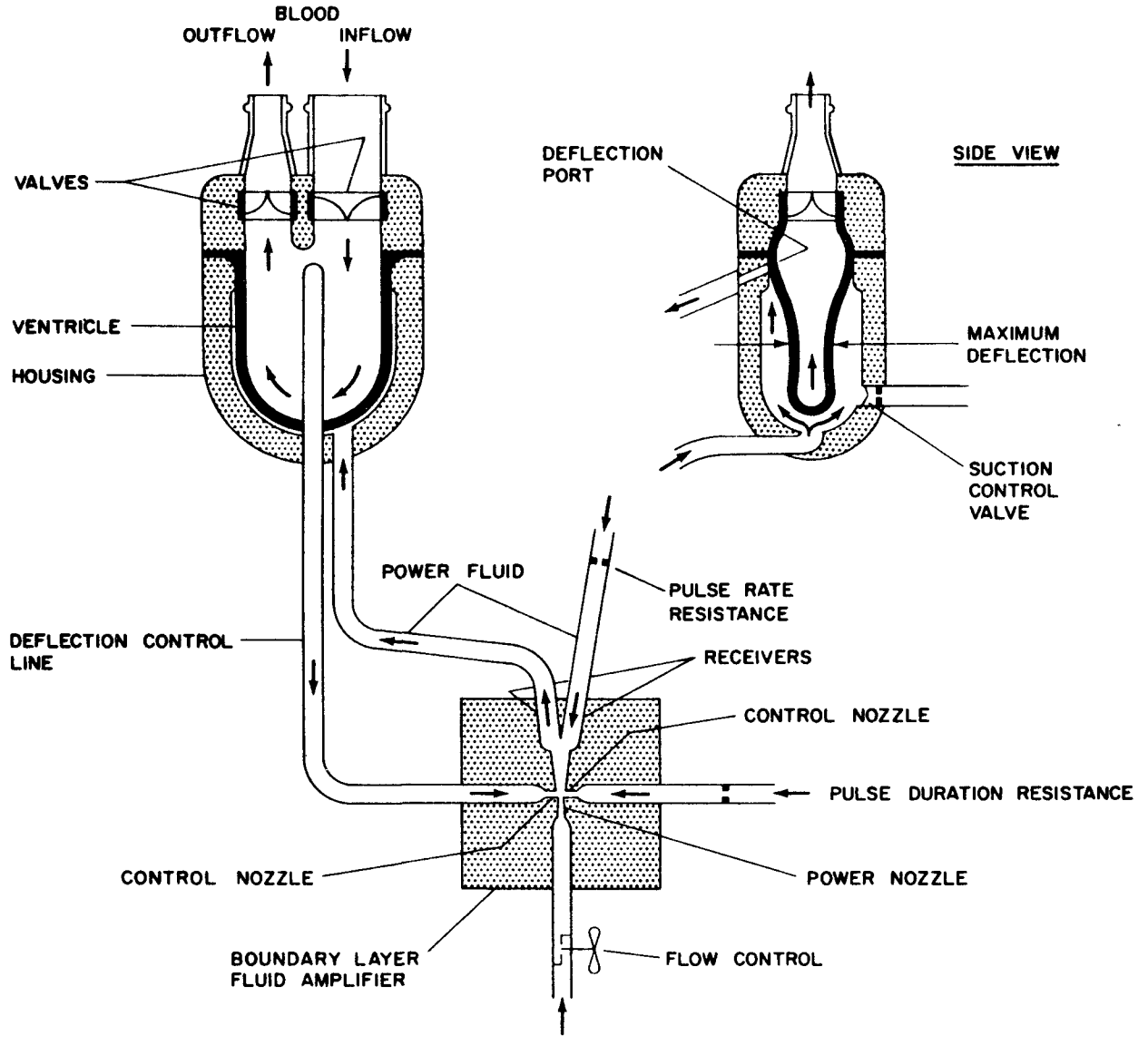

FIGURE 31. FLUIDIC AMPLIFIER HEART PUMP SCHEMATIC

3.01-68-087

The NASA system* utilizes a pressure servomechanism which converts an electrical signal into a pressure by means of an electronic mechanical feedback control system. It consists bascially of an electronic amplifier, proportional solenoid-actuated pneumatic valves, and a feedback pressure transducer. A physiologic pressure waveform is programmed on a function generator and the pressure servomechanism converts this output into dynamic drive pressure. The transducer-sensed atrial pressure is electronically multiplied by the output of the function generator to modulate the amplitude of the command signal to the pressure servo. Increases in atrial pressure proportionally increase the strength of contraction and produce higher systolic pressures to obtain automatic amplitude control. This sophisticated NASA system has excellent physiologic artificial heart operating characteristics.

5.12.3 Alternate Control Systems

The previously described control systems have been useful to the investigator by providing a means for evaluating the effects of artificial heart operating characteristics on physiological processes. However, the control power required by these systems makes them inefficient and unsuitable for use with an implantable power source. It is highly undesirable to use any significant amount of electrical power for control purposes in view of the inefficiency of converting thermal energy to electrical power at low power levels, and the complexity of the required supplemental power generation components (since the reference Stirling engine produces only pneumatic power). In addition, the solenoid valve is an inefficient user of electrical energy because of the power surges associated with each cycle. Electrical devices also have a high susceptibility to chloride ion corrosion and subsequent failure. The fluid amplifier artificial heart is an amazingly simple and inherently reliable device because of the minimum number of moving parts and the absence of electronics. Unfortunately, the bistable fluidic amplifier is an inefficient energy recovery device since the available output pressure is a maximum of 40 to 50 percent of the supply pressure. If these devices are used to drive the artificial heart directly (as in the referenced fluid amplifier heart), more than half of the available energy from the power source is used to obtain pulsatile switching control. This is a severe penalty which would result in a significant increase in the power source size, probably to the point of being impractical for implantation purposes. Consequently, it is necessary to design a control system which minimizes the parasitic power loss, and does not unduly compromise the inherent reliability of the simple fluid amplifier heart previously described.

5.12.3.1 Fluidic Amplifier Valve Actuation

In control systems where operation is intermittent and the cycle time is long, fluidic systems have a disadvantage because of continuous power consumption. While a fluidic device is operating, there is a constant flow of fluid through it, whether or not it is switching or acting in any way upon

* K. W. Hiller, W. Seidel, and W. J. Kolff, "An Electronic-Mechanical Control for an Intrathoracic Artificial Heart", Amer. Journal of Med. Electronics, July-Sept. 1963.

that flow. For example, in the fluid amplifier artificial heart, the power output is used to compress the heart during systole, but is wastefully vented during diastole. A partial vacuum is created by entrainment at the jet which provides a beneficial filling force during diastole, but the power recovery is quite small. The overall system power recovery, including pressure recovery by the fluidic amplifier and the parasitic vent loss during diastole, is only about 20 percent of the pneumatic supply power.

It is obvious, therefore, that a considerable power saving can be obtained if the fluid amplifier is used to actuate a valve instead of as the primary pneumatic drive mechanism, and if the output power is usefully stored between the valve actuation periods. A schematic diagram of a control system which satisfies these requirements is shown in Figure 32. The bistable fluidic amplifier pulse generator* (PG-1) is a capacitive timing device which stores the amplifier output and periodically directs a pneumatic pulse to actuate the spool valve and initiate diastole (see Figure 33). A similar pulse generator (PG-2) is then used to initiate systole. Pulse rate and duration of systole and diastole are controlled by adjusting the supply pressure to the pulse generators. A throttling valve on the high pressure inlet to the spool valve provides systolic pressure amplitude control.

Since the control system must be capable of sustaining a 3 g shock loading, the main spool valve must be latched in place between actuation pulses. A mechanical latch which automatically locks the spool in place at the end of spool displacement, and is released by the reverse pressure pulse, can be devised. The use of a mechanical latching device is objectionable from a reliability standpoint because of the possibility of jamming due to contamination or wear. The primary advantage of this control system is that maximum use is made of available pneumatic power (approximately 5 percent is required for actuation). If the spool valve were actuated and latched by continuous flow from a load insenstive bistable fluidic amplifier (no storage and timing circuit) as shown in Figure 34, the power loss would be approximately 20 to 30 percent, assuming 10 percent of the period each for systolic and diastolic valve actuation.

5.12.3.2 Vortex Control System

A rotary mechanical valve was considered because of the obvious reliability advantages of such a concept when compared with the oscillating-type spool or solenoid valve. This concept is illustrated in Figure 35 based on the use of vortex proportional fluidic control devices. The main valve is rotated at a specified frequency, which defines the pulse rate, by a rotary expander which is driven by a unidirectional vortex power amplifier. The location of the variable-area valve opening with respect to the outlet port permits adjustment of the relative duration of systole and diastole. The valve is positioned by the pressure differential across the spool locator which is adjusted by the push-pull vortex proportional power amplifier. A throttling valve on the high pressure inlet to the valve provides systolic amplitude control.

* Product Engineering, page 54, August 1, 1966.

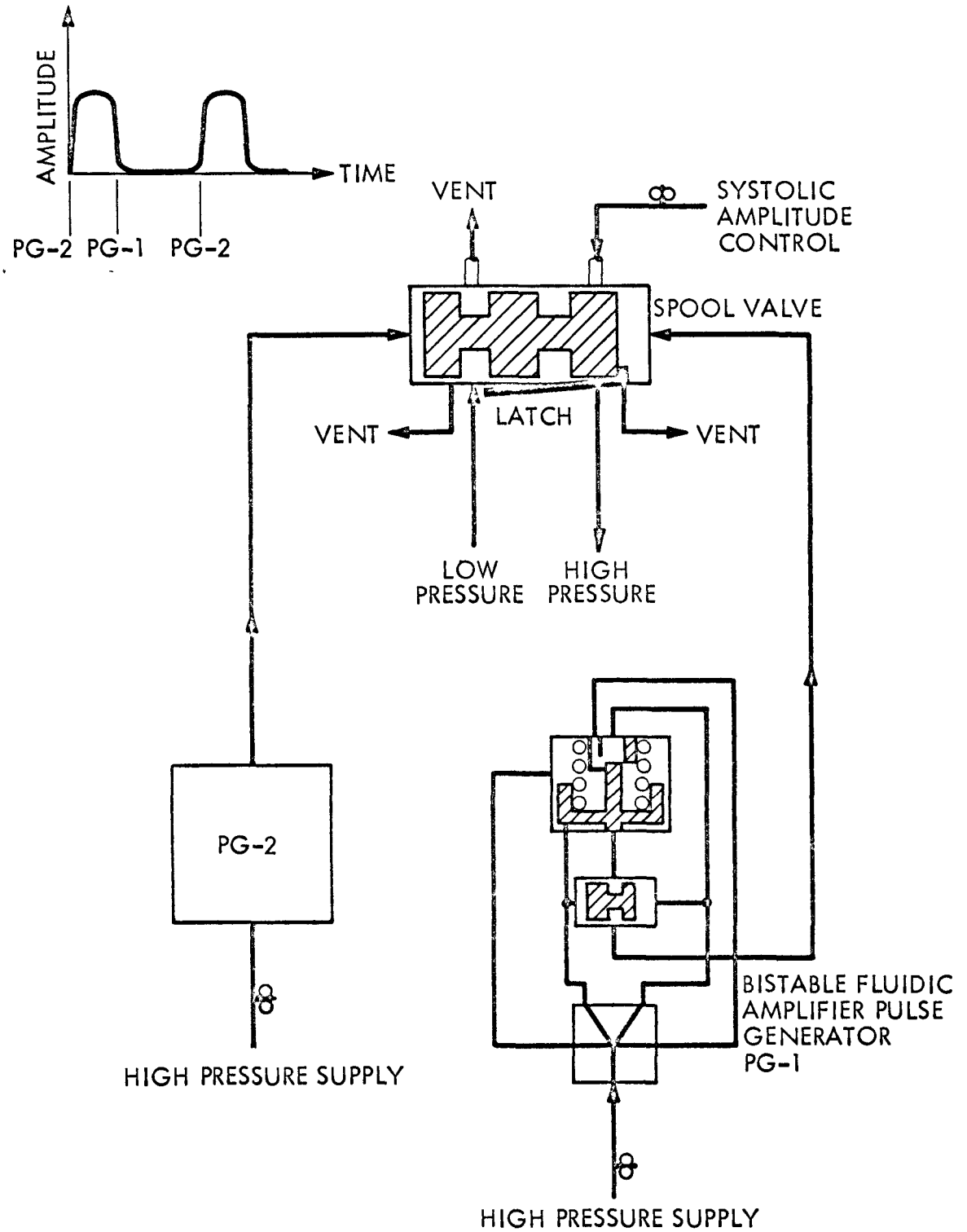

3.01-68-088

FIGURE 32. PULSE-OPERATED VALVE

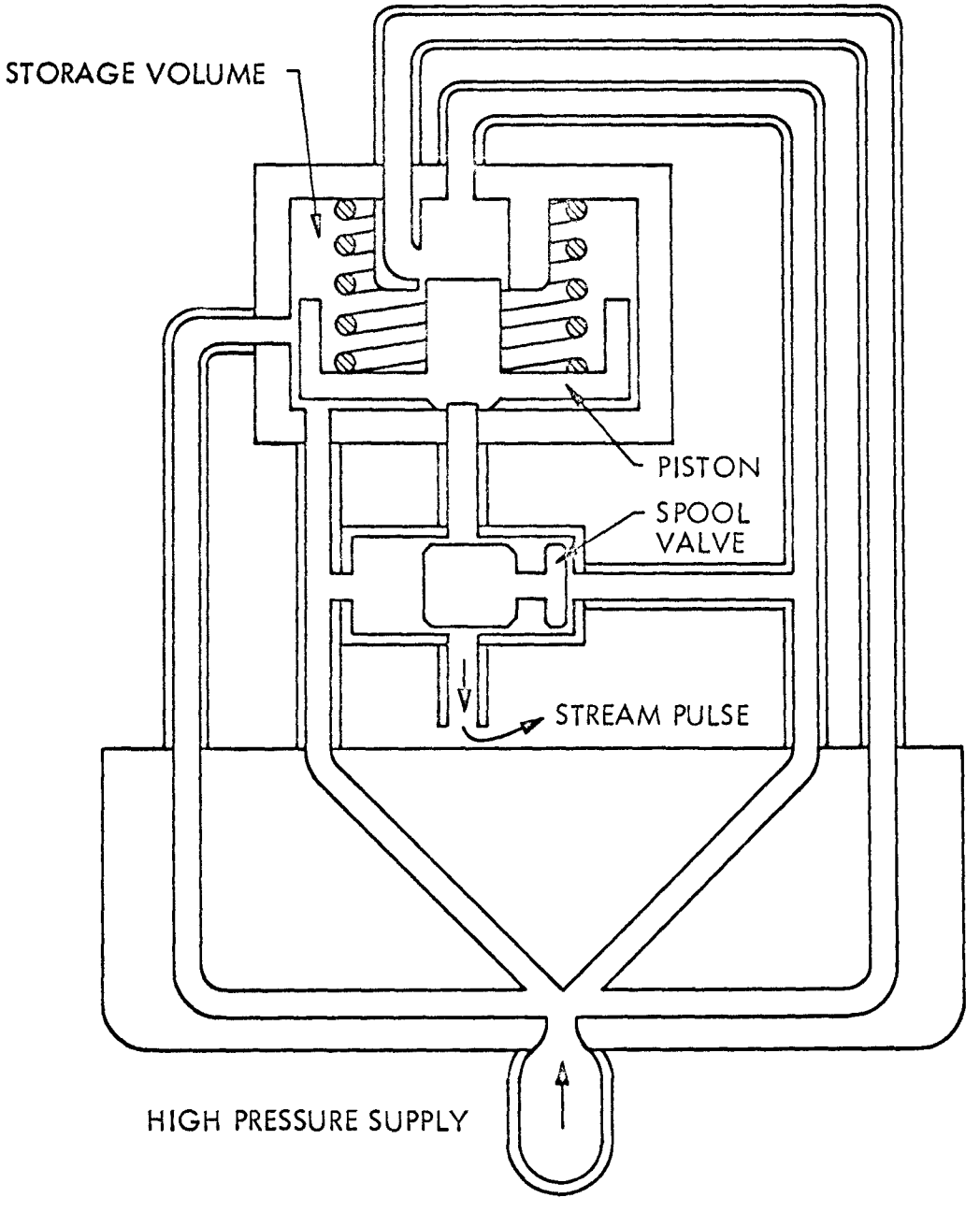

FIGURE 33. FLUID AMPLIFIER PULSE GENERATOR

3.01-68-069

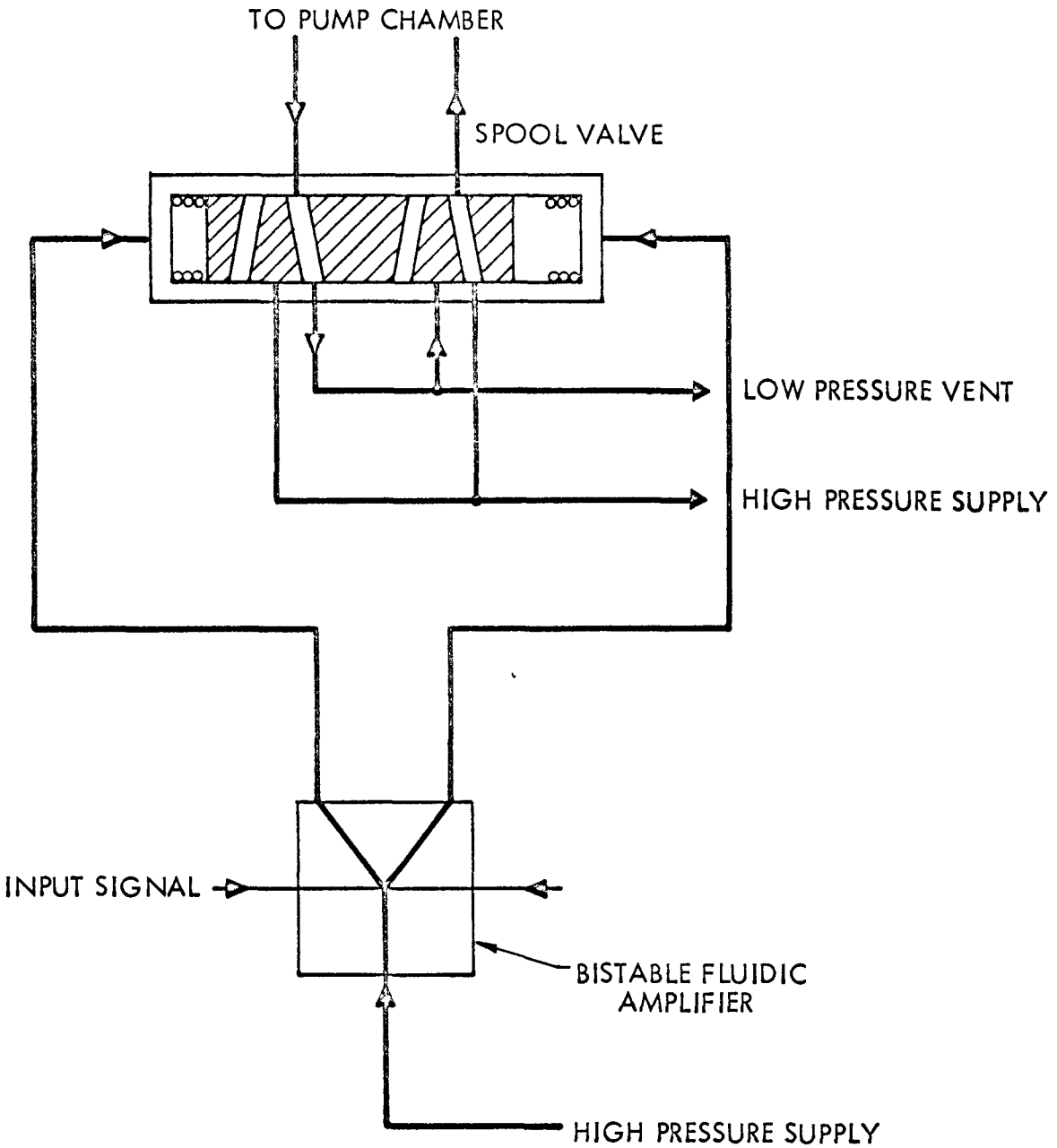

FIGURE 34. FLUIDIC ACTUATED SPOOL VALVE

301-68-090

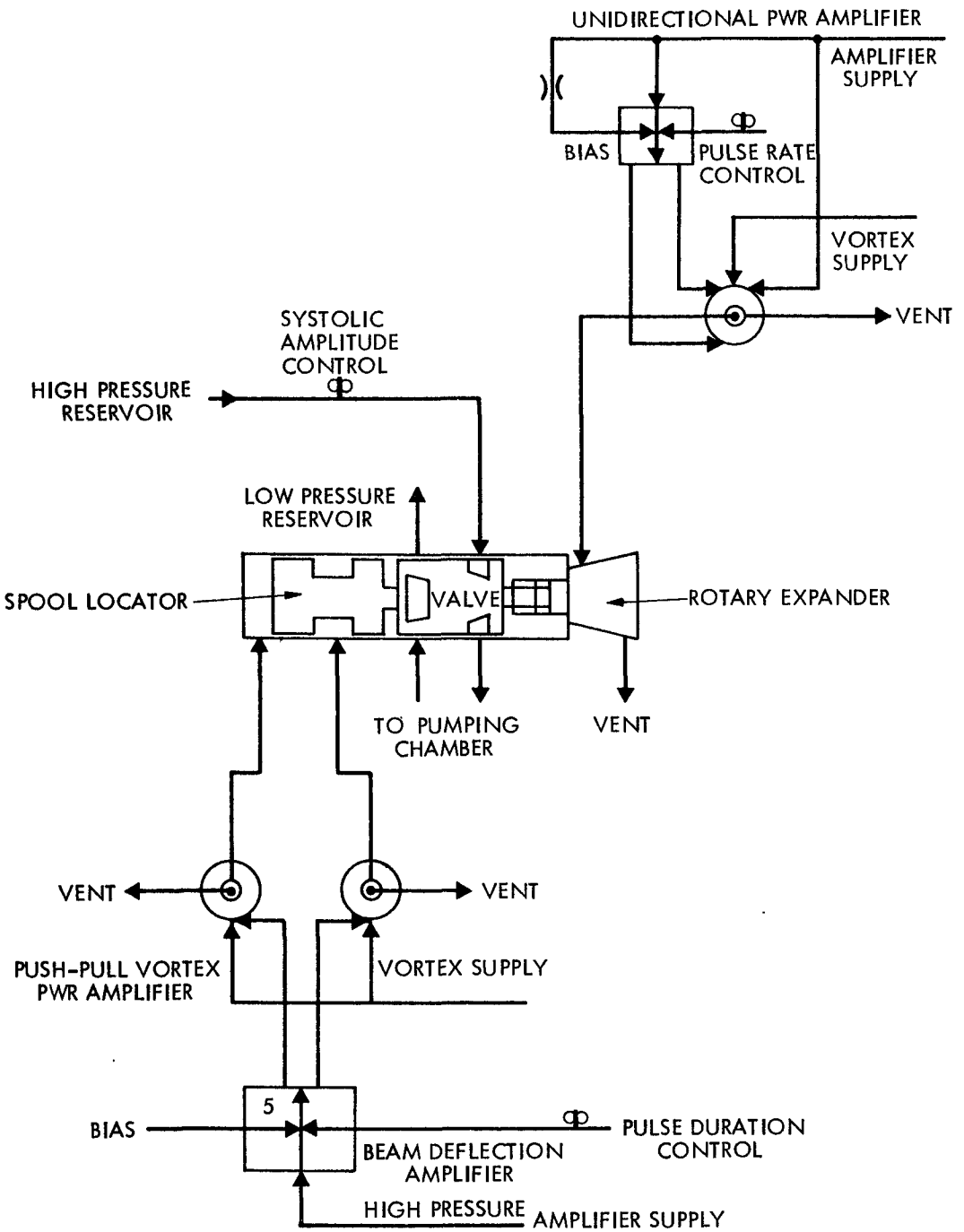

FIGURE 35. VORTEX CONTROL SYSTEM CONCEPT

3.01-68-001

A speed reducer would undoubtedly be required to obtain adequate efficiency from the rotary expander at such a low power output, since the required valve speed is only 30 to 80 rpm. Although the vortex amplifier is a reasonably good power recovery device, the control jets require a higher pressure stream than the main supply pressure. This is wasteful in a system which has a single high pressure gas reservoir. It is estimated that the total power required for this vortex control valve system would be approximately the same as for a spool valve driven by continuous flow from a load insensitive bistable fluid amplifier (about 30 percent of the total available power). The overall complexity and inefficiency of this system do not justify the highly desirable feature of rotary valve motion.

5.12.3.3 Electronic Control System

It has previously been stated that there is reason to believe that the natural autoregulatory control mechanisms may permit simple regulation by load sensitivity, complemented by atrial pressure response for flow balance compensation. In such case, close coupling with a fully pneumatic control system would provide the simplest and most direct solution. Should the body require a more complex control system, in which an artificial neural computer analyzes requirements and provides control signals which define pulse rate, duration of systole, systolic amplitude, etc., an electronic control system may well be required.

Two electronic control systems were previously described (the Detroit Coil Timer and the NASA control system). The Detroit Coil timer is based on simple on-off solenoid valves, and the NASA system on proportional solenoid valves. Assuming a solenoid electrical-to-mechanical conversion efficiency of 2 to 3 percent*, a 3-g holding force requirement , and actuation time equal to 10 percent of the pulse period, the required solenoid valve actuator power is approximately one electrical watt. If the electrical power is obtained from a thermoelectric converter (about 5 percent conversion efficiency), 20 thermal watts are required, or about half that required by the 7 watt Stirling engine. Approximately the same thermal power is required if the Stirling engine pneumatic power were used in an expander to generate the electric power for the solenoid.

It is apparent that the power required by a solenoid control system is excessive and would jeopardize system feasibility. The additional complexity of generating electrical power would add considerable to the size of the artificial heart system and compromise reliability. The advantages of control system simplcity, low power drain, compactness, and high reliability offered by a fully pneumatic system favor its selection.

5.12.4 Reference Control System

The reference control system is fully pneumatic to avoid the large power drain associated with electronic actuator devices, and uses the Stirling

* M. S. Blumberg, et. al., Artificial Heart Devices and Systems, Stanford Research Institute, Jan. 1966.

engine high and low pressure reservoirs for operating pressure differential. The direct-drive fluidic amplifier and fluidic amplifier-actuated spool valve control systems described above are coupled to reduce the control system power drain associated with each when used individually, and to retain the reliability advantage of a minimum of moving parts.

A schematic diagram of the reference control system is shown in Figure 36. A load sensitive, bistable fluidic amplifier (FA-1) is used as the primary switching element which directs the high pressure supply stream to the right ventricular pumping chamber during both systole and diastole, and also provides the pneumatic pressure required to actuate the sliding spool valve (SV-1) which cylically vents the opposite side of the right ventricular pumping chamber. The fluidic device also switches the sliding spool valve (SV-2) which directs the high pressure supply stream to the left ventricular pump and vents the opposite side of the pump. Since the maximum pressure recovery of a fluidic amplifier is only 40 to 50 percent of the supply pressure, its output is used to directly drive the right ventricle pumping chamber which only requires about 20 percent of the total heart pump power. As a consequence, the total control system power drain is considerably less than that of the complete fluidic amplifier heart pump; the total power loss is only 10 to 15 percent of the available pneumatic power.

Check valves (CV-1 and CV-2) are located in the fluidic amplifier lines leading to the right ventricular pump to provide positive venting of the pumping chamber to the system low pressure reservoir, and to minimize parasitic entrainment by the fluidic amplifier jet. The load sensitive bistable fluidic amplifier automatically switches at the end of systole and diastole when the pumping chamber reaches maximum displacement. The pumping chamber vent line is connected directly to the low pressure reservoir during systole so that the full available pressure differential is always applied for a firm systolic pulse. The duration of systole is therefore determined by the body autoregulatory mechanisms which control peripheral resistance. Control valve V-1 located in the right ventricle pumping chamber diastole vent line determines the duration of diastole and pulse rate. Control valve V-2 located in the left ventricle diastole vent line is required to adjust the left ventricular stroke displacement and maintain flow balance between the left and right ventricles. An atrial pressure sensor is required to provide the control signal for V-1 and V-2.

A timing circuit is provided to limit the pulse rate to a minimum permissible value consistent with normal physiological requirements, i.e., 60 to 70 bpm. During systole, a capacitive element (C) is fully charged to line pressure by the actuation of spool valve SV-1. Restrictors R-1 and R-2 control a fixed leakage flow rate to the fluidic amplifier device (FA-2). This leakage is normally vented to the low pressure reservoir. If the pulse rate is too low (below the minimum allowable rate of 60 to 70 bpm), the pressure in the capacitive element will be reduced by the controlled leakage to the point at which FA-2 will switch and direct and input signal to FA-1. This signal will automatically terminate the diastolic period and initiate systole.

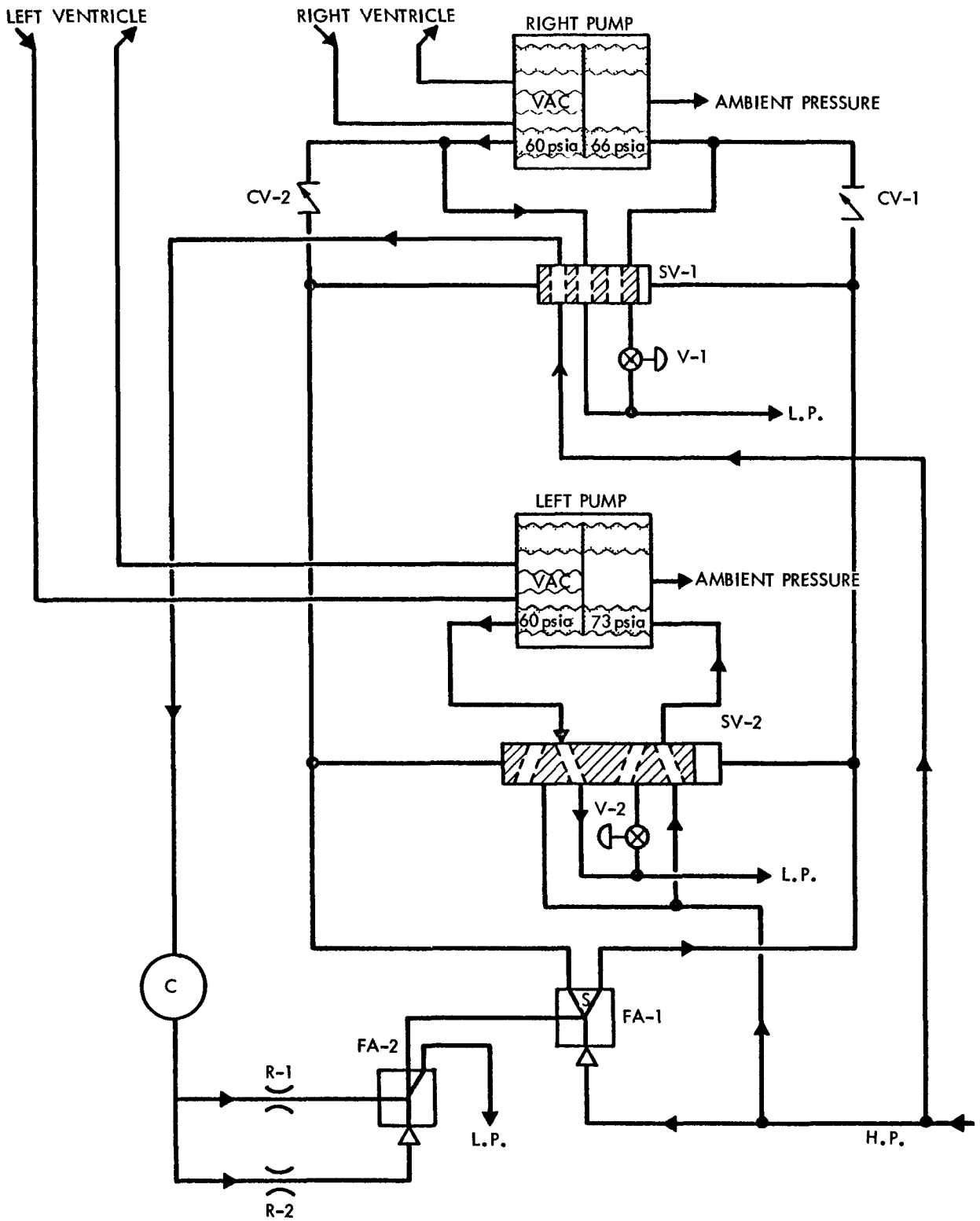

3.01-67-989

FIGURE 36. CONTROL SYSTEM SCHEMATIC DIAGRAM

5.13 ENGINE INTEGRATION

5.13.1 General Placement

The reference design of the artificial heart power supply consists of components or subassemblies at three different body locations. Interconnecting fluid lines are required between subassemblies and to connect the system to the artificial heart.

The main assembly of the power supply consists of heat source, engine, pumping chambers, gas reservoirs, gas-to-pumping fluid heat exchanger, and insulation. This assembly will be implanted in the abdominal cavity. The pumping fluid-to-blood heat exchanger is also implanted in the abdominal cavity and replaces a section of the abdominal aorta. A reference pressure bladder, which supplies the reference pressure for the pumping chamber, is located in the pleural cavity at the apex of the right lower lobe.

5.13.2 Engine Assembly

The engine assembly is shown in Figure 8. The development of the configuration shown was based on assumptions relative to the desirability of combining the heart engine components into a minimum number of packages, and to the development of shapes that would facilitate implant procedures and maximize patient comfort. The latter factor, of course, had to be considered in conjunction with both engine performance and reliability. Beyond the obvious criteria of making the engine as small as possible, it was assumed that an assembly which was very long in one dimension would be undesirable. It is anticipated that the reference engine configuration will require some revision when the exact implant location is selected.

Figure 37 shows in detail the arrangement of the heat source, displacer piston and cylinder, heater, regenerator, reversing system, thermal insulation, and nuclear shielding. The main feature of the reference design is that all of the reciprocating parts are in line; this configuration minimizes the dynamic loades on the bearings and seals and the weight of the oscillating pistons and shafts.

Every effort was made to minimize the effective length of this assembly to facilitate implantation. One of the primary factors which determines the overall length of the assembly is the stroke length of the reciprocating mass. The stroke length is particularly important for the reference system in that an increased stroke increases both the displacer and reversing cylinder lengths. Conversely, a decrease in stroke length increases the thermal losses through the displacer piston and cylinder and the surrounding thermal insulation. The reference design provides a qualitative balance between these factors. As observed in Figure 37, the source is also in line with the displacer and reversing piston. The alternate of placing the source on the side of the displacer cylinder was investigated and it was determined that this concept has several serious disadvantages: it complicates the thermal transport between the source and the heater; it perturbs the thermal gradients in the region surrounding the displacer cylinder and regenerator, resulting in greater thermal losses, mechanical

BLANK

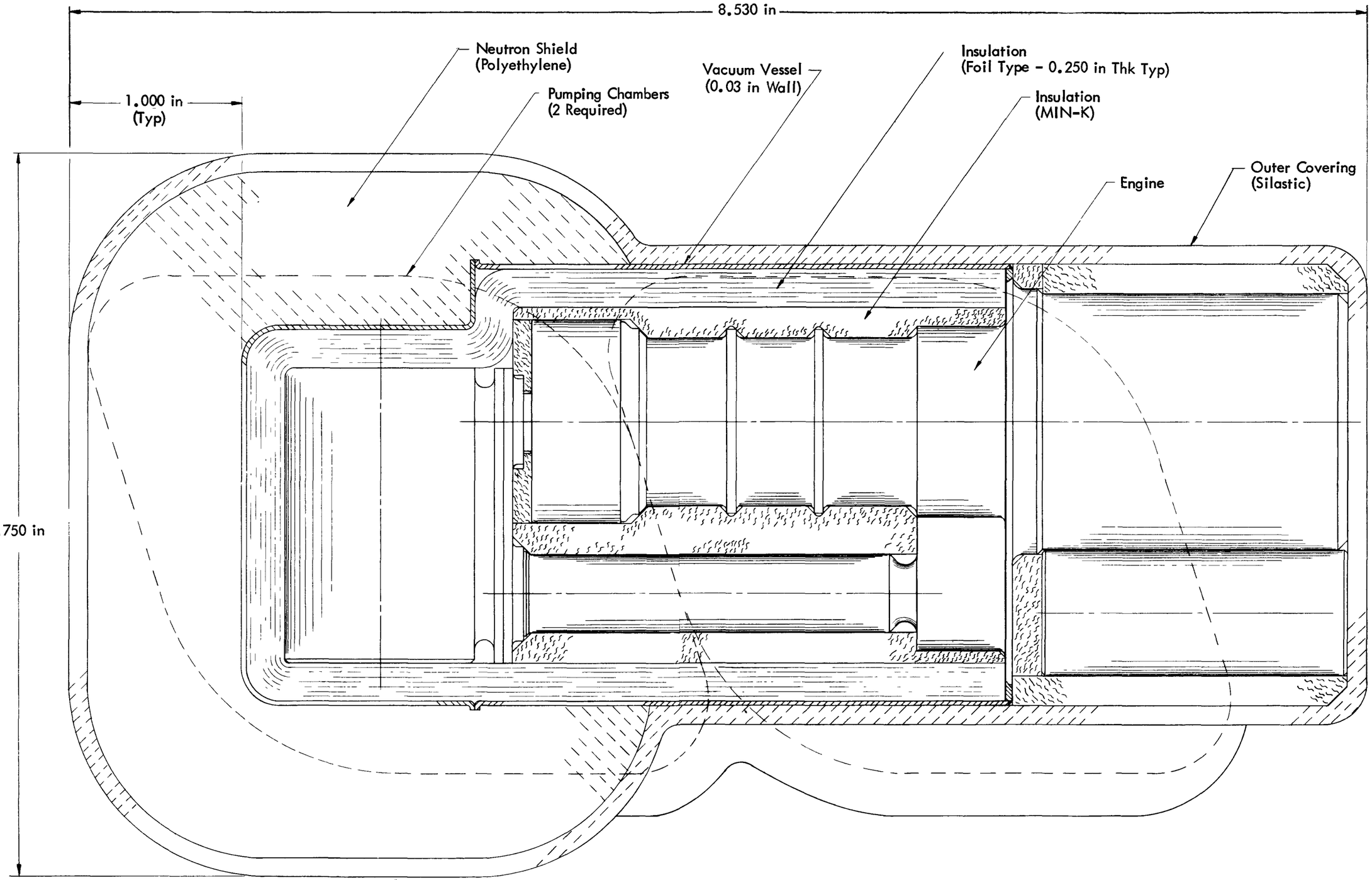
8.530 in
1.000 in
(Typ)
4.750 in
Neutron Shield
(Polyethylene)
Pumping Chambers
(2 Required)
Vacuum Vessel
(0.03 in Wall)
Insulation
(Foil Type - 0.250 in Thk Typ)
Insulation
(MIN-K)
Engine
Outer Covering
(Silastic)

3.01-68-092

BLANK

distortion, and more complex insulation; it results in a package configuration with an undesirable shape even though the length is decreased; and, it results in a less effective nuclear shield configuration.

The other design configurations which were adopted specifically to decrease the package length are the location of the shaft seal in the bottom displacer piston dome and the location of the check valves on the displacer cylinder wall. The inverted dome on the bottom of the displacer piston is not nearly as effective structurally for internal piston pressures as a convex dome. Acccordingly, the material thickness of the dome must be greater than that used in the upper dome. This increased thickness results in a greater parasitic heat loss between the cylinder wall and the cold chamber gas but the inverted dome was selected in spite of this fact to reduce the height of the assembly.

The analysis of the regenerator showed that an increase in overall system efficiency could be obtained if the length of this component was increased although the efficiency increase with length beyond the reference length is nominal. A longer regenerator could be incorporated by either increasing the length of the displacer cylinder (and stroke) or by extending the regenerator below the base of the displacer cyclinder. The increased displacer cylinder length was not acceptable because of the undesirable increase in the length of the main assembly and the extension of the regenerator below the displacer piston base was not adopted because of the increased flow losses which would be associated with such a design.

The selection of the basic engine assembly described above determines the overall length of the system but the final shape of the package is grossly affected by the two pumping chambers. As shown in Figure 37, these chambers are stacked in a way which results in an overall length comparable to that of the source, displacer cylinder and reversing system. Within limits, the pumping chambers could be larger in diameter and flatter or smaller in diameter and longer but these different shapes would result in a more irregular package.

Several alternates relative to the pumping chamber were considered. It is conceivable that the Stirling engine working fluid could be applied directly to an artificial heart which combines the functions of the flexible sack acting as an artificial heart and the pumping chambers employed in the reference design. The combination of these two functions into a single package would require a much more complex integration and would necessitate a very close coordination of effort between the heart and engine designers. This alternate, if practical, could result in a significant reduction in the weight and volume of the combined artificial heart and engine. This alternate was not pursued in the development of the reference design because of the complexity of the interface with the heart design but the potential benefits warrant careful evaluation of this concept in future programs.

The nuclear shielding surrounds the exposed surfaces of the source outside the thermal insulation. This design permits the use of a low temperature shielding material and minimizes the thermal losses with little loss in radiation shielding efficiency.

The low pressure reservoir is located adjacent to the reversing piston volume in the natural cavity created by extending the package line down from the regenerator.

5.13.3 Pumping Fluid-to-Blood Heat Exchanger

The pumping fluid-to-blood heat exchanger replaces a section of the abdominal aorta and is approximately 6 inches long and 1 inch in diameter. This assembly is described in Section 5.9.

5.13.4 Pressure Compensating Bladder

Control of the pressure within the left and right atrium is very critical. In the reference system, precise control by the control system maintains this pressure slightly above atmospheric pressure. However, compensation for gross changes in atmospheric pressure must also be provided and this is accomplished by pressurizing one volume of each pumping chamber to atmospheric pressure.

A fluid at atmospheric pressure is transfered between the pumping chamber and a flexible bladder located in the pleural cavity. Since the pleural cavity is at a pressure close to atmospheric, compensation for gross changes in atmospheric pressure (such as that associated with a change in altitude or meteorological effects) is accomplished automatically. It has been assumed that this flexible bladder, which has a capacity equivalent to the maximum stroke volume of both left and right vetricle, can be located at the apex of the right lower lobe in the pleural cavity.

5.13.5 Engine Support

The engine will be secured within the abdominal cavity by support members running from the outer portion of the engine assembly to suitable points on the bone structure of the patient. These external supports will fix the location and orientation of the major components. The neutron shield and lower portion of the engine are maintained in the proper configuration by the outer can of the evacuated thermal insulation. The pumping chambers and the low pressure reservoir are held in place by the connecting tubing and by the encapsulating material surrounding the entire assembly. The heater and heat source are supported by the displacer cylinder and regenerator structure.

5.13.6 Assembly Techniques

Detailed fabrication and assembly procedures have not been developed for the power supply since the design is only in the conceptual stage. However, it was considered desirable to define the major steps of the assembly to assure that the design presented could, in fact, be fabricated. These major assembly steps are given in sequence in the following paragraphs.

The displacer chamber and regenerator are assembled and welded to the upper and middle plates. The reverser piston and connecting rod are inserted through the lower chamber subassembly and the displacer piston is

assembled and welded in place. After alignment checks are satisfactorily completed, the entire assembly, and the displacer piston with seal ring and lower chamber plug with labyrinth seal, are inserted and electron beam-welded in place. The reversing piston cylinder and bottom cap are then added. The fuel capsule, already sealed into the special housing which forms the heater, is then welded onto the top plate to complete the assembly of the main engine parts.

After the check valves and plumbing are welded into place, the fibrous insulation is added to the outside of the regenerator and main chamber.

The foil insulation will have to be built up, layer by layer, over the thermally and radioactively hot source to assure the continuous cup arrangement necessary to provide a good heat barrier. The outer can will be installed and electron beam-welded in place to provide a high vacuum in the foil and fibrous insulation areas.

The plumbing and pumping chambers will then be welded in place (using all the open space available) and silastic will be cast around the entire package.

5.13.7 Summary of Power Source Volumes

The total volume of the power system is approximately 1800 cm^3. Major elements of this total are shown in Table 8.

TABLE 8 – SUMMARY OF POWER SOURCE VOLUMES

Engine and fuel, cm^3	290
Shield, cm^3	600
Pumping chambers, cm^3	570
Thermal insulation, cm^3	200
Miscellaneous, cm^3	140
Total volume, cm^3	1800

BLANK

6.0 PARAMETRIC ANALYSIS

6.1 OBJECTIVES

The purpose of the parametric analysis task was to provide information concerning the operation and performance of the engine under study. The primary objective of the task was the development of data from which a thorough understanding of the engine concept could be derived. Additional objectives included the identification of important system parameters and their effects on the overall system, and the determination of the dynamic behavior of the engine.

The specific objectives are grouped into three categories: the definition of the performance and operating characteristics of the modified Stirling engine, including the verification of the validity of the overall concept and the prediction of the engine operating characteristics; the identification of the important system parameters and their effects on the system, including the development of information to assist in component selection and in the selection of operating conditions; and the examination of the dynamic behavior of the system, including the verification of linear, reversing piston concept, the determination of system response to dynamic reservoir conditions, and a check for possible system instabilities.

6.2 APPROACH

Several analytical techniques of varying degrees of complexity and accuracy were developed to achieve the objectives of the parametric task. These techniques are classified under three major headings identified by the corresponding computer programs: the simplified technique (the digital code based on the Schmidt analysis); the intermediate technique (the MIMIC digital code and the associated analog program); and the detailed technique (the DSL/90 digital code).

The simplified technique was based on the classical Schmidt analysis of the Stirling engine. The derived algebraic equations used in this technique, however, were adjusted to account for all the non-ideal conditions except for the assumption of isothermal thermodynamic processes. These equations were programmed for an IBM 1130 computer. The intermediate technique was an actual system simulation using the lumped-node model, except for the assumption of

constant wall temperatures. This simulation was programmed for the IBM 7090 (94) computer and the PACE 231R-V analog computer. The detailed technique was also a system simulation, but the model had a finer node mesh than the intermediate technique simulation and included the wall nodes. This simulation was programmed for the IBM 7090(94) digital computer.

Specific advantages and limitations, in terms of model accuracy, computational costs, and computer scheduling, are associated with each technique. The simplified codes, using the on-site IBM 1130 computer, provided information quickly and inexpensively. The intermediate analog approach provided flexibility for parameter variation and dynamic response at a relatively modest cost. MIMIC provided basically the same information as the analog but the cost and the time required to obtain the data were greater. The detailed approach was the most accurate in terms of system simulation, but the cost associated with the use of this parametric program to obtain data was prohibitive.

In consideration of the advantages and limitations of each technique discussed above, the fundamental approach involved the use of the fast, less expensive techniques for the bulk of the analysis and the use of the more expensive and slower approaches to verify and extend the results of the more simplified techniques. Under this arrangement, the simplified technique was used to define the engine operating characteristics and the influence of parameters on system performance; and the intermediate analog approach was used to examine the dynamic behavior of the engine. The MIMIC and DSL/90 codes were used to confirm or supplement the results of the simplified and analog computations.

6.3 SIMPLIFIED ANALYTICAL TECHNIQUE

6.3.1 System Simultation Model

The simplified analytical technique considered the displacer piston and cylinder, the heater, and the regenerator as the components of the system simulation model. The other components were not included but were represented by appropriate selection of pressure levels for reservoirs and were included in the total energy summation. The check valves were represented as perfect valves (i.e., no delay or backflow) which opened and closed as a function of piston position.

The analysis was based on the classical, idealized Stirling engine Schmidt analysis which, in turn, is based on ideal frictionless flow, perfect regeneration and isothermal gas conditions. These assumptions permitted the development of algebraic expressions for the system pressure, mass flow and heat flow, which were used to derive equations for the modified Stirling engine with the non-ideal conditions (such as friction pressure drop and regenerator effectiveness) taken into account. The derivation of these equations is presented in Appendix M.

The two most important quantities which were developed from this analysis were the system gross output power and the input power to the gas. The input power to the gas is the sum of the power required to maintain the chambers at isothermal conditions and the power required to make up for the regenerator ineffectiveness. The input power to the gas is given by

$$Q_{in} = Q_A + Q_B + Q_R \qquad (6\text{-}1)$$

where:

$$Q_A = DP_{min}\,(A - X_1B)\left[\frac{1}{B}\left\{\log_e\left(\frac{A - X_1B}{A - X_2B}\right)\right\} + \left(\frac{A}{B} + \sigma_{nc}\right)\left\{\frac{1}{A-X_1B} - \frac{1}{A-X_2B}\right\}\right]$$

$$Q_B = DP_{max}\,(A-X_3B)\left[\frac{1}{B}\left\{\log_e\left(\frac{A-X_3B}{A-X_4B}\right)\right\} + \left(\frac{A}{B} + \sigma_{nc}\right)\left\{\frac{1}{A-X_3B} - \frac{1}{A-X_4B}\right\}\right]$$

$$Q_R = w\,C_p\,(T_{max} - T_{min})(1 - \epsilon_r)$$

$A = \sigma_d + 1$

$B = 1 + \tau$

C_p = gas specific heat

D = displacement volume

P_{min} = minimum pressure

P_{max} = maximum pressure

Q_A = heat transfer to chamber between X_1 and X_2

Q_B = heat transfer to chamber between X_3 and X_4

Q_R = regenerator ineffectiveness loss

T_{min} = cold chamber temperature

T_{max} = hot chamber temperature

w = average regenerator flow

X_1 = piston position where intake check valve closes

X_2 = piston position where extraction check valve opens

X_3 = piston position where extraction check valve closes

X_4 = piston position where intake check valve opens

ϵ_r = regenerator effectivness

σ_d = effective system dead volume

σ_{nc} = hot chamber clearance dead volume

τ = T_{min}/T_{max}

The gross output power is given by:

$$Q_{out} = \frac{\gamma}{\gamma - 1} P_{max} (1-\tau)(X_3-X_2) D \left(1 - \left(\frac{P_{min}}{P_{max}}\right)^{\frac{\gamma-1}{\gamma}}\right) \qquad (6\text{-}2)$$

where:

γ = gas specific heat ratio and other terms are defined as above.

The other energy terms which are also included as required system power are the insulation loss, the regenerator conduction loss and the effective piston conduction loss. The terms which must be deducted from the gross power include the frictional pressure loss, the pumping chamber efficiency loss, and the control power. All these energy terms are relatively independent of the isothermal assumption used in the analysis.

6.3.2 Computer Program Description

The basic algebraic expressions derived by modification of the Schmidt approach were formalized into a compute sequence and programmed for a digital computer. The general nature of the equations permitted several different versions of a computer program to be written depending on the desired input and output information. For example, if the piston position for the extraction point was specified, the maximum pressure was computed, but, if the maximum pressure was specified, then the extraction point was computed. As a consequence, the program was used either to calculate the system conditions and performance given the system configuration, or to compute the system configuration given system performance.

The particular version of the program presented in Appendix M computes the system performance given a fixed system configuration. This program requires as input the maximum and minimum temperature; the maximum and minimum pressures, the lengths, flow areas, and wetted perimeters of the heater and the regenerator; the displacement, stroke length, frequency and end clearance of the piston; the piston positions for closing of the check valves; the parasitic power for the pumping chamber inefficiency, the control system, and mechanical friction; and the physical properties of the gas. The program computes the piston positions for the opening of both check valves, the gross output power, the regenerator effectiveness, the flow friction power loss of the heater and regenerator, the parasitic conduction losses of the piston and regenerator, the required input power to the gas and the overall efficiency of the system. The program also computes the regenerator matrix configuration for a HEXCEL honeycomb design.

The principal value of this approach is the simplicity and ease with which an extensive analysis of the system may be performed. The program(s), written for the IBM 1130, has a very short running time. The different versions of the basic program permit an initial trade-off or semi-optimization study followed by an off-design study of a particular reference design.

6.3.3 Application and Results

The studies made with the simplified analytical technique were used to establish the reference system design and to perform a major portion of the component analysis, particularly for the heater and regenerator. The results of these studies are presented in the appropriate portions of Section 5.0 and summarized in Section 6.6.

6.4 INTERMEDIATE ANALYTICAL TECHNIQUE

6.4.1 System Simulation Model

The intermediate analytical technique considered the engine portion of the overall system and included the displacer piston and cylinder, the reversing piston and cylinder, the heater, the regenerator, and the check valves as components. The remainder of the system was represented by assumed time-dependent boundary conditions and by fixed parasitic losses. The boundary conditions were the temperatures and pressures of the reservoirs and the temperature of the heater wall.

This technique involved the analysis of a system dynamic simulation of the engine. The simulation was accomplished by writing the differential equations for the system and making an approximation by substituting finite-differences for the differentials with respect to the linear dimension. The finite-difference technique required that the system be divided into finite nodes which have lumped thermal capacitances. Thus the system equations become the interchange relationships between nodes and describe the conservation of mass and energy within individual nodes. The interchange equations are algebraic expressions and the conservation equations are integral equations with respect to time.

In comparing the integral equations of the wall node temperatures and the gas node temperatures, the wall nodes have equation time constants of the order of two or three orders of magnitudes larger than the gas node time constant. Thus, the wall node temperatures are essentially constant during gas node temperature excursions, and the assumption was made that the wall temperatures were constant. Expressions are derived only for the gas nodes.

The model has one gas node each in the displacer piston hot chamber, the piston cold chamber, the reversing piston upper chamber and the reversing piston lower chamber. The heater has three gas nodes and the regenerator has five gas nodes. The development of the system equations is shown in Appendix N. The temperature of the gas node in any chamber is determined by performing an energy balance on the node as given by:

$$T = \int \frac{1}{m}\left[T \Sigma w_i + \frac{H}{C_v}(T_W - T) + \gamma \Sigma w_i T_i - PA\frac{dx}{d\theta}\right]d\theta \qquad (6\text{-}3)$$

where:

m = mass of gas in node

w_i = flow of gas in or out of the node

H = heat transfer conductance between wall and gas

C_v = gas specific heat at constant volume

T_W = wall temperature

γ = gas specific heat ratio

T_i = temperature of incoming or outgoing gas

P = pressure of node gas

A = cross sectional area of chamber

x = piston displacement

The temperature of a gas node in either the heater or the regenerator is also determined by performing the energy balance given by:

$$T = \frac{\gamma - 1}{A} \int \frac{T}{P} \left[H (T_W - T) - \frac{w C_P}{2L} (T_A - T_C) \right] d\theta \qquad (6\text{-}4)$$

where:

C_p = gas specific heat at constant pressure

L = length of node

T_A = temperature of downstream gas node

T_C = temperature of upstream gas node

The pressure of a gas node is determined by using the equation of state:

$$P = \frac{mRT}{V} \qquad (6\text{-}5)$$

where:

V = volume of the node

R = gas constant

The mass of gas in each node is determined by performing a mass balance on the node as given by:

$$m = \int \Sigma w_i \, d\theta \qquad (6\text{-}6)$$

where:

$w_i = K \frac{P}{T} (\Delta P)$

K = flow coefficient

ΔP = pressure difference between nodes

The piston velocity and displacement is determined by performing a force balance on the piston by the equations:

$$\frac{dx}{d\theta} = \int \frac{1}{m_p} \left[\Sigma P_i A_i + F_f \right] d\theta \tag{6-7}$$

$$x = \int \frac{dx}{d\theta} \, d\theta \tag{6-8}$$

where:

m_p = mass of the piston

F_f = friction force

The two most important output quantities developed by this technique are the input power to the gas and the gross output power. The input power to the gas is given by the equation:

$$Q_{in} = \int \Sigma H (T_W - T) \, d\theta \tag{6-9}$$

where:

T = temperature of heater gas node

The gross output power is given by:

$$Q_{out} = \int C_p T_{HP} \left(1 - \left(\frac{P_{min}}{P_{max}} \right)^{\frac{\gamma-1}{\gamma}} \right) w_{HP} \, d\theta \tag{6-10}$$

where:

T_{HP} = extraction temperature

P_{min} = minimum gas pressure

P_{max} = maximum gas pressure

w_{HP} = extraction gas flow rate

In addition, the frictional pressure drop loss is given by:

$$Q_{DP} = \int \Delta P_{HP} \frac{w_R R T}{P} \, d\theta \tag{6-11}$$

where:

ΔP_{HP} = frictional pressure loss in heater and regenerator

w_R = regenerator gas flow rate

The dynamic simulation model also includes flow equations which represent leakages in the system. The leakages occur around the displacer piston, through the seal between the displacer chamber and the reversing chamber, around the reversing piston and as a result of possible backflow through the check valves.

6.4.2 Computer Program Description

The system simulation equations were programmed to be used as input to the MIMIC* digital computer program, a code for solving systems of ordinary differential equations on an IBM 7090(94) computer. MIMIC can be considered a digital analog simulator because a sorting algorithm in the program processor permits the input program to very closely resemble the original problem statement and permits the problem equations to be written in any order.

The MIMIC language uses a set of arithmetic operators and a set of functions. The arithmetic operators are standard Fortran symbols for addition, subtraction, multiplication and division. Four of the special functions available were used; these were:

1) R = EXP (A,B) $\quad R = B^A$

2) R = LIN(A,B,C,D) $\quad R = A \quad B \leq C \leq D$

$\quad R = 0 \quad D < C < B$

3) R = FSW(A,B,C,D) $\quad R = B \quad A < 0$

$\quad R = C \quad A = 0$

$\quad R = D \quad A > 0$

4) R = INT(A,B) $\quad R = B + \int_0^\theta A \, d\theta$

Note that the term B of the integral is the initial condition. The integration method is a high-order Runge-Kutta variable step integration routine in which the step size is automatically varied by the requirements of the problem to insure that the integration error does not exceed a given bound.

The input required by MIMIC are the problem equations together with the required problem input data to yield the desired output data. A listing of the problem equations as well as the required input and output parameters are shown in Appendix N. The required input data include: the thermodynamic and

* SEG-TP-67-31, "MIMIC Programming Manual," F. J. Sansom and H. E. Petersen, ASD, Wright-Patterson Air Force Base, Ohio, July 1967.

physical properties of the gas; the physical dimensions of the displacer chamber, reversing chamber, the heater and the regenerator; the pressures and temperatures of the reservoirs; the flow coefficients of the system flows; and the wall temperatures of the system. The output data, which are instantaneous values, include: the gas nodes temperatures and pressures; the system flows, the piston displacement and velocity; and the pertinent heat flows. The integrated heat flows are also output.

It should be noted that certain simplifications of the system model were included in the set of problem equations to limit the size of the problem. The mass balance equations for the heater and regenerator were not included in the problem; the assumption was made that the system pressure is essentially uniform at any instant and that the flow phenomenon through the heat exchangers can be represented by a flow resistance which connects the hot and cold displacer piston chambers. The only ramification of this assumption is that the dead volumes of the heat exchangers must be represented by some means; this was accomplished by placing equivalent volume end clearances in the hot and cold chambers.

The running time of this program is extremely long. The time constants for the gas temperature equations are of the order of 5×10^{-6} sec, which requires the same order of magnitude minimum integration interval. As a result the ratio of machine time to problem time is approximately 3500 or approximately 9 minutes of IBM 7094 machine time to solve for 0.15 seconds of problem.

The same basic system equations were programmed for the analog computer in order to circumvent the problem of the small integration interval. The analog has the distinct advantages of scaling the equations (so that the machine time-to-problem time ratio can be any value desired) and of having perfect integrators. The penalty of using an analog computer is the decrease in accuracy in the output parameters data.

Several additional features were included in the system equations developed for the analog models to take advantage of the ability to examine the engine performance over a long time duration. The boundary conditions (reservoir pressures) were provided by function generators which simulated the pressure excursions of the pumping chamber. The regenerator wall temperatures were determined by a temperature averaging process which adjusted the original input wall temperatures. In addition, equations were added which permitted a delay in the opening and closing of the check valves. These equations are presented in Appendix N.

6.4.3 Application of Intermediate Analytical Technique

Preliminary work was required to determine suitable wall temperatures to be used as input values to the programs. The average wall temperatures of the hot and cold chambers of the displacer piston were taken from the analysis of the heat transport down the cylinder (Appendix B). These temperatures were based on the thermal profiles of the chambers for given average gas temperatures. The heater wall temperature is an input parameter so that the gas temperature in the hot chamber is dependent on the heater wall temperature selected. The regenerator wall temperatures were based on preliminary work

done with a dynamic modeling program* to determine the longitudinal temperature distribution with a matrix regenerator. This work verified the linear nature of the temperature distribution as predicted by Hausen.** Therefore, a linear temperature distribution was input to the programs. It should be noted that all the wall temperatures must be adjusted until the temperature conditions of the gas are matched to the wall temperatures in order to develop a good approximation to the actual steady state values.

The system reference conditions and dimensions for the analysis were taken from the results of the simplified analytical investigations; this arrangement was necessary in order to limit the range of parameters to be investigated.

The three objectives of the intermediate analytical technique were: to provide a normalization check for the simplified analytical technique; to investigate features (such as leakages and the reversing piston) which are not included in the Schmidt analysis; and, to investigate the system dynamics and cyclic nature of the system parameters. In view of the specific advantages of the two computer program approaches (the high accuracy of the digital program and the ability of the analog to investigate long-term transients and accommodate readily adjustable input parameters), MIMIC was used to provide the normalization check and the analog was used to attain the other two objectives.

The normalization check was performed by running both MIMIC and the simplified code with the same system physical dimensions and boundary conditions and comparing the results. Normalization was considered to be accomplished when the parameters or effects causing any difference between the two methods could be identified and adjustment factors could be determined. The investigation of the special features and the system dynamics and varying the problem parameters to ascertain the effect of those parameters on the system. The parameters investigated included the displacer piston leakage, the labrynth seal leakage, the reversing piston leakage, the check valve backflow, system pressure ratio, the system dead volume, the system minimum temperature, and the regenerator heat transfer area. In addition, the system response to dynamic reservoir pressures and the verification of operation of the sealed reversing piston were included in the analog studies.

The results of the intermediate analytical technique computer programs are summarized in Section 6.6.

6.5 DETAILED ANALYTICAL TECHNIQUE

6.5.1 System Simulation Model

The detailed analytical technique considered essentially the same basic system and method of analysis as the intermediate analytical technique. The basic difference between the two approaches was an attempt to improve the simulation by dividing the hot and cold chambers into finer nodes and by including the equations of the wall nodes.

* IBM 1130 Continuous System Modeling Programs 1130-CX-13X.

** M. Jakob, "Heat Transfer" Vol. II, John Wiley and Sons, New York, 1957, pp 289-296, 320-325.

The detailed model has three gas nodes in the hot chamber, two gas nodes in the cold chamber and the same number of gas nodes in the other components as the intermediate model. This arrangement results in ten nodes representing the displacer piston cylinder, six nodes for the displacer piston, two nodes for the reversing piston cylinder, two nodes for the reversing piston cylinder, one node for the heater wall and five nodes for the regenerator wall. The development of the system equations is shown in Appendix O, along with a schematic model with nodes.

The equations which were changed from those used in the intermediate model include the chamber pressure equation, the chamber gas temperature equations and the addition of the cylinder node temperature equations and the heat exchange wall temperature equations. The general chamber pressure equation is:

$$P = \int \frac{\gamma R}{AV}\left[\frac{q_o}{C_p} + \Sigma(w_i T + w_i (T_i - T)\ \rho(w_i) + \frac{PA}{R}\frac{dx}{d\theta}\right]d\theta \qquad (6\text{-}12)$$

where:

γ = gas specific heat ratio

R = gas constant

A = cross-section area of chamber

V = volume of chamber

q_o = total heat flow into the chamber from the wall

C_p = gas specific heat at constant pressure

w_i = gas flow in or out of the chamber

T = chamber gas node temperature where w_i occurs

T_i = temperature of gas flow in or out of chamber

$\rho(w_i)$ = function which is one if w_i is negative, otherwise zero

x = displacement

θ = time

The general chamber gas node temperature is given by:

$$T = \int \frac{RT}{PV}\left[\Sigma\, w_i\ (T_i - T) + \frac{q_o}{C_p} + \frac{V}{C_p}\frac{dP}{d\theta}\right]d\theta \qquad (6\text{-}13)$$

The general chamber wall node temperature equation is:

$$T_W = \int \frac{1}{m_W C_{pW}} \Sigma q_i \, d\theta \qquad (6\text{-}14)$$

where:

m_W = mass of the wall node

C_{pW} = specific heat of wall node

q_i = individual energy transported to or from the node

The gas nodes in the heat exchangers are the same as the intermediate method but the general regenerator wall node temperature is given by:

$$T_{WB} = \int \frac{1}{m_{WB} C_{pWB}} \left[H \, (T_{WB} - T_B) + \frac{K}{L} \, (T_{WA} + T_{WC}) \right] d\theta \qquad (6\text{-}15)$$

where:

m_{WB} = mass of the wall node

C_{pWB} = specific heat of the wall node

H = heat transfer conductance between gas and wall

T_B = temperature of adjacent gas node

K = longitudinal conductance between wall nodes

L = length of wall node

T_{WA} = temperature of adjacent upstream wall node

T_{WC} = temperature of adjacent downstream wall node

6.5.2 Computer Program Description

The system simulation equations were programmed to be used as input to the DSL/90* digital computer program,an IBM developed program for solving systems of ordinary differential equations on an IBM 7090(94) computer. DSL/90 has basically the same features of MIMIC except that the functional capability as a simulator language is more sophisticated and on a larger scale. DLS/90 permits the use of a maximum of 300 integrators and/or memory elements as compared with MIMIC's maximum of 95 integrators and/or first-order transfer functions.

* TR-02.355 "DSL/90 Digital Simulation Language Users Guide", W. M. Syn and D. C. Wyman, IBM Systems Development Division, San Jose, California.

The DSL/90 language uses arithmetic operators and functions. The standard Fortran symbols for addition, subtraction, multiplication, division and exponentiation are used. The only special function used of those available is:

$$R = \text{INTGRL } (A,B) \qquad R = A + \int_0^{\theta} B \, d\theta$$

It should be noted that subfunctions and subroutines can be used in DSL/90 as in standard Fortran IV language. There are five integration schemes available in DSL/90: a fourth order Runge-Kutta with variable or fixed integration steps; a variable step, fifth order, predictor-corrector Milne integration; a fixed integration interval Simpson's rule; a trapezoidal integration; and a rectangular integration.

The required input to DSL/90 is basically the same as MIMIC except that the number of input quantities is greater since the wall characteristics are also included. The output is also basically the same but is increased in number because of the larger number of nodes.

The running time of the problem is extremely long. The time constant for the gas temperature equations are of the order of 1×10^{-6} sec. This required integration interval added to the increase in the number of equations makes the running time approximately 20 times that of MIMIC. The ratio of machine time-to-problem time is approximately 70,000 or approximately 9 minutes of IBM 7094 machine time to solve for 7.7 milliseconds of problem time.

6.5.3 Application of Detailed Analytical Technique

The main objective of the detailed analytical technique was to determine the effect of considering a more precise model than was used in the intermediate analysis. The validity of the assumption of constant wall temperatures was of particular interest, although the identification of other phenomena occurring in the system was also important.

The analysis was performed by selecting a reference design and running the program long enough to examine the engine operation. The problem initial conditions were selected from the results of the analysis performed with the intermediate technique to reduce the required running time.

6.6 SUMMARY

The results of the parametric analysis are grouped according to the objectives which were to be accomplished. The first objective (determining the performance and operating characteristics of the engine) was accomplished using a combination of the three basic techniques. Results of the DSL/90 runs confirmed that the wall temperatures in the system are essentially constant during the time period equivalent to one cycle. This finding permitted the assignment of confidence to the use of the MIMIC model to yield results which would be a good approximation of those obtained with DSL/90.

The comparison of the results of the simplified and intermediate techniques, however, indicated that there existed a significant difference between

the two methods. Since it is desirable to formulate a good representation of the system and at the same time use a simple method for the analysis, a normalization process was developed to resolve the differences. The basic difference between the two models is the assumption of isothermal conditions in the simplified model as opposed to the variable temperatures used in the MIMIC model. The increase in system temperature during compression in the dynamic model results in a higher pressure response in MIMIC than in the simplified model, and yields more available power. For example, comparing the two models for the case where gas extraction occurs at the same piston position, the dynamic model achieved a pressure ratio of 1.25, whereas the simplified model achieved a pressure ratio of 1.13 with a corresponding lower (by 50%) available power per cycle.

Since the inconsistency in available power was caused by the erroneous pressure response, the results of the two analyses were normalized by the adjustment of another parameter which compensated for the temperature. For example, if the unswept volume in the simplified model is adjusted, the analysis yielded results which correlated well with those of the dynamic model. With the normalization of the three techniques, a consistent model of the system was established from which performance and operating characteristics of the engine could be determined. A typical plot of system characteristics as determined by MIMIC and the analog are shown in Figures 38 and 39.

The second objective of identifying the important system parameters and their effects on the system performance was accomplished by using the simplified technique and the analog approach. The simplified model was used to assist in the evaluation of components and typical analysis and results are presented in Appendix A. The simplified model was also used to determine the effects of the more general system parameters, such as the system maximum temperature, the regenerator effectiveness, system unswept volume and system pressure level. These parameters, except for system pressure, were investigated for a system with the same geometry and the same output power. The system pressure level, however, could not be compared on a similar basis as the other parameters since the pressure level dictates the engine size for a given output power. Therefore, two systems were considered - one at a minimum pressure of 15 psia and the other at 60 psia. The results of these investigations are plotted in Figure 40.

The analog was used to investigate other parameters and features of the engine. The parameters considered with the intermediate technique on the analog computer included the displacer piston leakage, the labyrinth seal leakage, the reversing piston leakage, the system pressure ratio, system unswept volume, and the regenerator surface area. The analysis was performed by using the influence-coefficient approach, where a reference design is specified and one parameter is varied at a time. Thus, the engine output power was not held constant. In addition, the regenerator surface area was selected as a parameter because the definition of regenerator effectiveness in the dynamic model was not clearly established. The effect of the parameters on system output power and thermodynamic efficiency is shown in Figures 41 and 42.

The use of the dynamic simulation model for the study of system parameters proved somewhat more difficult than the use of the simplified model. In the simplified model, there were a prescribed number of independent

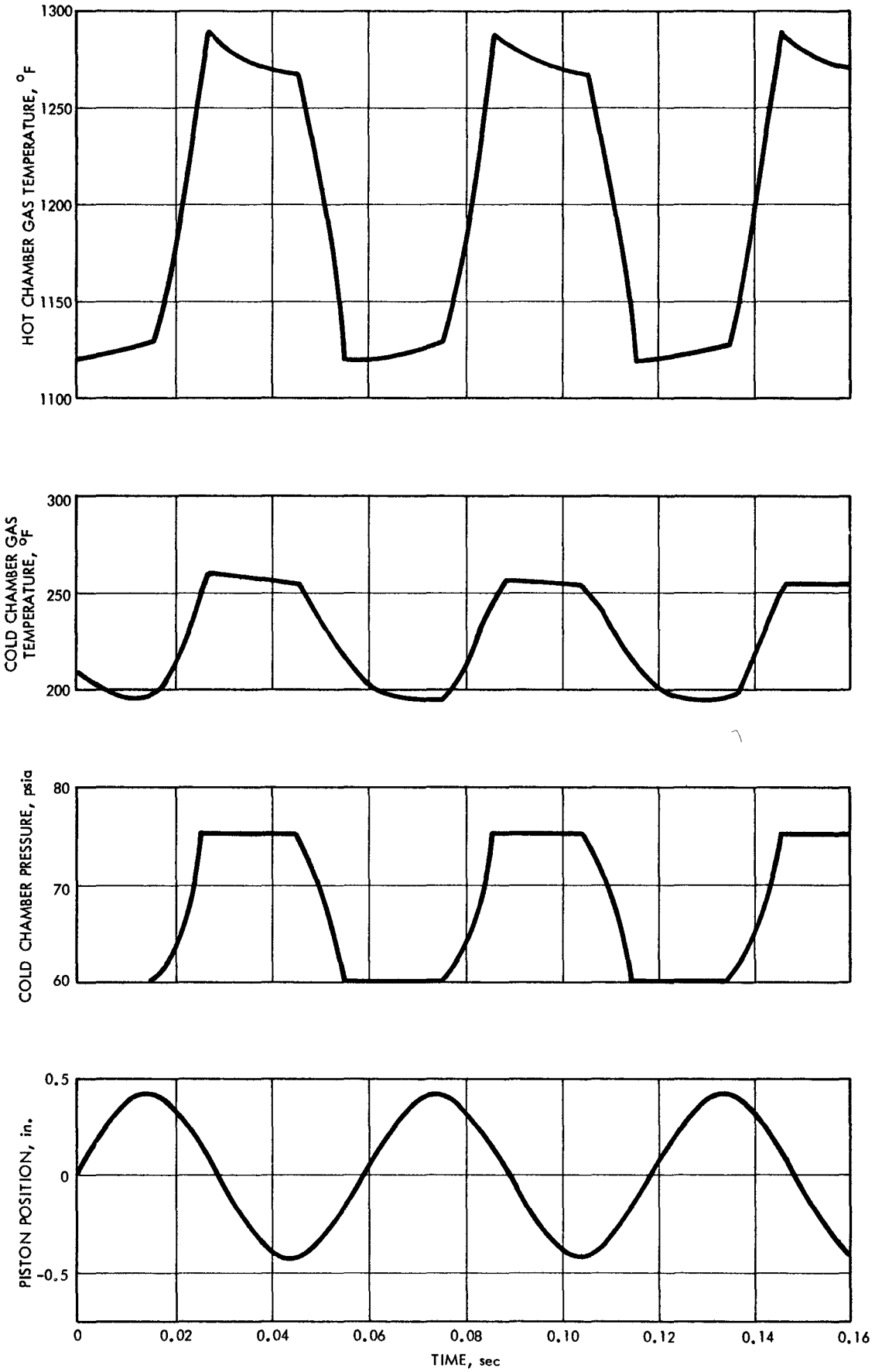

FIGURE 38. TYPICAL RESULTS FROM DYNAMIC MODEL (DIGITAL)

3.01-67-991

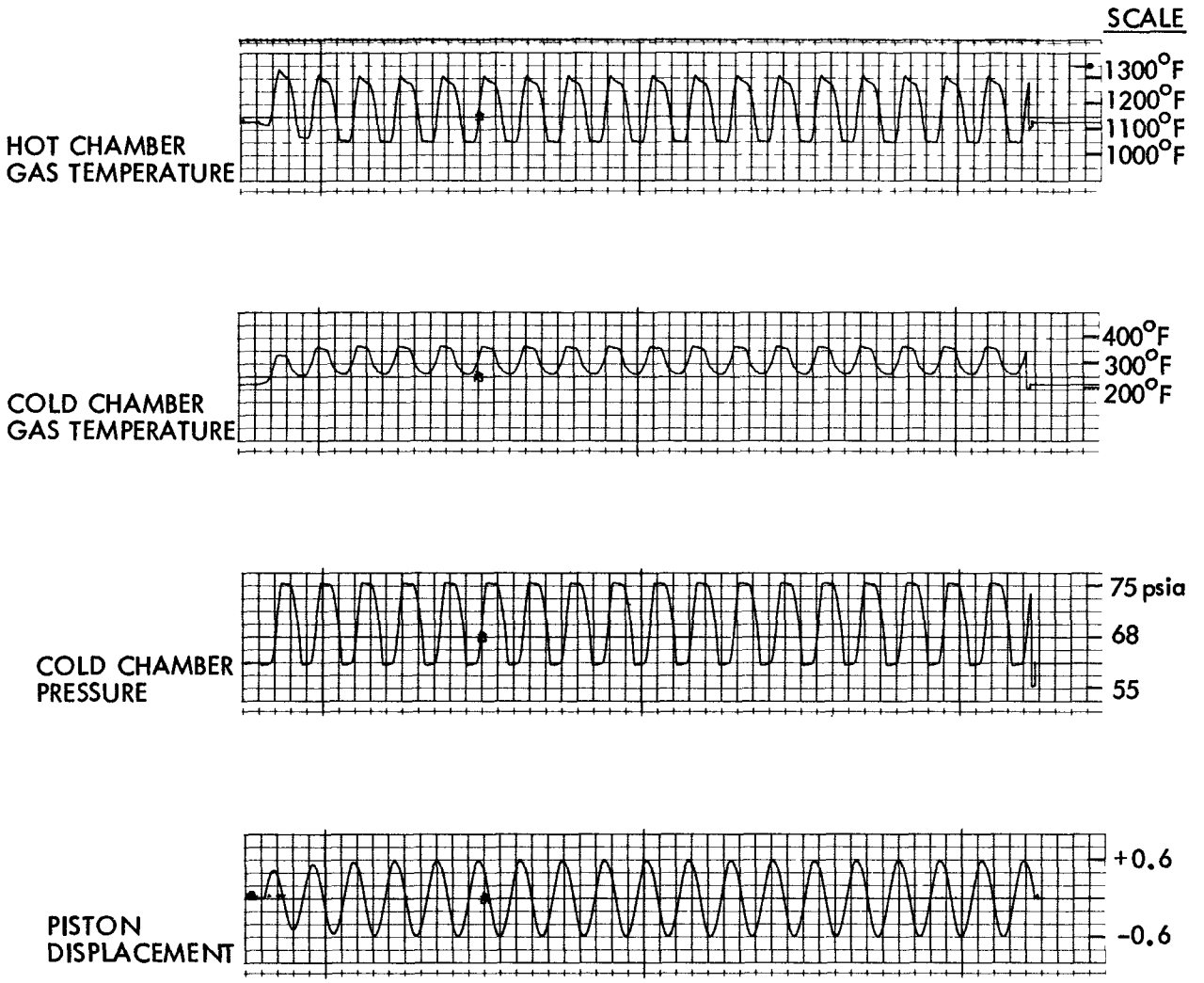

FIGURE 39. TYPICAL RESULTS FROM DYNAMIC MODEL (ANALOG)

3.01-67-992

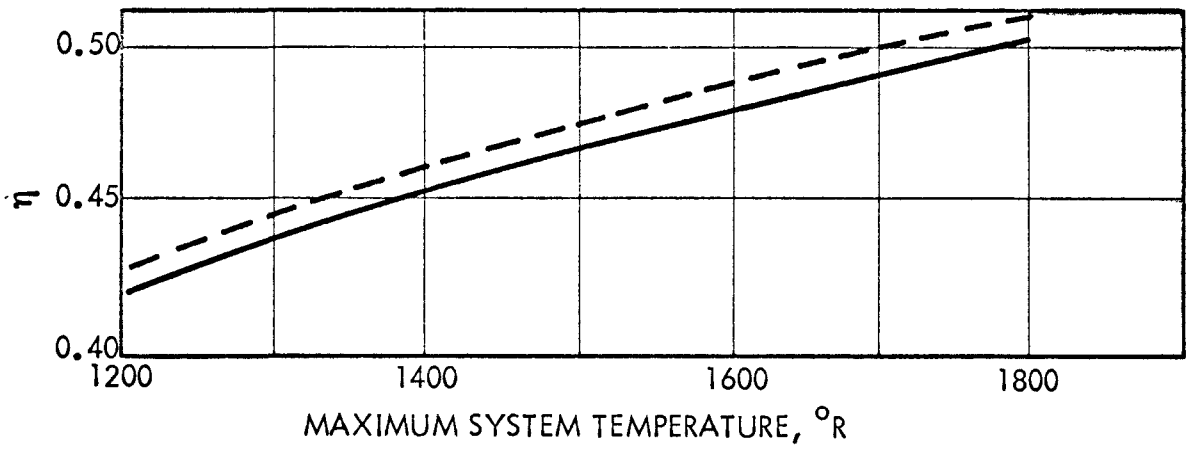

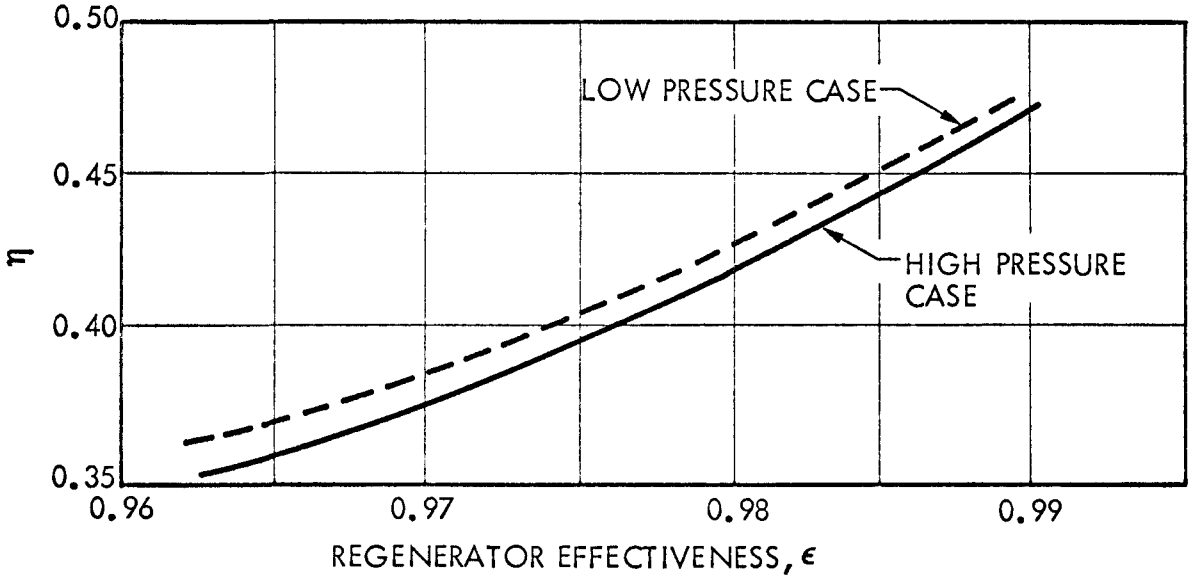

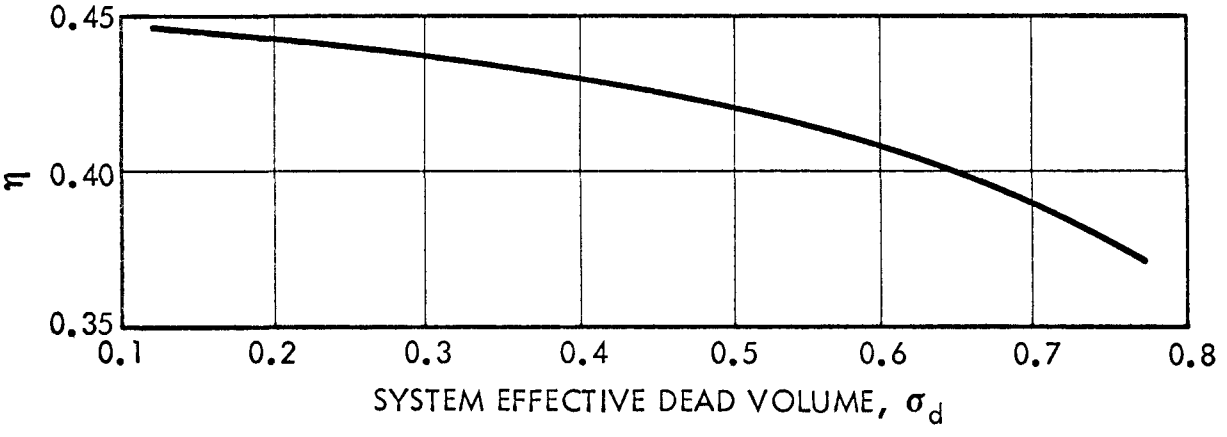

3.01-68-093

FIGURE 40. EFFECT OF SYSTEM PARAMETERS ON RELATIVE EFFICIENCY

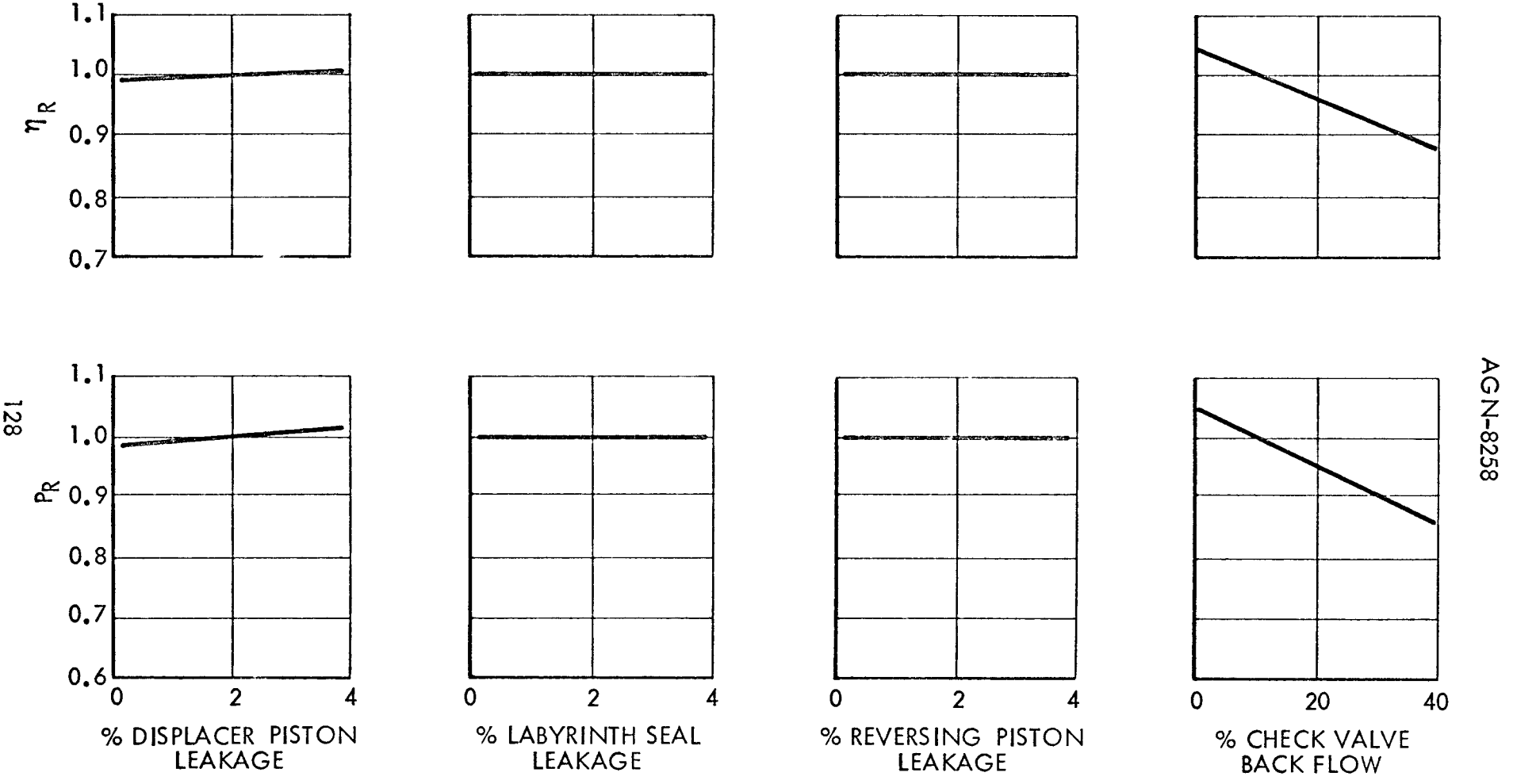

FIGURE 41. EFFECT OF SYSTEM LEAKAGES ON RELATIVE THERMODYNAMIC EFFICIENCY, η_R, AND RELATIVE GROSS OUTPUT POWER, P_R

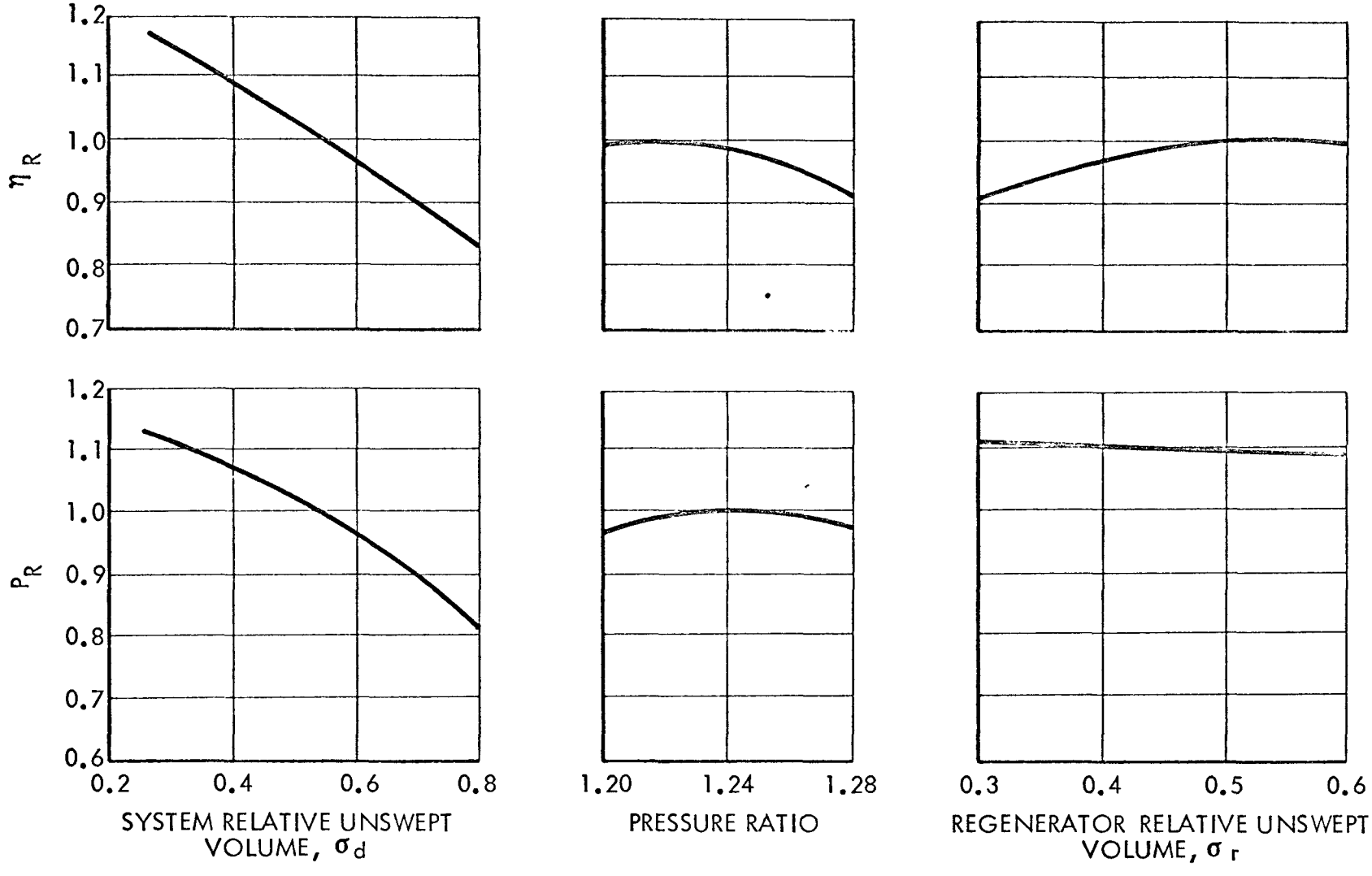

FIGURE 42. EFFECT OF SYSTEM PARAMETERS ON RELATIVE THERMODYNAMIC EFFICIENCY, η_R, AND RELATIVE GROSS OUTPUT POWER, P_R

parameters (e.g., displacement, unswept volume, temperature, pressure, etc.) and a number of dependent system parameters (e.g., output power, efficiency, etc.). The parametric analysis was performed by varying the independent parameters one at a time and observing the effect on the dependent parameters. For the dynamic model, however, some of the previously independent parameters become dependent. For example, varying the regenerator surface area increased the regenerator pressure drop, which increased the cycle frequency and decreased the stroke which, in turn, increased the system unswept volume. Some of these parameters could be adjusted to their original values but this approach proved too difficult in the case of several parameters. Although this parametric dependency limited the amount of definitive parametric analysis performed by this model, important insight to the system operational dynamics was achieved.

The results of the simplified and analog parametric analyses were used to assist in the evaluation of the performance of the reference system design. The two parameters which define the system performance are the gross output power and the gross thermal power. These two parameters were determined by performing an overall system energy balance as shown below:

Available output power	7.0 watts
Reversing piston power	0.9
Operational control power	1.0
Pumping chamber and line losses	0.5
Check valves loss	0.3
Gross output power	9.7 watts
Thermal power to gas	23.7 watts
Regenerator conduction loss	2.3
High temperature insulation loss	1.7
Piston and cylinder conduction loss	6.0
Gross thermal power	33.7 watts

The system gas thermodynamic power terms which included the available output power, the reversing piston power, and the thermal power to gas were calculated using the analog computer. The thermal power to gas includes losses due to regenerator ineffectiveness and due to energy transport from the gas to the cylinder wall. The operational control power requirement was established in Section 5.11. The pumping chamber and line losses were estimated and the check valve loss was determined in Section 5.5. The regenerator, high temperature insulation and the piston-cylinder conduction losses were determined in their respective component analysis sections which are described in Sections 5.3, 5.4 and 5.1 respectively.

A summary of the engine conditions that result in the above thermodynamic performance is given in the following table:

Average hot chamber temperature, ^{o}F	1200
Average cold chamber temperature, ^{o}F	250
Low pressure reservoir pressure, psi	60
High pressure reservoir pressure, psi	74
Engine speed, rpm	1000
Engine displacement, in^3	1.32
Relative unswept volume, hot chamber	0.2
Relative unswept volume, cold chamber	0.2
Relative unswept volume, regenerator	0.6
Regenerator effectiveness, %	0.98
Piston stroke, in.	1.5
Piston length, in.	1.3
Piston diameter, in.	1.06
Piston and cylinder material	Hastelloy C
Maximum fuel temperature, ^{o}F	1300

The third objective of examining the dynamic behavior was performed using the analog computer. As previously indicated, this method provided valuable insight into the parametric relationships of the system. The linear reversing piston concept was studied in some detail since this driving mechanism was part of the model in the study of the system parameters. Two different concepts were studied: a system where high pressure gas was injected through ports into the reversing piston chamber to drive the system; and the reference case, in which power is delivered to the reciprocating mass directly from the displacer cylinder.

The investigation of system response to dynamic reservoir conditions and the question of possible system instabilities both led back to the reversing piston concepts. The operation of the system is ultimately dependent on the ability to provide sufficient continuous energy to the piston system to overcome aerodynamic and frictional losses. If this criterion is satisfied, the engine will continue to operate through any reasonable system pressure excursion, although perhaps not of design output power or efficiency. Therefore, the desirable approach is to over-design the energy input mechanism and dissipate the excess energy.

The ported concept inputs energy to the piston by injecting high pressure gas to the reversing piston. The dissipation of any excess energy is inherent on this design and is accomplished by returning the high pressure gas to the reservoir system. Thus, the design involves merely the proper selection of the port location to accommodate the lowest anticipated pressure level. The reference concept inputs energy through the differential area caused by the connecting rod. The dissipation of energy requires a dashpot mechanism, so the design involves selecting the proper differential area and an adequate dash pot concept.

BLANK

7.0 COMPARATIVE ANALYSIS

Only the Stirling and Rankine power conversion cycles have been proposed for use in implantable power sources. Consequently, this discussion will be restricted to these cycles and to the general types of engines being proposed for this application. The comparative analysis concentrates on the power conversion process, although interface considerations are discussed where these are critical.

7.1 LOW-SPEED STIRLING ENGINE

One of the concepts proposed as an implantable power supply can be described by the following general characteristics:

- Operates on the Stirling cycle, with work being extracted in the form of a pressurized gas.
- Linear concept used for Stirling engine with work required to support oscillation provided directly by the displacer cylinder.
- Operates at speed equivalent to heart rate so that direct coupling between engine output and artificial heart is possible.
- Operates at pressure level of circulatory system (and at the pressure ratio of the left ventricle) so that direct coupling between engine and circulatory support system is possible.
- Regenerator is integral with displacer piston.

These characteristics were considered by Aerojet during the early phase of the program reported herein and all except the first two were rejected for technical reasons.

7.1.1 Engine Description

The following conditions were assumed, in addition to those listed above, to define the configuration and performance of this type Stirling engine.

Maximum Gas Temperature, ^{o}F	1200
Minimum Gas Temperature, ^{o}F	200
Regenerator Volume	0.5 x (Displacement)
Unswept Volume at Hot & Cold End	0.05 x (Displacement)
Minimum Gas Pressure, psia	14.7
Displacer Cylinder L/D	0.9
Engine Speed, cycles/sec	2.5
Gross Power (to achieve 7 watts net), watts	10
Regenerator Material	Steel Wool

7.1.2 Engine Size

Maximum power density and efficiency are achieved if gas is extracted from the engine at a pressure ratio of about 1.28 or at 18.8 psia. For this condition, an isothermal (Schmidt) analysis indicates a power density of 192 ft lb/ft^3-stroke. A gross output of 10 watts at 2.5 cycles/sec. requires an engine displacement of about 26 in^3. This compares with the displacement of 2.1 in^3 for the engine originally proposed by Aerojet and 1.35 in^3 for the reference conceptual design. The internal dimensions of the displacer piston for the low-speed Stirling engine are 3.9 in. dia and 3.5 in. long. The piston area is 12.1 $in.^2$, the stroke is about 2.2 in. and the regenerator length is about 1.1 in.

7.1.3 Heat Losses

The parasitic heat loss through the regenerator will be very large because of the large cross-sectional area. The regenerator matrix consists of steel wool which is filled with helium. The thermal conductivity of the helium alone is about 0.12 Btu/hr-ft-^{o}F and the conductivity of the regenerator matrix is estimated to be about 0.20 Btu/hr-ft-^{o}F. Consequently, the heat loss by simple conduction through the regenerator will be about 27 watts.

The large size of the displacer cylinder results in other large parasitic heat losses, particularly as a result of the mechanical pumping of heat. The net result is poor efficiency which is caused by the low power density resulting from the low engine speed and low pressure.

7.1.4 Heat Transfer Into Gas

The integration of the regenerator with the displacer piston is occasionally proposed as a modification to the Stirling engine. The main disadvantage of this approach is the difficulty in transfering heat into and out of the engine gas. With a separate regenerator, the gas can be made to flow through a separate heater in which the flow geometry and heat transfer geometry are of the designer's choice. The integral regenerator requires heat to be transfered to the gas through the piston ends. Various techniques

can be employed to maximize this heat transfer, such as increasing the surface area and promoting gas circulation, but these techniques require other compromises and are limited in effectiveness.

In this evaluation, it is assumed that gas circulation in the hot and cold chamber is improved by providing nozzles at the entrance and exit of the regenerator. It is difficult to calculate exact heat transfer conditions because the flow conditions depend on the exact location and characteristics of these nozzles and also on piston position. However, two different techniques were used to estimate the heat transfer conditions at mid-stroke.

In the first technique, the gas space was divided into two concentric volumes. The thermal resistance was assumed to consist of the outer layer of gas and the thermal capacitance was assumed to be concentrated at the surface between the two gas volumes. It was also assumed that heat was transfered to the gas from both the cylinder end and the piston face. Calculations indicated that a temperature difference of about 600°F was required to transfer 50 watts to the gas.

The second method of estimating heat input to the gas was to treat the hot chamber as if it were a gas passage in which laminar flow was occurring. The hydraulic diameter was twice the chamber height. Again assuming that heat was transfered to the gas from both surfaces, the calculated temperature difference required to transfer 50 watts to the gas was 560°F.

While neither of the above techniques yields very accurate results, the general agreement between the two calculated temperature differences indicates that the values are probably nearly correct. It is more likely that heat will be transfered to the gas only through the cylinder end, rather than through both the cylinder end and piston face. If this is the case, then the required temperature difference is increased by a factor of four. The conditions described are for mid-piston stroke; heat transfer will be better when the piston is closer to the cylinder end and poorer when it is farther away.

It is theoretically possible to operate an engine with a temperature difference of this order (600°F) in the hot chamber since such a difference is within the temperature capability of potential radioisotope fuels. The major difficulty is that parasitic heat losses, already high, would be increased even further. However, it is an unacceptable technique for heat rejection from the cold chamber since heat must be rejected at about 100°F and the cold chamber temperature must be as low as possible.

7.1.5 Summary

The performance of an engine of the type described above will be marginal due to the low power density, high parasitic heat loss and poor heat transfer into and out of the displacer cylinder. The power density can be increased by increasing the pressure level and engine speed. However, this will increase the parasitic heat loss through the regenerator if the length is decreased and will degrade heat transfer into the engine if the

diameter is decreased. The best solution is to separate the regenerator and displacer piston (so that a heater can be added) and to increase the engine speed.

Operation of the engine at the heart rate does not eliminate the requirement for components performing the functions of the pumping chambers incorporated in the Aerojet concept. The engine operates at about the pressure ratio required by the left ventricle but some provision must be made for the lower pressure ratio required for the right ventricle. In addition, a barrier to prevent diffusion of engine gas into the blood must be provided for both left and right ventricle systems. Control of the engine may also be complicated by the very close coupling between the engine and the circulatory system.

7.2 RECIPROCATING STEAM ENGINE

The primary advantage of the Stirling cycle when compared with other thermodynamic cycles, is that the Stirling engine can achieve very high thermodynamic efficiencies (about 20%). This minimizes the size, weight and cost of the shielded radioisotope heat source, as well as the heat load on the body.

There is little doubt that a small, completely-closed Rankine cycle system could be made to operate but the concept has several inherent disadvantages. These include the following:

- Liquid-Vapor Interface Problems: Condensed liquid must be reliably returned to the boiler feed pump suction regardless of the orientation of the system. A possible solution to this problem involves the utilization of surface tension forces in small capillary passages. Boiling interface problems may require the use of a once-through (Sultzer type) boiler. Although the concepts of capillary action condensate return and a once-through boiler represent acceptable solutions to the liquid-vapor interface problem, the incorporation of these concepts create new problems, particularly with regard to water purity.

- Water Conditioning: Water chemistry in a Rankine system will change with time, even though high purity water is provided initially and care is taken in the selection of materials of construction. The normal procedure in steam plants involves a continuous adjustment of water conditions by additives or purification techniques. If the water condition is not controlled: the water may become more corrosive to materials of construction; scale may form on boiler surfaces, reducing the flow and heat transfer; corrosion products may precipitate on sliding surfaces, causing increased friction and wear; and dissolved materials may affect the surface tension, disrupting the condensate collection system if it depends on surface tension.

- Thermodynamic Efficiency: The major disadvantage of the small reciprocating steam engine is low thermal efficiency. Detailed calculations in Appendix P show that the maximum practical efficiency which may be achieved from a reciprocating steam engine is 10 to 13%. The equivalent Stirling engine efficiency is about 24%, indicating that the Stirling engine has an efficiency advantage of about a factor of two.

7.3 POSITIVE DISPLACEMENT ROTARY STEAM ENGINE

The rotary vane-type steam engine did not appear to warrant separate performance analysis and none was conducted. Generally, the comments made regarding the reciprocating steam engine also apply to the rotary engine. The rotary engine has an additional parasitic heat loss due to the short conduction path across the vane. If saturated steam is used, as has been suggested, then the initial condensation losses are much larger than those calculated for the reciprocating steam engine (See Appendix P).

BLANK

8.0 IDENTIFICATION OF MAJOR PROBLEMS

The potential problems associated with the development of an implantable power source have been categorized as fundamental and developmental in the following discussion. Fundamental problems are those whose solution requires favorable results from research not yet conducted. Developmental problems are those whose solution is simply a question of design, testing, quality control, etc. Most of the fundamental problems relate to interface areas, either with the radioisotope fuel or with the body.

None of the problems identified to date indicate that the implantable power source cannot be developed using straightforward engineering development techniques or that the resultant system will fail to satisfy any of the performance criteria.

8.1 FUNDAMENTAL PROBLEMS

8.1.1 Size

The size of the engine is within the specified limits but the unit would be more satisfactory if it could be made smaller. Some reduction in size appears possible by design modification but more significant reductions could be made:

- If the neutron dose rate at the surface of the shield can be increased (the shield thickness and volume reduced)
- If the size of the encapsulated source can be reduced by showing that the helium generated by alpha decay of plutonium is retained within the fuel material. This would also result in a decrease in shield volume.
- If the circulatory support system can pump asynchronously (the size of the pumping chambers can be reduced)

8.1.2 Control

The minimum circulatory support system control requirements for normal activity are not known. The nature of the input control signal is also un-

certain. Final design of the control system cannot proceed until these questions have been resolved.

8.1.3 Materials Compatibility

Selection of materials for use in contact with blood is uncertain. This affects engine design, primarily with regard to the heat exchanger.

8.1.4 Penetration of Equipment by Body Fluids

Body fluids are extremely corrosive to many metals. Many of the corrosive elements, particularly the metal and chloride ions, readily penetrate elastic materials such as silicone rubber. A means must be found to keep these corrosive elements from reaching the bellows in the pumping chamber or bellows life will be adversely affected.

8.2 DEVELOPMENTAL PROBLEMS

8.2.1 Bellows Life

Some development of fabrication and quality control techniques may be required to achieve adequate bellows uniformity and life.

8.2.2 Stability of Thermal Insulation

Some development effort may be required to assure the stability of the vacuum required to maintain the low thermal conductivity of the evacuated foil insulation.

8.2.3 Bearing Materials

Existing technology cannot be applied directly to the solution of the bearing requirements, in that life requirements are longer and loads are much lighter than normal design conditions. Additional testing under specific bearing conditions is required.

8.2.4 Leakage of Gas from Engine

Long term retention of the engine working gas may be a problem; it may be necessary to include a small makeup gas supply in the system.

APPENDIX A

HEATER AND REGENERATOR

A. INTRODUCTION

The parametric analyses of the heater and regenerator were performed with the aid of the cycle analysis code described in Appendix M. In general, the analyses were performed with all controlled parameters constant except that parameter being studied and engine swept volume. The relationships which define the operational characteristics of the heater and regenerator as used in the computer code are derived in this Appendix. Section B establishes that the flow is laminar in both the heater and regenerator. The equations for pressure drop and fluid flow loss through the regenerator are developed in Sections C and D. The effects of variable flow on the regenerator fluid flow and heat transfer are derived in Sections E and F, respectively. The equations for heat transfer in the heater fins are developed in Section G.

B. FLOW REGIME IN HEATER AND REGENERATOR

The goal is to define the flow regime in the heater and regenerator. The method utilized assumes laminar flow, with Graetz's number less than 10, and develops equations based on engine parameters which shows that the Reynold's number is less than 2100. Parameters such as D_e, A_c, A, P, h, and L are eliminated from the equations. By definition:

$$D_e = \frac{4A_c}{Pm} = [4\ V] \cdot \frac{1}{A} \qquad \text{(A-1)}$$

$$N_R = \frac{D_e G}{\mu} = \left[\frac{4\omega}{\mu}\right] \cdot \frac{L}{A} \qquad \text{(A-2)}$$

$$Y = \frac{hA}{\omega C_p} = \left[\frac{4.36\ K}{\omega C_p\ 4V}\right] \cdot A^2 \qquad \text{(A-3)}$$

It is assumed that the power loss due to pressure drop through the regenerator is given by:

$$PRR = f \frac{L}{D_e} \frac{\omega^3}{2g\rho^2 A_c^2} = \frac{64}{N_R} \frac{L}{D_e} \frac{\omega^3}{2g\rho^2 A_c^2}$$

$$= \left[\frac{8\omega^3}{g\rho^2 V^3} \right] AL^3 \qquad \text{(A-4)}$$

Combining Equations (A-2) and (A-4) yields:

$$N_R = \left[\frac{8g\rho^2 V^3 PRR}{\mu^3} \right]^{1/3} \frac{1}{A^{4/3}} \qquad \text{(A-5)}$$

Combining Equations (A-3) and (A-5) yields:

$$N_R = \left[\frac{8g\rho^2 V^3 PRR}{\mu^3} \right]^{1/3} \left[\frac{4.36\ K}{\omega C_p\ 4V\ Y} \right]^{2/3}$$

$$= \left[\frac{(4.36)^2\ g\ V\ PRR}{2\mu\ P_R^2\ Y^2\ Q^2} \right]^{1/3} \qquad \text{(A-6)}$$

For the regenerator

μ	$>$	0.056 lb/ft-hr
PRR	$<$	2650 ft-lb/hr (1 watt)
Y	$>$	100 ($\sim$ 98% effectiveness)
Q	$>$	2 · D Hz
V	$<$	D

$$\therefore N_R \cong \frac{110}{Hz^{2/3} D} \qquad \text{(A-7)}$$

where: Hz is in cycles/sec and
D is in in^3.

Several analyses indicate that a power output of seven watts requires that

$$HzD > 10$$

$$N_R \approx 11 \cdot Hz^{1/3} \quad \text{and} \qquad \text{(A-8)}$$

for reasonable values of Hz, the flow through the regenerator is laminar. For the heater,

$$\mu > 0.1 \text{ lb/ft-hr}$$

The selection of the value of Y for the heater is more difficult. Since the wall temperature of the heater is constant, it can be shown that, for a 20°F average temperature rise through the heater,

$$Y \approx L_N [1 + 20/\Delta T_1] \qquad \text{(A-9)}$$

For reasonable values of ΔT_1 (say 100°F; 50°F is used in reference design):

$$Y > 0.18$$

$$N_R = 620 (Hz)^{1/3} \quad \text{and,} \qquad \text{(A-10)}$$

for engine speeds below 38.5 cps or 2190 cpm, N_R is laminar.

C. PRESSURE DROP THROUGH REGENERATOR - AVERAGE FLOW

The temperature of the gas varies as it passes through the regenerator. The effect on pressure drop can be estimated, assuming a constant flow rate, from:

$$\Delta P = \int_0^L f \frac{1}{D_e} \frac{v^2}{2g} \rho \, dx \qquad \text{(A-11)}$$

For laminar flow

$$f = \frac{64}{N_R}$$

$$\Delta P \cong \frac{64\ \bar{\omega}\ \bar{\mu}}{2g\ D_e^2\ A_c} \int \frac{1}{P}\ dx$$

$$\approx \frac{64\ \bar{\omega}\ \bar{\mu}\ R}{2g\ D_e^2\ A_c\ P} \int T\ dx \qquad \text{(A-12)}$$

Since:

$$T \cong T_{min} + \Delta T\ \frac{x}{L} \qquad \text{(A-13)}$$

$$\Delta P \cong \frac{64\ \bar{\omega}\ \bar{\mu}\ RL}{2g\ D_e^2\ A_c\ P\Delta T} \int_{T_{min}}^{T_{max}} T\ dT$$

$$\cong \frac{64\ \bar{\omega}\ \bar{\mu}\ L}{2g\ D_e^2\ A_c\ \rho_{max}}\ \frac{(1+\tau)}{2} \qquad \text{(A-14)}$$

D. <u>POWER LOSS DUE TO PRESSURE DROP THROUGH REGENERATOR - AVERAGE FLOW</u>

$$PRR = \int_o^L f\ \frac{1}{D_e}\ \frac{v^2}{2g}\ \rho Q\ dx$$

$$= \frac{64\ \bar{\omega}^2\ \bar{\mu}}{2g\ D_e^2\ A_c} \int_o^L \frac{1}{\rho^2}\ dx \qquad \text{(A-15)}$$

Since:

$$T \approx T_{min} + \frac{x}{L}\ \Delta T \qquad \text{(A-16)}$$

$$PRR = \frac{64\ \bar{\omega}^2\ \bar{\mu}}{2g\ D_e^2\ A_c} \left[\frac{R}{P}\right]^2 \frac{L}{\Delta T} \int_{T_{min}}^{T_{max}} T^2\ dT$$

$$= \frac{64\ \bar{\omega}^2\ \bar{\mu}\ L}{2g\ D_e^2\ A_c\ P_{max}^2}\ \frac{(1+\tau+\tau^2)}{3} \qquad \text{(A-17)}$$

E. VARIABLE FLOW FLUID DYNAMIC LOSSES

The flow losses through the heater and regenerator are variable as a result of displacer piston cycling and pressure changes. The effect of the variable flow on the pressure drop and fluid dynamic losses are analyzed below for a half cycle starting at bottom dead center.

The mass of gas in the hot chamber, engine pressure level and piston position can be approximated by:

$$W = [0.5 + 0.5 \cos\beta\theta + \sigma]\, PD/RT \qquad \text{(A-18)}$$

$$P = P_{LP} + \Delta P\,(1 - 2x/s) \qquad \text{where } x < s/2 \text{ and,}$$

$$= P_{LP} \qquad \text{where } x > s/2 \qquad \text{(A-19)}$$

$$x = [1 - \cos\beta\theta]\, s/2 \qquad \text{(A-20)}$$

So:

$$\omega = -\frac{dW}{d\theta} = -\left[0.5\beta \sin\beta\theta + (0.5 + 0.5\cos\beta\theta + \sigma)\frac{dP}{Pd\theta}\right]\frac{PD}{RT} \qquad \text{(A-21)}$$

$$\frac{dx}{d\theta} = \beta s \sin\beta\theta/2 \qquad \text{(A-22)}$$

$$\frac{dP}{d\theta} = -\Delta P\beta \sin\beta\theta \qquad \text{where } x < s/2 \text{ and,}$$

$$\frac{dP}{d\theta} = 0 \qquad \text{where } x > s/2 \qquad \text{(A-23)}$$

or

$$\frac{dP}{d\theta} = -\Delta P\beta \sin\beta\theta\, \gamma(\theta) \qquad \text{where } \gamma(\theta) = 1 \text{ for } \theta < \frac{\theta_o}{4} \qquad \text{(A-24)}$$

$$\gamma(\theta) = 0 \text{ for } \frac{\theta_o}{4} < \theta < \frac{\theta_o}{2}$$

$$\frac{2\omega}{\beta D\rho} = \sin\beta\theta\left[1 + (1 + \cos\beta\theta + 2\sigma)\frac{\Delta P}{P}\,\gamma(\theta)\right] \qquad \text{(A-25)}$$

The value of $\psi = (1 + \cos\beta\theta + 2\sigma)\,\Delta P/P$ is a slowly varying function. For example, if $P_{max} = 73.3$ psi, $P_{min} = 60$ psi, and $\sigma = 0.1$

ψ = 0.400, 0.388, 0.352, and 0.267 for

$\beta\theta$ = 0, 27, 54, and 90^o respectively.

$$\therefore \quad \frac{2\omega}{\beta D\rho} \cong \sin\beta\theta \left[1 + \psi\ \gamma(\theta)\right]$$

$$\overline{\frac{2\omega}{\beta D\rho}} = \frac{1}{\pi}\left[\int_{o}^{\pi/2} \sin z\ (1 + \bar{\psi})\ dz + \int_{\pi/2}^{\pi} \sin z\ dz\right] = (2 + \bar{\psi})/\pi$$

$$\overline{\left(\frac{2\omega}{\beta D\rho}\right)^2} = \frac{1}{\pi}\left[\int_{o}^{\pi/2} \sin^2 z\ (1 + \bar{\psi})^2\ dz + \int_{\pi/2}^{\pi} \sin^2 z\ dz\right] =$$

$$= 0.25\left((1 + \bar{\psi})^2 + 1\right) \qquad \text{(A-26)}$$

As shown in Sections B and C, the regenerator losses are:

$$\Delta P \cong \frac{64\ \bar{\mu}\ L}{2g\ D_e^2\ A_c\ \rho_{max}} \left(\frac{1 + \tau}{2}\right)\ \bar{\omega} \quad \text{and,}$$

$$PRR = \frac{64\ \bar{\mu}\ L}{2g\ D_e^2\ A_c\ \rho_{max}^2} \left(\frac{1 + \tau + \tau^2}{3}\right) \overline{\omega^2}$$

Therefore:

$$\Delta P = \frac{32\ L^2\ \bar{\mu}\ Hz\ (2 + \bar{\psi})}{2g\ D_e^2\ \sigma_R} \left(\frac{1 + \tau}{2}\right) \qquad \text{(A-27)}$$

$$PRR = \frac{(1 + \bar{\psi})^2\ 8\bar{\mu}\ D}{g\ \sigma_R} \left(\frac{\pi Hz\ L}{D_e}\right)^2 \left[\frac{1 + \tau + \tau^2}{3}\right] \qquad \text{(A-28)}$$

F. VARIABLE FLOW HEAT TRANSFER IN THE REGENERATOR

A simplified regenerator model is assumed to determine the approximate effect of variable flow through the regenerator. The wall temperature is assumed to be time independent and linear with axial position for the purpose of analysis. Further, the inlet gas temperature is assumed to be constant and the flow rate is assumed to be sinusoidal The model is shown schematically in Figure A-1.

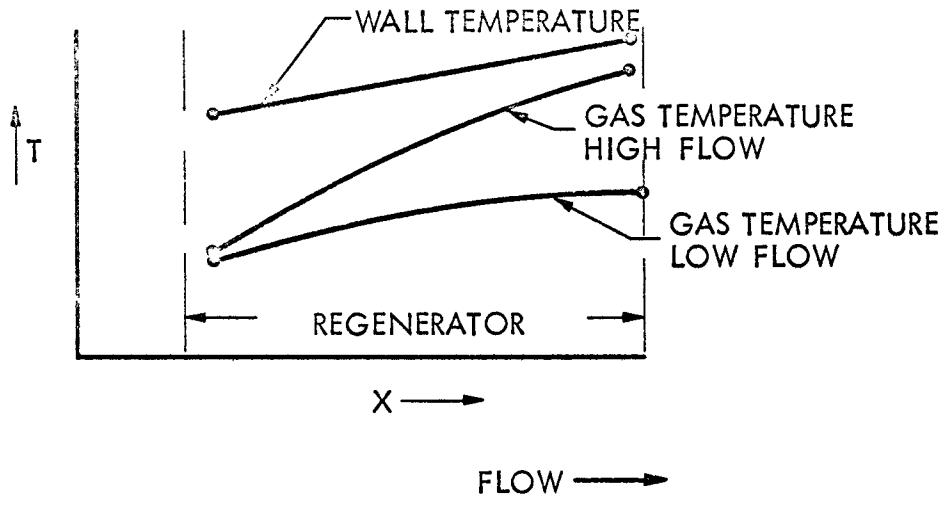

Figure A-1

At a particular flow rate:

$$\omega C_p \, dT = hP \, [T_w - T] \, dx \qquad \text{(A-29)}$$

Let $\alpha = T_w - T$ and

ΔT_w = maximum temperature difference between regenerator wall at regenerator inlet and outlet. Then:

$$\frac{d\alpha}{dx} + \frac{Y}{L}\alpha = \frac{\Delta T_w}{L} \qquad \text{(A-30)}$$

Using Laplace transforms:

$$L(\alpha) = \frac{\Delta T_o}{\left[s + \frac{Y}{L}\right]} + \frac{\Delta T_w}{s\left(s + \frac{Y}{L}\right)L}$$

or $$\alpha(x) = \Delta T_o \, e^{-\frac{Yx}{L}} + \frac{\Delta T_w}{Y}\left(1 - e^{-\frac{Yx}{L}}\right) \qquad \text{(A-31)}$$

For the regenerator, $Y \approx 100$ at average flow:

$$\alpha(L) \approx \Delta T_w / Y = \frac{WC_p \, \Delta T_w}{hA} \qquad \text{(A-32)}$$

For a constant flow rate, ω_o, the total heat content of the gas flowing over a 1/2 cycle is given by:

$$q_c = \int_o^{\theta^o/2} \omega_o \left(\frac{\omega_o C_p \Delta T_w}{hA}\right) d\theta = \frac{\omega_o C_p \Delta T_w}{hA} \frac{\theta^o}{2} \qquad \text{(A-33)}$$

For a variable flow, $\omega = \frac{\pi}{2} \bar{\omega} \sin\beta\theta$, so:

$$q_v = \int_o^{\theta^o/2} \omega \left(\frac{\omega C_p \Delta T_w}{hA}\right) d\theta = \left(\frac{\pi}{2}\right)^2 \frac{\bar{\omega}^2 C_p \Delta T_w}{hA} \int_o^{\theta^o/2} \sin\beta\theta \, d\theta$$

$$= \frac{\pi^2}{8} \frac{\bar{\omega}^2 C_p \Delta T_w}{hA} \qquad \text{(A-34)}$$

If $\bar{\omega} = \omega_o$ and $q_c = q_v$, then:

$$\left(\frac{hA}{2\bar{\omega}C_p}\right)_{\text{variable}} = \frac{\pi^2}{8} \left(\frac{hA}{2\omega_o C_p}\right)_{\text{average}}$$

or

$$NTU_{\text{variable}} = \frac{\pi^2}{8} NTU_{\text{average}} \qquad \text{(A-35)}$$

Therefore, the variable flow heat exchanger has the same heat transfer performance as a constant flow heat exchanger if the NTU is increased by a factor of $\pi^2/8$.

G. THERMAL CONDUCTION IN HEATER FINS

MODEL:

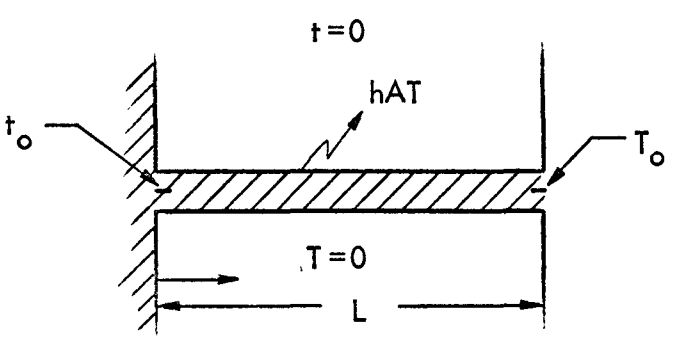

DERIVATION:

$$\frac{d^2T(x)}{dx^2} - \left(\frac{2h}{kt}\right) T(x) = 0$$

or

$$\frac{d^2T(x)}{dx^2} - B^2\, T(x) = 0 \qquad \text{(A-36)}$$

With the boundary conditions:

$$T(o) = T_o \text{ and,} \qquad \text{(A-37)}$$

$$\frac{dT(L/2)}{dx} = 0, \text{ symmetry,} \qquad \text{(A-38)}$$

a general solution to Equation (A-36) becomes:

$$T(x) = C_1 \cosh Bx + C_2 \sinh Bx$$

$$\frac{dT(x)}{ax} = B\left[C_1 \sinh Bx + C_2 \cosh Bx\right] \qquad \text{(A-39)}$$

Applying boundary conditions:

$$T(x) = T_o\left[\cosh Bx - \tanh (BL/2) \sinh Bx\right] \qquad \text{(A-40)}$$

$$T(o) = T_o \qquad \text{(A-41)}$$

$$T(L/2) = T_o/\cosh BL/2 \qquad \text{(A-42)}$$

$$\Delta T = T_o - T(L/2) = T_o\,(\cosh BL/2 - 1)/\cosh BL/2 \qquad \text{(A-43)}$$

For the reference design:

$$T_o \approx 60^oF + \Delta T/2 \qquad \text{(A-44)}$$

$$\Delta T \simeq 120^oF \left[\frac{\cosh BL/2 - 1}{\cosh BL/2 + 1}\right] \qquad \text{(A-45)}$$

Figure A-2 shows the value of ΔT as a function of BL

For the reference design

$$BL = \sqrt{\frac{2h}{kt}}\, L \simeq \sqrt{\frac{2 \times 100 \times 12}{10 \times 0.0418}}\ \frac{0.1972}{12} = 1.24$$

Therefore $\Delta T \approx 10^oF$

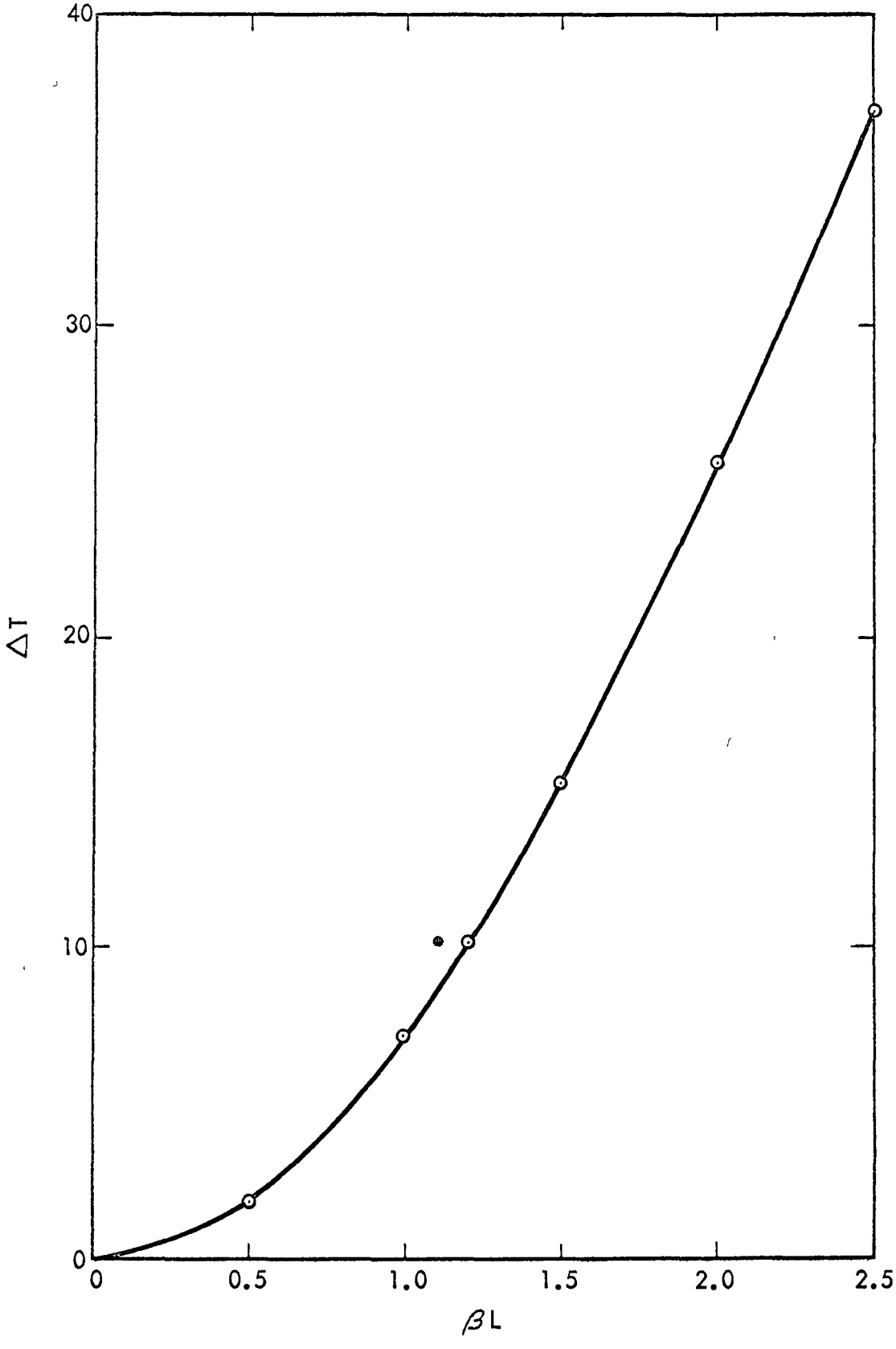

FIGURE A-2. HEATER ΔT AS A FUNCTION OF βL

3.01-68-035

NOMENCLATURE

A	Heat transfer area
A_c	Total flow area
B	$(2h/kt)^{\frac{1}{2}}$
C_v	Constant
D	Engine swept volume
D_e	Equivalent hydraulic diameter
f	Fluid flow friction coefficient
g	Gravitational constant
G	Weight flow per unit area
Gz	Graetz's number
h	Heat transfer coefficient
Hz	Engine speed
K	Thermal conductivity of gas
L	Length or Laplace transform
N_R	$hA/2\omega C_p$ (regenerator) $\frac{hA}{\omega C_p}$ (heater)
P	Pressure
ΔP	Pressure drop
P_R	Prandtl's number
PRR	Flow power loss
P_{LP}	Low pressure reservoir pressure
Pm	Wetted perimeter
Q	Volumetric flow rate
q	Total heat flow
R	Gas constant
s	Stroke or Laplace transform variable
t	Fin thickness
T	Gas temperature
T_w	Wall temperature
T_{max}	Hot chamber average temperature
T_{min}	Cold chamber average temperature
ΔT_ω	Maximum regenerator wall temperature less minimum regenerator wall temperature
ΔT_1	Temperature increment between heater wall and T_{max}
v	Velocity
V	Flow volume

W	Weight
x	Position
Y	$hA/\omega C_p$
z	Integration variable
α	$T_w - T$
β	2π Hz
$\gamma(\theta)$	$1 \quad \theta < \theta_o/4$
	$0 \quad \frac{\theta^o}{4} < \theta_o/2$
θ	Time
θ_o	Oscilation period
μ	Viscosity
$\bar{\mu}$	Average viscosity
ρ	Density
ρ_{max}	Density at T_{max}
σ	Unswept volume/D toward hot chamber of unit being considered
σ_R	Regenerator flow volume/D
τ	T_{min}/T_{max}
ψ	$(1 + \cos\beta\theta + 2\sigma)\ \Delta P/P$
ω	Gas mass flow rate

APPENDIX B
HEAT TRANSPORT DOWN CYLINDER

A. NODAL HEAT TRANSFER

MODEL:

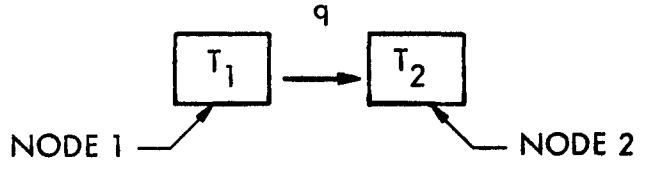

$$q = B\left[T_1 - T_2\right] \tag{B-1}$$

$$C_1 \frac{dT_1}{d\theta} = -B\left[T_1 - T_2\right] \tag{B-2}$$

$$C_2 \frac{dT_2}{d\theta} = B\left[T_1 - T_2\right] \tag{B-3}$$

$$\frac{dT_1}{d\theta} = -B_1\left(T_1 - T_2\right) \tag{B-4}$$

$$\frac{dT_2}{d\theta} = B_2\left(T_1 - T_2\right) \tag{B-5}$$

Using Laplace transforms:

$$(S + B_1)\,\mathcal{T}_1 - B_1\mathcal{T}_2 = T_{10} \tag{B-6}$$

$$(S + B_2)\,\mathcal{T}_2 - B_2\mathcal{T}_1 = T_{20} \tag{B-7}$$

$$\text{Thermal Resistance} = \frac{\Delta x}{2\ KWt_1} + \frac{\Delta x}{2\ KWt_2}$$

$$= \frac{\Delta x}{2\ KW}\ [b_1 + b_2] \qquad \text{(B-8)}$$

Therefore:
$$B = \frac{2\ KW}{\Delta x\ (b_1 + b_2)} \qquad \text{(B-9)}$$

$$B_1 = \frac{B}{W\Delta x t_1\ \rho\ C}\ \frac{2K}{\Delta x^2\ \rho\ C}\ \frac{b_1}{b_1 + b_2} \qquad \text{(B-10)}$$

Similarly:

$$B_2 = \frac{2K}{\Delta x^2\ \rho\ C}\ \frac{b_2}{b_1 + b_2} \qquad \text{(B-11)}$$

$$B_1 + B_2 = \frac{2K}{\Delta x^2\ \rho\ C} \qquad \text{(B-12)}$$

$$\frac{B_1}{B_1 + B_2} = \frac{b_1}{b_1 + b_2} \qquad \text{(B-13)}$$

$$T_1 = T_{10} + \frac{b_1}{b_1 + b_2}\left(T_{20} - T_{10}\right)\left(1 - e^{-\frac{2K\theta}{\Delta x^2\ \rho\ C}}\right) \qquad \text{(B-14)}$$

$$\left[S^2 + \left(B_1 + B_2\right)S\right] \mathcal{T}_1 = \left(S + B_1 + B_2\right)T_{10} + B_1\left(T_{20} - T_{10}\right) \qquad \text{(B-15)}$$

$$\mathcal{T}_1 = \frac{T_{10}}{S} + \frac{B_1}{S\left(S + B_1 + B_2\right)}\left(T_{20} - T_{10}\right) \qquad \text{(B-16)}$$

$$T_1 = T_{10} + \frac{B_1}{B_1 + B_2}\left(T_{20} - T_{10}\right)\left(1 - e^{-\left(B_1 + B_2\right)\theta}\right) \qquad \text{(B-17)}$$

Since the node configuration is symmetrical:

$$T_2 = T_{20} - \frac{B_2}{B_1 + B_2}\left(T_{20} - T_{10}\right)\left(1 - e^{-\left(B_1 + B_2\right)\theta}\right) \qquad \text{(B-18)}$$

Equation (B-18) is used as a basis of the computer code. Equations for B_1 and B_2 are developed in the following sections.

B. WALL CONDUCTION MODE

MODEL:

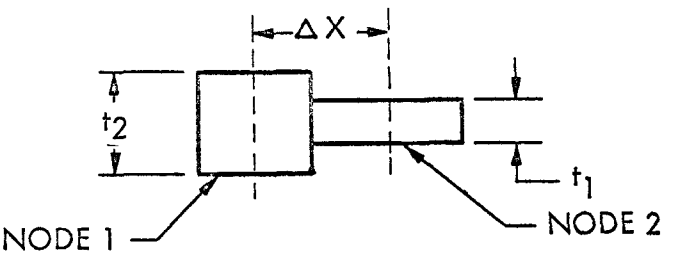

C. HEAT FLOW ACROSS GAS GAP

$$\text{Thermal Conductance} = \frac{K_G\, W\Delta x}{\delta} = B \tag{B-19}$$

$$B_1 = \frac{B}{\delta \Delta x W t_1 \rho C} = \frac{K_G\, b_1}{\delta \rho C} \tag{B-20}$$

$$B_2 = \frac{K_G\, b_2}{\delta \rho C} \tag{B-21}$$

$$B_1 + B_2 = \frac{K_G}{\delta \rho C}\left[b_1 + b_2\right] \tag{B-22}$$

Therefore:

$$T_1 = T_{10} + \frac{b_1}{b_1 + b_2}\left(T_{20} - T_{10}\right)\left(1 - e^{-\frac{K_G}{\delta \rho C}(b_1 + b_2)\theta}\right) \tag{B-23}$$

D. DOME CONDUCTION

MODEL:

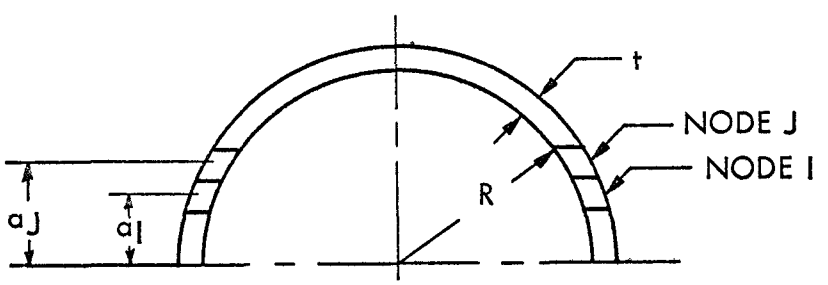

Thermal resistance between adjacent nodes, I and J

$$\frac{1}{B} = \frac{1}{2\pi kt}\int \frac{dz}{x} \tag{B-24}$$

$$dz = \sqrt{\left(\frac{ax}{ay}\right)^2 + 1}\ dy \tag{B-25}$$

$$\frac{dx}{ay} = -\frac{Y}{x} = -\frac{y}{(R^2 - y^2)^{\frac{1}{2}}} \tag{B-26}$$

$$dz = \frac{R}{\sqrt{R^2 - y^2}}\ dy \tag{B-27}$$

$$x = \sqrt{R^2 - y^2} \tag{B-28}$$

$$\text{Thermal Resistance} = \frac{R}{2\pi kt}\int_{a_I}^{a_J} \frac{dy}{R^2 - y^2} = \frac{1}{2\pi kt}\left[\tanh^{-1}\frac{a_J}{R} - \tanh^{-1}\frac{a_I}{R}\right] \tag{B-29}$$

$$q = \frac{2\pi\ kt\ \Delta T}{\left[\tanh^{-1}\frac{a_J}{R} - \tanh^{-1}\frac{a_I}{R}\right]} \tag{B-30}$$

$$C_J = 2\pi R\left[a_J - a_I\right] t\ \rho C \tag{B-31}$$

$$B_J = \frac{K}{R\rho C\left[\tanh^{-1}\frac{a_J}{R} - \tanh^{-1}\frac{a_I}{R}\right]} \tag{B-32}$$

NOMENCLATURE

B	=	Thermal conductance
B_1, B_2	=	B/C_1, B/C_2 respectively
C_1, C_2	=	Nodal thermal capacitance
t_1, t_2	=	Nodal thicknesses
b_1, b_2	=	$1/t_1$, $1/t_2$ respectively
T_1, T_2	=	Nodal temperatures
T_{10}, T_{20}	=	Initial nodal temperatures
S	=	Laplace transform variable
q	=	Heat flow
K, K_G	=	Metal, gas thermal conductivity
W	=	Width (into paper in sketches)
Δx	=	Node length (see sketch)
Θ	=	Time
ρ	=	Density
C	=	Heat capacitance
δ	=	Gas gap width
$\mathcal{T}_1$, $\mathcal{T}_2$	=	Laplace transforms of T_1, T_2
x, y, a_J, a_I, R		Defined by sketch in Section D
C_J	=	Thermal capacitance of dome node J
t	=	Thickness of dome wall

APPENDIX C

DERIVATION OF FLUID DYNAMICS FORMULA FOR CHECK VALVE

A. MODEL

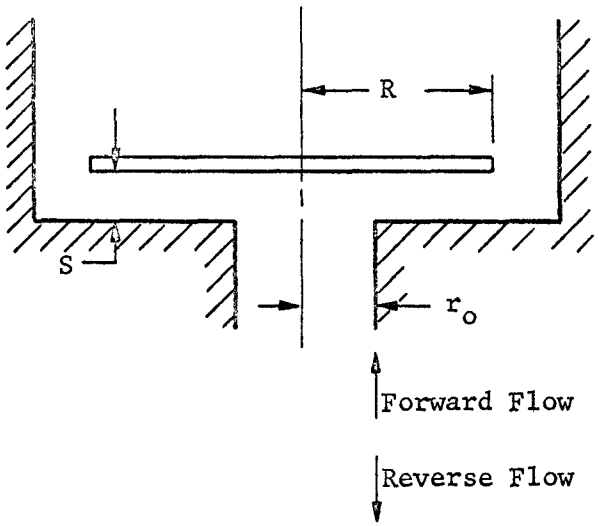

B. FORWARD FLOW

Assuming a velocity head loss at R,

$$P = P_o - \frac{V^2}{2g}\rho - \int_{r_o}^{r} f \frac{V^2}{2g} \frac{\rho}{D_e} dr \qquad \text{(C-1)}$$

$$P_1 = P_o - \left[\frac{V^2}{2g}\rho\right]_R - \int_{r_o}^{R} f \frac{V^2}{2g} \rho/D_e \, dr \qquad \text{(C-2)}$$

or $$2g\,\Delta P/\rho = (P_o - P_1)\, 2g/\rho = \left[V^2\right]_R + \int_{r_o}^{R} f \frac{1}{D_e} V^2 \, dr$$

$$f = \frac{64u}{D_e V \rho} \quad \text{for laminar flow}$$

$$V = \frac{Q}{2\pi r\delta}$$

$$\frac{2g\ \Delta P}{\rho} = \left(\frac{Q}{2\pi R\delta}\right)^2 + \int_{r_o}^{R} \frac{8\mu Q}{\pi\delta^3\rho}\ \frac{dr}{r}$$

or

$$\frac{1}{2}\,Q^2 + \frac{C_3}{\delta}\,Q - \frac{C_4}{2}\,\delta^2\,\Delta P = 0$$

or, using quadradic equation,

$$Q = \frac{C_3}{\delta}\left[\left[1 + \frac{C_4\delta^4\Delta P}{C_3^{\,2}}\right]^{\frac{1}{2}} - 1\right] \qquad \text{(C-3)}$$

$$F = \pi r_o^{\,2}\,\Delta P + \int_{r_o}^{R} (P - P_1)\,2\pi r\,dr \qquad \text{(C-4)}$$

Combining equations (C-1), (C-2) and (C-4) yields:

$$F = \pi R^2\,\Delta P - \frac{\rho}{2g}\left[\int_{r_o}^{R} 2\pi r\,V^2\,dr + \int_{r_o}^{R} 2\pi r dr \int_{r_o}^{r} \frac{f\,V^2}{D_e}\,dr\right]$$

Performing the integrations gives:

$$F/\pi R^2 = \Delta P - \rho/g\left\{\left(\frac{Q}{2\pi\delta R}\right)^2 \mathrm{Ln}\ R/r_o + \frac{2\mu Q}{\pi\delta^3\rho}\left[\mathrm{Ln}(R/r_o)^2 - 1 + \left(\frac{r_o}{R}\right)^2\right]\right\}$$

$$a = F\ .\ g/\pi R^2\ t_p\rho_p$$

$$a = C_5\,\Delta P - C_6\left(\frac{Q}{\delta}\right)^2 - C_7\left(\frac{Q}{\delta^3}\right) \qquad \text{(C-5)}$$

The computer program solves Equation (C-3) using a current δ and ΔP impressed by the engine and reservoir. The results are used in Equation (C-5) to determine acceleration. This acceleration is used to determine a new δ for the next time increment. Accelerations caused by any spring forces are added to the acceleration caused by fluid dynamic forces.

C. REVERSE FLOW

The derivation of this case is similar except that a velocity head loss is assumed to occur at r_o rather than R. Equations (C-3) and (C-5) apply with the following adjustment of constants.

$$C_3 = 16\mu \pi r_o^2 \text{ Ln } R/r_o/\rho$$

$$C_4 = 8\pi^2 r_o^2 g/\rho$$

$$C_6 = \rho(.5 (R/r_o)^2 - .5 - \text{Ln } R/r_o)/ + p \rho_p$$

D. TYPICAL RESULTS

Table C-1 shows a tabulation of a number of typical runs. Figures C-1 through C-6 show a number of typical position plots.

NOMENCLATURE

F	=	Force on disk
a	=	Acceleration of disk
R	=	Disk diameter
r	=	Inlet diameter
P	=	Pressure absolute
P_o	=	Pressure inlet
P_1	=	Pressure outlet
ΔP	=	Total pressure drop
f	=	Friction factor
μ	=	Viscosity
Q	=	Volumetric flow rate
D_e	=	Equivalent diameter = 2δ
ρ	=	Gas density
V	=	Velocity
δ	=	Valve opening
t_p	=	Plate thickness
ρ_p	=	Plate density
C_3	=	$16\mu\ \pi R^2\ \text{Ln}\ R/r_o/\rho$
C_4	=	$8\pi^2\ R^2\ g/\rho$
C_5	=	$g/t_p\ \rho_p$
C_6	=	$C_5\ \text{Ln}\ R/r_o/4\pi^2 R^2$
C_7	=	$\frac{2\mu}{\pi t_p \rho_p}\left\{\text{Ln}\ (R/r_o)^2 - 1 + (\frac{r_o}{R})^2\right\}$

TABLE C-1 – SUMMARY OF TYPICAL CHECK VALVE CALCULATIONS

Run No.	Maximum Opening, in.	r_o, in.	R, in.	Spring Engagement	Spring Constant, lb/in.	Pressure Loss, watts	Back Flow, %	Energy Loss to B.F, watts	Total Energy Loss per Stroke
201	0.020	0.100	0.200	0	0	0.652	2.0	0.140	0.792
202	0.020	0.150	0.200	0	0	0.119	3.5	0.245	0.364
203	0.020	0.100	0.150	0	0	0.201	2.32	0.162	0.363
204	0.025	0.100	0.150	0.020	0.25	0.161	1.32	0.092	0.253
205	0.030	0.100	0.150	0.020	0.25	0.178	0.18	0.012	0.190
206	0.030	0.100	0.150	0.025	0.25	0.144	3.68	0.258	0.402
207	0.030	0.100	0.150	0.025	0.50	0.153	0.98	0.070	0.223
208	0.030	0.100	0.150	0.025	1.00	0.176	1.38	0.097	0.273
209	0.030	0.100	0.150	0	0	0.136	4.67	0.326	0.462
210	0.030	0.100	0.150	0.025	1.00	0.210	6.3	0.440	0.650
211	0.030	0.100	0.150	0.020	0.50	0.244	0.123	0.0086	0.253
212	0.030	0.100	0.150	0.020	1.00	Bounded Closed at #2.9 millisec			
213	0.030	0.100	0.150	0.025	0.40	0.149	1.24	0.087	0.236
214	0.030	0.100	0.150	0.025	0.60	0.157	0.24	0.016	0.173
215*	0.030	0.100	0.150	0.025	0.70	0.164	0.012	0.0008	0.164
216	0.060	0.100	0.150	0	0	0.099	12.3	0.84	0.939

*Selected design

RUN NO. 205	
MAX POSSIBLE OPENING	.030
SPRING ENGAGEMENT	.010
INLET DIAMETER	.100
DISC DIAMETER	.150
SPRING CONSTANT	.25
ENERGY TO OPERATE	.178
ENERGY LOSS TO BACK FLOW	.012
TOTAL ENERGY CONSUMED PER CYCLE	.190

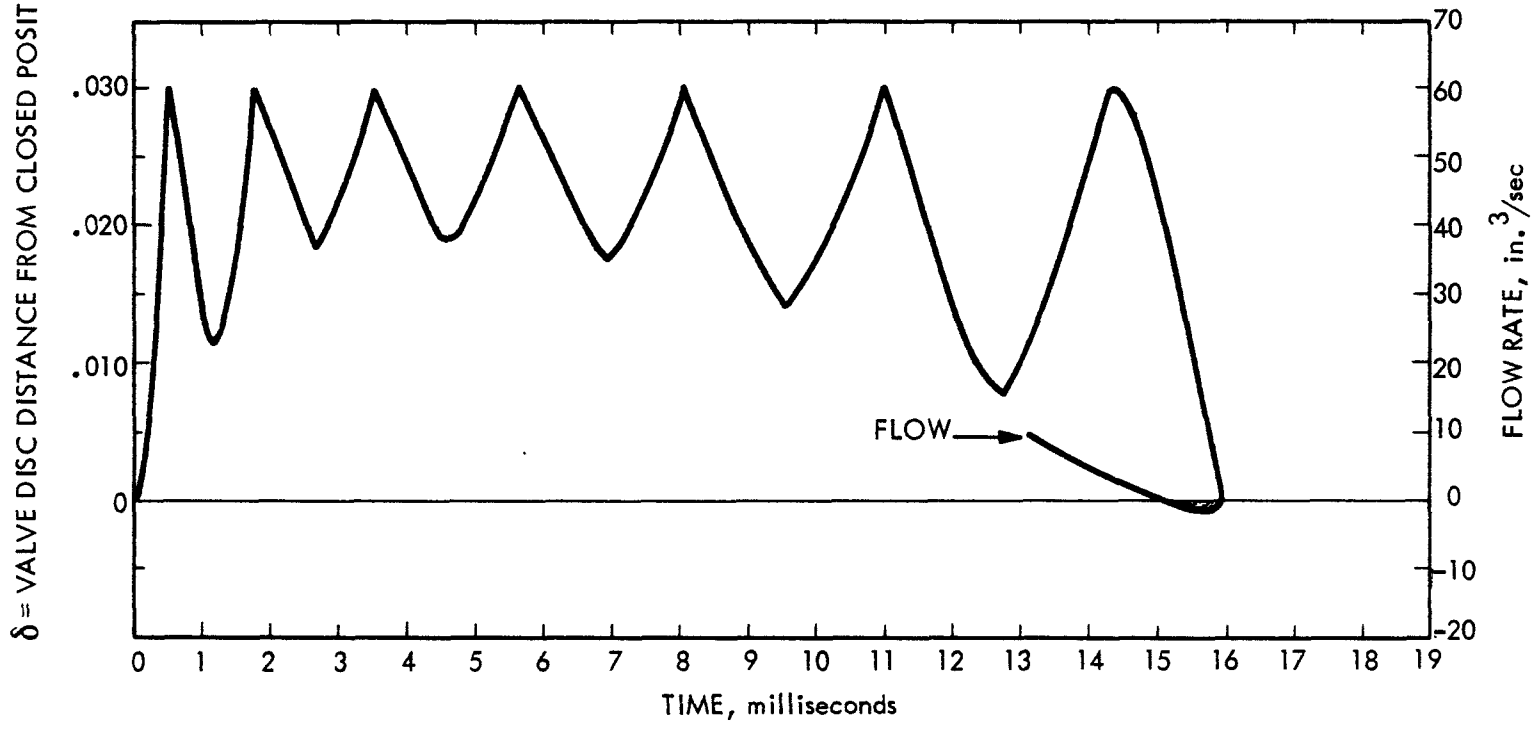

FIGURE C-1. CHECK VALVE PERFORMANCE

RUN NO. 206	
MAX POSSIBLE OPENING	.030
SPRING ENGAGEMENT	.005
INLET DIAMETER	.100
DISC DIAMETER	.150
SPRING CONSTANT	.25
ENERGY TO OPERATE	.144
ENERGY LOSS TO BACK FLOW	.258
TOTAL ENERGY CONSUMED PER CYCLE	.402

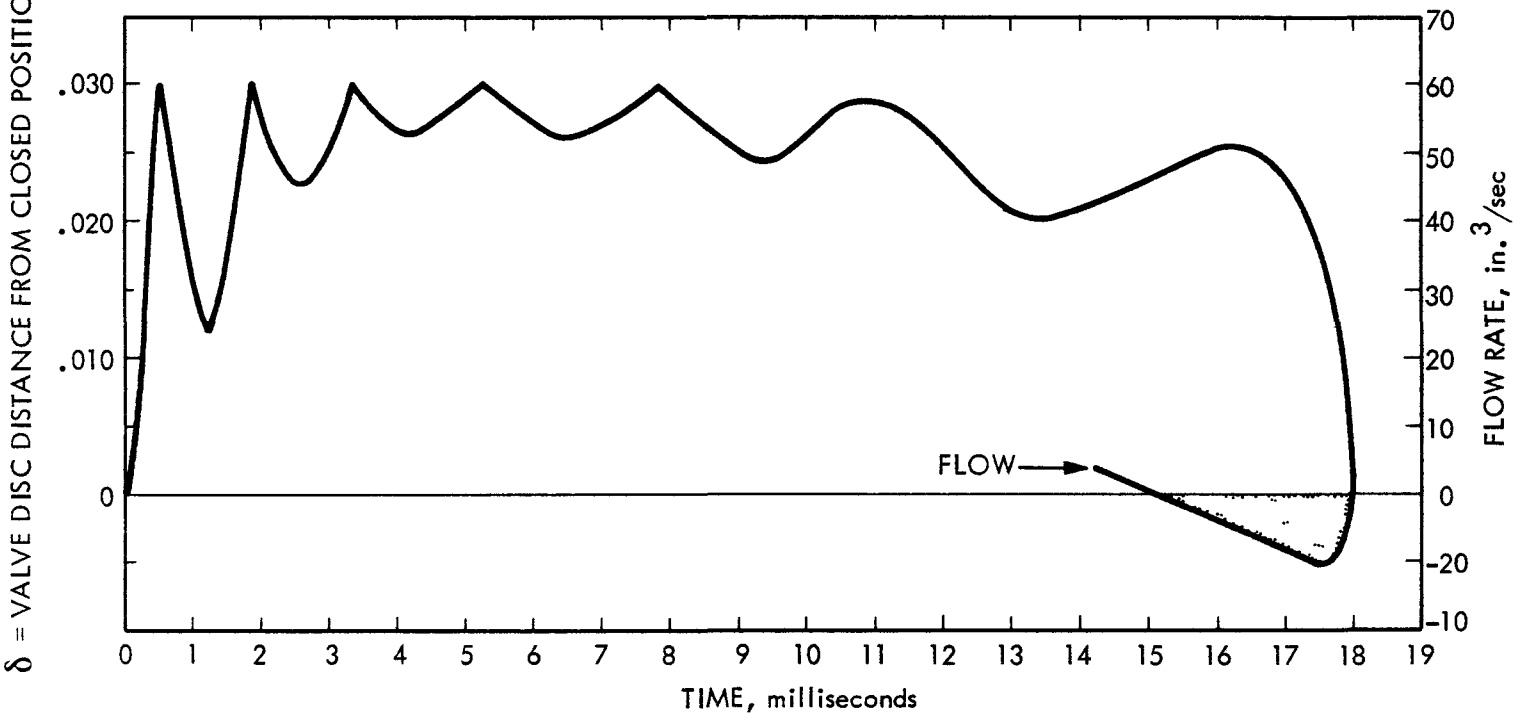

FIGURE C-2. CHECK VALVE PERFORMANCE

RUN NO. 207	
MAX POSSIBLE OPENING	.030
SPRING ENGAGEMENT	.005
INLET DIAMETER	.100
DISC DIAMETER	.150
SPRING CONSTANT	.50
ENERGY TO OPERATE	.153
ENERGY LOSS TO BACK FLOW	.070
TOTAL ENERGY CONSUMED PER CYCLE	.223

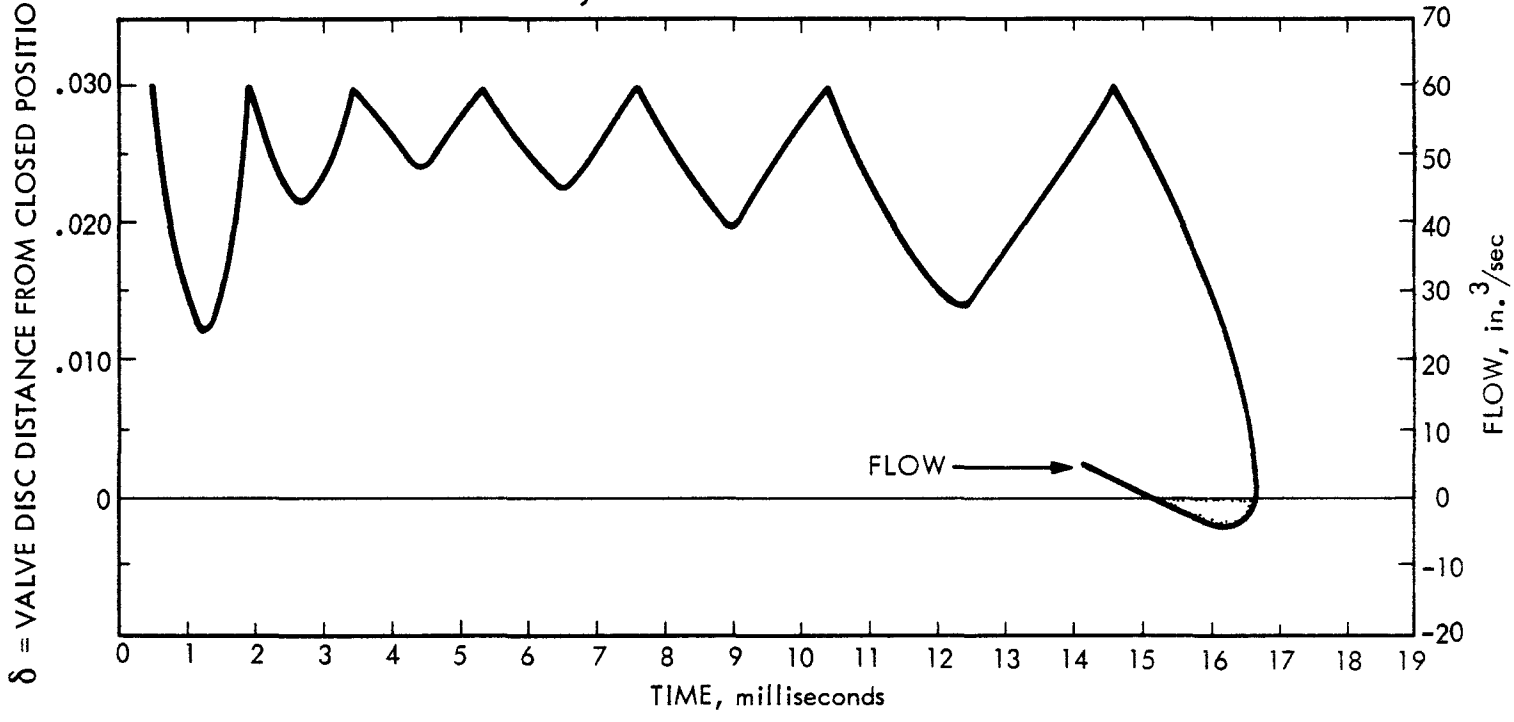

FIGURE C-3. CHECK VALVE PERFORMANCE

RUN NO. 208

MAX POSSIBLE OPENING	.030
SPRING ENGAGEMENT	.005
INLET DIAMETER	.100
DISC DIAMETER	.150
SPRING CONSTANT	.100
ENERGY TO OPERATE	.176
ENERGY LOSS TO BACK FLOW	.097
TOTAL ENERGY CONSUMED PER CYCLE	.273

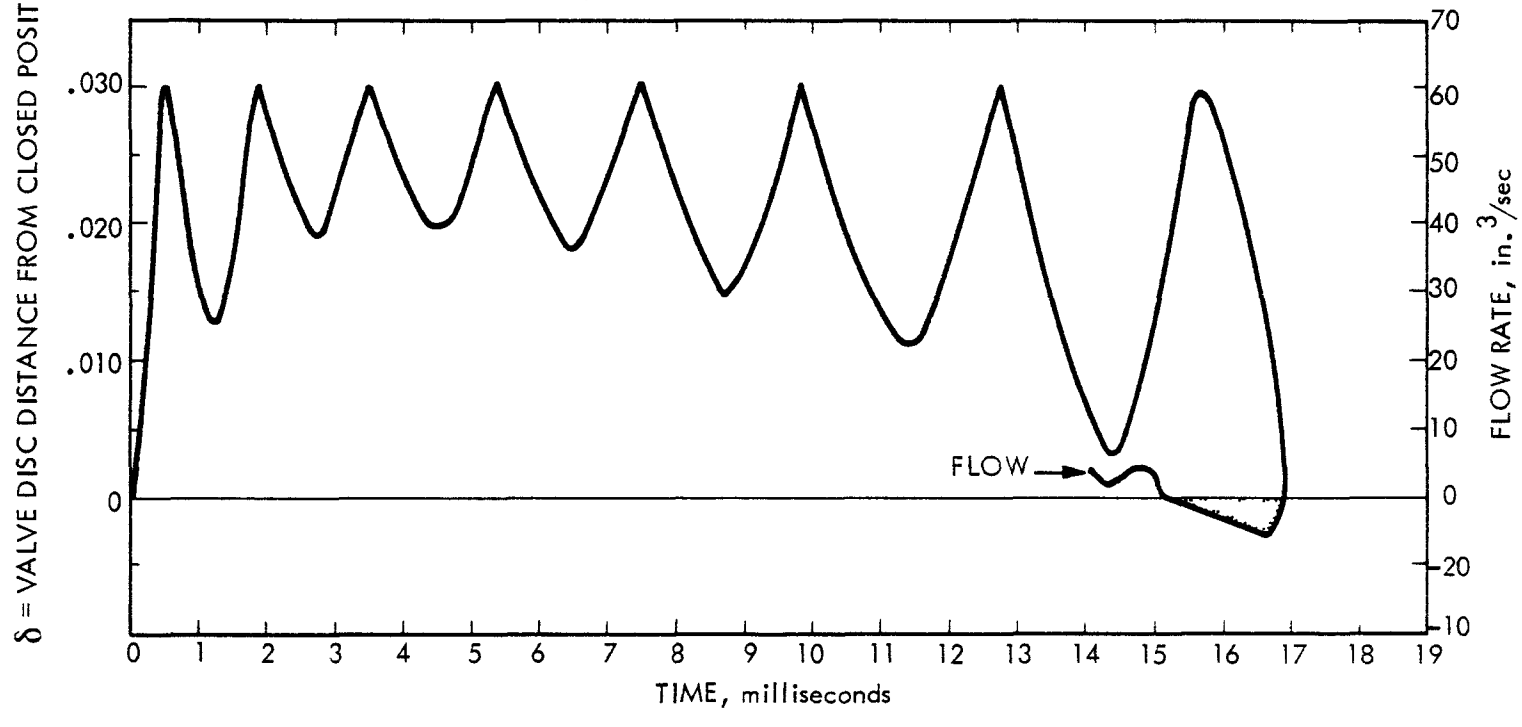

FIGURE C-4. CHECK VALVE PERFORMANCE

RUN NO. 209	
MAX POSSIBLE OPENING	.030
SPRING ENGAGEMENT	0
INLET DIAMETER	.100
DISC DIAMETER	.150
SPRING CONSTANT	0
ENERGY TO OPERATE	.136
ENERGY LOSS TO BACK FLOW	.326
TOTAL ENERGY CONSUMED PER CYCLE	.462

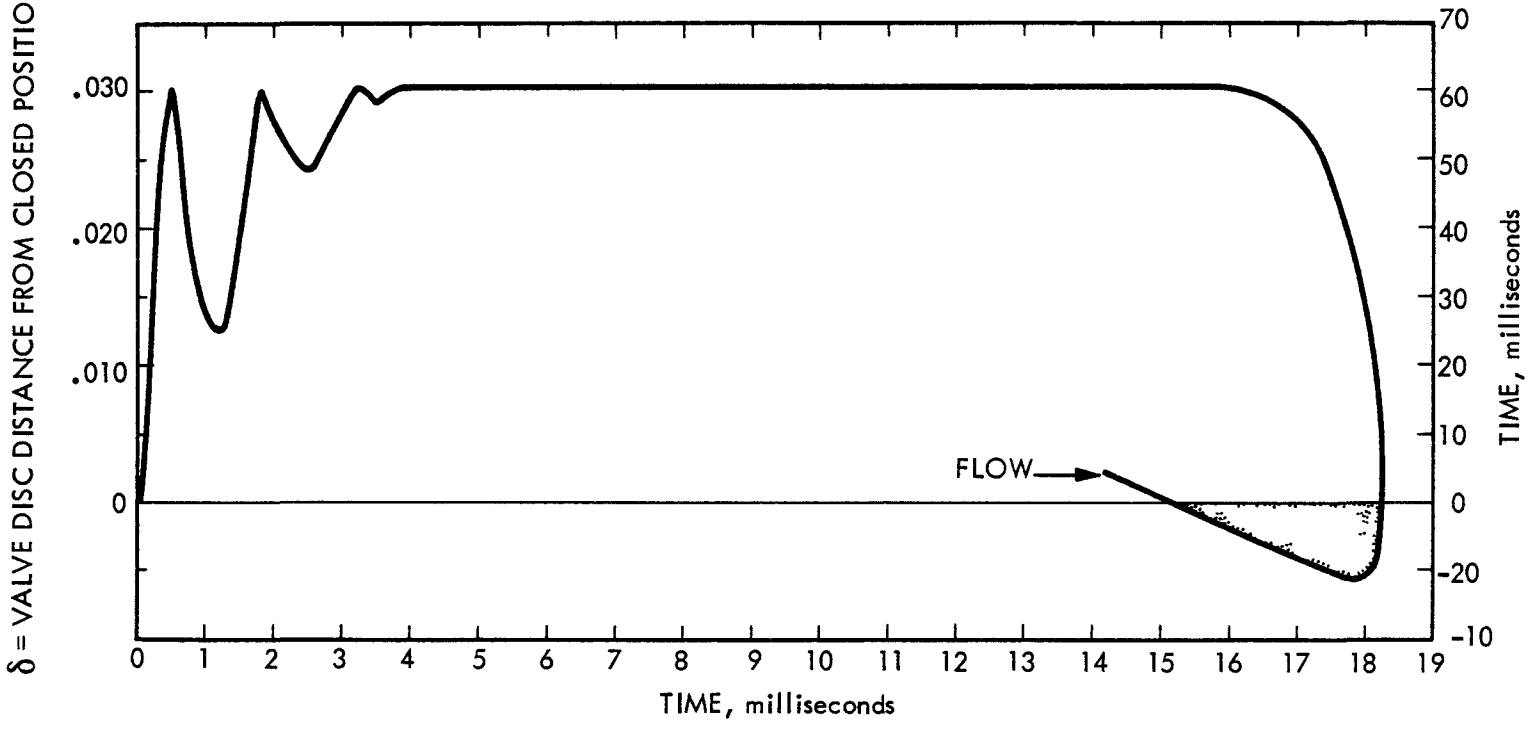

FIGURE C-5. CHECK VALVE PERFORMANCE

RUN NO. 215	
MAX POSSIBLE OPENING	.030
SPRING ENGAGEMENT	.005
INLET DIAMETER	.100
DISC DIAMETER	.150
SPRING CONSTANT	.70
ENERGY TO OPERATE	.164
ENERGY LOSS TO BACK FLOW	.0008
TOTAL ENERGY CONSUMED PER CYCLE	.164

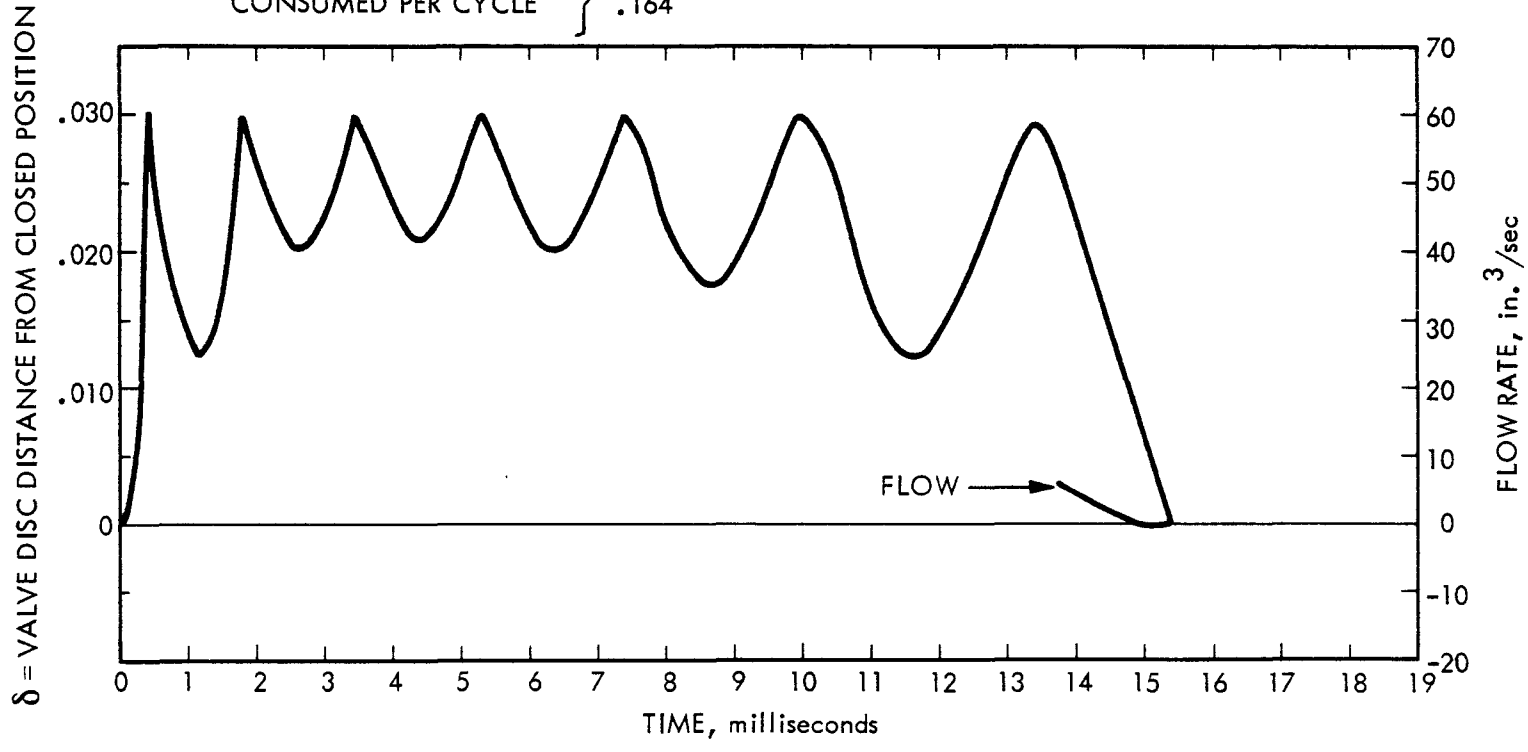

FIGURE C-6. CHECK VALVE PERFORMANCE - REFERENCE DESIGN

APPENDIX D

REVERSING PISTON OPERATION

A. REVERSING SYSTEM

1) Model

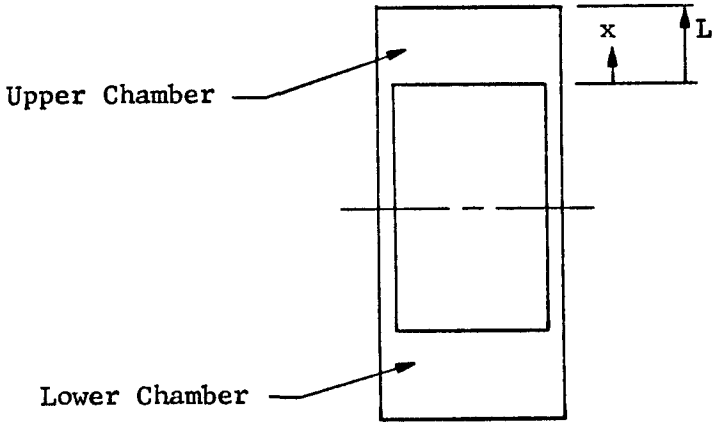

2) Derivation of Equation

$$P_u A - P_l A = M \frac{d^2x}{dt^2}$$

$$P_u = P_o V_o^{\,2}/(V_o - Ax)^{\gamma}$$

$$P_l = P_o V_o^{\,2}/(V_o + Ax)^{\gamma}$$

Since $$\frac{d^2x}{dt^2} = v \frac{dv}{dx}$$

$$v^2 = v_o^{\,2} + \frac{2P_o A}{M} \int_o^x ((1 + \frac{x}{L})^{-\gamma})\, dx$$

$$v^2 = v_o^{\,2} + \frac{2P_o V_o}{(\gamma-1)M} \left[2 - (1 + z)^{1-\gamma} - (1 - z)^{1-\gamma}\right]$$

and

$$v_o^2 = -\frac{2P_oV_o}{(\gamma-1)M}\left[2 - (1+z_L)^{1-\gamma} - (1-z_L)^{1-\gamma}\right]$$

$$T = 4\left[\frac{(\gamma-1)M\,V_o}{2P_oA^2}\right]^{\frac{1}{2}}\int_o^{z_L} dz/\left[(1+z_L)^{1-\gamma} + (1-z_L)^{1-\gamma} - (1+z)^{1-\gamma} - (1-z)^{1-\gamma}\right]^{\frac{1}{2}}$$

The intergral is a definite integral which can be integrated on a computer. Noting that $f = \frac{1}{T}$

$$f = \left[\frac{-2P_oA^2}{(\gamma-1)MV_o}\right]^{\frac{1}{2}}/4I(z_L)$$

where $I(z_L)$ is the definite integral in the preceeding equation.

B. WORK ADDITION SYSTEM

The work addition is obtained by considering the pressure forces acting on the area of the rod between displacer and reversing piston projected on the top surface of the displacer piston and bottom surface of the reversing piston.

Figure D-1 shows pressure traces for the system. The top chart shows the pressures layed out over a complete cycle and illustrates the action between the hot chamber and lower reversing piston pressures. The bottom chart is the top chart folded around the vertical top dead center line. The shaded area is proportional to the cyclic work applied to the reciprocating mass.

Assuming linear lines and check valve opening position at mid-stroke,

$$WK = .5\,(P_{HP} - P_{LP})\,A_RS$$

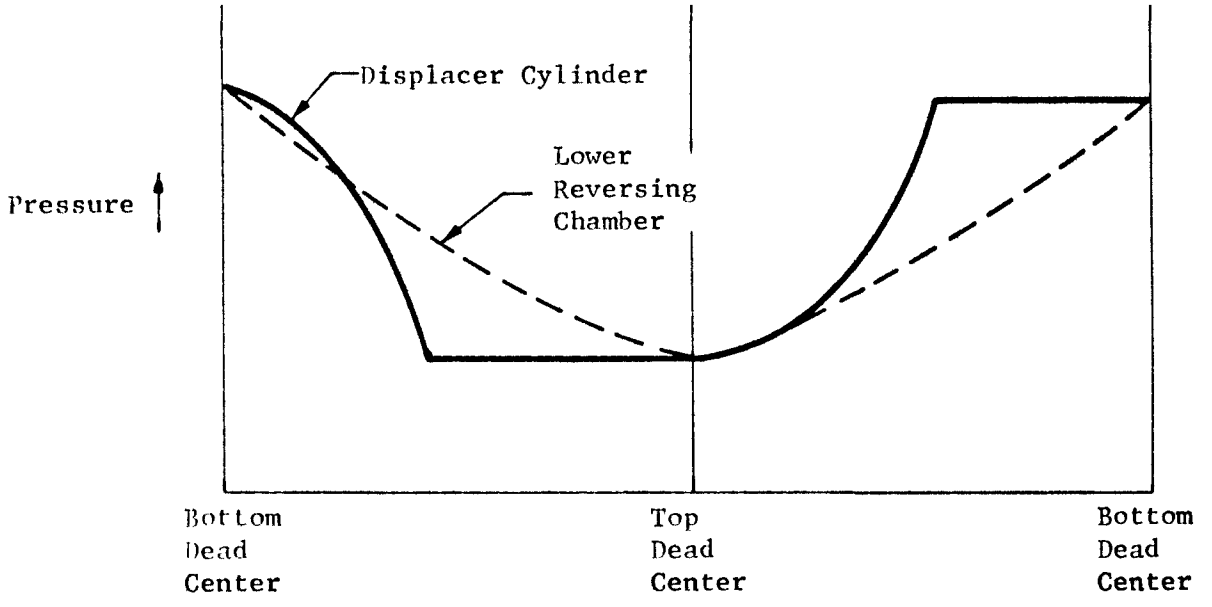

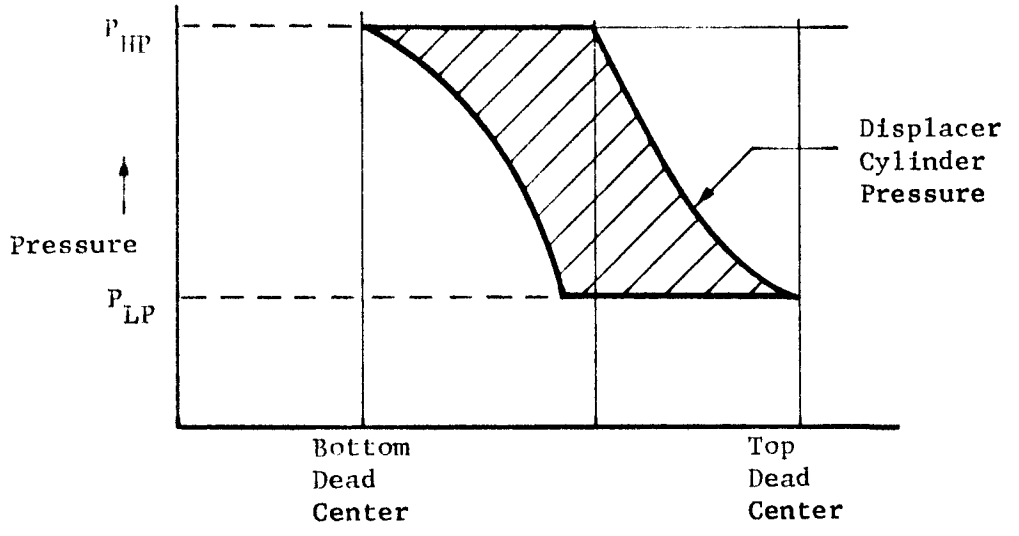

3.01-68-042

FIGURE D-1. PRESSURE TRACES

NOMENCLATURE

P	=	Pressure
A	=	Area reversing piston
A_R	=	Area rod
M	=	Mass of reciprocating mass
x	=	Position variable
L	=	(cylinder length - piston length)/2
V	=	Volume
v	=	Velocity
z	=	x/L
z_L	=	(x/L) at x = max.
γ	=	C_p/C_v ratio for working fluid
f	=	Frequency
T	=	Period
$I(z_L)$	=	See text
S	=	Stroke
WK	=	Work per cycle

Subscripts

o	=	reversing piston at mid-stroke
u	=	upper
l	=	lower
HP	=	high pressure reservoir
LP	=	low pressure reservoir

APPENDIX E
SEALS AND BEARING ANALYSES

A. MAXIMUM ACCELERATION FORCE

The forces operating on the reciprocating mass system were established by an examination of the acceleration forces developed during normal operation.

Assuming a sinasoidal operation, the forces can be calculated by:

$$X = \frac{S}{2} \sin\beta\theta$$

$$\dot{X} = \frac{S}{2} \beta \cos\beta\theta$$

$$\ddot{X} = -\frac{S}{2} \beta^2 \sin\beta\theta = \frac{F}{M} = \text{acceleration}$$

$$F = \frac{MS\beta^2}{2} \sin\beta\theta$$

$$F_{max} = \frac{MS\beta^2}{2} = \frac{0.1 \times 1.5 \times 4\pi^2 (16.6)^2}{32.2 \times 12 \times 2}$$

$$F_{max} = 2.1 \text{ lb}$$

B. TWISTING MOMENT

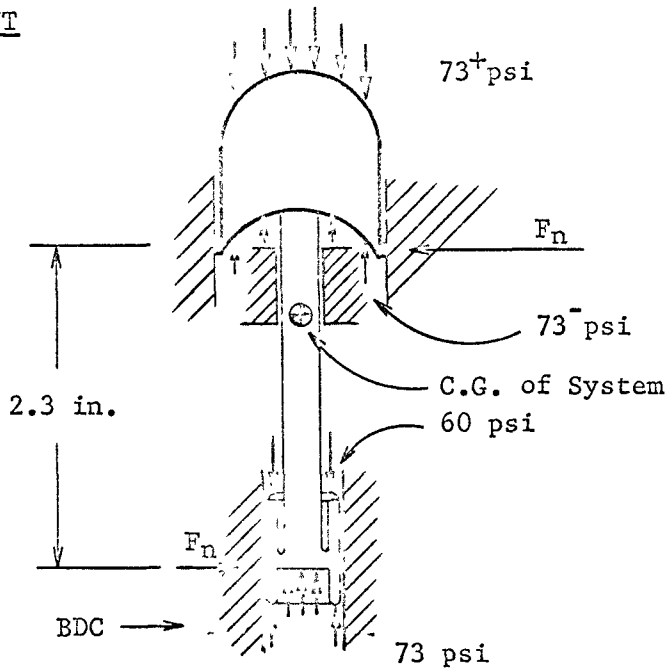

FIGURE E-1

A potential problem is the twisting moment which would result from a center of gravity which is not precisely on the axial centerline due to manufacturing or material eccentricities (See Figure E-1). Assuming a dislocation of 0.010 in. (which, in a symmetrical body of rotation of about 1 in. diameter is very unlikely),the moment created would be M = 2.1 x 0.010 in. = 0.021 inch lb. Normal forces are required on both the displacer piston and reversing piston to counteract this moment. The magnitude of these forces is:

$$F_n = \frac{0.021}{2.3} = 0.0091 \text{ lb}$$

This force is negligible compared to the weight of the reciprocating mass.

C. PRESSURE FORCES ON REVERSING PISTON

A condition more serious than that discussed in B above (but even less likely) is that associated with a force developed momentarily at the bottom dead center or top dead center position if the reversing piston assumes a slightly cocked attitude. A condition can be hypothesized (see Figure E-2) where skew position of the piston results in a pressure unbalance which tends to force the piston to one side of the cylinder. This solution was analyzed by calculating the normal forces developed as follows:

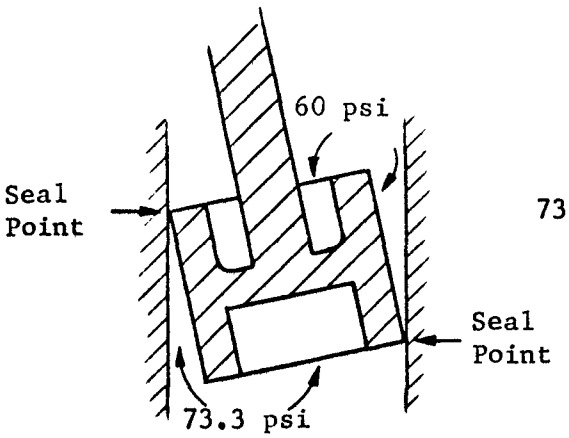

Axial Cross Section

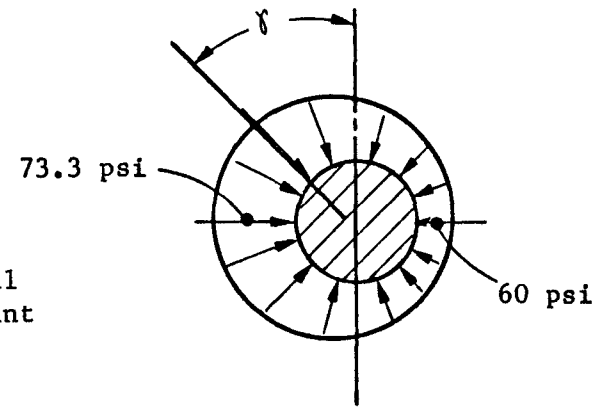

Transverse Cross-Section with Pressure Distribution on Surface Indication

FIGURE E-2

Assume $$P = P_A + \frac{\Delta P}{2}(1 + \sin\gamma)$$

$$\frac{\text{Force}}{L} = R\int_0^{2n}\left[\left(P_A + \frac{\Delta P}{2}\right) + \frac{\Delta P}{2}\sin\gamma\right]\sin\gamma\, d\gamma$$

$$= \frac{R\Delta P}{2}\int_0^{2\pi}\sin^2\gamma$$

$$= \frac{R\Delta P}{2}\left[\frac{1}{2}\gamma - \frac{1}{2}\sin^2\gamma\right]_0^{2\pi}$$

$$= \frac{\pi R\Delta P}{2}$$

$$\text{Force} = \frac{\pi R\Delta P L}{2}$$

$$R = 0.5/2$$

$$\Delta P = 13.3$$

$$L_p = 0.5 \text{ in.}$$

$$\text{Force} = \frac{\pi \times 0.25 \times 13.3 \times 0.5}{2} = 2.6 \text{ lb}$$

This represents a very conservative estimate, since the clearance between piston and cylinder wall is so small that pressure differences of the type postulated could not develop.

D. DISPLACER PISTON LEAKAGE

The leakage rate across the displacer piston was examined as follows:

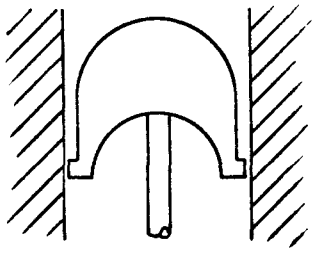

FIGURE E-3

Assume $\Delta P = 0.1$ psi

$(Q/fD_v) = 0.04$ (shown to be acceptable by the analog computer studies)

ρ = density of helium at 73.3 psi and 250°F

$= 2.22 \times 10^{-5}$ lb/in.^{3}

$D = 1.02$ in.

$L = 0.0625$ in.

Assuming an entrance and exit loss of 1.5 velocity heads:

$$\Delta P = f_R \frac{L}{D_e} \frac{V^2}{2g} \rho + 1.5 \frac{V^2}{2g} \rho$$

$$= \frac{64 \mu}{D_e V \rho} \frac{L}{D_e} \frac{V^2 \rho}{2g} + 1.5 \frac{Q^2 \rho}{2g (\pi^2 \delta^2 D^2)}$$

$$= \frac{8 \mu L}{\pi g \delta^3 D} \left(\frac{Q}{f D_v}\right) \left(f D_v\right) + 4.35 \times 10^{-9} \left[\frac{Q}{f D_v \delta}\right]^2 \left(f D_v\right)^2$$

$$= 1.93 \times 10^{-7} \frac{L}{\delta^3} \left(\frac{Q}{f D_v}\right) + 2.25 \times 10^{-6} \left(\frac{Q}{f D_v}\right) \frac{1}{\delta^2}$$

Since $\left(\frac{Q}{f\ D_v}\right) = 0.04 \quad L = 0.0625$ in.

$$\Delta P = 4.82 \times 10^{-10}/\delta^3 + 3.60 \times 10^{-9}/\delta^2 = 0.1 \text{ psi}$$

By trial and error

$$\delta = 0.00169 \text{ inches}$$

E. REVERSING PISTON LEAKAGE

The reversing piston was examined by establishing the continuous energy loss due to the leakage around the piston. As in the preceding case, the friction losses are much greater than entrance and exit losses. Neglecting the latter;

$$\Delta P = f \frac{L}{D_e} \frac{V^2}{2g} \rho = \frac{64\ \mu}{D_e V \rho} \frac{L}{D_e} \frac{V^2}{2g} \rho$$

$$= \frac{32 \mu\ L\ Q}{g\ D_e^{\ 2}\ (\pi\ D\ \delta)} \quad \text{where} \quad D_e = 2\ \delta$$

$$Q = \frac{g\ \delta^3 \pi D}{8\ \mu L}\ \Delta P$$

Since $E_{\Delta\theta} = \left[\Delta\ P\ Q\right]_{\Delta\theta} = \frac{g\ \delta^3 \pi D \Delta P^2}{8\ \mu L}$

$$\overline{E} = \frac{g\ \pi \delta^3 D}{8\ \mu L} \left(\frac{2}{T}\right) \int_0^{\pi/2} (\Delta P_{max})^2 \sin^2 \beta\theta\ d\theta$$

Letting

$$y = \beta\theta$$

and

$$\beta = \frac{2\pi}{T}$$

$$\therefore \quad y = \frac{2\pi}{T}\ \theta$$

$$\bar{E} = \frac{g\,\pi\delta^3 D\,(\Delta P_{max})^2}{4\,\mu L T\,(\frac{2\pi}{T})} \int_0^{\pi} \sin^2 y\,dy$$

Solving the integral:

$$\int_0^{\pi} \sin^2 y\,dy = \frac{1}{2^y} - \frac{1}{4}\sin^2 y \Big|_0^{\pi} = \frac{\pi}{2}$$

$$\therefore \quad \bar{E} = \frac{g\,\pi\delta^3 D\,\Delta P_{max}^2}{16\,\mu L}$$

$$\bar{E} = 1.2 \times 10^9 \times \delta^3 \text{ watts}$$

For $\delta = 0.0001 = 10^{-4}$ inch

$$\bar{E} = 1.2 \times 10^{-3} \text{ watts}$$

$$= 0.0012 \text{ watts}$$

For $\delta = 0.0005 = 5 \times 10^{-4}$ inch

$$\bar{E} = 1.2 \times 10^9 \times 1.25 \times 10^{-10}$$

$$= 0.14 \text{ watt}$$

To allow for 0.0008 in. wear (on the diameter) over the 10 year life, a radial tolerance of 0.0001 must be held during fabrication.

F. LABYRINTH SHAFT SEAL LEAKAGE

The clearance for this shaft was established in a manner similar to that described in the previous section. Then:

$$\bar{E} = \frac{g\,\pi\delta^3 D\,\Delta P^2_{max}}{16\,\mu L}$$

$$\bar{E} = 3.3 \times 10^8\,\delta^3$$

$\therefore$ for $\delta = 0.0001$, $\bar{E} = 0.00033$ watts

for $\delta = 0.0005$, $\bar{E} = 0.04$ watts

G. SHAFT SEAL - LABYRINTH TYPE DESIGN

A labyrinth-type shaft seal was considered as an alternate design. An analysis was performed to determine the optimum labyrinth seal geometry using the formula given in "Close Clearance Orifices" by Andrew Lenkei, Product Engineering, April 26, 1965.

$$W = 5.7\ KA \frac{P_1}{\left[RT_1\right]^{\frac{1}{2}}} \left(\frac{1-\left(P_m/P_1\right)^2}{m - Ln\,P_m/P_1}\right)^{\frac{1}{2}} \left[1-\left(\frac{1}{\frac{8.5C}{L_p - L + 7.2C}}\right)\right]^{\frac{1}{2}}$$

$$N_R = \frac{2WC}{AMG}$$

For low Reynold's number flow, the flow coefficient, K, is approximated by the relationship:

$$K \approx \left[\frac{N_R}{75 + 32L/C}\right]^{\frac{1}{2}}$$

Combining the equations for W, N_R and K, and rearranging yields:

$$\frac{1}{W} \alpha \frac{1}{Z}(Z + 0.426X) \left(YZ + Ln\ P_{1/P_m}\right)\left[\frac{1 - 1.3Z - X}{1 + 7.2Z - X}\right] = \Psi$$

For a fixed Z and Y, there is an optimum X (land-to-pitch ratio) to result in minimum flow. The optimum X can be determined by differentiating the equation and letting

$$\frac{\partial X}{\partial X} = \frac{\partial\,(1/W)}{\partial X} = 0 \quad \text{for a maximum}$$

$$\text{The optimum } X = C2\left[1 - \left[1 - \frac{C_1C_2 - C_oC_2 + C_oC_1}{C_2^2}\right]^{\frac{1}{2}}\right]$$

Where:

$$C_o = 2.35Z$$
$$C_2 = 1 + 7.2Z$$
$$C_1 = 1 - 1.3Z$$

Figure E-4 shows a plot of Ψ and $X_{optimum}$ as a function of Z. To obtain a maximum Ψ or minimum flow, Figure E-4 shows that a minimum Z and a value of X approaching unity should be used.

$$\text{Since} \quad X = L/L_p \cong 1 \quad L \approx L_p$$

or the optimum land-to-pitch ratio for low Reynold's number flow systems is 1. A labyrinth seal with this land to pitch ratio is more commonly known as a sleeve seal.

NOMENCLATURE

A	=	Flow area
C	=	Radial clearance - shaft-to-land
C_o, C_1, C_2	=	Defined in text
C.G.	=	Center of gravity
D	=	Diameter
D_e	=	Equivalent diameter
D_v	=	Swept volume
E	=	Energy
F	=	Force
f	=	Frequency
f_R	=	Friction factor
g	=	Gravitation acceleration
K	=	Flow coefficient

L = Length (for labyrinth, L is land length)

L_p = Pitch - single labyrinth land and valley

L_t = Total labyrinth length

M = Mass

n = Number of labyrinth lands

N_R = Reynold's number

P = Pressure

Q = Flow rate

R = Gas constant

S = Stroke

T = Period

T_e = Temperature

V = Velocity

W = Mass flow rate

X = L/L_p

y = L_t/C

Z = C/L_p

β = $\frac{2\pi}{T}$

γ = Azmuth angle

δ = Clearance

θ = Time

μ = Viscosity

ρ = Density

Ψ = Define by Equation 4 but proportion to 1/W

Subscript 1 = upstream conditions

Subscript m = downstream conditions.

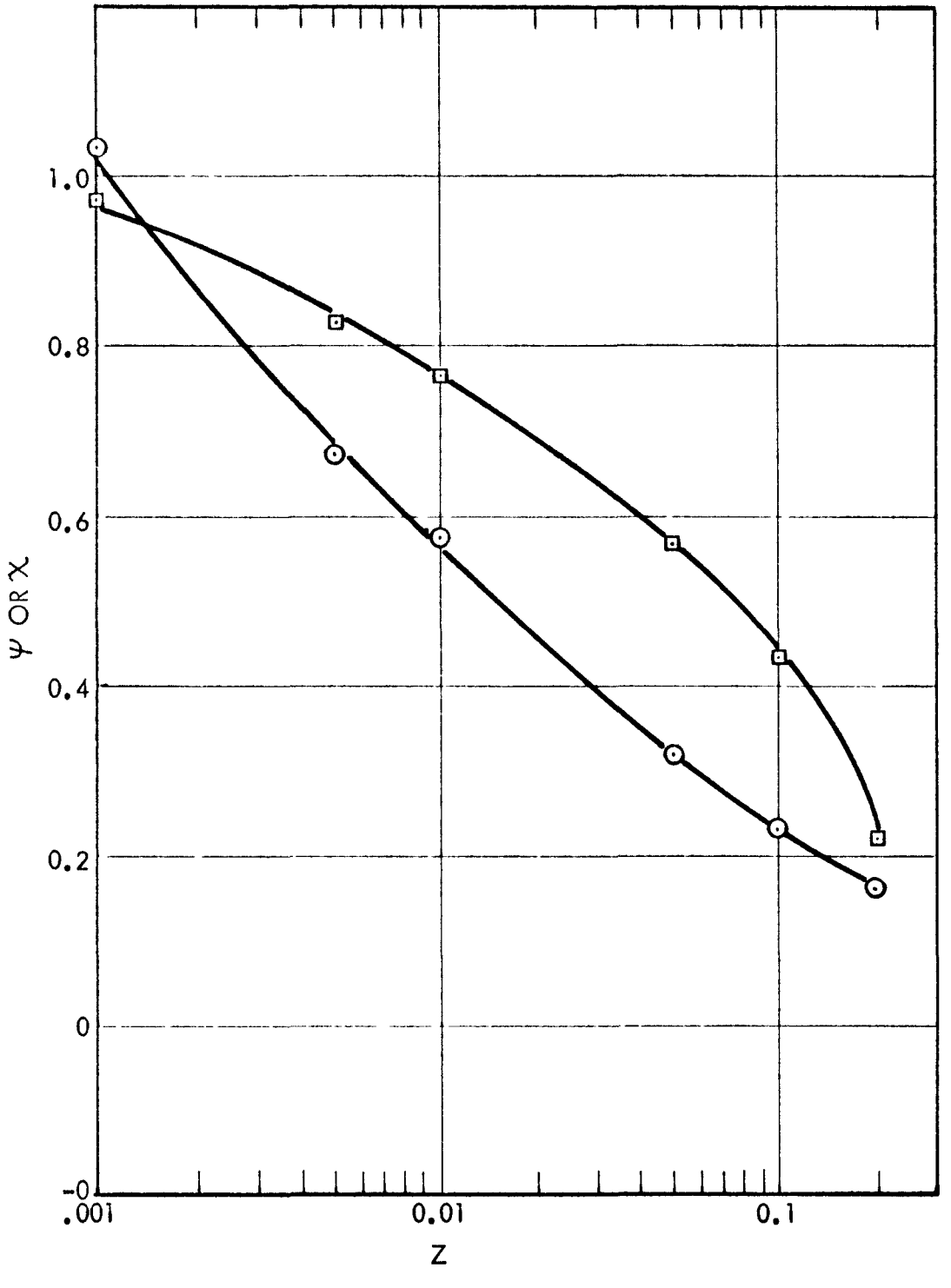

FIGURE E-4. LABYRNTH SEAL PARAMETERS

3.01-68-043

BIBLIOGRAPHY

1) Bibliograph on Solid Lubricants, NASA SP-5037, February 1966.

2) Technology Survey - Solid Lubricants, NASA SP-5059, May 1966.

3) Load and Temperature as Related to Solid Film Lubricant Wear Life, Goerge Murphy, Jr., January 1967, AD 649-102.

4) Friction and Wear of Composite Solid Lubricating Materials, G. L. Thomas, AD-636-402.

5) Dry - Film Lubricants from Molybdenum Disulfide Bonded with Microfibrous Boehmite, V. G. Fitzsimmons, December 1966, AD-645-889.

6) Radiometaic Study of the Wear Characteristics of Dry Film Lubricants, E. A. Jennings, August 1966.

7) Bonded-Coating Lubricated Metal Parts, Alfred Disapio, September 5, 1960, Product Engineering.

APPENDIX F
PUMPING CHAMBER AND ENGINE INTERACTION

A. MODEL

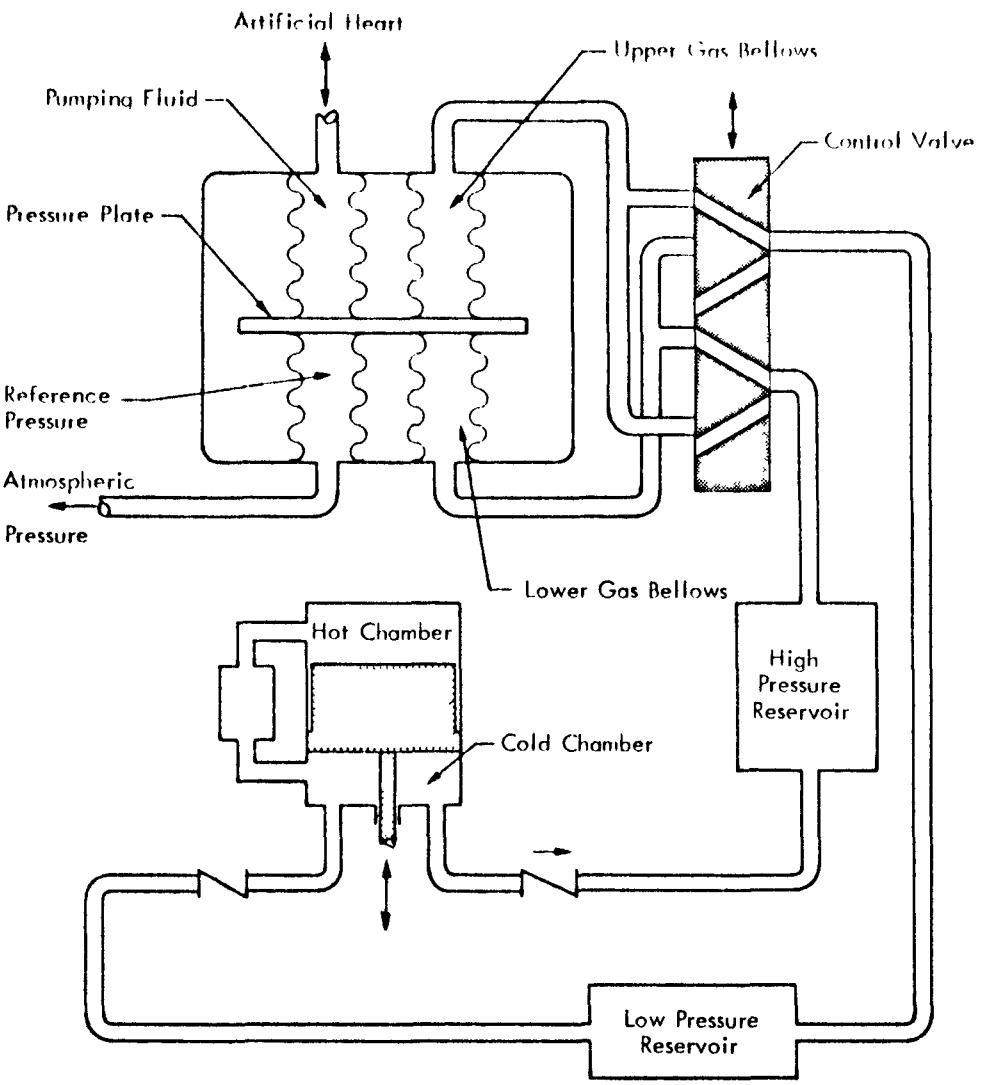

B. ANALYSIS

A computer code was written to evaluate the interaction between the engine, pumping chamber and artificial heart. Simplifying assumptions were made for each of the major assemblies to minimize the complexity of the code; the basic assumptions are listed below:

1) With the exception of the engine hot chamber, the gas in all volumes was assumed to be at a constant temperature.

2) The Stirling engine was assumed to be a perfect Schmidt-type engine with no frictional or aerodynamic losses.

3) The engine was assumed to have an unswept-to-swept volume ratio of 0.378 in both the hot and the cold chambers.

4) The pressure plate and bellows in the pumping chamber were assumed to have no inertia. (The combined bellows have a linear spring constant with a zero net force when half of the pumping fluid stroke volume is in the pumping chamber.)

5) The check valve was assumed to act in an ideal manner.

6) Valve switches were assumed to be accomplished instantaneously.

7) The artificial heart was assumed to be depicted by the following model:

$$Q_{systole} = C_1 (P_R - P_o)$$

$$Q_{diastole} = C_2 (P_{oo} - P_R)$$

where:

$Q_{systole}$ = Rate at which pumping fluid flows from the pumping chamber to the artificial heart as determined by the flow resistance of the vascular system.

$Q_{diastole}$ = Rate at which pumping fluid flows from the artificial heart to the pumping chamber as determined by the flow resistance of the artificial heart valves.

C_1, C_2 = Proportionality constants.

P_o = Pressure in the ventricle at which blood starts to flow from the ventricle to the aorta.

P_{oo} = Pressure in the ventricle at which blood starts to flow from the atrium to the ventricle.

P_R = Pumping fluid pressure.

The heart cycle was arbitrarily subdivided into 156 intervals. The engine is assumed to have an oscillation 1/15.6 that of a heart cycle. The number of the 156 intervals alloted to systole is an input variable.

An examination of the model shows that there are six basic configurations which depend on both the control valve and check valve settings. The six basic configurations are listed in Table F-1.

TABLE F-1

BASIC COMBINATIONS - INTERCONNECTED VOLUMES

Case	Volume	Interconnected Spaces
Case I (Diastole)	a	Engine, HP reservoir, upper gas bellows
	b	LP reservoir, lower gas bellows
Case II (Diastole)	a	HP reservoir, upper gas bellows
	b	LP reservoir, lower gas bellows
	c	Engine
Case III (Diastole)	a	HP reservoir, upper gas chamber
	b	Engine, LP reservoir, lower gas bellows
Case IV (Systole)	a	Engine, HP reservoir, lower gas bellows
	b	LP reservoir, upper gas bellows
Case V (Systole)	a	HP reservoir, lower gas bellows
	b	LP reservoir, upper gas bellows
	c	Engine
Case VI (Systole)	a	HP reservoir, lower gas bellows
	b	Engine, LP reservoir, upper gas bellows

The computer program calculates the combined response of the engine, pumping chamber, and artificial heart interval by interval. For each interval, the flow rate to or from the artificial heart calculated for the preceding interval is assumed to persist. This assumption permits the determination of new upper and lower gas bellows volumes.

At the start of each interval, the computer determines which of the basic configurations listed in Table F-1 exists, and calls one of six subroutines, each of which depict one of the six basic configurations. In each subroutine, new pressures, based on the new volumes for the two gas bellows and engine position, are calculated for each volume in the system. This pressure calculation is based on a conservation of mass. In addition, the subroutine determines if the position of either of the check valves should be modified for the next interval.

On the return to the main program from one of the six subroutines, a force balance is made on the pressure plate to determine the pumping fluid pressure required to maintain equilibrium. Bellows forces are included in this force balance. Based on the revised pumping fluid pressure, a new pumping fluid flow rate is calculated and the next interval calculation is started.

A convenient set of initial conditions is to assume that the system is at constant pressure. Accordingly, it requires a number of heart cycles for the system to reach equilibrium.

The program input data includes hot volume temperature, cold volume temperature, engine swept volume, area ratio of gas to pumping fluid bellows, average pumping fluid pressure, average system gas pressure, HP and LP reservoir volume, four artificial heart constants (see assumption 7), pumping fluid stroke volume, combined spring constants of all bellows, pneumatic power required for other than pumping chamber, intervals for systole, and number of heart cycles analyzed prior to printout.

The output consists of a print out for every fifth interval. The output information includes interval number, engine position, all gas and pumping fluid pressures, and the volume of pumping fluid transfered to the artificial heart.

APPENDIX G
TYPICAL BELLOWS ANALYSIS

A. STATEMENT OF PROBLEM

This Appendix presents a typical stress and deflection analysis for one of several sets of bellows specified in the reference conceptual pumping chamber. The large bellows containing the pumping fluid has been selected for analysis. This bellows can be subjected to either the maximum and minimum differential pressure at any point in its travel; therefore, it is necessary to consider four stress points, at the ID and OD, as listed below:

Case	Pressure Differential	Compression
I	maximum	minimum
II	minimum	minimum
III	maximum	maximum
IV	minimum	maximum

The following bellows criteria are assumed:

1) Maximum pressure differential, 65 psi external
2) Minimum pressure differential, 60 psi external
3) Mean diameter, 2.65 in.
4) Stroke, 1 in.
5) Modulus of elasticity, 16×10^{-6} psi
6) Minimum spring constant desired.

B. ANALYSIS

This analysis is based on the technique described by Zierak and Juderslehan*. The nomographs and curves presented in this reference were converted into curves for titanium alloys to simplify the analysis for the pumping

*Zierak, S. J. and Juderslehan, P., "Nomograms and Charts for Welded Diaphragm Metal Bellows Design", Design News, 26 Oct. 1967

chambers. These curves are reproduced as Figures G-1 and G-2. Figure G-3 shows the fatigue curve used for the bellows analysis.

As shown in Figure 26 of the main text, the minimum spring constant for a fixed mean diameter, ΔP, ID uncorrected pressure stress, and length is provided by a bellows with a span-to-mean-diameter ratio of approximately 1.3. For this bellows:

$$K_{minimum} = 1.61 \times 10^5 \, D_m^3 \, \Delta P^2 / \sigma_{PID}^2 \, L$$

For this calculation

$$K_{minimum} = 1.27 \times 10^{10} / \sigma^2_{PID} L$$

Assume $L = 0.4$ in. and $\sigma_{PID} = 85{,}000$ psi

$$K_{minimum} = 4.4 \text{ lb/in.}$$

$$K_o = 11 \quad \text{(see Figure G-1)}$$

$$h = 4.2 \left[\frac{D_m L K}{K_o} \right]^{\frac{1}{4}} \text{ mils}$$

$$= 3.4 \text{ mils}$$

$$S = 1.3 \times D_m = 0.345 \text{ in.}$$

$$\sigma_{\delta ID} = -3{,}700 \frac{h^2 \delta}{D_m^2 L} = 15{,}200 \, \delta \text{ psi (See Figure G-2)}$$

Assume that δ goes from 4 to 5 in.

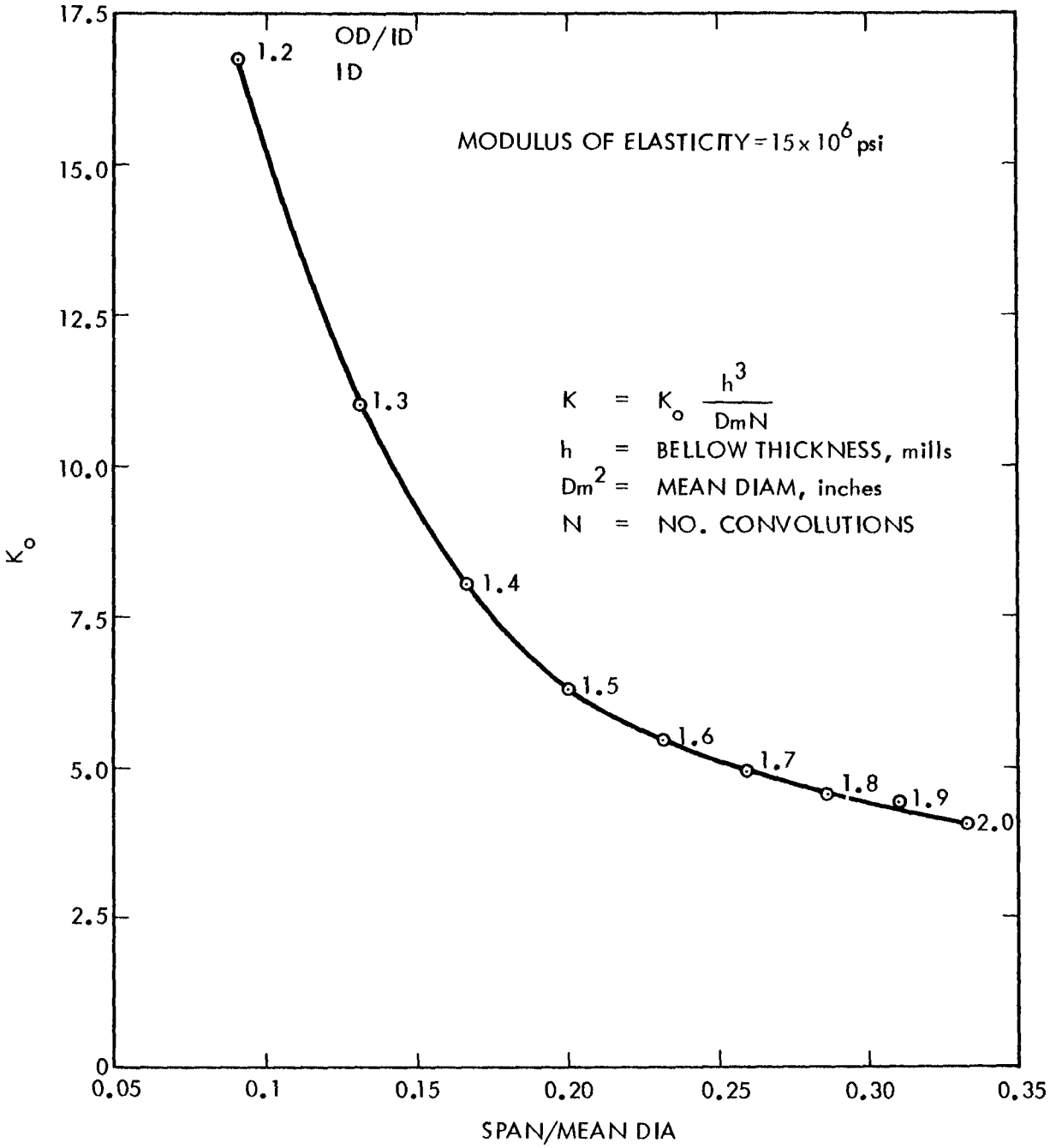

FIGURE G-1. EFFECT OF SPAN ON NESTED RIPPLE BELLOWS SPRING CONSTANT

3.01-68-044

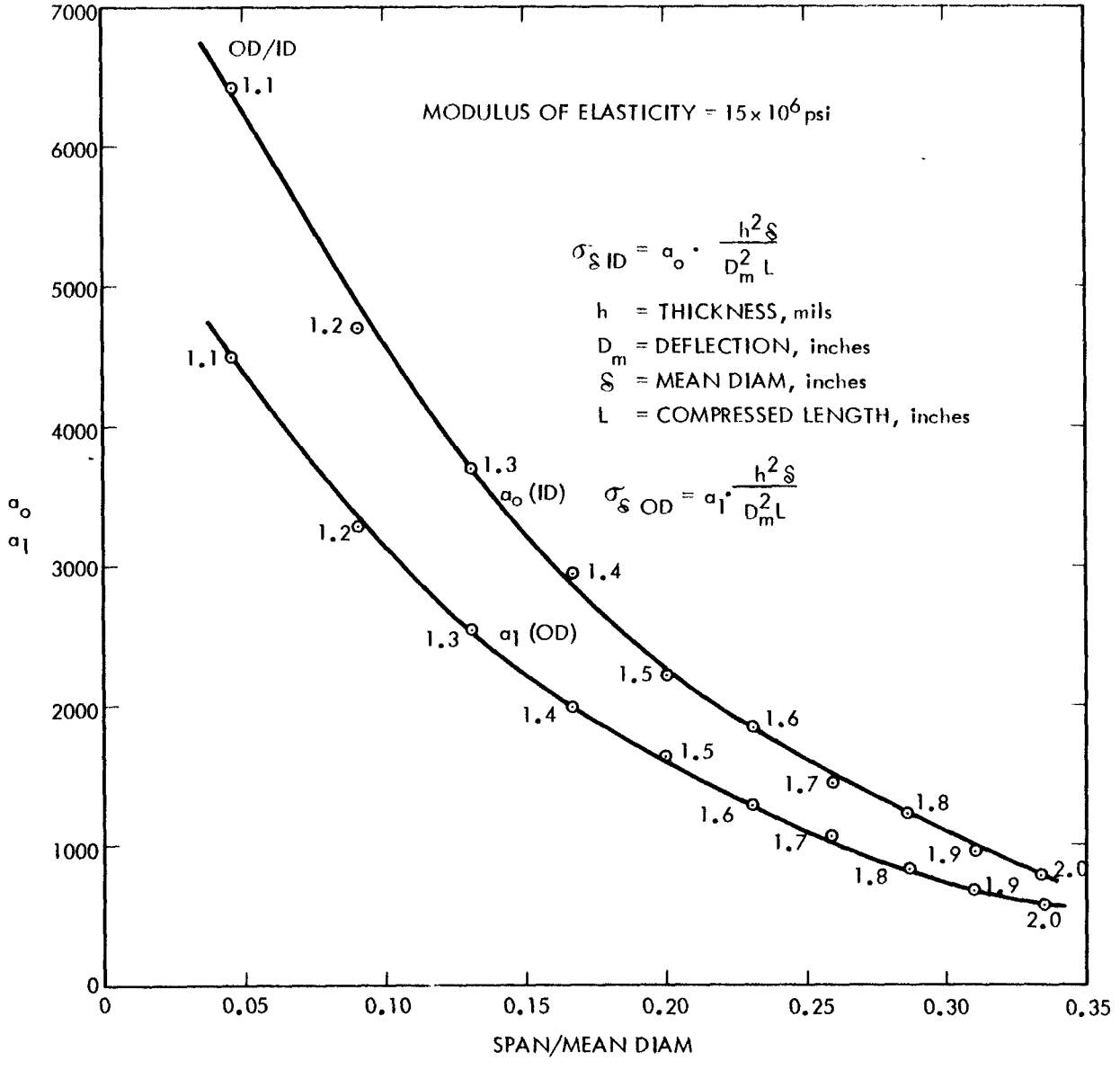

FIGURE G-2. DEFLECTION STRESSES FOR NESTED RIPPLE BELLOWS

3.01-68-045

3.01-68-046

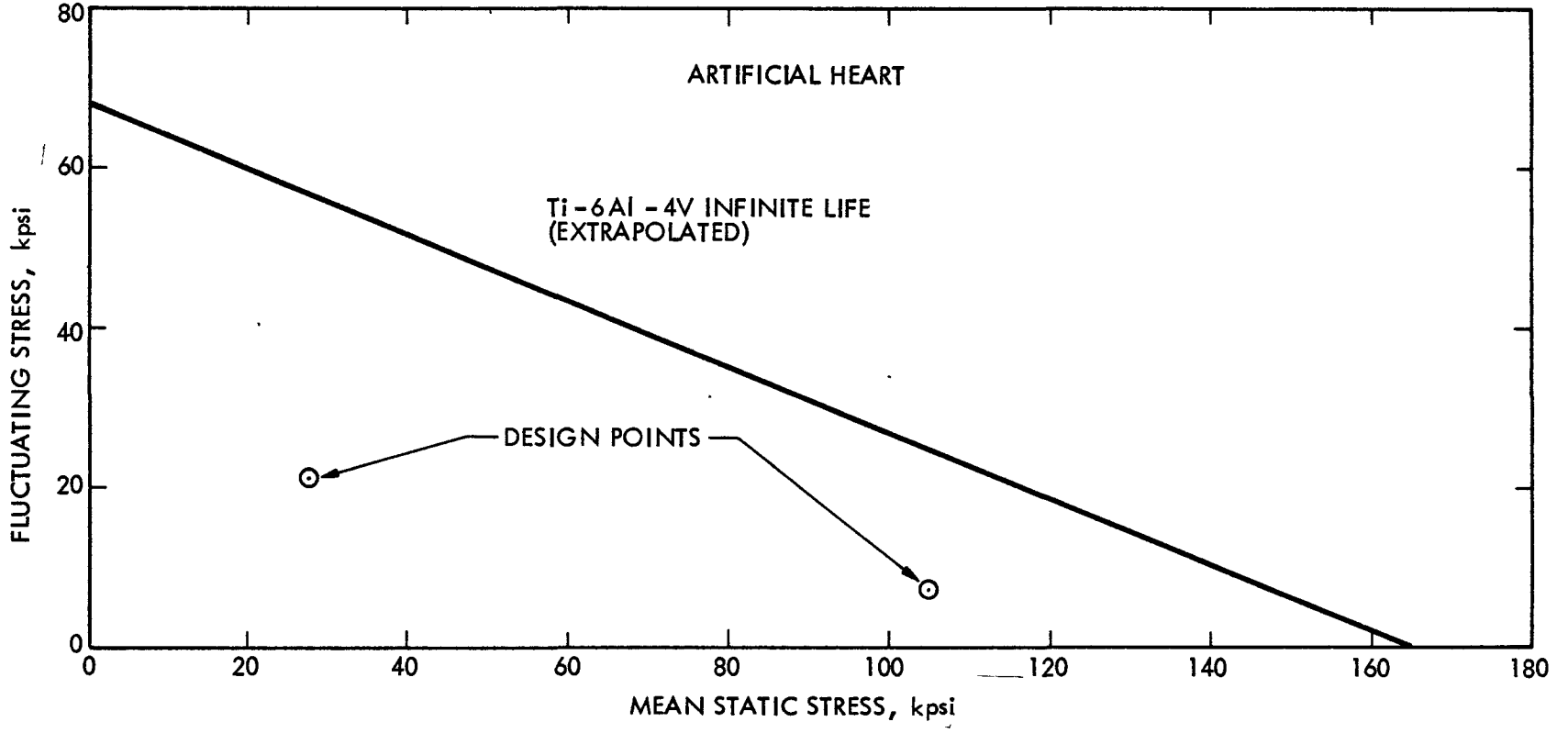

FIGURE G-3. PUMPING BELLOWS STRESSES AS RELATED TO FATIGUE CURVES

AGN-8258

Stress on ID

Stress in kpsi

Case	I	II	III	IV
σ_{PID}	+ 85.0	+ 78.5	+ 85.0	+ 78.5
$\sigma_{\delta ID}$	- 60.5	- 60.5	- 75.5	- 75.5
Net Stress	+ 24.5	+ 18.0	+ 9.5	+ 3.0
Stress K_s*	+ 49.0	+ 36.0	+ 19.0	+ 6.0

Range of ID Stress = + 6.0 to 49.0 kpsi

σ_{ID} = 27.5 $\pm$ 21.5 kpsi

Stress on OD

$$\sigma_{\delta OD} = 2{,}500 \frac{h^2 \delta}{D_m^2 L} = -10{,}300\ \delta$$ (See Figure G-2)

$$\sigma_{POD} = 0.725\ \sigma_{PID}$$

Case	I	II	III	IV
σ_{POD}	- 61.6	- 57.0	- 61.6	- 37.0
$\sigma_{\delta OD}$	- 40.9	- 40.9	- 51.0	- 51.0
Net Stress	-102.5	- 97.9	-112.6	-108.0
Stress K_s	-102.5	- 97.9	-112.6	-108.0

Range of OD Stress = -97.9 to -112.6 kpsi

σ_{OD} = -105.2 $\pm$ 7.4 kpsi

The two controlling stress points are plotted in Figure G-3. The calculated stresses are well below the controlling maximum stress line for the Ti-6A-4V alloy.

*Factor of 2 stress concentration on all tensile stress.

NOMENCLATURE

ΔP	=	differential pressure
K	=	spring constant
D_m	=	mean diameter
L	=	bellows compressed length
K_o	=	empirical factor
S	=	span
h	=	bellows wall thickness
δ	=	compressive deflection from free length
σ_{PID}	=	pressure stress on ID
σ_{POD}	=	pressure stress OD
$\sigma_{\delta ID}$	=	deflection stress ID
$\sigma_{\delta OD}$	=	deflection stress OD
σ_{ID}	=	net stress OD

Positive stresses indicate tension

APPENDIX H
HEAT REJECTION EQUIPMENT

A. INTRODUCTION

In Section 5.9 of this report, two sets of assumed operating parameters are delineated. Each of these sets of parameters are controlling for one of the two main heat exchangers in the heat rejection system. For the pumping fluid-to-blood heat exchanger, the maximum blood temperature is the critical parameter; therefore the low flow, maximum heat load condition is controlling and this occurs when minimum mechanical power is being delivered to the blood. For the gas-to-pumping fluid heat exchanger, the maximum performance of the heat exchanger should occur when maximum mechanical power is being delivered to the blood so that maximum efficiency is obtained.

For the gas-to-pumping fluid heat exchanger, the following conditions apply:

Heat rejection, 25 watts; pumping fluid rate, 24 l/min forward and reverse; systole-diastole duration, 1:1. Approximately 22 watts must be transfered by the gas-to-pumping fluid heat exchanger.

For the pumping fluid-to-blood heat exchanger, the following conditions apply:

Heat rejection, 30 watts; pumping fluid rate, 12 l/min during systole and 6 l/min during diastole; average blood flow rate, 2.4 l/min; systole-diastole duration 1:2; relative blood flow during systole, 1; relative flow during 70% diastole, 0.2; relative flow during remaining 30% diastole, 0; aorta size, 2.5 cm; inlet blood temperature, 39°C; heart pulse rate, 1 beat/sec.

It is further assumed that 22.5 watts are dissipated in the pumping fluid-to-blood heat exchanger which replaces a section of the abdominal aorta and 7.5 watts are dissipated in the artificial heart.

B. PUMPING FLUID-TO-BLOOD HEAT EXCHANGER - BLOOD SIDE

Assumed blood properties:

Density = 1.04 gr/cc = 0.0376 lb/in.^{3}

Thermal conductivity = 0.36 Btu/hr ft ^oR

Kinematic viscosity = 0.0169 $\longrightarrow$ 0.0269 cm^2/sec = 0.0026 $\longrightarrow$ 0.0042 in.^{2}/sec

Heat capacity = 1 cal/gr ^oC = 1 Btu/^oR

Average flow rate = 2.4 l/min = 2.44 in.^{3}/sec

	Systole	Diastole 70%	Diastole 30%
Percent of time	33.3	46.7	20
Flow rate, in.^{3}/sec	5.72	1.15	0
Flow rate, lb/sec	0.210	0.042	0
Reynold's Number	1740 2800	348 572	0
Flow regime	laminar	laminar	static
Graetz's Number (L = 6 in.)	4,200	840	0
Nusselt's Number (ND/K)	28.4	16.5	4.36
h, Btu/hr ft^2 ^oR	123.2	71.5	19.0
Velocity, in/sec	7.36	1.47	0
Energy absorption, watts	35.4	20.5	6.5

From the forgoing, the average h for the whole cardiac cycle and the bulk blood flow rise during systole are 78.2 Btu/hr ft^2 ^oF and 0.18^oF respectively.

Assuming that the heat flow from the pumping fluid side is relatively constant, the temperature rise in the stainless steel wall of the heat exchanger during each diastole can be estimated. The thermal capacity of a 6 in. long, 1 in. diameter, 20 mil thick wall stainless steel tube is approximately 0.01 Btu/^oF $\cong$ 10 watt-sec/^oF. The wall temperature rise during diastole

$$\simeq \frac{(22.5 - 20.5)\ 0.467 + (22.5 - 5.5)^{0.2}}{10 \text{ watt sec}/^oF} \text{ watt-sec} \approx 0.43^oF.$$

Since the maximum blood temperature increase is limited to 7.2°F (4°C), the average film temperature differential must be 7.2°F minus the bulk temperature rise during systole minus half of the tube wall temperature rise during diastole or 6.8°F. Then:

$$A = \frac{\bar{Q}}{h\Delta T_{Film}} = \frac{(22.5)\ (3.412)}{(78.2)\ (6.8)} = 0.144\ ft^2 = 20.8\ in^2 \quad \text{and}$$

$$L = \frac{A}{\pi D} = \frac{20.8}{\pi x 1} = 6.6\ in.$$

C. PUMPING FLUID-TO-BLOOD HEAT EXCHANGER - PUMPING FLUID SIDE

The pumping fluid is assumed to have properties similar to water at approximately 110°F as follows:

Density $\simeq$ 1 gr/cc = 0.036 lb/in.^{3}
Thermal conductivity $\simeq$ 0.36 Btu/hr ft °R
Kinematic viscosity $\simeq$ 0.0066 cm^2/sec $\simeq$ 0.00103 in.^{2}/sec
Heat capacity = 1 cal/gr °C $\simeq$ 1 Btu/°R
Flow rate = 12 l/min = 12.2 in.^{3}/sec forward
= 6 l/min = 6.1 in.^{3}/sec reverse
= 24 l/min = 24.4 in.^{3}/sec maximum
Prandtl number $\simeq$ 4.24

The controlling factor is the pressure drop. Assuming an annular flow passage, the value of equivalent diameter to area is:

$$D_e/A_c = \frac{2\delta}{\pi D\delta} = \frac{2}{\pi} = 0.636\ in.^{-1}$$

$$N_{Re} = \frac{VD_e\rho}{\mu} = \frac{D_eW}{A\ \mu} = \frac{0.636 \times (6.1 \longrightarrow 12.2)}{0.00103}$$

N_{Re} = 3770 reverse
= 7550 forward

Flow in the forward direction is turbulent, with a friction factor $\approx$ 0.035

$$\Delta P = f \frac{L}{D_e} \frac{V^2}{2g} \rho = \frac{f}{\pi^2} \frac{L(\emptyset)^2}{D_e D^2 \delta^2} \frac{\rho}{2g}$$

$$= \frac{(0.035)\ (6.6)\ \ (24.4)^2\ \ (0.036)}{(2\ \pi^2)\delta^3 (2)\ (32.2)\ (12)} = \frac{3.24 \times 10^{-4}}{\delta^3}$$

For $\Delta P \approx 0.1$ psi

$\delta^3 \simeq 3.24 \times 10^{-3}$ in.^{3}

$\delta = 0.15$ inch

Using the Colburn Equation:

$$h \approx 0.023 \frac{K}{D_e} (N_{Re})^{0.8} (Pr)^{0.4} .$$

$$= \frac{(0.023)(0.036)}{0.15/12} (3770 \longrightarrow 7550)^{0.8} (4.24)^{0.4}$$

$= 850$ Btu/hr ft^2 ^oR reverse flow

$= 1500$ Btu/hr ft^2 ^oR forward flow

$\bar{h} = (1,500)\ (0.333) + (850)\ (0.667) = 1070$

Average $\Delta T_{Film} \simeq \frac{Q}{hA} = \frac{(22.5)\ (3.412)\ (144)}{(1070\pi)\ (1)\ (6.6)} = 0.50^oF$

Average ΔT(bulk systole) $\simeq \frac{Q}{WC_p} \approx 0.048^oF$

Average ΔT(bulk diastole) $\simeq 0.096^oF$

Temperature differential across tube $= \frac{Qt}{KA} = \frac{(22.5)\ (3.412)\ (0.020)\ (12)}{(10)\ (\pi)\ (1)\ (6.6)} = 0.09^oF$

Average temperature of pumping fluid $\approx 110^oF$

D. HEAT TRANSFER IN ARTIFICIAL HEART

To estimate the heat dissipated in the artificial heart, it is assumed that the artificial heart consists of 18 square inches of 30 mil-thick silicone rubber with a conductivity of 0.121 Btu/hr ft ^oR. The heat transfer coefficients for the blood and pumping fluid are assumed to be those obtained in the pumping fluid-to-blood heat exchanger.

$$\frac{1}{U} = \frac{1}{h_{\text{pump fl.}}} + \frac{1}{h_{\text{blood}}} + \left(\frac{t}{K}\right)_{\substack{\text{silicone} \\ \text{rubber}}} = 0.0345$$

$$U = 29.0 \text{ Btu/hr ft}^2\,^{\circ}\text{F} = 0.0591 \frac{\text{watts}}{\text{in}^2\,^{\circ}\text{F}}$$

$$Q = UA\Delta T = (0.0591)\ (18)\ (7.8) = 8.3 \text{ watts}$$

This value of Q is larger than the assumed value of 7.5 watts so that the analysis tends to be conservative.

E. GAS-TO-PUMPING FLUID HEAT EXCHANGER

Contrary to the case for the pumping fluid-to-blood heat exchanger, the controlling condition for the gas-to-pumping fluid heat exchanger is the full engine power condition. The reason for this change in condition is that this heat exchanger must perform best at the full engine output to provide for the highest efficiency at this point. In the pumping fluid-to-blood heat exchanger, the maximum allowable blood temperature was the controlling factor.

The secondary controlling factors in this heat exchanger are the pressure drops on both the liquid and gas sides and the heat transfer coefficient on the gas side.

The geometry specified for this heat exchanger is a concentric tube arrangement, with the pumping fluid flowing through the central tube and the engine working fluid flowing through the annulus.

The size of the central tube can be determined from pumping fluid pressure drop considerations. The maximum flow rate of the pumping fluid is 24.2 $\text{in.}^3/\text{sec}$. The Reynold's number is:

$$N_{Re} = \frac{4W}{\pi D \mu} = \frac{18{,}050}{D} \quad \text{where D is in inches.}$$

The flow is turbulent for diameters below several inches so that a friction factor of ~ 0.026 can be assumed. The frictional pressure drop per foot is:

$$\frac{d\Delta P}{dl} = \frac{f}{D} \frac{V^2}{2g} \rho = 0.00117 \text{ psi/in.}$$

The pressure drop for a 5/8 in. diameter tube is 0.012 psi/inch, which is the correct order of magnitude. The heat transfer coefficient is:

$$h = 0.023\ K/D\ (N_R)^{0.8}\ (Pr)^{0.4} = 1100\ \text{Btu/hr ft}\ ^{o}F$$

The gas side of the heat exchanger has a laminar flow with a Wc_p of 0.6 Btu/hr ^{o}F. The Graetz number is:

$$N_{Gz} = \frac{Wc_p}{KL} = \frac{0.6}{(0.1)\ (L)} = \frac{6}{L}$$

For L (0.6 ft):

$$N_{Nu} = 1.75\ (N_{Gz})^{1/3}$$

$$h = 1.75\ \frac{k}{D_e}\ \left(\frac{6}{L}\right)^{1/3} = 0.318/D_e L^{1/3}$$

where: D_e and L are in feet.

Assuming $D_e = 0.020$ in. and $L \approx 1$ in.

$$h \approx 435\ \text{Btu/hr ft}\ ^{o}R$$

The tube effective heat transfer coefficient $= \frac{K}{t}$

$$\approx \frac{10}{.02/12} \approx 6000\ \text{Btu/hr ft}^2\ ^{o}F$$

The overall heat transfer coefficient

$$U = \left[\Sigma\ \frac{1}{h}\right]^{-1} = \left[\frac{1}{1100} + \frac{1}{435} + \frac{1}{6000}\right]^{-1} = 287\ \text{Btu/hr ft}^2\ ^{o}R$$

Of the overall heat load to the pumping fluid, approximately 22 watts is transfered from the gas to the pumping fluid in the heat exchanger and the remaining is transfered directly to the pumping fluid in the pumping chambers. The total gas ΔT is, therefore:

$$\Delta T_G = \frac{Q}{Wc_p} = \frac{(22)\ (3.412)}{0.6} = 125^{o}F$$

The required heat transfer area is given by:

$$A = \frac{Q}{U\Delta T_G} \ln \frac{\Delta T_G + \Delta T_o}{\Delta T_o}$$

Where: ΔT_o is the temperature difference between pumping fluid and the exit gas. The value of $\Delta T_o \approx 2^{\circ}F$ is used to provide a cold chamber temperature of $250^{\circ}F$.

$$A = \frac{(22.0)(3.412)}{287} \quad \frac{\text{LN } \frac{127}{2}}{127} = 0.00855 \text{ ft}^2 = 1.23 \text{ in.}^{-2}$$

Since the diameter $\approx$ 0.75 in.,the required heat exchanger length is approximately 0.52 inches. To provide a suitable margin, a one inch length is used.

The pressure drop is:

$$\Delta P = f \frac{L}{D_e} \frac{V^2}{2g} \rho = \frac{32\ \mu LV}{g\ D_e^{\ 2}} = \frac{4\ \mu L\emptyset}{\pi g D\ D_e^{\ 3}}$$

for $Q = 7.32 \text{ in.}^3/\text{sec}$, $D_e = 0.020$ in., $\mu = 1.3 \times 10^{-6}$ lb/in.sec

$$\Delta P = \frac{(64)\ (1.3 \times 10^{-6})\ (7.32)\ (1)}{(\pi)\ (32.2)\ (0.75)(0.02)^3\ \ (12)} = 0.0835 \text{ psi}$$

This pressure drop is acceptable.

NOMENCLATURE

A	Heat transfer area
A_c	Fluid flow area
C_p	Heat capacitance (constant pressure)
D	Diameter
D_e	Equivalent diameter
f	Fluid friction coefficient
g	Gravitational constant
h	Heat transfer coefficient
K	Thermal conductivity
L	Length
N_{Re}	Reynold's number
N_{Gz}	Graetz's number
Pr	Prandtl's number
ΔP	Pressure drop
Q	Heat flow
t	Wall thickness
ΔT	Temperature difference
ΔT_G	Temperature difference gas
ΔT_o	Exit gas temperature less pumping fluid temperature
U	Overall heat transfer coefficient
V	Velocity
W	Weight flow rate
δ	Gap
$\emptyset$	Volumetric flow rate
ρ	Density
μ	Viscosity

APPENDIX I
FUEL CAPSULE ANALYSES

The radioisotope heat source capsule will be implanted in a patient for 1 to 10 years, but it is possible that the radioisotope could become lost in the public domain for an indefinite period. If such were to happen, the worst case conditions would occur at about one half-life of the fuel after encapsulation (87.5 years). At that time,the helium gas pressure buildup resulting from decay of the Pu-238, combined with the decrease in gas pressure as the heat source temperature decays, results in the peak lifetime capsule pressure.

From discussion with PuN source manufacturers,* it has been determined that only a small portion of the helium formed during decay will be on an exposed surface (even in the event of minor pellet cracking) such that it will be released as gas. Therefore, it is assumed that PuN fuel can be prepared which releases only 25% of the He as gas.

If the initial capsule temperature, with the fuel in place in the power system, is 1250°F, the temperature after one half-life is:

$$T_o = \frac{1250 - 100}{2} + 560 = 1085^{\circ}R$$

The moles of released helium formed after one half-life from a 35 w(t) Pu-238 source will be:

$$N_g = \frac{(.25)(35\ w)\ (1 - e^{-\lambda t})}{(0.55\ \frac{w}{gm\ Pu\text{-}238})(238\ \frac{gms\ Pu\text{-}238}{mole})} = 0.0334 \text{ moles}$$

* Memo to R. L. Newacheck from P. Underhill-NEMO, "Meeting with BMI Representatives" dtd 29 November 1967 and communication with Mr. Daniel F. Askey, Associate Chief, Plutonium Technology and Materials Thermodynamics Division, BMI, dtd December 5, 1967.

The internal pressure from helium after one half-life will be:

$$P_{He} = (14.7)(0.0334)\left(\frac{1085}{492}\right)\left(\frac{22400}{V_g}\right)$$

$$= \frac{24,250}{V_g}, \text{ where } V_g = \text{gas volume in } cm^3$$

Since $V_g = V_t$ (container cavity volume) - V_f (crystalline fuel volume),

and $$V_f = \frac{(35\ w)}{\left(0.55 \frac{w}{gm\ Pu\text{-}238}\right)} \left(\frac{252\ gms\ PuN}{238\ gm\ Pu\text{-}238}\right) \left(\frac{1}{14.25 \frac{gms\ PuN}{cc\ PuN}}\right)$$

$$= 4.72 \text{ cc, then}$$

$$V_g = (16.38)\left(\frac{\pi}{4} D^2 L\right) - 4.72, \text{ where}$$

D and L are the diameter and length, respectively, of the inner fuel container cavity in inches.

The total gas pressure in the capsule is given by:

$$P_g = P_{He} + P_o, \text{ where } P_o, \text{ the initial gas pressure, is}$$

$$P_o = 14.7\left(\frac{1250 + 460}{460}\right) = 54 \text{ psi.}$$

P_o is negligible in comparison to P_{He}, so that

$$P_g \cong P_{He} = \frac{24,250}{(16.38)\left(\frac{\pi}{4} D^2 L\right) - 4.72} = \frac{1,880}{(D^2 L) - 0.367}$$

The hoop stress in the fuel container walls is:

$$\sigma = P_g \frac{D_o^2 + D^2}{D_o^2 - D^2}, \text{ where } D_o \text{ is the container OD.}$$

Let $X = \frac{D_o}{D}$, then $\sigma = P_g\left(\frac{X^2 + 1}{X^2 - 1}\right)$, and

$$\sigma = \frac{1,880}{D^2 L - 0.367}\left(\frac{X^2 + 1}{X^2 - 1}\right).$$

For the tungsten -25% rhenium container proposed, the yield strength at the temperature of interest is approximately 75,000 psi. Using a safety factor of 5 gives a working stress, σ, of 15,000 psi. Thus,

$$D^2L = 0.367 + 0.155 \left(\frac{X^2 + 1}{X^2 - 1}\right).$$

The selected solution is D = 0.74 in. and t = 0.185 in. which results in an L/D ratio of 1.9. This combination of dimensions results in a weight and size for the shielded, encapsulated fuel system which is reasonable and provides adequate material thickness for the capsule seal weld.

The proposed encapsulation consists of an inner container of tungsten - 25% rhenium (W-25Re) encased in an outer jacket of Hastelloy C. The inner container material is selected for its strength, weldability and compatibility with the proposed fuel form. The outer jacket provides environmental protection for the primary container.

The wall thickness however has been set at 0.170 in. of W-25Re in consideration of the shielding requirements. The total thickness of the pressure vessel, then, is 0.170 + 0.030 = 0.20 inches. This thickness satisfies the strength requirements of a flat-ended pressure vessel containing 5000 psi.

The reference capsule dimensions are shown in Figure I-1 and listed in Table I-1 below.

TABLE I-1 - FUEL CAPSULE DIMENSIONS

Thickness W-25Re side wall end plate, in.	0.17
Thickness cladding (Hastelloy C), in.	0.03
Inside diameter, in.	0.74
Inside length, in.	1.40
Outside diameter, (W-25Re), in.	1.08
Length (W-25Re), in.	1.74
Outside diameter (Hastelloy C), in.	1.142
Length, (Hastelloy C), in.	1.80
Fuel pellets	
Number	4
Inside diameter, in.	0.50
Outside diameter, in.	0.74
Length, in.	0.35

3,01-68-047

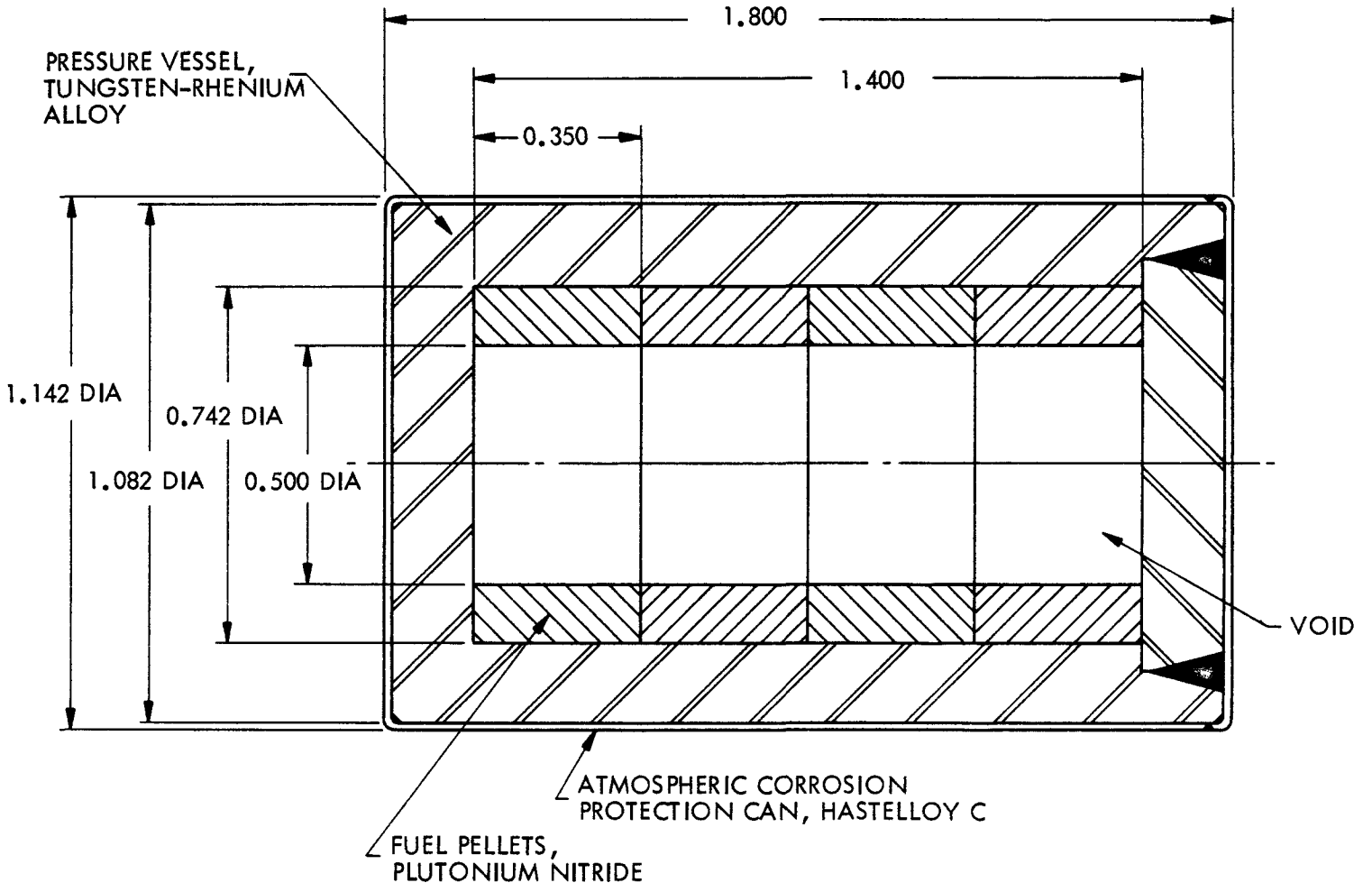

FIGURE I-1. REFERENCE FUEL CAPSULE DESIGN

The W-25Re container will be sealed by TIG or electron beam welding and the Hastelloy C container will be sealed by electron beam welding. The dimensions shown in Table I-1 assume no clearances between parts but the exact dimensions will change slightly prior to fabrication.

The total volume occupied by the fuel, assuming an 88% densification, is

$$\frac{4.72}{.88} = 5.38 \text{ cm}^3 = .33 \text{ in.}^3$$

The maximum pressure buildup, assuming that 25% of the helium formed is released as a gas, is ~ 5,000 psi. The safety factor of 5 used in establishing the pressure vessel wall thickness provides a reasonable margin for the disputed amount of helium build-up since the maximum pressure would only be 4 x 5000 or ~ 20,000 psi.

BIBLIOGRAPHY OF LITERATURE REVIEWED

1) W. M. Rutherford, G.N. Huffman, and D. L. Coffey, "Preparation and Neutron Counting of 238 PuO_2 Depleted in 180." Nuclear Applications, Vol. 3, June 1967.

2) G. M. Matlack, C. F. Metz, "Radiation Characteristics of Plutonium-238", Report No. LA-3696, September 1967.

3) R. W. Dayton, S. J. Paprocki, "Progress Relating to Civilian Applications During July 1965", Report No. BMI-1738, August 1965.

4) D. H. Stoddard, and E. L. Albencsius, "Radiation Properties of Pu-238 etc." Report No. DP-984, July 1965.

5) W. M. Pardue, et. al., "An Evaluation of Plutonium Compounds as Nuclear Fuels", Report No. BMI-1698, October 1964.

6) W. M. Pardue, et. al., "Synthesis, Fabrication, and Chemical Reactivity of Plutonium Mononitride," Report No. BMI-1693, September 1964.

7) Internal Memo SD-612, December 1967, "Minutes of Day Meeting with W. M. Pardue and Daniel Askey of BMI-Columbus".

APPENDIX J
SHIELDING CALCULATIONS

A. SUMMARY

Calculations were performed to determine tungsten and polyethylene shield thicknesses required to maintain the surface dose close to 50 mrem/hr. The reference design uses a PuN, 35 watt(t) heat source prepared from highly purified plutonium*. The source dimensions are 0.738 in. outside diameter and 1.4 in. long. The metal pressure vessel consists of 0.17 in. of W-25Re and 0.0425 in. of Hastelloy C, and the shield is 1.125 in. of borated polyethylene.

With the above configuration, the total surface dose is comprised of 2.4 mrem/hr of gamma and 49 mrem/hr of neutron radiation. Since the total dose is predominately from the neutron contribution the addition of polyethylene changes the surface dose as shown in Figure J-1.

Alternate neutron absorption materials (see Figure J-2) were examined. The best of these, lithium hydride, causes materials compatibility and encapsulating problems while providing less than a 10% improvement in neutron absorption.

During the final shielding design work, experimental verification of the calculated surface dose of 51.4 mrem/hr (considered accurate to within a factor of + 1.5 and - 2.0, exclusive of source emission spectra variation) must be undertaken.

B. SOURCE DATA

The neutron and gamma source intensities were obtained for a 35 watt PuN heat source assumed to have radiation characteristics of pure Pu-238. Tables J-1 and J-2 present the neutron and gamma source strengths**.

* G. M. Matlack and C. F. Metz, "Radiation Characteristics of Plutonium-238*, LA-3696, September 1967.

**D. H. Stoddard, and E. L. Albenesius, "Radiation Properties of Pu-238, etc." Report No. DP-984, July 1965.

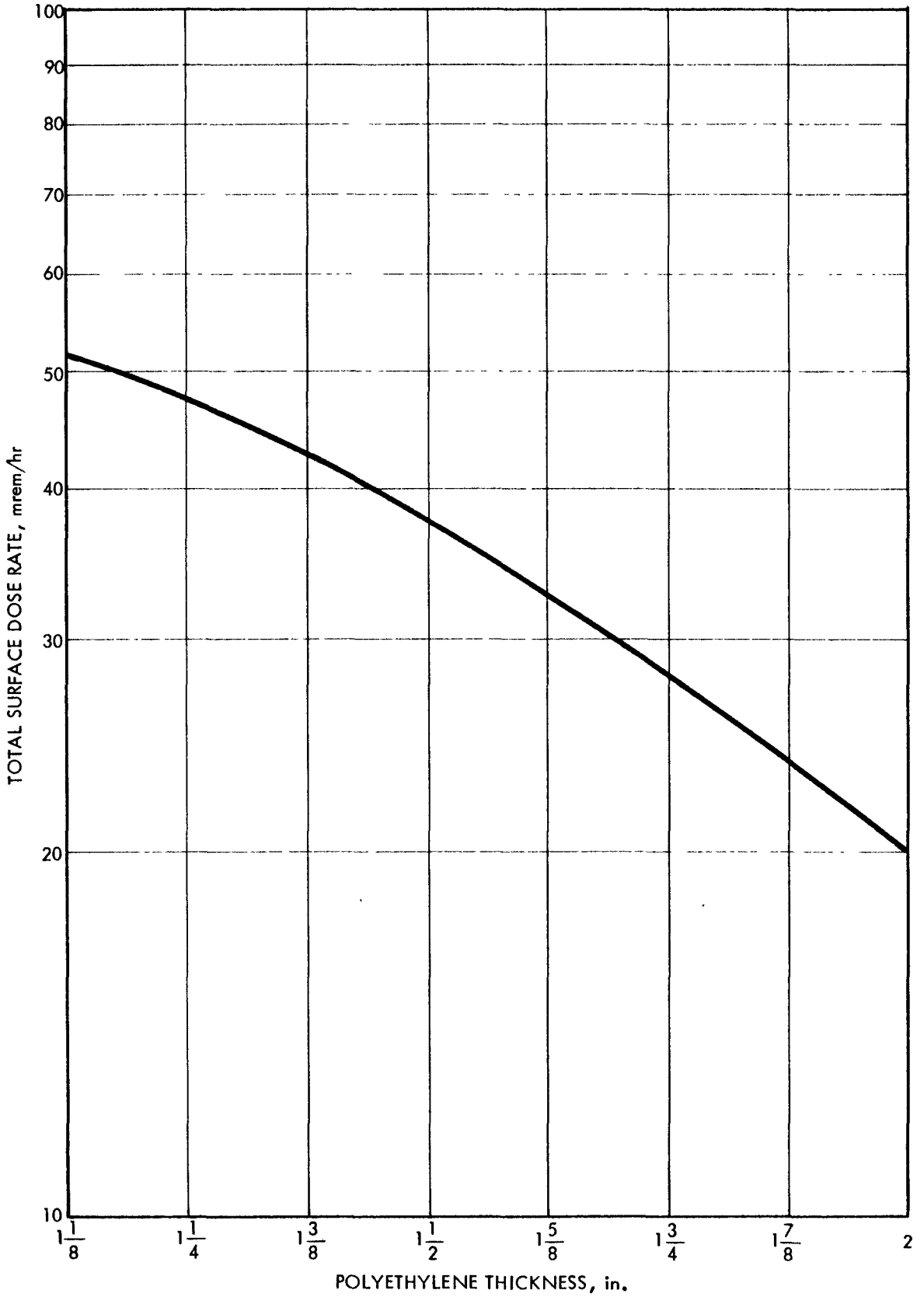

FIGURE J-1. SURFACE DOSE RATE FOR A 35 watt PuN HEAT SOURCE

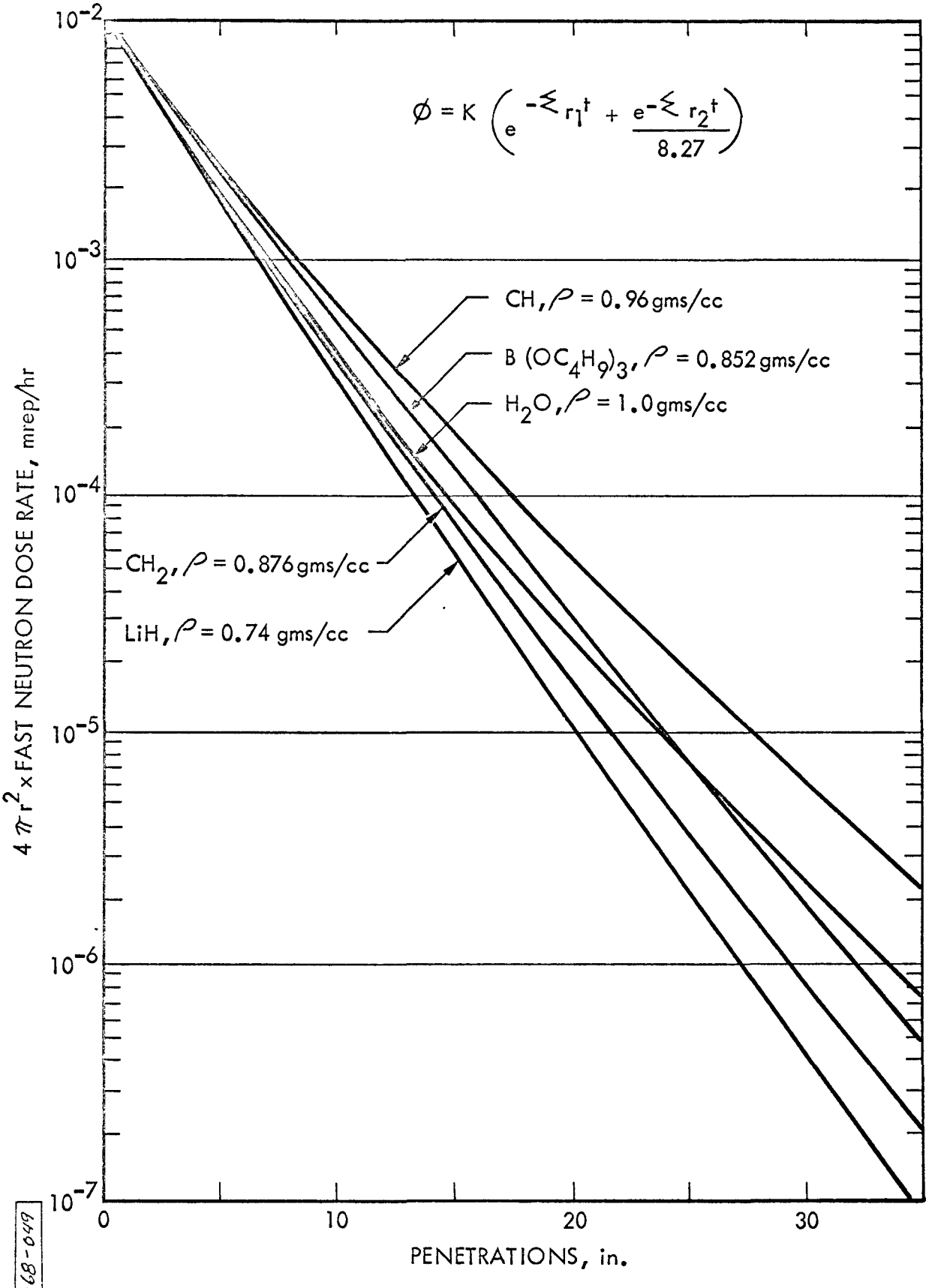

3.01-68-049

FIGURE J-2. DOUBLE EXPONENTIAL FAST NEUTRON ATTENUATION DUE TO A UNIT POINT ISOTROPIC FISSION

TABLE J-1 – GAMMA EMISSION SPECTRA FOR A PuN HEAT SOURCE

E, Mev	γ Emission Rate, γ/sec-gram
0.16	2.1×10^{8}
0.31	3.3×10^{5}
1.50	2.07×10^{3}
2.70	7.1×10^{2}

TABLE J-2 – NEUTRON EMISSION SPECTRA FOR A PuN HEAT SOURCE (SPONTANEOUS FISSION ONLY)

En, Mev	Abundance, n/sec- gram product
0 - 0.5	2.2×10^{2}
0.5 - 1.0	2.9×10^{2}
1.0 - 2.0	5.9×10^{2}
2.0 - 3.0	3.6×10^{2}
3.0 - 4.0	1.8×10^{2}
4.0 - 5.0	1.3×10^{2}
5.0 - 6.0	7.2×10^{1}
6.0 - 7.0	2.4×10^{1}
8.0 -10.0	6.3×10^{0}
10.0 -13.0	3.1×10^{0}

C. ANALYTICAL METHOD

The analyses performed to determine the gamma contribution to the radial surface dose rate employed the following cylindrical source representation for the source shield configuration:

$$\phi_{\gamma} = \frac{BS_{v}R_{o}^{2}F(\theta, b_{2})}{2(a + z)k}$$

where:

ϕ_{γ} = surface gamma dose rate, mrem/hr

S_{v} = volume source strength of PuN, Mev/cc-sec

R_{o} = radius of source material

B = buildup factor

a = distance from the surface of the PuN source to the surface of the polyethylene shield, cm

z = effective self-absorption distance of an equivalent line source, cm

k = conversion factor from Mev/cm^2-sec to mrem/hr

$$F(\theta, b_2) = \int_o^{\theta} e^{-b \sec\theta} \, d\theta$$

$$\theta = \tan^{-1} \frac{h}{2 (a + z)}$$

h = height of PuN source cylinder

$$b_2 = \Sigma \mu_i t_i + \mu_s Z$$

μ_i = macro-cross section of shield material, cm^{-1}

t_i = thickness of shield material, cm

μ_s = macro-cross section of source material, cm^{-1}

The neutron contribution to the radial surface dose rate was determined by the following cylindrical source representation:

$$\phi_n = \frac{S_n R_o^2 F(\theta, b_2)}{2 (a + z) c}$$

where:

ϕ_n = surface neutron dose rate, mrem/hr

S_n = volume source strength of PuN, n/cc-sec

z = effective neutron self-absorption distance of an equivalent line source, cm

c = conversion factor from n/cm^2-sec to mrem/hr

$$b_2 = \sum \Sigma_i t_i + \Sigma_s Z$$

Σ_i = fast neutron removal cross section of shield material, cm^{-1}

Σ_s = fast neutron removal cross section of the PuN source material, cm^{-1}

The remaining symbols are as previously defined.

APPENDIX K
ISOTROPIC INSULATION THICKNESS ANALYSIS

A. MODEL

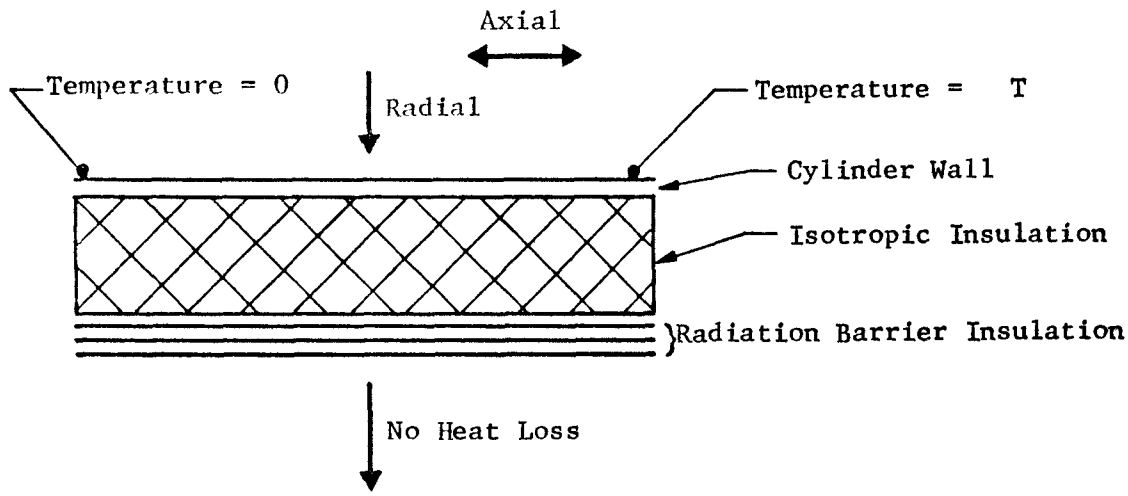

B. ASSUMPTIONS

1) The radiation barrier acts as a single sheet of material with axial thermal conductivity K_o and thickness t_o.

2) The cylinder has a linear temperature gradient from 0 to ΔT.

3) The radial and axial heat conduction through isotropic insulation can be treated separately.

4) No significant radial heat transfer occurs in radiation barrier-type insulation.

5) No axial heat transfer occurs out of either end of the radiation barrier.

C. AXIAL HEAT FLOW IN RADIATION BARRIER INSULATION

$$T(x)'' - c^2 T(x) = -c^2 T1(x) \qquad \text{(K-1)}$$

with boundary conditions

$$T1(x) = x\,\Delta T/L: \quad \text{Laplace } T1(x) = \Delta T/s^2 L$$

$$T(o)' = 0$$

$$T(L)' = 0$$

Taking Laplace transform of Equation (K-1):

$$(s^2 - c^2)\,\mathcal{T}(s) = -c^2\,\Delta T/s^2 L + sT_o + T(o)'$$

Rearranging:

$$\mathcal{T}(s) = (sT_o - c^2 \Delta T/s^2 L)/(s^2 - c^2) \qquad \text{(K-2)}$$

The inverse Laplace transform of Equation (K-2) is:

$$T(x) = T_o \cosh(cx) - c\Delta T/L \int_o^x \int_o^x \sinh(cx)\,dx\,dx$$

or

$$T(x) = T_o \cosh(cx) - \Delta T \sinh(cx/cL) + \Delta Tx/L \qquad \text{(K-3)}$$

and

$$T(x)' = T_o \sinh(cx) - \Delta T/L \cosh(cx) + \Delta T/L \qquad \text{(K-4)}$$

Since $T(L)' = 0$

$$T_o = \Delta T/cL \left[\frac{\cosh(cL) - 1}{\sinh(cL)}\right] \qquad \text{(K-5)}$$

The total heat flow through the radiation barrier occurs at $T(x)'' = 0$

$$T(x_o)'' = c^2 T_o \cosh(cx_o) - c\Delta T/L \sinh(cx_o) = 0$$

or

$$\tanh(cx_o) = \tanh(cL/2) \qquad \text{(K-6)}$$

$$Q = \pi D K_o t_o T(x_o)' \qquad \text{(K-7)}$$

Combining Equations (K-4), (K-5), (K-6), and (K-7) yields:

$$Q = (\pi D K_o t\,\Delta T/L) \tanh(cL/4) \tanh(cL/2)$$

D. AXIAL FLOW IN ISOTROPIC INSULATION

$$Q_m = \pi D K_m t_m \Delta T/L$$

E. TOTAL AXIAL HEAT FLOW

$$Q_{total} = Q + Q_m$$

The results, using values given in nomenclature list, are shown in Table K-1.

TABLE K-1

AXIAL HEAT FLOW

cL	t_m, inches	Q, watts	Q_m, watts	T total, watts
.6	3.84	.14	1.98	2.12
1.0	1.38	.37	.71	1.08
1.6	.54	.83	.28	1.11
2.0	.35	1.16	.18	1.34
2.6	.20	1.63	.10	1.73
3.0	.15	1.90	.08	1.98
3.6	.11	2.24	.06	2.30
4.0	.09	2.43	.04	2.83
0	0	3.32	0	3.32

NOMENCLATURE AND ASSUMED VALUES

$T(x)$	=	Effective temperature in radiation barrier insulation
$T1(x)$	=	Temperature along cylinder wall
ΔT	=	$T1(L) - T1(x)$ [$1000^{\circ}R$]
L	=	Length of cylinder [3 inches]
K_m	=	Thermal conductivity of isotropic insulation [0.02 Btu/hr-ft-$^{\circ}F$]
K_o	=	Axial thermal conductivity of radiation barrier insulation [6.5 Btu/hr-ft-$^{\circ}R$]
t_m	=	Thickness of isotropic insulation
t_o	=	Effective thickness of radiation barrier insulation [.020 in.]
C	=	$(k_m/k_o t_m t_o)^{\frac{1}{2}}$
x	=	Position variable
x_o	=	Position where axial conduction is greatest
s	=	Laplace transform variable
$\mathcal{T}(s)$	=	$\mathcal{T}$ = Laplace $(T(x))$
T_o	=	$T(o)$
Q	=	Axial heat flow in radiation barrier
Q_m	=	Axial heat flow in isotropic insulation
Q_{total}	=	$Q + Q_m$
D	=	Diameter of cylinder [1 inch]

APPENDIX L

CRITICAL PROPERTIES OF MATERIALS

A. INTRODUCTION

Materials properties strongly effect the design and performance of three components:

- Displacer piston and cylinder
- Pumping chamber bellows
- Fuel capsule

Materials for each of the above applications are reviewed in the following sections. General classes of materials that appear satisfactory are identified and data are presented on the more promising materials.

B. DISPLACER PISTON AND CYLINDER

The requirements established for this component are:

1. Operating Temperature:

Maximum temperature	1500°F
Normal temperature	1300-1350°F
Temperature gradient	1000°F/in.
Environment	helium vacuum

2. Other Properties:

Weldability	TIG/EB
Machinability	Close tolerance thin section
80,000 hour creep strength	
Dimensional stability	
Minimum thermal conductivity	

A number of materials, including magnesium, aluminum, titanium, stainless steels, nickel based alloys, and refractory metals, were investigated for this application.

Aluminum and aluminum alloys, magnesium, and magnesium alloys and titanium alloys were eliminated from further consideration because of insufficient elevated temperature strength capability and high conductivity. Refractory metal alloys (Nb, Ta) were eliminated because of high conductivity and difficult fabrication.

The austentic stainless steels and nickel based alloys appear most appropriate for the intended application. Table L-1 compares critical properties of these materials. Based on this presentation, the nickel based alloys appear to satisfy the requirements better than stainless steels.

Three solid solution alloys and one precipitation hardened (Inconel 718) alloy are listed in Table L-1. The K/yield strength ratio of the latter is much lower than any of the other nickel based alloys, because of the very high yield strength of this alloy. A-286, Hastelloy C and Hastelloy X are the next best alloys. A-286 is a super stainless steel, which is precipitation hardenable through titanium and aluminum additions. Both Hastelloy C and X are solid solution strengthened alloys in which deliberate precipitation is not induced through such additions. All the alloys are sufficiently weldable and machinable to satisfy the requirements for this application. However, the precipitation hardened alloys will require postweld heat treatment if uniform mechanical properties are desired.

80,000 hour creep data are not available for any of these alloys, although an extrapolation can be made from existing data using Larson-Miller techniques.

Dimensional stability of these alloys is satisfactory; none undergo phase changes that would cause dimensional instabilities.

The materials recommended for the displacer piston and cylinder are, in order of preference, Hastelloy C, Hastelloy X, and Inconcel 718.

TABLE L-1 – PROPERTIES OF SELECTED MATERIALS

Alloy	Test Temp, °F	Ultimate Tensile, ksi	Yield Strength ksi	Elong., %	Mod of Elasticity x10^6 psi	Conduct., Btu/hr-ft	K/ Y.S
304	300	67	38	30.5	26.5	8.8	0.23
	1000	55	18.5	43.5	19.2	13.2	0.71
	1300	34.3	15.0	35.5	---	14.8	1.0
	1500	19.4	---	---	16.0	16.0	---
316	300	76.0	31.0	53.0	---	8.8	0.28
	1000	69.2	21.0	---	23.4	11.9	0.56
	1300	46.0	19.5	42.0	22.0	22.0	0.67
	1500	27.5	18.5	42.0	21.3	14.0	0.75
347	300	74.5	34.0	47.0	27.5	9.0	2.6
	1000	59.6	---	36.4	22.8	13.0	---
	1300	40.0	24.0	51.0	20.7	14.0	0.58
	1500	23.0	19.5	76.0	19.4	14.5	0.75
310	300	87.5	35.0	47.0	27.5	9.0	0.26
	1000	73.0	22.0	36.0	23.0	13.0	---
	1300	45.3	20.5	30.0	21.2	15.5	0.75
	1500	25.4	16.5	---	19.8	17.2	1.04
Inconel	600	99	38	50	29.1	8.7	0.23
	1000	95	36	50	25.8	11.7	0.325
	1200	74	34	26	23.2	12.5	0.37
	1600	18	12	76	16.6	13.0	1.0
Hastelloy C	300	87	38	39	29	6	0.16
	1000	80	34	41	25	9.4	0.28
	1300	70	34	46	23	10.5	0.31
	1500	54	32	42	22	11.5	0.36
Hastelloy X	300	110	50	40	27	7.1	0.14
	1000	93	41	45	24	11.0	0.27
	1350	72	36.5	37	22	12.8	0.35
	1500	52	33.0	33.5	21	14.6	0.44
Inconel 718	300	165	140	12	27	7.5	0.05
	1000	150	125	10	25	10.4	0.08
	1300	132	130	10	22	12	0.11
	1500	88	75	---	21	12.6	0.17
A-286 (sheet)	300	125	80	19	27	8.8	0.11
	1000	108	74	17	24	13.0	0.17
	1300	69	54	10	22	15.2	0.28
	1500	32	25	30	20	16.5	0.66
Incoloy 800 (rod)	400	77.3	36.0	39.0	28	(500°F)9.1	0.25
	1000	75.0	21.5	56.0		11.5	0.54
	1300	42.4	26.9	51.0			
	1500	24.8	14.2	91.0		14.5	1.0

C. PUMPING CHAMBER BELLOWS

The requirements established for this component are:

1.	Operating temperature	200-250°F
2.	Environment	helium-vacuum-liquid
3.	Stress level	maximum allowable cyclic stress
4.	Stress cycles	$3\text{-}5 \times 10^8$
5.	Other Properties:	
	High stress fatigue limit	
	Minimum modulus of elasticity	
	Resistance to stress corrosion	
	Weldable by TIG or EB	
	Low permeability to helium.	

A number of materials were reviewed to establish values for modulus of elasticity and fatigue strength. The results of this review are presented in Table L-2.

In evaluating the various classes of materials, it appears that the titanium alloys offer an almost satisfactory balance between modulus and fatigue strength, particularly the 6Al-4V alloy. It should be recognized that the 68,000 psi value will be reduced somewhat at 200 to 250°F, although the nickel based alloys and stainless steels will be less sensitive to temperature.

All the alloys listed in Table L-2 satisfy the fabricability, permeability to helium and environmental capability requirements. It will be necessary, however, to avoid conditions which could lead to stress corrosion (i.e. alternate wet/dry conditions and low chloride concentrations) if stainless steels (including 17-7 PH and AM 350) or the titanium alloys are employed. Stress corrosion could occur in these alloys due to their highly stressed condition.

Diffusion of helium through these materials at 200-250°F should be investigated, but is not expected to be severe.

D. FUEL CAPSULE CLADDING

The requirements established for this component are:

TABLE L-2 — COMPARATIVE MATERIALS PROPERTIES FOR BELLOWS APPLICATION

Material	Temp, °F	Elastic Modulus x 10^6 psi	Fatigue Strength, ksi	Temp. °F
6061 Aluminum	200	9.9	19 (10^8 cycles)	room
	300	9.5		
7039 Aluminum	100	10	30 (10^8 cycles)	room
7075 Aluminum	200	9.5	16 (10^7 cycles)	300°F
	300	8.9	22 (10^7 cycles)	room
Ti-5Al-2.5 Sn	200	15		
	300	14.9	75 (10^7 cycles)	room
Ti-6Al-4V	200	15		
	300	14.9	68 (10^7 cycles)	room
AISI Type 304	200	28		
	300	27	100 (10^7 cycles)	room
17-7PH	200	28	82 (10^7 cycles)	room
	300	27		
AM-350	200	29	60 (10^7 cycles)	room
	300	27		
Inconel-750	200	31	64 (10^6 cycles)	room
	300	30		
Inconel-718	200	28		
	300	27	90 (10^7 cycles)	RT
Beryllium Copper	Room	17.0 Tension	32 (10^8 cycles)	RT annealed
	Room	6.5 Torsion	42 (10^8 cycles)	RT hardened

1. Operating Temperature:

Maximum temperature	1400-1500°F
Environment	Helium, vacuum, air (air exposure would only occur at lower temperatures)

2. Other Properties:

Maximum creep rupture strength at operating temperature

Good shielding characteristics

Impact strength and toughness

Corrosion resistance

For this application, the combined requirements of high Z, high density and elevated temperature capability restricts the material selection greatly. Restricting the selection to metallics, because of the impact strength requirement, the candidates are lead, uranium, tantalum, and tungsten. Higher Z, more dense materials (Re, Os, Ir, etc.) are possible candidates, although they are impractical from a cost viewpoint.

Lead and uranium must be eliminated in consideration of the operating temperature in view of the melting point and high temperature strength of such materials. Table L-3 compares the properties of tantalum and tungsten with air, water and stainless steel.

TABLE L-3 – COMPARISON OF SHIELDING MATERIALS

Material	Melting Point, °C	Density, g/cc	Absorption Coefficient (1 Mev), cm^{-1}
Air	0	0.00129	7.7×10^{-5}
Water	0	1.0	0.071
Stainless Steel	1400-1427	7.8	0.462
Tungsten	2410	19.3	1.25
Tantalum	2996	16.6	1.08

Tantalum and tungsten have similar melting points and have γ absorption coefficients that are not greatly different. Thus, either of these materials or alloys of these materials could be utilized in this application without a severe penalty. Figures L-1 and L-2 compare the ultimate strengths of several materials including unalloyed tungsten, unalloyed tantalum, tantalum-10 tungsten and tungsten-rhenium. It is apparent from these data that either the unalloyed metals or the alloys have satisfactory strength at the temperatures of interest. These materials will function equally well in a vacuum or a high purity inert gas but these atmospheres must be maintained at high purity relative to N_2 or H_2 to prevent severe embrittlement of the tantalum alloy. Operation in air, obviously must be carefully controlled since, although tantalum is one of the more oxidation resistant refractory metals, air is not considered an appropriate environment for this class of alloys. If contact with air is anticipated, the temperature of the metal should be maintained below 500°C (932°F) for tungsten and below 600°C (1100°F) for tantalum alloys. The possibility of encapsulating the refractory metal in a Hastelloy C or X can could

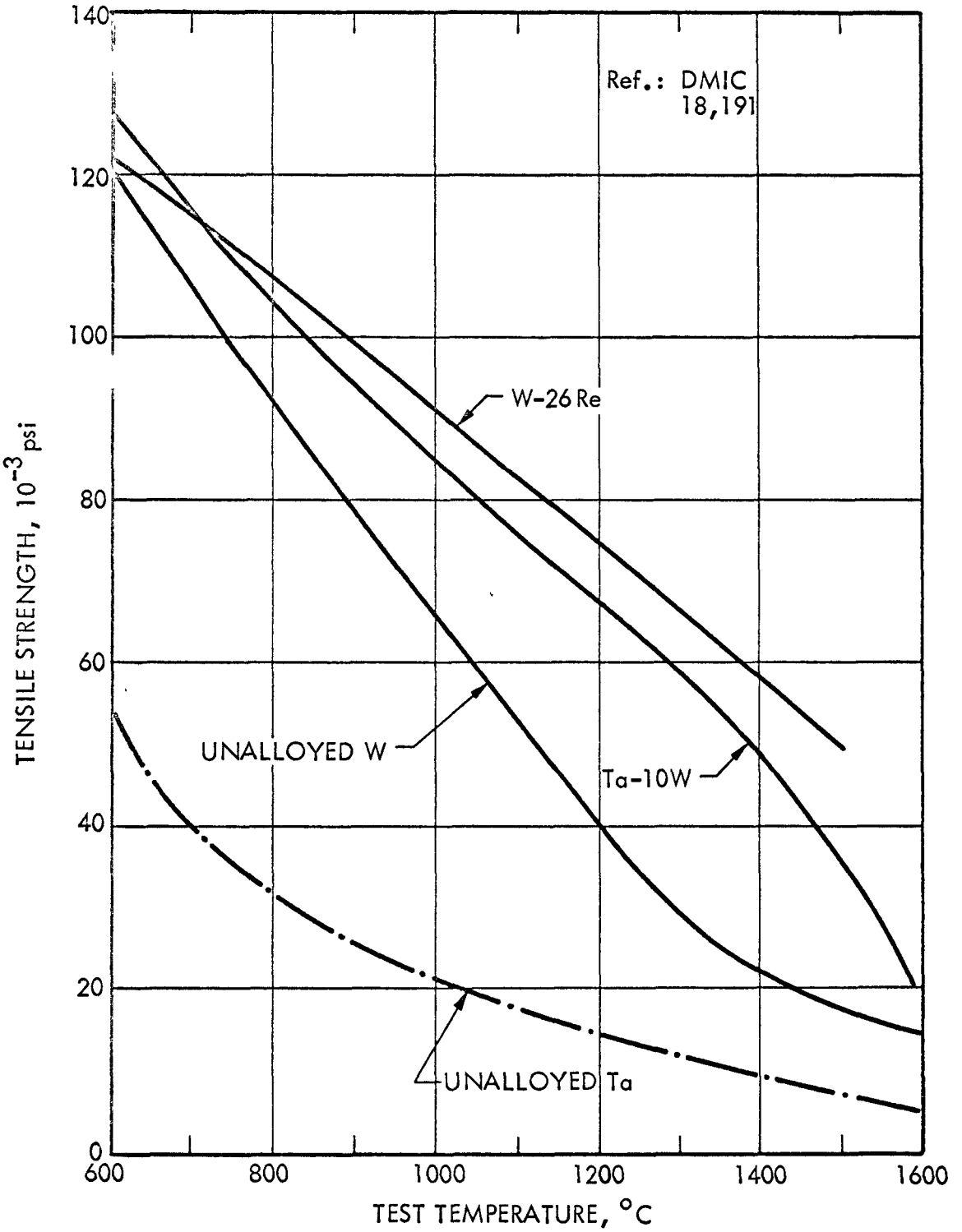

3,01-68-050

FIGURE L-1. COMPARATIVE MECHANICAL PROPERTIES OF SELECTED REFRACTORY METALS

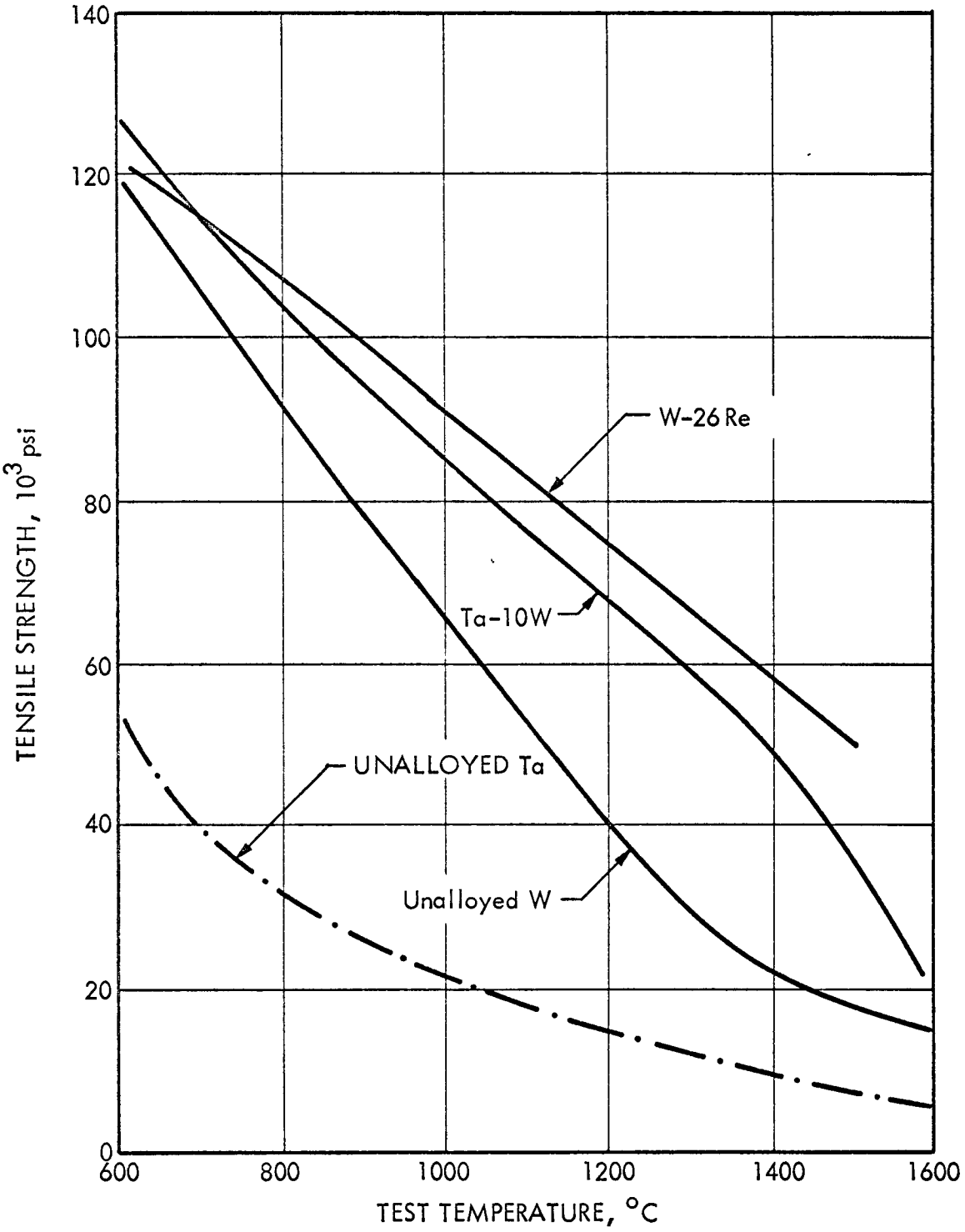

FIGURE L-2. COMPARATIVE MECHANICAL PROPERTIES OF SELECTED REFRACTORY METALS (Ref. DMIC 185,191)

3.01-68-051

be considered, as could use of oxidation resistant coatings to minimize oxidation.

The impact strength of these materials after extended exposure at temperature when tested at temperature is not greatly affected, provided the atmosphere was relatively uncontaminated. However, the room temperature impact properties are greatly degraded after extended operation, particularly where some contaminants are present in the environment. This property deficiency should also be considered in the decision regarding encapsulation in a non-refractory metal outer container.

Weldability of the tantalum alloys, particularly by TIG or EB, is generally good, although high purity atmospheres must be maintained if TIG welding is employed to avoid weld embrittlement. Unalloyed tungsten is difficult to weld by TIG techniques; electron beam techniques would probably provide a more satisfactory weldment. A tungsten-26 wt% rhenium alloy should weld satisfactorily by either technique although careful welder qualification must precede any welding.

Although several tungsten and tantalum alloys have the characteristics required for this application, tungsten (or a tungsten alloy) is more attractive than tantalum because of the higher density and the tungsten-rhenium alloy appears to be the best choice in view of the superior fabrication characteristics of this alloy.

APPENDIX M

SIMPLIFIED PARAMETRIC ANALYSIS TECHNIQUE

A basic assumption is made in the analysis which allows the system equations to be written as algebraic expressions. This assumption is that isothermal conditions exist in the hot and cold displacer piston chambers and is the basis for the classical Schmidt analysis for the Stirling engine. The derivation of the Schmidt equations is contained in several sources* and the final forms of equations are as follows:

1. System Pressure

$$P = (m_t \, RT_c/D) \Big/ (\tau \, V_n/D + V_c/D + \sigma_d) \qquad \text{(M-1)}$$

where

$$\sigma_d = \tau\sigma_{nd} + \left[\frac{\tau \ln \tau}{\tau - 1}\right] \sigma_r + \sigma_{cd} \qquad \text{(M-2)}$$

$$\frac{dP}{d\theta} = -P \left[\tau d(V_n/D) \Big/ d\theta + d(V_c/D)\, d\theta\right] \Big/ \left[\tau V_n/D + V_c/D + \sigma_d\right] \qquad \text{(M-3)}$$

2. Mass Flow

$$W/D = (1/RT)\left[Pd(V/D) \Big/ d\theta + (V/D)\, dP/d\theta\right] \qquad \text{(M-4)}$$

---

* F. A. Creswich, "Thermal Design of Stirling-Cycle Machines", SAE Paper 949C.

3. Heat Flow

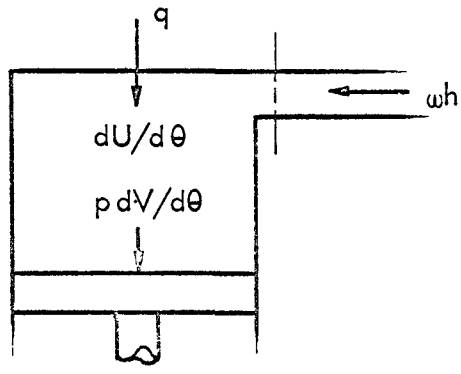

$$q/D = (V/D)\, dP/d\theta \qquad \text{(M-5)}$$

These equations can be adapted to represent the modified Stirling engine which extracts work as pressurized gas. Assume extraction of the gas begins at a piston position x_2 and ends at x_3 and that in-flow of gas begins at x_4 and ends at x_1 where all x's are measured from top-dead-center and as a fraction of total stroke. It is apparent that, between x_2 and x_3, the system pressure is constant and equal to P_{max}, and between x_4 and x_1 the constant pressure is equal to P_{min}. Also, between piston positions x_3 and x_4 and between x_1 and x_2 the total mass in the system is constant. Therefore, using Equation (M-1)

$$P_{min} = \frac{(m_t\, RT_c/D)}{\tau\, x_1 + (1 - x_1) + \sigma_d} \qquad \text{(M-6)}$$

$$P_{max} = \frac{(m_t\, RT_c/D)}{\tau\, x_2 + (1 - x_2) + \sigma_d} \qquad \text{(M-7)}$$

Dividing yields:

$$\frac{P_{min}}{P_{max}} = \frac{\tau\, x_2 + 1 - x_2 + \sigma_d}{\tau\, x_1 + 1 - x_1 + \sigma_d} \qquad \text{(M-8)}$$

or $$x_2(\tau - 1) + (1 + \sigma_d) = \frac{P_{min}}{P_{max}}\left[x_1\,(\tau - 1) + (1 + \sigma_d)\right] \qquad \text{(M-9)}$$

Rearranging and solving for x_2 gives:

$$x_2 = x_1 \frac{P_{min}}{P_{max}} - \left(\frac{P_{min}}{P_{max}} - 1\right)\left(\frac{1 + \sigma_d}{1 - \tau}\right) \qquad \text{(M-10)}$$

Similarly, for x_4:

$$x_4 = x_3 \frac{P_{max}}{P_{min}} - \left(\frac{P_{max}}{P_{min}} - 1\right)\left(\frac{1 + \sigma_d}{1 - \tau}\right) \qquad \text{(M-11)}$$

The extracted volume of gas may also be determined using Equation (M-1). If the system mass is conserved, then the pressure equation at piston position x_2 is given by Equation (M-7) and the pressure equation of x_3 is:

$$P_{max} = \frac{m_t \, RT_c/D}{\tau \, x_3 + (1 - x_3) + \sigma_d + \Delta V/D} \qquad \text{(M-12)}$$

where ΔV is the additional volume to conserve mass and maintain the pressure, and is also the extracted volume. Therefore, combining Equations (M-7) and (M-12) and solving for ΔV gives:

$$x_3(\tau - 1) + (\sigma_d + 1) + \Delta V/D = x_2(\tau - 1) + (\sigma_d + 1) \qquad \text{(M-13)}$$

or

$$\Delta V/D = (1 - \tau)(x_3 - x_2) \qquad \text{(M-14)}$$

The available power of the extracted gas is given by:

$$W_k = \frac{\gamma}{\gamma - 1} P_{max} \, \Delta V \left(1 - \left(\frac{P_{min}}{P_{mas}}\right) \frac{\gamma - 1}{\gamma}\right) \qquad \text{(M-15)}$$

The average flow rate through the regenerator may be computed by the mass displaced by the displacer piston during a stroke. With the piston at bottom-dead-center, the mass of gas at T_{max} is:

$$M = D(P_{max} \, (1 + \sigma_{nd})/RT_{max}) \qquad \text{(M-16)}$$

At top-dead-center, the mass is:

$$M = DP_{min} \, (\sigma_{nd})/RT_{max} \qquad \text{(M-17)}$$

Thus the difference between the two masses is the mass of gas sent through the regenerator during a half cycle, or

$$M = D(P_{max}(1 + \sigma_{nd}) - P_{min}(\sigma_{nd})/RT_{max} \quad \text{(M-18)}$$

Then the flow rate is merely the mass displaced times the number of half cycles per unit time.

The regenerator performance is defined by its effectiveness, which is a function of the number of heat transfer units. The NTU of the regenerator is:

$$NTU = hA/w\ C_p \quad \text{(M-19)}$$

where:

$$h = 4.36\ k/d_n$$

$$d_n = 4.0\ A_R/PERR$$

The effectiveness is related to the NTU by the relationship:*

$$\epsilon_r = 1 - \frac{0.82}{(NTU)^{0.956}} \quad \text{(M-20)}$$

The determination of the power loss due to pressure drop in the heater and regenerator are developed in the following manner. For the regenerator:

$$dP_{rr} = dP\,\frac{w}{\rho} = \rho f\,\frac{dx}{dH}\,\frac{V^2}{2g}\,\frac{w}{\rho} \quad \text{(M-21)}$$

Assuming the Reynold's number is in the laminar range:

$$dP_{rr} = \frac{64\,\mu}{VD_H}\,\frac{dx}{D_H}\,\frac{V^2}{2g}\,\frac{w}{\rho}$$

$$= \frac{64\,\mu}{2g\,D_H^{\,2}}\,V\,\frac{w}{\rho}\,dx$$

$$= \frac{64\,\mu}{2g\,D_H^{\,2}A}\,\left(\frac{w}{\rho}\right)^2 dx \quad \text{(M-22)}$$

* Kays, William and London, A. L., "Compact Heat Exchangers," McGraw Hill Book Co., 2nd Edition 1964.

Noting that

$$A = \frac{\sigma_r D}{L} \tag{M-23}$$

$$\frac{w}{\rho} = \frac{w RT}{P} = \frac{w R}{P}\left[T_{max} - (T_{max} - T_{min})\frac{x}{L}\right]$$

$$= \frac{w R T_{max}}{P}\left[1 - (1 - \tau)\frac{x}{L}\right] \tag{M-24}$$

$$\frac{w R T_{max}}{P} = 2 D Hz$$

Therefore

$$dP_{rr} = \frac{64\mu L}{2g D_H^2 \sigma_r D}(2 D Hz)^2\left[1 - (1 - \tau)\frac{X}{L}\right]^2 dx$$

$$= \frac{256\mu L D Hz^2}{2g D_H^2 \sigma_r}\left[1 - 2(1 - \tau)\frac{x}{L} + (1 - 2\tau + \tau^2)\frac{x^2}{L^2}\right] dx \tag{M-25}$$

Integrating yields:

$$P_{rr} = \frac{256\mu L D Hz^2}{2g D_H^2 \sigma_r}\left[x - 2(1 - \tau)\frac{x^2}{2L} + (1 - 2\tau + \tau^2)\frac{x^3}{3L^2}\right]_o^L \tag{M-26}$$

Evaluating the integral and combining terms gives:

$$P_{rr} = \frac{256\mu L^2 D Hz^2}{2g D_H^2 \sigma_r}(1 + \tau + \tau^2)/3 \tag{M-27}$$

The power loss in the heater is derived in a similar manner except the velocity term is independent of x and there is no τ term.

The energy transferred to and from the gas in the hot and cold chambers is determined by integrating and summing the energy transfer required to maintain the chambers at constant temperature.

Using Equation (M-5), the net energy transferred to the hot chamber may be determined in the following manner over the part of the stroke between x_1 and x_2.

$$\frac{q}{D} = (V_n/D)\frac{dP}{d\theta} = (V_n + C)/D\left[\frac{[m_t RT_c/D][\tau\, d(V_n/D)/d\theta + d(V_c/D)/d\theta]}{[\tau(V_n/D) + V_c/D + \sigma_d]^2}\right] \quad \text{(M-28)}$$

Since $V_n + V_c = D$, then

$$\frac{q}{D}d\theta = (V_n + C)/D\left[\frac{[m_t RT_c/D][\tau d(V_n/D) + d(D-W_n/D)]}{[(\tau - 1)(V_n/D) + (\sigma_d + 1)]^2}\right.$$

$$= \frac{\left((V_n + C)/D\right)(m_t RT_c/D)(\tau-1)(d(V_n/D))\right)}{[(\tau-1)(V_n/D) + (\sigma_d + 1)]^2} \quad \text{(M-29)}$$

Then

$$\int \frac{Z\, dz}{(MZ + N)^2} = \frac{1}{M^2}\left[\log_e (MZ + N) + \frac{N}{MZ + N}\right] \quad \text{(M-30)}$$

$$\int \frac{dz}{(MZ + N)^2} = -\frac{1}{M(MZ + N)} \quad \text{(M-31)}$$

Let $\sigma_d + 1 = A$, $1 - \tau = B$, $m_t RT_c/D = K$.

Integrating yields:

$$\frac{q}{D}\Delta\theta = K(-B)\left[\frac{1}{(-B)^2}\left(\log_e -B\frac{V_n}{D} + A\right) + \frac{A}{-B\frac{V_n}{D} + A} - \frac{C/D}{-B(-B\frac{V_n}{D} + A)}\right]_{x_1}^{x_2}$$

$$= K\left[\frac{1}{B}\log_e \frac{A - x_1B}{A - x_2B}\right] - \frac{A}{B(A - x_2B} + \frac{A}{B(A - x_1B)} - \frac{C/D}{(A - x_2B)}$$

$$+ \frac{C/D}{(A - x_1B)}$$

$$= K\left[\frac{1}{B}\left(\log_e \frac{A - x_1B}{A - x_2B}\right)\right] + \left(\frac{A}{B} + \frac{C}{D}\right)\left[\frac{1}{A - x_1B} - \frac{1}{A - x_2B}\right] \quad \text{(M-32)}$$

Since $m_t RT_c/D = P_{min}(A - x_1 B)$ at x,

$$\frac{q}{D}\Delta\theta = P_{min}(A - x_1 B)\left[\frac{1}{B}\left[\log_e \frac{A-x_1 B}{A-x_2 B}\right] + \left(\frac{A}{B} + \frac{C}{D}\right)\left[\frac{1}{A-x_1 B} - \frac{1}{A_1-x_2 B}\right]\right] \quad \text{(M-33)}$$

The heat transferred during the stroke from x_3 to x_4 is derived in a similar manner.

The equations for the system energy losses are standard form equations and need not be derived. These include the regenerator ineffectiveness loss equation which is of the form

$$Q_R = w\, C_p\, (T_{max} - T_{min})(1 - \epsilon_r), \quad \text{(M-34)}$$

the piston and cylinder conduction loss equation which is of the form:

$$Q_c = \frac{K_P A_P}{L_P}(T_{max} - T_{min}), \text{ and} \quad \text{(M-35)}$$

the regenerator conduction loss equation which is of the form:

$$Q_R = \frac{K_{rw} A_{rw}}{L_{rw}}(T_{max} - T_{min}) \quad \text{(M-36)}$$

The complete set of equations is shown as a Fortran Listing, in Figure M-1, with nomenclature shown in Table M-1.

FIGURE M-1.

```
C  IMPLANTABLE POWER SUPPLY   SCHMOT METHOD

      DIMENSION NAME(25)
    2 FORMAT(25A2)
    3 FORMAT(6E12.5)
   10 FORMAT(' INPUT DATA',5X,25A2,//)
   11 FORMAT(5X,'TMIN=',E12.5,5X,'TMAX=',E12.5,6X,'HEA=',E12.5,7X,
     2'HL=',E12.5,8X,'D=',E12.5,//,8X,'S=',E12.5,6X,'XLH=',E12.5,5X,
     3'XLC=',E12.5,7X,'AR=',E12.5,7X,'RL=',E12.5,//,7X,'X1=',E12.5,7X,
     4'X3=',E12.5,5X,'PMIN=',E12.5,5X,'PMAX=',E12.5,7X,'AK=',E12.5,//,
     57X,'HZ=',E12.5,7X,'CP=',E12.5,8X,'R=',E12.5,5X,'PERH=',E12.5,5X,
     6'PERR=',E12.5,/)
   12 FORMAT(6X,'TKH=',E12.5,6X,'TKC=',E12.5,6X,'AMU=',E12.5,5X,'AMU1=',
     2E12.5,6X,'PRL=',E12.5,//,6X,'PRC=',E12.5,6X,'PRF=',E12.5,5X,
     3'TKP=',E12.5,7X,'TP=',E12.5,7X,'PL=',E12.5,//,7X,'QI=',E12.5)
   13 FORMAT(///2X,'OUTPUT DATA'//)
   14 FORMAT(6X,'TAU=',E12.5,4X,'SIGHD=',E12.5,4X,'SIGCD=',E12.5,5X,
     2'SIGR=',E12.5,5X,'SIGD=',E12.5,//,7X,'X2=',E12.5,7X,'X4=',E12.5,
     36X,'VEX=',E12.5,7X,'WK=',E12.5,6X,'PRG=',E12.5,//,7X,'CR=',E12.5,
     47X,'DH=',E12.5,7X,'DP=',E12.5,5X,'RNTU=',E12.5,6X,'REF=',E12.5,//,
     55X,'DELT=',E12.5,6X,'PRH=',E12.5,6X,'PRR=',E12.5,6X,'PR1=',E12.5,
     67X,'QA=',E12.5,/)
   15 FORMAT(7X,'QR=',E12.5,7X,'QP=',E12.5,6X,'QPR=',E12.5,7X,'QC=',
     2E12.5,8X,'Q=',E12.5,//,7X,'ZN=',E12.5,6X,'EFF=',E12.5,5X,'QLLP=',
     3E12.5,5X,'SIDE=',E12.5)
      READ(2,2)(NAME(I),I=1,25)
      READ(2,3)TMIN,TMAX,HEA,HL,D,S,XLH,XLC,AR,RL,X1,X3,PMIN,PMAX,AK,
     2HZ,CP,R,PERH,PERR,TKH,TKC,AMU,AMU1,PRI,PRC,PRF,TKP,TP,PL,QI
      WRITE(3,10)(NAME(I),I=1,25)
      WRITE(3,11)TMIN,TMAX,HEA,HL,D,S,XLH,XLC,AR,RL,X1,X3,PMIN,PMAX,AK,
     2HZ,CP,R,PERH,PERR
      WRITE(3,12)TKH,TKC,AMU,AMU1,PRI,PRC,PRF,TKP,TP,PL,QI
      WRITE(3,13)
      TAU=TMIN/TMAX
      SIGHC=XLH/S
      SIGCD=XLC/S
      SIGHD=HEA*HL/D+SIGHC
      SIGR=AR*RL/D
      SIGD=TAU*SIGHD+SIGCD+(TAU*SIGR/(TAU-1.))*ALOG(TAU)
      A=SIGD+1.
      B=1.-TAU
      X2=X1*PMIN/PMAX-(PMIN/PMAX-1.)*(A/B)
      X4=X3*PMAX/PMIN-(PMAX/PMIN-1.)*(A/B)
      VEX=B*(X3-X2)
      WK=(AK/(AK-1.))*PMAX*VEX*(1.-(PMIN/PMAX)**((AK-1.)/AK))*D
      PRG=WK*HZ
      CR=(2.*HZ*CP*D)*(PMAX*(1.+SIGHD)-PMIN*SIGHD)/(R*TMAX)
      DH=4.0*HEA/PERH
      DP=4.0*AR/PERR
      RNTU=1.09*PERR*RL*(TKH+TKC)/(DP*CP)
      REF=1.0-.82/((RNTU)**.956)
      DELT=(1.0-REF)*(TMAX-TMIN)
      PRH=256.*AMU*D*(HZ*HL/DH)**2/(64.4*(SIGHD-SIGHC))
      PRR=(256.*AMU1*D/(64.4*SIGR))*(HZ*RL/DP)**2*((1.0+TAU+TAU**2.0)/3.)
     1)
```

FIGURE M-T. (Continued)

```
 PRD =(PRG-2.*(PRH+PRP+PRF))/.7376-PRI-PRC
 QA=D*PMIN*(A-X1*B)*(ALOG((A-X1*B)/(A-X2*B))/B+((A/B)+SIGHD)*(1./(A
2-X1*B)-1./(A-X2*B)))
 QB=D*PMAX*(A-X3*B)*(ALOG((A-X3*B)/(A-X4*B))/B+((A/B)+SIGHD)*(1./ A
2-X3*B)-1./(A-X4*B)))
 QR=CP*(1.-REF)*B*TMAX/2.
  QC=SQRT(12.56*D/S)*TKP*B*TMAX*TP/PI
 ZN=1.1547*AR/DP**2.0
 QRR=0.34741E-06*DP/RL*(TMAX-TMIN)*ZN
 Q= (QA+QB)*HZ/778.+QR+QC+QI+QKP
 EFF=PRD/(Q *1055.)
 DELP=0.00345*(1.0+TAU)*AMU1*HZ*(PL/DR)**2.0/SIGR
 SIDE=6.9284*DP
 WRITE(3,14)TAU,SIGHD,SIGCD,SIGR,SIGT,X2,X4,VEX,WK,PRG,CP,DH,DR,
2RNTU,REF,DELT,PRH,PRP,PRD,QA
 WRITE(3,15)QB,QR,QRR,QC,Q,ZN,EFF,DELP,SIDE
 CALL EXIT
 END
```

TABLE M-1

NOMENCLATURE

Symbol	Definition
A	Surface or cross-section area or defined variable
B	Defined variable
C_p	Specific heat at constant pressure
C	Hot chamber dead volume
D	Displacement
D_H	Hydraulic diameter
f	Flow friction factor
g	Gravitational acceleration
h	Convective heat transfer coefficient
Hz	System cycle frequency
k	Thermal conductivity
L	Length
m	Mass
M	Mass
NTU	Number of heat transfer units
P	Pressure
P_{rr}	Regenerator flow friction power loss
q	Heat flow
R	Gas constant
T	Temperature
V	Volume or velocity
w	Flow rate
W_k	Available power
x	Linear position
X_1	Dimensionless piston position where inlet check valve closes
X_2	Dimensionless piston position where exhaust check valve opens
X_3	Dimensionless piston position where exhaust check valve closes
X_4	Dimensionless piston position where inlet check valve opens
γ	Gas specific heat ratio
ϵ	Effectiveness

TABLE M-1 (Continued)

Symbol	Definition
θ	Time
μ	Gas viscosity
ρ	Gas density
σ	Dimensionless component dead volume
τ	Temperature ratio
Subscripts	
c	Cold chamber volume
cd	Cold chamber dead volume
d	Overall dead volume
n	Hot chamber volume
nd	Hot chamber dead volume
min	Minimum
max	Maximum
p	Piston
r	Regenerator
rw	Regenerator wall
t	Total
Fortran	
AK	γ
AMU	μ at T_{max}
AMU1	μ at $(T_{max} + T_{min})/2$
AR	Regenerator flow area
Cp	C_p
CR	wC_p
D	D
DELP	Regenerator pressure loss
DELT	Temperature difference between heater wall and gas
DH	Heater hydraulic diameter
DR	Regenerator hydraulic diameter
EFF	System overall net efficiency
HFA	Heater flow area
HL	Heater length

TABLE M-1 (Continued)

Portran	Definition
HZ	Hz
PERH	Heater wetted perimeter
PERR	Regenerator wetted perimeter
PL	Piston length
PMAX	P_{max}
PMIN	P_{min}
PRC	Control power requirement
PRF	Piston friction power loss
PRG	Gross output power
PRH	Heater flow friction power loss
PRL	Pumping chamber power loss
PRO	Net output power
PRR	Regenerator flow friction power loss
Q	Heater power
QA	Heat input to system on downstroke
QB	Heat input to system on upstroke
QC	Conduction heat loss down cylinder and piston
QI	Insulation heat loss
QR	Regenerator ineffectiveness heat loss
QRR	Regenerator conduction heat loss
R	R
REF	ϵ_r
RL	Regenerator length
RNTU	NTU
S	Stroke
SIDE	Regenerator honeycomb side length
SIGCD	σ_{cd}
SIGD	σ_d
SIGHD	σ_{cd}
SIGR	σ_r
TAU	τ
TKC	Gas thermal conductivity of T_{min}
TRH	Gas thermal conductivity of T_{max}

TABLE M-1 (Continued)

Fortran	Definition
TKP	Piston thermal conductivity
TMAX	T_{max}
TMIN	T_{min}
TP	Piston and cylinder wall thickness
VEX	Extracted volume
WK	W_K
X1	X_1
X2	X_2
X3	X_3
X4	X_4
XLC	Cold chamber end clearance
XLH	Hot chamber end clearance
ZN	Number of channels in regenerator

APPENDIX N

INTERMEDIATE PARAMETRIC ANALYSIS TECHNIQUE

The analytical representation of the system is shown in Figure N-1 with the system divided into finite nodal elements. The analysis is performed assuming that the metal node temperatures are constant and that the gas temperatures are transient.

The formulation of the system equations require the development of six fundamental equations which describe the gas pressure and temperature of the compression and expansion spaces, the gas temperature of the heat exchanger nodes, the mass in any space, the flow phenomenon of the system, and the piston dynamics. There are additional auxiliary equations but these need not be derived since they merely represent the calculation of dummy variables, output parameters or problem constants.

TEMPERATURE EQUATIONS

The equations for the gas temperatures in the hot and cold displacer piston chambers and the upper and lower reversing piston chambers are developed from the same basic equation. This basic temperature equation is derived by performing an energy balance on a generalized gas control volume as shown below.

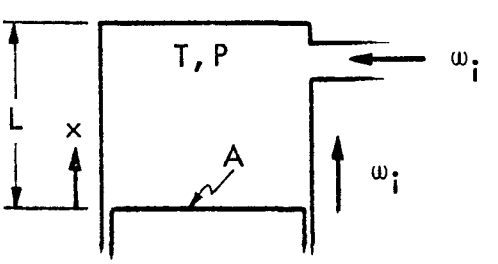

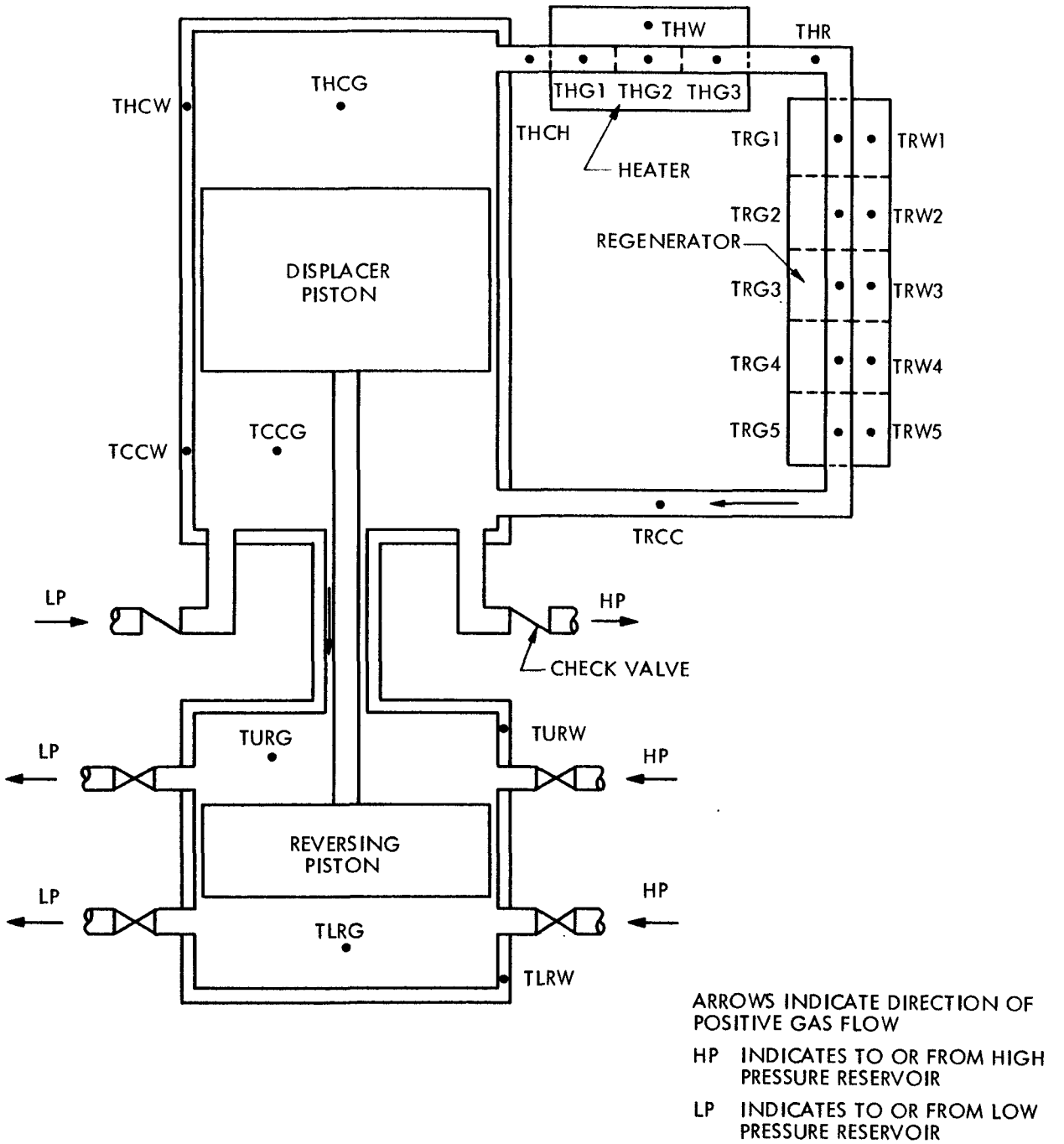

FIGURE N-1. INTERMEDIATE ANALYTICAL MODEL NODAL NETWORK

Assuming energy flow into the control volume as positive, the energy transfer from the chamber wall to the gas in a small time increment, $\delta\theta$, is:

$$\delta Q = H (T_w - T) \delta\theta \qquad \text{(N-1)}$$

The energy transfer by the enthalpy content of the incoming or outgoing gas is:

$$\delta Q = \Sigma \delta m C_p T = \gamma C_r \Sigma w_i T_i \qquad \text{(N-2)}$$

The mechanical work done on or by the gas is:

$$\delta Q = - P\delta V = -P \frac{dV}{d\theta} \delta\theta = -PA \frac{dx}{d\theta} \delta\theta \qquad \text{(N-3)}$$

The internal energy change in the gas is:

$$\delta Q = \frac{d}{d\theta} (mC_v T)\delta\theta - C_v T \frac{dm}{d\theta} \delta\theta + C_v m \frac{dT}{d\theta} \delta\theta$$

$$= C_v T \Sigma w_i \delta\theta + C_v m \frac{dT}{d\theta} \delta\theta \qquad \text{(N-4)}$$

Summing the energy terms:

$$C_v T \Sigma w_i + C_v m \frac{dT}{d\theta} = H(T_w - T) + \gamma C_v \Sigma w_i T_i - PA \frac{dx}{d\theta} \qquad \text{(N-5)}$$

Rearranging and solving for T yields:

$$T = \int \frac{1}{m} \left[T \Sigma w_i + \frac{H}{C_v} (T_w - T) + \gamma \Sigma w_i T_i - PA \frac{dx}{d\theta} \right] d\theta \qquad \text{(N-6)}$$

Note that T_i is dependent on the direction of the gas flow and will be the volume temperature during outflow and the outlet temperature of the adjacent node during inflow to the volume.

The equations for the gas temperatures in the heater and regenerator nodes are developed from the same basic equation. This basic temperature equation is derived by performing an energy balance on a generalized gas element as shown below:

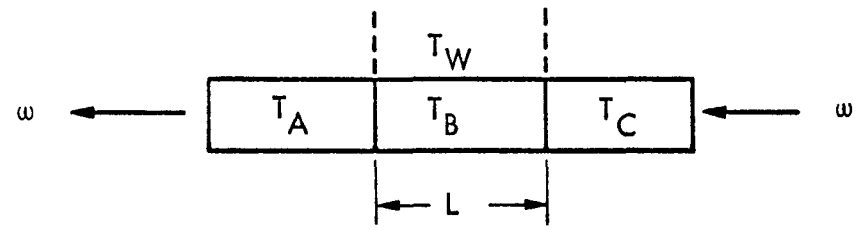

The control volume is bounded by gas elements at average temperatures T_A and T_C and a wall at temperature T_W. The energy transfer from the wall to the gas in a small time increment, $\delta\theta$, is:

$$\delta Q = H(T_W - T_B)\delta\theta \qquad \text{(N-7)}$$

The enthalpy rise of the gas of flow rate w is given by:

$$\delta\theta = \frac{d}{dy}(w\, C_p\, T)\, \delta y \delta\theta$$

$$= \left[w\, C_p \frac{dT}{dy} + C_p\, T \frac{dw}{dy}\right] \delta y \delta\theta \qquad \text{(N-8)}$$

The internal energy rise of the gas is

$$\delta Q = \frac{d}{d\theta}(mC_v T)\delta\theta = \frac{d}{d\theta}\left(\frac{AP}{RT}\, \delta y\, C_v T\right)\delta\theta$$

$$= \frac{A}{\gamma - 1}\frac{dP}{d\theta}\, \delta y \delta\theta \qquad \text{(N-9)}$$

Solving for $\frac{dP}{d\theta}$ by equating the flow rate change to decrease in content in control volume yields:

$$\frac{dw}{dy}\, \delta y \delta\theta = -\frac{d}{d\theta}\left(\frac{PA\, \delta y}{RT_B}\right) \delta\theta$$

$$\frac{dw}{dy} = \frac{A}{R}\left[\frac{1}{T_B}\frac{dP}{d\theta} - \frac{P}{T_B{}^2}\frac{dT}{d\theta}\right]$$

$$\frac{dP}{d\theta} = \frac{P}{T_B}\frac{dT_B}{d\theta} - \frac{RT_B}{A}\frac{dw}{dy} \qquad \text{(N-10)}$$

Combining the above equations gives:

$$\frac{A}{\gamma - 1}\left[\frac{P}{T_B}\frac{dT_B}{d\theta} - \frac{RT_B}{A}\frac{dw}{dy}\right] = H(T_W - T_B) - \left[w\,C_p\frac{dT_B}{dy} + C_pT_B\frac{dw}{dy}\right] \qquad \text{(N-11)}$$

Assuming that there is no net storage of gas in any of the heat exchanger element permits the simplification of Equation (N-11) to:

$$\frac{A}{\gamma - 1}\frac{P}{T_B}\frac{dT_B}{d\theta} = H(T_W - T_B) - w\,C_p\frac{dT_B}{dy} \qquad \text{(N-12)}$$

By linearizing the temperature into finite differences in length, the following approximation may be made:

$$\frac{dT_B}{dy} = \frac{\Delta T}{\Delta y} = \frac{1}{L}\left[\frac{T_A + T_B}{2} - \frac{T_B + T_C}{2}\right] = \frac{T_A - T_C}{2L} \qquad \text{(N-13)}$$

Therefore, solving for T_B in Equation (N-12) yields:

$$T_B = \frac{\gamma - 1}{A}\int^{T_B}\frac{T_B}{P}\left[H\,(T_W - T_B) - \frac{w\,C_p}{2L}\,(T_A - T_C)\right]d\theta \qquad \text{(N-14)}$$

Note that if the node of interest is the end node of a heat exchanger, the $(T_A - T_C)$ term becomes either $(2T_A - T_B - T_C)$ or $(T_A + T_B - 2T_C)$.

The temperature between com-onents is flow-direction dependent and in each case is the outlet temperature of a component. The outlet temperature of a component is an extrapolation of the gas temperature gradient within the component.

PRESSURE EQUATIONS

The pressure in each of the expansion or compression spaces is calculated using the equation of state. For a generalized volume:

$$P = \frac{mRT}{V} = \frac{mRT}{A(L - X)} \qquad \text{(N-15)}$$

MASS EQUATIONS

The mass of gas in each of the expansion or compression spaces is calculated using a mass balance on a control volume. The net content within the volume is determined by integrating the net flow into the volume:

$$m = \int \Sigma w_i \, d\theta \tag{N-16}$$

FLOW EQUATIONS

The gas flow between two points is assumed to be a direct function of the pressure difference between the two points. This assumption is correct if the pressure losses of the flowing gas are due to friction alone. The pressure drop equation for frictional flow is:

$$P_A - P_B = \rho f \frac{L}{D} \frac{V^2}{2g} \tag{N-17}$$

For low Reynold's number the friction factor is equal to $64/R_e$. Therefore:

$$P_A - P_B = \rho \frac{64\mu}{\rho VD} \frac{L}{D} \frac{V^2}{2g} \tag{N-18}$$

$$= \frac{32\mu L}{\rho D^2 g A} (\rho AV) \tag{N-19}$$

Using the definition of flow and the equation of state:

$$w = \frac{D^2 gA}{32\mu LR} \frac{P}{T} (P_A - P_B) \tag{N-20}$$

PISTON DYNAMICS

The piston velocity and displacement is determined by performing a force balance on the piston. The forces on the piston are the pressure forces and friction forces or:

$$\Sigma P_i A_i + F_f = m \frac{d^2x}{d\theta^2} \tag{N-21}$$

The velocity is given by:

$$\frac{dx}{d\theta} = \int \frac{1}{m}\left[\Sigma P_i A_i + F_f\right] d\theta, \qquad \text{(N-22)}$$

and the displacement is given by:

$$x = \int \frac{dx}{d\theta}\, d\theta \qquad \text{(N-23)}$$

The energy accounting equations are not necessary for the simulation of the system, but are necessary for the determination of the integrated system heat flows which are used for the evaluation of the engine performance. The equations include heater power to gas:

$$Q_{in} = \int H(T_W - T_B)\, d\theta, \qquad \text{(N-24)}$$

gross available power, which is the available expansion energy between the two pressure levels:

$$Q_{out} = \int C_p\, T_{HP}\left(1 - \left(\frac{P_{LP}}{P_{HP}}\right)^{\gamma-1/\gamma}\right) W_{HP}\, d\theta, \qquad \text{(N-25)}$$

power required by the reversing piston if the flow-through concept is used:

$$Q_{RP} = \int C_p\, T_{HP}\left(1 - \left(\frac{P_{LP}}{P_{HP}}\right)^{\gamma-1/\gamma}\right) W_{RP}\, d\theta, \text{ and} \qquad \text{(N-26)}$$

frictional power loss:

$$Q_{DP} = \int (P_A - P_B)\, \frac{w\, RT}{P}\, d\theta \qquad \text{(N-27)}$$

The complete set of equations is shown as a Fortran listing in Figure N-2 with nomenclature shown in Table N-1.

Additional equations which are included in analog computer approach are shown in Figure N-3.

FIGURE N-2.

```
IMPLANTABLE POWER SUPPLY SIMULATION MIMIC VERSION

INPUT CONSTANTS AND PARAMETERS
                    CON(DT,DTMAX,DTMIN)
                    PAR(KONHG,KONCG,CVG,CPG,JCON,RCON)
                    PAR(DC,DDP,DRC,DRP,DROD)
                    PAR(LRC,PORT,MP,FRIC,ZERO)
                    PAR(AFH,PERH,LH,AFR,PERR,LR)
                    PAR(LHC,LCC,XLL,XUL,PLP,PHP)
                    PAR(KPL,KLP,KHP,KSL,KRPL)
                    PAR(KHPRC,KLPRC,MHCGIC,MCCGIC,MURGIC,MLRGIC)
                    PAR(THCW,TCCW,THW,TRW1,TRW2,TRW3)
                    PAR(TRW4,TRW5,TURW,TLRW,TLPG,THPG)
DUMMY CONSTANTS EQUATIONS
          TEQ     = FSW(T,FALSE,TRUE,FALSE)
 TEQ      C1      = .35*C2*DC*DC
 TEQ      C2      = 17.952*KONHG/CVG
 TEQ      C3      = CPG/CVG
 TEQ      C4      = .7854*DC*DC/(CVG*JCON)
 TEQ      C5      = JCON*(C3-1.)/AFH
 TEQ      C6      = 4.36*KONHG*PERH/DHH
 TEQ      C7      = 1.5*CPG/LH
 TEQ      C8      = JCON*(C3-1.)/AFR
 TEQ      C9      = 2.18*(KONHG+KONCG)*PERR/DHR
 TEQ      C10     = 2.5*CPG/LR
 TEQ      C11     = 1.2732*RCON/(DC*DC)
 TEQ      C12     = 386./MP
 TEQ      C13     = C14-.7854*DROD*DROD
 TEQ      C14     = .7845*DDP*DDP
 TEQ      C15     = .35*C16*DRC*DRC
 TEQ      C16     = 17.952*KONCG/CVG
 TEQ      C17     = .7854*DRC*DRC/(CVG*JCON)
 TEQ      C18     = 1.2732*RCON/(DRC*DRC)
 TEQ      C19     = C20-.7854*DROD*DROD
 TEQ      C20     = .7854*DRP*DRP
 TEQ      C21     = C6*LH/3.0
 TEQ      RATIO   = PLP/PHP
 TEQ      GAM     = (C3-1.)/C3
 TEQ      PROD    = EXP(GAM,RATIO)
 TEQ      C22     = CPG*THPG*(1.-PROD)
 TEQ      DHH     = 4.0*AFH/PERH
 TEQ      DHR     = 4.0*AFR/PERR
 TEQ      KRH1    = 1.5241*LH/(DHH*DHH*AFH)
 TEQ      KRH2    = .82967*LR/(DHR*DHR*AFR)
SWITCHING FUNCTIONS EQUATIONS
          FHP     = FSW(DHP,0.0,1.0,1.0)
          FLP     = FSW(DLP,0.0,1.0,1.0)
          FRF1    = FSW(DPHC,0.0,1.0,1.0)
          FRF2    = FSW(DPHC,1.0,0.0,0.0)
          FSLP    = FSW(DPSL,0.0,1.0,1.0)
          FSLN    = FSW(DPSL,1.0,0.0,0.0)
          FRPLP   = FSW(DPRPL,0.0,1.0,1.0)
          FRPLN   = FSW(DPRPL,1.0,0.0,0.0)
          FUHPP   = FSW(DPUHP,0.0,1.0,1.0)
          FUHPN   = FSW(DPUHP,1.0,0.0,0.0)
```

FIGURE N-2. (Continued)

```
          FULPP  = FSW(DPULP,0.0,1.0,1.0)
          FULPN  = FSW(DPULP,1.0,0.0,0.0)
          FLHPP  = FSW(DPLHP,0.0,1.0,1.0)
          FLHPN  = FSW(DPLHP,1.0,0.0,0.0)
          FLLPP  = FSW(DPLLP,0.0,1.0,1.0)
          FLLPN  = FSW(DPLLP,1.0,0.0,0.0)
          FURI   = FSW(XL-PORT,0.0,0.0,1.0)
          FURO   = FSW(XL+PORT,1.0,0.0,0.0)
          DIREC  = FSW(XDOTL,1.0,0.0,-1.0)
TEMPERATURE EQUATIONS
          QHCG1  = THCG*(WR+WPL)
          QHCG2  = (C1/(LHC-XL)+C2*(LHC-XL))*(THCW-THCG)
          QHCG3  = -C3*(WR*THCH+WPL*THCPL)
          QHCG4  = C4*PHC*XDOTL
          THCG   = INT((QHCG1+QHCG2+QHCG3+QHCG4)/MHCG,1580.0)
          QCCG1  = -TCCG*(WR+WPL+WLP-WHP-WSL)
          QCCG2  = (C1/(LCC+XL)+C2*(LCC+XL))*(TCCW-TCCG)
          QCCG3  = C3*(WR*TRCC+WPL*TCCPL+WLP*TLPG-WHP*TCCG-WSL*TCCSL)
          QCCG4  = -C4*PCC*XDOTL
          TCCG   = INT((QCCG1+QCCG2+QCCG3+QCCG4)/MCCG,670.0)
          QHG11  = C6*(THW-THG1)
          QHG12  = C7*WR*(2.*THCH-THG1-THG2)
          THG1   = INT((C5*THG1/PHC)*(QHG11+QHG12),1610.0)
          QHG21  = C6*(THW-THG2)
          QHG22  = C7*WR*(THG1-THG3)
          THG2   = INT((C5*THG2/PHC)*(QHG21+QHG22),1660.0)
          QHG31  = C6*(THW-THG3)
          QHG32  = C7*WR*(THG2+THG3-2.*THR)
          THG3   = INT((C5*THG3/PHC)*(QHG31+QHG32),1680.0)
          QRG11  = C9*(TRW1-TRG1)
          QRG12  = C10*WR*(2.*THR-TRG1-TRG2)
          TRG1   = INT((C8*TRG1/PHC)*(QRG11+QRG12),1570.0)
          QRG21  = C9*(TRW2-TRG2)
          QRG22  = C10*WR*(TRG1-TRG3)
          TRG2   = INT((C8*TRG2/PHC)*(QRG21+QRG22),1580.0)
          QRG31  = C9*(TRW3-TRG3)
          QRG32  = C10*WR*(TRG2-TRG4)
          TRG3   = INT((C8*TRG3/PHC)*(QRG31+QRG32),1200.0)
          QRG41  = C9*(TRW4-TRG4)
          QRG42  = C10*WR*(TRG3-TRG5)
          TRG4   = INT((C8*TRG4/PHC)*(QRG41+QRG42),1010.0)
          QRG51  = C9*(TRW5-TRG5)
          QRG52  = C10*WR*(TRG4+TRG5-2.*TRCC)
          TRG5   = INT((C8*TRG5/PHC)*(QRG51+QRG52),820.0)
          QURG1  = -TURG*(WURI-WURO+WSL-WPPL)
          QURG2  = (C15/(LRC-XL)+C16*(LRC-XL))*(TURW-TURG)
          QURG3  = C3*(WURI*TURP-WURO*TULP+WSL*TURSL-WRPL*TURPL)
          QURG4  = C17*PUR*XDOTL
          TURG   = INT((QURG1+QURG2+QURG3+QURG4)/MURG,660.0)
          QLRG1  = -TLRG*(WLRI-WLRO+WRPL)
          QLRG2  = (C15/(LRC+XL)+C16*(LRC+XL))*(TLRW-TLRG)
          QLRG3  = C3*(WLRI*TLHP-WLRO*TLLP+WRPL*TLRPL)
          QLRG4  = -C17*PLR*XDOTL
          TLRG   = INT((QLRG1+QLRG2+QLRG3+QLRG4)/MLRG,660.0)
          THCH   = FRF1*THCG+FRF2*(1.5*THG1-.5*THG2)
          THR    = FRF1*(1.5*THG3-.5*THG2)+FRF2*(1.5*TRG1-.5*TRG2)
          TRCC   = FRF1*(1.5*TRG5-.5*TRG4)+FRF2*TCCG
          THCPL  = THCG*FRF1+THCW*FRF2
          TCCPL  = TCCW*FRF1+TCCG*FRF2
```

FIGURE N-2. (Continued)

```
          TCCSL  = FSLP*TCCG+FSLN*TCCW
          TURSL  = FSLP*TURW+FSLN*TURG
          TURPL  = FRPLP*TURG+FRPLN*TURW
          TLRPL  = FRPLP*TLRW+FRPLN*TLRG
          TUHP   = FUHPP*THPG+FUHPN*TURG
          TULP   = FULPP*TURG+FULPN*TLPG
          TLHP   = FLHPP*THPG+FLHPN*TLRG
          TLLP   = FLLPP*TLPG+FLLPN*TLPG
PRESSURE EQUATIONS
          PHC    = C11*MHCG*THCG/(LHC-XL)
          PCC    = C11*MCCG*TCCG/(LCC+XL)
          PUR    = C18*MURG*TURG/(LRC-XL)
          PLR    = C18*MLRG*TLRG/(LRC+XL)
MASS EQUATIONS
          MHCG   = INT(-WP-WPL,MHCGIC)
          MCCG   = INT(WR+WPL+WLP-WHP,MCCGIC)
          MURG   = INT(WURI-WURO,MURGIC)
          MLRG   = INT(WLRI-WLRO,MLRGIC)
FLOW EQUATIONS
          KRH    = PHC/(KRH1+KRH2)
          WR     = KRH*DPHC
          WPL    = KPL*DPHC
          WHP    = KHP*DHP*FHP
          WLP    = KLP*DLP*FLP
          WSL    = KSL*DPSL
          WURI   = KHPRC*FURI*DPUHP
          WURO   = KLPRC*FURO*DPULP
          WLRI   = KHPRC*FURO*DPLHP
          WLRO   = KLPRC*FURI*DPLLP
          WRPL   = KRPL*DPRPL
          DPHC   = PHC-PCC
          DHP    = PCC-PHP
          DLP    = PLP-PCC
          DPSL   = PCC-PUR
          DPRPL  = PUR-PLR
          DPUHP  = PHP-PUR
          DPULP  = PUR-PLP
          DPLHP  = PHP-PLR
          DPLLP  = PLR-PLP
DYNAMIC EQUATIONS
          PFORC  = C13*PCC-C14*PHC-C19*PUR+C20*PLR
          XDOT   = INT(C12*(PFORC+DIREC*FRIC),50.0)
          XDOTL  = LIN(XDOT,XL,XLL,XUL)
          XL     = INT(XDOTL+ZERO*(QIN+QOUT+QRP+QDP),0.0)
ENERGY ACCOUNTING EQUATIONS
          QIND   = C21*(3.*THW-THG1-THG2-THG3)
          QIN    = INT(QIND,0.0)
          QRPD   = C22*(WUPI+WLPI)
          QRP    = INT(QRPD,0.0)
          QOUTD  = C22*WHP
          QOUT   = INT(QOUTD,0.0)
          QDPD   = DPHC*WR*RCON*TRG3/(PHC*JCON)
          QDP    = INT(QDPD,0.0)
HEADINGS AND OUTPUT PARAMETERS
                   HDR(T,XL,XDOTL,QIN,QRP,QOUT)
                   HDR(THG1,THG2,THG3,TRG1,TRG2,TRG3)
                   HDR(TRG4,TRG5,THCG,TCCG,TURG,TLRG)
                   HDR(PHC,PCC,PUR,PLR,WR,WPL)
                   HDR(WHP,WLP,WURI,WURO,WLRI,WLRO)
```

FIGURE N-2. (Continued)

```
HDR(WSL,WPPL,THCH,THP,TPCC,QDP)
HDR(MHCG,MCCG,MURG,MLRG)
HDR(QIND,QRPD,QOUTD,QDPD)
HDR
OUT(T,XL,XDOTI,QIN,QPP,QOUT)
OUT(THG1,THG2,THG3,TPG1,TPG2,TRG3)
OUT(TPG4,TRG5,THCG,TCCG,TURG,TLRG)
OUT(PHC,PCC,PUR,PLR,WP,WPI)
OUT(WHP,WLP,WURI,WURO,WLRI,WLRO)
OUT(WSL,WPPL,THCH,THP,TPCC,QDP)
OUT(MHCG,MCCG,MURG,MLRG)
OUT(QIND,QRPD,QOUTD,QDPD)
OUT
FIN(T,.150)
END
```

FIGURE N-3.

ADDITIONAL EQUATIONS FOR ANALOG SIMULATION

```
REGENERATOR WALL TEMPERATURE EQUATIONS
          HTIME  = (T+1.0)/2.0
          DTHRP  = INT(FRF1*THR,1700.0)
          THRPA  = DTHRP/HTIME
          DTHRN  = INT(FRF2*THR,1640.0)
          THRNA  = DTHRN/HTIME
          DTRCP  = INT(FRF1*TRCC,730.0)
          TRCPA  = DTRCP/HTIME
          DTRCN  = INT(FRF2*TRCC,670.0)
          TRCNA  = DTRCN/HTIME
          TRWH   = (THRPA+THRNA)/2.0
          TRWC   = (TRCPA+TRCNA)/2.0
          DELTT  = (TRWH-TRWC)/5.0
          TRW1   = TRWH-DELTT/2.0
          TRW2   = TRW1-DELTT
          TRW3   = TRW2-DELTT
          TRW4   = TRW3-DELTT
          TRW5   = TRW4-DELTT
CHECK VALVE EQUATIONS
          U1     = (DPCVO-DPCVC)/2.0
          U2     = (DPCVO+DPCVC)/2.0
          HPCV   = DHP-U1+U2*FCVH
          FCVH   = FSW(HPCV,-1.0,1.0,1.0)
          FCVHF  = (FCVH+1.0)/2.0
          WHP    = KHP*FCVHF*DHP
          LPCV   = DLP-U1+U2*FCVL
          FCVL   = FSW(LPCV,-1.0,1.0,1.0)
          FCVLF  = (FCVL+1.0)/2.0
          WLP    = KLP*FCVLF*DLP
```

TABLE N-1

NOMENCLATURE

Symbols	Definition
A	Surface or cross-sectional area
C_p	Specific heat at constant pressure
C_v	Specific heat at constant volume
D	Diameter
f	Flow friction factor
F_f	Sliding friction force
g	Gravitational acceleration
H	Heat transfer conductance
L	Length
m	Mass
P	Pressure
Q	Heat flow
R	Gas constant
T	Temperature
V	Volume or velocity
w	Flow rate
x	Piston displacement
y	Linear displacement
γ	Gas specific heat ratio
θ	Time
μ	Gas viscosity
ρ	Gas density
Subscripts	
dp	Pressure drop power
hp	High pressure reservoir
lp	Low pressure reservoir
out	Output power
rp	Reversing piston power
w	Wall

TABLE N-1 - Continued

FORTRAN	Definition
AFH	Heater flow area
AFR	Regenerator flow are
CPG	C_p
CVG	C_v
DC	Displacer piston chamber diameter
DDP	Displacer piston diameter
DROD	Connecting rod diameter
DRP	Reversing piston diameter
FRIC	F_f
JCON	Conversion factor 9336 in-lb/Btu
KHP	Engine outlet check valve flow coefficient
KHPRC	Reversing chamber inlet flow coefficient
KLP	Engine inlet check valve flow coefficient
KLPRC	Reversing chamber outlet flow coefficient
KONCG	Gas thermal conductivity at hot temperature
KONHG	Gas thermal conductivity at cold temperature
KPL	Displacer piston leakage flow coefficient
KRPL	Reversing piston leakage flow coefficient
KSL	Labyrinth seal leakage flow coefficient
LCC	Cold chamber equivalent end clearance
LH	Heater length
LHC	Hot chamber equivalent end clearance
LR	Regenerator length
LRC	Upper or lower reversing chamber length
MCCG	Instantaneous mass of gas in cold chamber
MCCGIC	Initial mass of gas in cold chamber
MHCG	Instantaneous mass of gas in hot chamber
MHCGIC	Initial mass of gas in hot chamber
MLRG	Instantaneous mass of gas in lower reversing chamber
MLRGIC	Initial mass of gas in lower reversing chamber
MP	Mass of piston assembly
MURG	Instantaneous mass of gas in upper reversing chamber

TABLE N-1 - Continued

FORTRAN	Definition
MURGIC	Initial mass of gas in upper reversing chamber
PCC	Cold chamber pressure
PERH	Heater wetted perimeter
PERR	Regenerator wetted perimeter
PHC	Hot chamber pressure
PHP	High pressure reservoir pressure
PLP	Low pressure reservoir pressure
PLR	Lower reversing chamber pressure
PORT	Distance from midstroke where reversing ports open
PUR	Upper reversing chamber pressure
QDP	Pressure drop power loss
QDPD	Instantaneous pressure drop power loss
QIN	Heater power to gas
QIND	Instantaneous heater power to gas
QOUT	Gross available output power
QOUTD	Instantaneous gross available output power
QRP	Reversing piston required power
QRPD	Instantaneous reversing piston required power
RCON	Gas constant
T	Time
TCCG	Cold chamber gas temperature
TCCW	Cold chamber wall temperature
THCG	Hot chamber gas temperature
THCH	Gas temperature between hot chamber and heater
THCW	Hot chamber wall temperature
THGn, n=1,2,3	Heater gas temperatures
THPG	High pressure reservoir gas temperature
THR	Gas temperature between heater and regenerator
THW	Heater wall temperature
TLPG	Low pressure reservoir gas temperature
TLRC	Lower reversing chamber gas temperature

TABLE N-1 - Continued

FORTRAN	Definition
TLRW	Lower reversing chamber wall temperature
TRCC	Gas temperature between cold chamber and regenerator
TRGn, n=1,...,5	Regenerator gas temperatures
TRWn, n=1,...,5	Regenerator wall temperatures
TURG	Upper reversing chamber gas temperature
TURW	Upper reversing chamber wall temperature
WHP	Engine outlet flow to high pressure reservoir
WLP	Engine inlet flow from low pressure reservoir
WLRI	Lower reversing chamber inlet flow
WLRO	Lower reversing chamber outlet flow
WPL	Displacer piston leakage
WR	Regenerator flow
WRPL	Reversing piston leakage
WSL	Labryinth seal leakage
WURI	Upper reversing chamber inlet flow
WURO	Upper reversing chamber outlet flow
XDOTL	Piston velocity
XL	Piston displacement from midstroke
XLL	Lower piston stroke limit
XUL	Upper piston stroke limit
ZERO	Value of zero

APPENDIX O

DETAILED PARAMETRIC ANALYSIS TECHNIQUE

The analytical representation of the system is shown in Figure O-1. with the model divided into finite nodal elements. The nodal elements in the heat exchangers are constant in size but the nodes in the expansion and compression spaces are of variable size depending on the piston position.

The formulation of the system equations requires the development of seven fundamental equations which describe the gas pressure, gas temperature and wall temperature of the compression and expansion space nodes, the gas temperature and wall temperature of the heat exchanger nodes, the flow phenomena of the system, and the piston dynamics. There are additional auxiliary equations but these need not be derived since they are merely representations of boundary conditions or calculations of dummy variables, output parameters, and problem constants.

EXPANSION AND COMPRESSION SPACES

The equations for the displacer piston hot and cold chambers and the reversing piston upper and lower chambers are derived in the same manner and are represented by three basic equations. The first of these is the pressure equation for the expansion or compression space. Assume a control volume with an instantaneous volume V_A, pressure P_A, and temperature T_A. There is net heat and mass flow in or out of the volume as shown below.

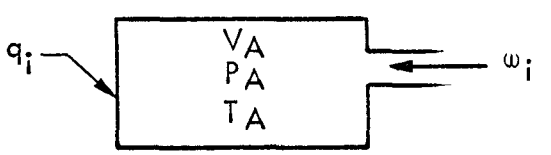

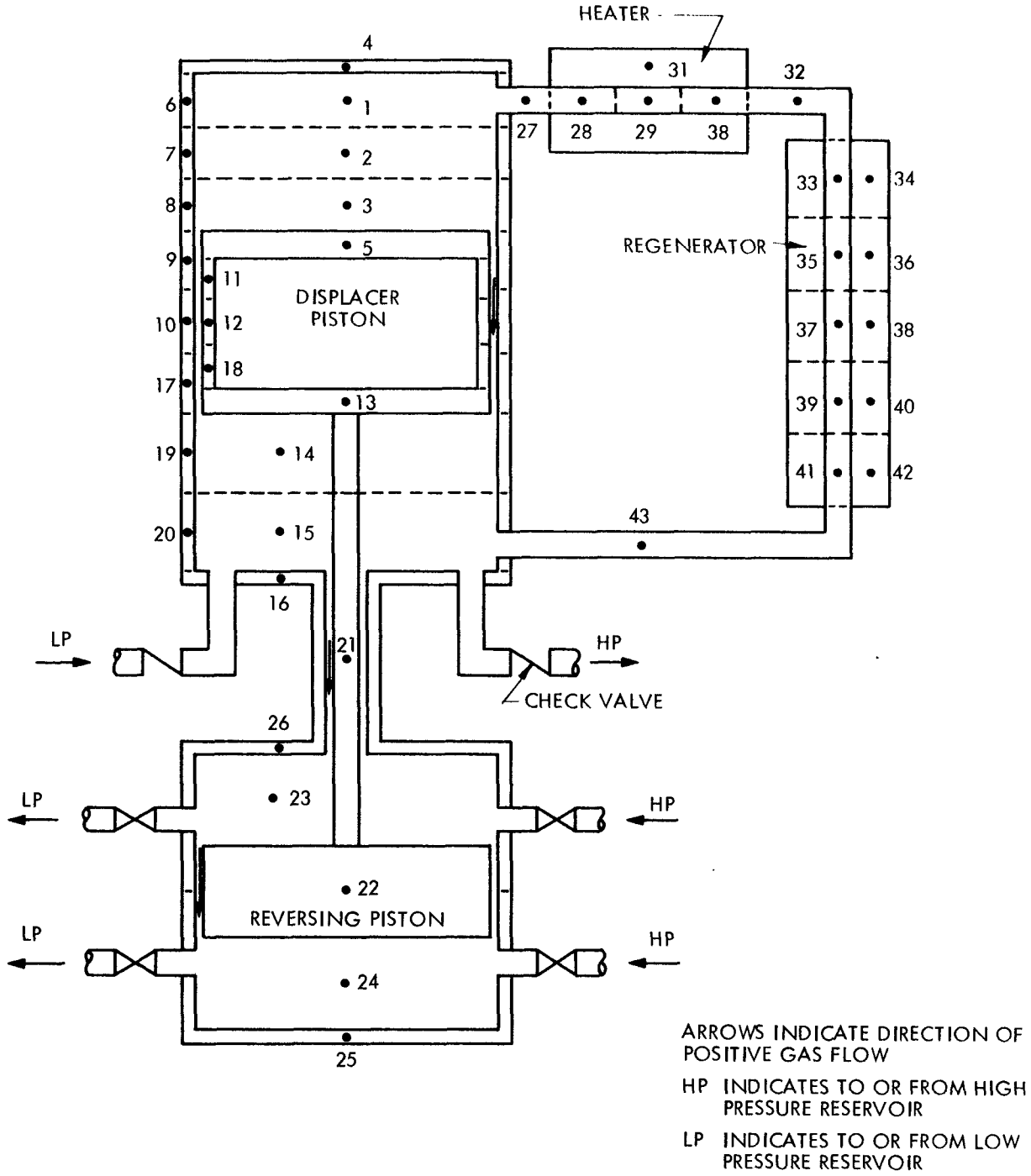

FIGURE O-1. DETAILED ANALYTICAL MODEL NODAL NETWORK

3.01-68-053

The temperature of the mass flow is T_i if the flow is in and T_A if the flow is out of the volume. Let:

$$W_i = w_i \delta\theta \tag{0-1}$$

$$\Sigma W_i = W_o \tag{0-2}$$

$$\Sigma W_i T_i = (WT)_o \tag{0-3}$$

$$\Sigma q_i = q_o \tag{0-4}$$

First, mixing the incoming gas with control volume, gas at constant pressure resulting in a new volume temperature, T_A' or:

$$W[T_A' - T_A] = \Sigma W_i \, [T_i - T_A'] \tag{0-5}$$

or

$$T_A' = \frac{(WT)_o + W_A T_A}{W_A + W_o} \tag{0-6}$$

Adding the heat flows into the total resultant gas volume at constant pressure results in a temperature T_A'' or:

$$(W_A + W_o) \, C_p \, (T_A'' - T_A') = q_o \delta\theta \tag{0-7}$$

or

$$T_A'' = T_A' + \frac{q_o \delta\theta}{(W_A + W_o) C_p} \tag{0-8}$$

Assuming that an adiabatic process occurs due to the motion of the piston and results in a new volume, V_B,

$$V_B = V_A'' \left(\frac{P_A}{P_B}\right)^{1/\gamma} = \frac{(W_A + W_o) R T_A''}{P_A} \left(\frac{P_A}{P_B}\right)^{1/\gamma} \tag{0-9}$$

Substituting T_A for T_A'' and T_A' and simplifying yields:

$$V_B = V_A \left[\frac{(WT)_o}{W_A T_A} + 1 + \frac{q_o \delta\theta}{W_A C_p T_A}\right] \left(\frac{P_A}{P_B}\right)^{1/\gamma} \tag{0-10}$$

Noting:

$$(WT_o) = \Sigma W_i T_i = \Sigma w_i T_i \delta\theta = (wT)_o \delta\theta \tag{0-11}$$

$$\frac{V_B}{V_A} = 1 + \frac{\delta V}{V_A} \qquad (0\text{-}12)$$

$$\left(\frac{P_A}{P_B}\right)^{1/\gamma} = \left(\frac{P_B}{P_A}\right)^{-1/\gamma} = \left(1 + \frac{\delta P}{P_A}\right)^{-1/\gamma} \simeq \left(1 - \frac{1}{\gamma}\frac{\delta P}{P_A}\right) \qquad (0\text{-}13)$$

Substituting Equations (0-11), (0-12), and (0-13) into (0-10) and neglecting all second order terms yields:

$$1 + \frac{\delta V}{V_A} \simeq 1 + \frac{(wT)_o \delta\theta}{W_A T_A} + \frac{q_o \delta\theta}{W_A C_p T_A} - \frac{1}{\gamma}\frac{\delta P}{P_A} \qquad (0\text{-}14)$$

Using the equation of state, $P_A V_A = W_A R T_A$, and converting to differential form:

$$\frac{P_A}{W_A R T_A}\frac{dV}{d\theta} = \frac{(wT)_o}{W_A T_A} + \frac{q_o}{W_A C_p T_A} - \frac{1}{\gamma}\frac{V_A}{W_A R T_A}\frac{dP}{d\theta}$$

or

$$\frac{P_A}{R}\frac{dV}{d\theta} = (wT)_o + \frac{q_o}{C_p} - \frac{1}{\gamma}\frac{V_A}{R}\frac{dP}{d\theta} \qquad (0\text{-}15)$$

By definition, $(wT)_o = \Sigma w_i T_i$

$$w_i T_i = w_i T_i \text{ if } w_i \text{ is inward}$$
$$w_i T_i = w_i T_A \text{ if } w_i \text{ is outward.}$$

or $$w_i T_i = w_i T_A + w_i (T_i - T_A)\, \rho(w_i) \qquad (0\text{-}16)$$

where

$$\rho(w_i) = 1.0 \qquad w_i < 0$$
$$= 0 \qquad w_i > 0$$

Therefore

$$\frac{q_o}{C_p} + \Sigma(w_i T_A + w_i (T_i - T_A)\, \rho(w_i)) = \frac{V_A}{\gamma R}\frac{dP}{d\theta} + \frac{P_A}{R}\frac{dV}{d\theta} \qquad (0\text{-}17)$$

Now, assume there are N connected volumes in a particular expansion space. Also assume that all volumes are at identical pressures and all are of equal volume. Then Equation (0-17) may be written for each volume and, by summing all the equations, the interflows between connected volumes may be eliminated from the pressure equation. This may be shown by examining any two adjacent volumes and summing the interflow at their boundary. Thus the interflow w_i, appears in the equations of the j^{th} and $(j + 1)^{th}$ volumes as follows:

$$w_i T_j + w_i (T_{j+1} - T_j)\rho(w_i)$$

$$- w_i T_{j+1} - w_i (T_j - T_{j+1}) [1 - \rho(w_i)]$$

$$= w_i (T_{j+1} - T_j) [-1 + \rho(w_i) + 1 - \rho(w_i)] = 0$$

Hence all interflows cancel, leaving the expression:

$$\frac{q_o}{C_p} + \Sigma(w_i T_A + w_i (T_i - T_A)\ \rho(w_i)) = \frac{1}{\gamma R} V \frac{dP}{d\theta} + \frac{P}{R} \frac{dV}{d\theta} \qquad (0\text{-}18)$$

where $V = NV_A = A(L \pm X)$

w_i is external flows only.

Solving for P gives:

$$P = \int \frac{\gamma R}{A(L \pm X)} \left[\frac{q_o}{C_p} + \Sigma(w_i T_A + w_i (T_i - T_A)\ \rho(w_i)) \pm \frac{P_A}{R} \frac{dx}{d\theta}\right] d\theta \qquad (0\text{-}19)$$

The temperature equations for the gas nodes in the expansion or compression spaces are derived in a similar manner. Using the relationship of Equation (0-9), the temperature after the adiabatic process is

$$T_B = T_A'' \left(\frac{P_B}{P_A}\right)^{\gamma - 1/\gamma} \qquad (0\text{-}20)$$

or

$$1 + \frac{\delta T}{T_A} = \frac{T_A''}{T_A} \left(\frac{P_B}{P_A}\right)^{\gamma - 1/\gamma} \qquad (0\text{-}21)$$

As in Equation (0-13)

$$\left(\frac{P_B}{P_A}\right)^{\gamma-1/\gamma} \simeq 1 + \frac{\gamma - 1}{\gamma}\frac{\delta P}{P_A} \qquad (0\text{-}22)$$

Substituting Equations (0-6), (0-8) and (0-22) into (0-21) gives:

$$1 + \frac{\delta T}{T_A} = \left[\frac{(WT)_o + W_A T_A}{T_A(W_A + W_o)} + \frac{q_o \delta\theta}{(W_A + W_o)C_p T_A}\right]\left[1 + \frac{\gamma - 1}{\gamma}\frac{\delta P}{P_A}\right]$$

$$= \frac{1}{1 + \frac{W_o}{W_A}}\left[\frac{(WT)_o}{W_A T_A} + \frac{q_o \delta\theta}{W_A C_p T_A} + 1\right]\left[1 + \frac{\gamma - 1}{\gamma}\frac{\delta P}{P_A}\right] \qquad (0\text{-}23)$$

Now

$$\frac{1}{1 + \frac{W_o}{W_A}} = \frac{1}{1 + \frac{w_o \delta\theta}{W_A}} \simeq 1 - \frac{w_o \delta\theta}{W_A} \qquad (0\text{-}24)$$

Substituting Equation (0-24) into (0-23) and neglecting second order terms yields:

$$1 + \frac{\delta T}{T_A} = \frac{(wT)_o \delta\theta}{W_A T_A} + \frac{q_o \delta\theta}{W_A C_p T_A} + 1 - \frac{w_o \delta\theta}{W_A} + \frac{\gamma - 1}{\gamma}\frac{\delta P}{P_A} \qquad (0\text{-}25)$$

Collecting terms and converting to differential form gives:

$$\frac{dT_A}{d\theta} = \frac{1}{W_A}\left[(wT)_o - w_o T_A + \frac{q_o}{C_p} + \frac{\gamma - 1}{\gamma}\frac{W_A T_A}{P_A}\frac{dP}{d\theta}\right] \qquad (0\text{-}26)$$

Using previous definitions and the equation of state:

$$\frac{dT_A}{d\theta} = \frac{RT_A}{P_A V_A}\left[\Sigma\, w_i(T_i - T_A) + \frac{q_o}{C_p} + \frac{V_A}{C_p}\frac{dP}{d\theta}\right] \qquad (0\text{-}27)$$

Integrating yields:

$$T_A = \int \frac{RT_A}{P_A V_A}\left[\Sigma\, w_i(T_i - T_A) + \frac{q_o}{C_p} + \frac{V_A}{C_p}\frac{dP}{d\theta}\right]d\theta \qquad (0\text{-}28)$$

where $V_A = \frac{A}{N}(L \pm X)$

The temperature equations for the wall nodes in the expansion or compression spaces are developed simply be performing an energy balance on the metal nodal element.

$$mC_p \frac{dT}{d\theta} = \Sigma q_i$$

or

$$T = \int \frac{1}{m C_p} \Sigma q_i \, d\theta \qquad (0\text{-}29)$$

There are several different mechanisms for transfer of energy to and from a wall node. Since the variable cylinder wall nodes require all the modes of energy transport, a generalized variable node as shown will be examined.

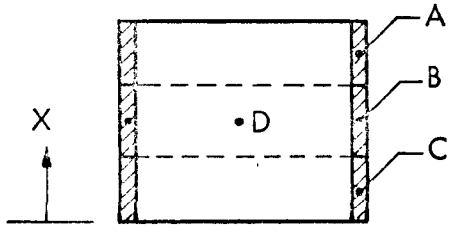

The first mode of energy transport is by convection from the gas to the metal node and the transfer area is dependent on the piston position.

$$q_i = hA \frac{(L - X)}{L} (T_D - T_B) \qquad (0\text{-}30)$$

The second mode is conduction to the adjacent nodes and the conduction length is dependent on piston position:

$$q_2 = K \frac{(T_A - T_B)}{(\frac{L - X}{N})} + K \frac{(T_B - T_C)}{(\frac{L - X}{N})} \qquad (0\text{-}31)$$

The third mode is radiation to the surrounding nodes and the surface area is dependent on piston position.

$$q_3 = \Sigma\sigma F_{B\text{-}n} A \frac{(L - X)}{L} (T_B^4 - T_n^4)$$

$$\simeq \Sigma 4\sigma F_{B\text{-}n} A \frac{(L - X)}{L} T_B^3 (T_B - T_n) \qquad (0\text{-}32)$$

Note that this mode of energy transfer is considered at the high temperature nodes.

The fourth mode is energy transfer due to the moving boundaries of the node:

$$q_4 = Ax \frac{dx}{d\theta} C_p (T_C - T_B) + Ax \frac{dx}{d\theta} C_p (T_A - T_B) \qquad (0\text{-}33)$$

Since the mass of the wall nodal element is also dependent on piston position Equation (0-29) becomes:

$$T = \int \frac{L}{m_o (L - X) C_p} (q_1 + q_2 + q_3 + q_4)\, d\theta \qquad (0\text{-}34)$$

Note that if the node of interest is in the negative x direction the (L - X) terms become (L + X).

HEAT EXCHANGER EQUATIONS

The equations for the heater and regenerator nodes are derived in the same manner and are represented by two basic equations. The first is the temperature equation for a heat exchanger gas node. Assume a set of nodes as shown below; where T_W is the wall temperature and T is the gas temperature and the gas is flowing at a rate w.

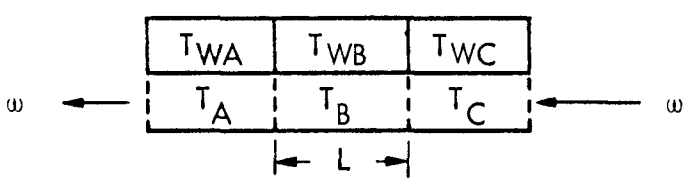

Using the derivation in Appendix N, the temperature of the gas node is:

$$T_B = \int \frac{\gamma - 1}{A} \frac{T_B}{P} \left[H (T_{WB} - T_B) - \frac{wC_p}{2L} (T_A - T_C) \right] d\theta \qquad (0\text{-}35)$$

Note that if T_B is an end node and T_C is the inlet gas temperature, then the $(T_A - T_C)$ term would become $(T_A + T_B - 2T_C)$; or if T_A is the exit temperature, then the term would be $(2T_A - T_B - T_C)$.

The second equation defines the wall temperature of the heat exchanger. Using the model as shown, the heat transfer to the gas from the wall node is

$$\delta Q = H(T_{WB} - T_B)\delta\theta \qquad (0\text{-}26)$$

Using the linearizing approach of finite nodes, the conduction heat transfer to adjacent nodes is:

$$\delta Q = \left[\frac{K}{L}(T_{WC} - T_{WB}) - \frac{K(T_{WB} - T_{WA})}{L}\right]\delta\theta \qquad (0\text{-}37)$$

The internal energy rise in the wall node is:

$$\delta Q = mC_p\,\delta T_{WB} \qquad (0\text{-}38)$$

Performing an energy balance on the node and converting the equation to differential form yields:

$$mC_p\frac{dT_{WB}}{d\theta} = H(T_{WB} - T_B) + \frac{K}{L}(T_{WC} + T_{WA} - 2T_{WB})$$

or

$$T_{WB} = \int \frac{1}{mC_p}\left[H(T_{WB} - T_B) + \frac{K}{L}(T_{WC} + T_{WA} - 2\,T_{WB})\right]d\theta \qquad (0\text{-}39)$$

Note again that the term $(T_{WC} + T_{WA})$ must be adjusted if the node of interest is a end node.

FLOW EQUATIONS

The flow between two points is assumed to be a direct function of the pressure difference between the two points. This assumption is correct if the pressure losses of the flowing gas are due to friction alone as shown in Appendix N. From that derivation, the flow equation is:

$$w = C\frac{(P_A + P_B)}{T}(P_A - P_B) \qquad (0\text{-}40)$$

PISTON DYNAMICS

The piston velocity and displacement is determined by performing a force balance on the piston as shown in Appendix N. The velocity of the piston is given by:

$$\frac{dx}{d\theta} = \int \frac{1}{m}(\Sigma\, P_i A_i + F_f)d\theta \qquad (0\text{-}41)$$

and the displacement is given by:

$$x = \int \frac{dx}{d\theta}\,d\theta \qquad (0\text{-}42)$$

The complete set of system equations is shown in Figure 0-2, with nomenclature listed in Table 0-1. The basic temperature, pressure, flow and dynamic equations are listed together with precomputed problem constants, dummy variables and computed required output parameters.

It should be noted that a particular temperature convention is used in anticipation of increased accuracy for analog computation. Temperatures for nodes 1 through 12 and 27 through 37 are referenced to a temperature T_o and the remaining nodes are referenced to T_∞. For example:

$$T_1{}^{o}\,\text{Don} = T_o - T_1{}^{o}\,\text{Rankine}$$

$$T_{13}{}^{o}\,\text{Wes} = T_{13}{}^{o}\,\text{Rankine} - T_\infty$$

It should also be noted that the model shows inlet ports to the reversing piston and that this is merely to achieve flexibility in the design simulation. For a sealed reversing piston, the inlet and outlet flow coefficient's would set to zero.

FIGURE O-2.

```
*       DSL-90 IMPLANTABLE POWER SUPPLY SIMULATION
*            P.QUILICI - W.TAMAI
*
INCON ICPH  =  66.6, ICT1  = 200.0, ICT2  = 200.0, ICT3  = 200.0,     ...
      ICPC  =  66.6, ICT14 = 150.0, ICT15 = 150.0, ICT5  = 200.0,     ...
      ICT6  = 200.0, ICT7  = 200.0, ICT8  = 200.0, ICT9  = 360.0,     ...
      ICT10 = 680.0, ICT11 = 360.0, ICT12 = 680.0, ICT13 = 150.0,     ...
      ICT16 = 150.0, ICT17 = 310.0, ICT18 = 310.0, ICT19 = 150.0,     ...
      ICT20 = 150.0, ICT21 = 113.0, ICP23 =  66.6, ICT23 =  75.0
INCON ICP24 =  66.6, ICT24 =  75.0, ICT22 =  75.0, ICT25 =  75.0,     ...
      ICT26 =  75.0, ICXOUT=  50.0, ICX   =   0.0, ICT34 = 309.0,     ...
      ICT36 = 497.0, ICT38 = 685.0, ICT40 = 532.0, ICT42 = 344.0,     ...
      ICT33 = 309.0, ICT35 = 497.0, ICT37 = 685.0, ICT39 = 532.0,     ...
      ICT41 = 344.0, ICT31 = 150.0, ICT28 = 203.0, ICT29 = 209.0,     ...
      ICT30 = 215.0, ICQH  =   0.0, ICT4 = 200.0 ,ICQOUT= 0.0
PARAM CPG   = 1.240, KG    =3.24E-6,GAM   = 1.66 , R     = 4640.,     ...
      TDPH  = 0.020, CPDP  = 0.11 , RHODP = 0.28 , SIGMA =3.31E-14,   ...
      SH5T2 = 0.00 , SH5T4 = 0.00 , DDP   = 1.303, DC    =1.3430,     ...
      TWALL = 0.010, CPW   = 0.11 , RHOW  = 0.282, KW    =1.51E-4,    ...
      LP    = 2.5  , DELTAP= 0.001, KDP   =1.51E-4,TDPW  =0.005  ,    ...
      KROD  =1.51E-4,DROD  = 0.125, LROD  = 2.0  , TCYB  =0.030
PARAM RHOROD= 0.282, CPROD = 0.11 , DRP   = 0.36 , LRP   =2.5    ,     ...
      LRPC  = 6.25 , DELRP = 0.001, KRP   =1.51E-4,TRPC  =0.010  ,     ...
      DRPC  = 0.40 , RHORP = 0.282, CPRP  = 0.11 , RHORPC =0.282 ,     ...
      CPRPC = 0.11 , MPRP  = 0.10 , DEMS  =7.4E-6, RO    =0.125  ,     ...
      G     =386.0 , VIS   =1.85E-6,LT    = 5.0  , A     =0.354
PARAM AH    =0.165 , LH    = 1.5  , RHOH  = 0.282, CPH   = 0.11 ,     ...
      HH    =2.78E-4,DEH   = 0.164, PERH  = 165.0, PHG   =3.454 ,     ...
      LHG   = 1.5  , AHG   =0.1355, CPHG  = 1.24 , AR    =0.312,      ...
      LP    = 1.2  , RHOR  =0.001 , CPR   =  0.11, KR    =5.48E-5,    ...
      PRG   = 25.6 , LRG   =1.2   , ARG   =  0.25, CPRG  =1.24  ,     ...
      AEH   =0.1355, LEH   =1.50  , DEP   =  0.25, AEP   =0.049
PARAM LEPH  = 1.0  , DER   =0.030 , AER   =  0.25, LER   =1.2   ,     ...
      LEPC  = 3.0  , DECV  =0.25  , AECV  = 0.049, LECV  = 50.0 ,     ...
      U1    = 0.1  , U2    =0.1   , PHPBAR= 73.3 , PLPBAR= 60.0 ,     ...
      PUI   = 0.0  , TLP   =  0.0, I     = 1.03 , TO    =1860. ,     ...
      TINF  = 560. , TBEAT = 0.6  , TS    =  100., F     = 0.05 ,     ...
      G6    = 0.001, FF    = 2.50 , OMEGA = 420. , KLS   =1.51E-4
PARAM ALS   = 0.01 , LLS   = 1.00 , ADP   = 1.33 , AROD  =0.0123,     ...
      ARP   =0.102 , AT    = 0.049, HHG   =8.6E-5, HRG   =3.62E-4,     ...
      K20   = 5.0E-8,LAMBDA=0.0   , THP   = 150.0,  JAY=9238.0
PARAM TIME=0.0
CONTRL DELT=0.00001,FINTIM=0.0300
PARAM GATE=1,INDEX=0
INTGER GATE,INDEX
PRINT 0.0006,TIME,PH,T1,T2,T3,T4,PC,T14,T15,T5,T6,T7,T8,T9,T10,T11,  ...
      T12,T13,T17,T18,T19,T20,WPL,P23,T23,P24,T24,T26,XOUT,X,W1,W2,   ...
      W3,W4,T34,T36,T38,T40,T42,    T33,T35,T37,T39,T41,T31,T28,T29,  ...
      T30,QH,WLS
NOSORT
      GO TO (100,200),GATE
*
*       DUMMY CONSTANTS
*
 100  GATE=2
```

FIGURE O-2. (Continued)

```
PI=3.141527
B12=3.0*CPG/ADP*JAY
C1=3.0*KG*ADP
C2=2.0*C1
C3=0.6666667*PI*KG/0.350
B8=1.0/CPG
B10=(GAM-1.0)/3.0
B11=ADP/R
B9=3.0*R/ADP
B7=2.0*CPG/(ADP-AROD)*JAY
C19=2.0*KG*ADP
C18=2.0*C19
C20=PI*KG/0.350
B1=(GAM-1.0)/2.0
B2=(ADP-AROD)/R
B3=2.0*R/(ADP-AROD)
E2=1.0/(ADP*TDPH*CPDP*RHODP)
C15=CPG
C7=4.0*SIGMA*PI*DDP*SH5T2
C8=4.0*SIGMA*ADP*SH5T4
E1=3.0/(PI*DC*TWALL*CPW*RHOW)
C4=6.0*KW*PI*DC*TWALL
C5=0.5*C4
C6=0.5/E1
C9=2.0*C6
C10=C4
C11=C9*3.0*LP
E3=3.0/C11
C14=KG*PI*DDP*LP/(3.0*DELTAP)
C17=C9
C12=6.0*KDP*PI*DDP*TDPW/LP
E4=3.0/(PI*DDP*TDPW*RHODP*CPDP*LP)
E5=1.0/(ADP*TDPH*RHODP*CPDP)
C24=2.0*KROD*AROD/LROD
E6=1.0/(ADP*TCYB*RHOW*CPW)
C25=KLS*ALS/LLS
C21=4.0*PI*DC*TWALL*KW
C16=KG*PI*DDP*LP/(3.0*DELTAP)
C31=(1.0-0.666667*LP)*PI*DC*TWALL*RHOW*CPW
E7=2.0/(PI*DC*TWALL*RHOW*CPW)
C22=2.0*KW*PI*DC*TWALL
C23=PI*DC*TWALL*RHOW*CPW/4.0
E8=1.0/(AROD*RHOROD*CPROD*LROD)
C26=2.0*KG*ARP
C28=2.0*PI*KG/0.350
B20=GAM-1.0
B21=(ARP-AROD)/R
B22=CPG/(ARP-AROD)*JAY
B23=R/(ARP-AROD)
B24=CPG/ARP*JAY
B25=ARP/R
B26=R/ARP
E9=0.5/(ARP*TDPH*RHORPC*CPRPC)
E10=1.0/(ARP*TCYB*RHORPC*CPRPC)
C13=3.0*KDP*PI*DDP*TDPW/LP
C27=KG*PI*DRP*LRP/(2.0*DELRP)
C29=2.0*KRP*PI*DRPC*TRPC/LRPC
C30=PI*DRPC*TRPC*LRP*RHORPC*CPRPC/2.0
G1=ADP
```

```
      G2=(ADP-ARDD)
      G4=(ARP-ARDD)
      G5=ARP
      K1=PI*DELTAP**3*G*DDP*DENS/(8.0*VIS)
      K4=PI*DDP*DELTAP/R
      K5=SQRT(RO)*G*DELRP**3/(6.64*VIS*R)
      K6=3.404*RO*DELRP*(LT/AT)
      K7=K5*6.64/4.70
      K8=LRP/2.0-RO
      K9TRM1=LRP/2.0-A-RO
      K9TRM2=LRP/2.0+A-RO
      K9=K7*(1.0/K9TRM1+1.0/K9TRM2)
      K10=K7*(1.0/K9TRM1-1.0/K9TRM2)
      G10=1.0/(AH*LH*RHOH*CPH)
      G11=3.0*R/(AHG*LHG*CPHG)
      G12=5.0/(AR*LR*RHOR*CPR)
      G13=5.0*R/(ARG*LRG*CPRG)
      G14=(DEH**2*G*AEH)/(32.0*R*LEH*VIS)
      G15=(DEP**2*G*AEP)/(32.0*R*LEPH*VIS)
      G16=(DER**2*G*AER)/(32.0*R*LER*VIS)
      G17=(DEP**2*G*AEP)/(32.0*R*LEPC*VIS)
      G18=(DECV**2*G*AECV)/(32.0*R*LECV*VIS)
      HTRHS=HH*PERH*LH
      HTRH=HHG*PHG*LHG
      HTRHG=HHG*PHG*LHG/3.0
      WHG=CPHG/2.0
      KK=5.0*KR*AR/LR
      REGR=HRG*PRG*LRG/5.0
      REGRG=HRG*PRG*LRG/5.0
      WRG=CPRG/2.0
  200 CONTINUE
SORT
*
*     DISPLACER PISTON EQUATIONS
*
      DPH=     INTGRL( 0.0,B12*Y9/(L-X))
      PH=ICPH+DPH
      T1=INTGRL(ICT1,-B9*(T0-T1)/(PH*(L-X))*(Q1+Y9+Y2-Y7*RHO(Y5)))
      T2=INTGRL(ICT2,-B9*((T0-T2)/(PH*(L-X))*(Q2+Y9+Y7*PSI(Y5)          ...
                                                -Y8*RHO(Y6))))
      T3=INTGRL(ICT3,-B9*(T0-T3)/(PH*(L-X))*(Q3+Y9+Y4+Y8*PSI(Y5)))
      T4=INTGRL(ICT4,-E6*(E1T4-E4T5-E4T6-E4T7-E4T8))
      DPC=     INTGRL( 0.0,B7*Y19/(L+X))
      PC=ICPC+DPC
      T14=INTGRL(ICT14,B3*(T14+TINF)/(PC*(L+X))*(Q14+Y19+Y12            ...
                                                      -Y18*RHO(Y17)))
      T15=INTGRL(ICT15,B3*(T15+TINF)/(PC*(L+X))*(Q15+Y19+Y14+Y15        ...
                                              +Y16A+Y16C-Y18*PSI(Y17)))
      T5=INTGRL(ICT5,-E2*(E5+E3T5-E5T6-E5T7-E5T8+E4T5))
      T6=INTGRL(ICT6,-E1*(E4T6+E1T6-E6T7)/(L-X))
      T7=INTGRL(ICT7,-E1*(E4T7+E5T7+E6T7-E7T8)/(L-X))
      T8=INTGRL(ICT8,-E1*(E4T8+E5T8+E7T8-E8T9)/(L-X))
      T9=INTGRL(ICT9,-E3*(E8T9-E9T11-E9T10))
      T10=INTGRL(ICT10,-E3*(E9T10-E10T12-E10T17))
      T11=INTGRL(ICT11,-E4*(E5T11+E9T11-E11T12))
      T12=INTGRL(ICT12,-E4*(E11T12+E10T12-E12T18))
      T13=INTGRL(ICT13,E5*(E13-E13T14-E13T18-E13T21))
      T16=INTGRL(ICT16,E6*(E15T16-E16T26-E16T20))
      T17=INTGRL(ICT17,E3*(E10T17-E17T18-E17T19))
```

FIGURE O-2. (Continued)

```
      T18=INTGRL(ICT18,E4*(E12T18+E13T18+E17T18))
      T19=INTGRL(ICT19,E7*(E17T19+E14T19-E19T20)/(L+X))
      T20=INTGRL(ICT20,E7*(E19T20+E15T20+E16T20)/(L+X))
      T21=INTGRL(ICT21,E8*(E13T21-E21T22))
      WPL=K1*(ICPH-ICPC+DPH-DPC)+K4*PH*XDOT/(T0+TINF+T13-T15)
*
*     REVERSING PISTON EQUATIONS
*
      DP23=      INTGRL( 0.0 ,B22*Y30/(LRPC-X))
      P23=ICP23+DP23
      T23=INTGRL(ICT23,B23*(T23+TINF)/(P23*(LRPC-X))*(Q23+Y21+Y23     ...
                                                      +Y25+Y15C))
      DP24=      INTGRL( 0.0 ,B24*Y31/(LRPC+X))
      P24=ICP24+DP24
      T24=INTGRL(ICT24,B26*(T24+TINF)/(P24*(LRPC+X))*(Q24+Y23A+Y27+Y29))
      T22=INTGRL(ICT22,E9*(E21T22-E22T23-E22T25-E22T26))
      T25=INTGRL(ICT25,E10*(E24T25-E25T26+E22T25))
      T26=INTGRL(ICT26,E10*(E16T26+E22T26+E23T26+E25T26))
      XDOT=ICXDOT+INTGRL( 0.0 ,(-G1*PH+G2*PC-G4*P23+G5*P24            ...
                -GAMMA(XDOT)*(F+G6*XDOT)+FF*COS(OMEGA*TIME))*G/MPRP)
      X=INTGRL(ICX,XDOT)
      W1=(PHP+P23)*(PHP-P23)/(T22+TINF)*(GAMMA2+GAMMA4*ALTERM)
      W2=(P23+PLP)*(P23-PLP)/(T22+TINF)*(GAMMA3+GAMMA5*(2.0-ALTERM))
      W3=(PHP+P24)*(PHP-P24)/(T22+TINF)*(GAMMA3+GAMMA4*ALTERM)
      W4=(P24+PLP)*(P24-PLP)/(T22+TINF)*(GAMMA2+GAMMA4*ALTERM)
      ALTERM=ALPHA1(X,A)
      WDIL=(P24+P23)*(ICP24-ICP23+DP24-DP23)/                          ...
                                    (T22+TINF)*(K10+K9*BETA(X,A))
*
*     DUMMY DISPLACER PISTON EQUATIONS
*
      Y1=-WR*(T0-T1)+Y2
      Y2=-WR*(T1-T27)*RHO(WR)
      Y3=-WPL*(T0-T3)+Y4
      Y4=-WPL*(T3-T5)*RHO(WPL)
      F1T2=C1*(T2-T1)/(L-X)
      F1T4=C2*(T4-T1)/(L-X)
      F1T6=C3*(T6-T1)*(L-X)
      Q1=-B8*(F1T2+F1T4+F1T6)
      F2T7=C3*(T7-T2)*(L-X)
      F2T3=C1*(T3-T2)/(L-X)
      Q2=-B8*(F2T7+F2T3-F1T2)
      F3T5=C2*(T5-T3)/(L-X)
      F3T8=C3*(T8-T3)*(L-X)
      Q3=-B8*(F3T5+F3T8-F2T3)
      YH=Q1+Q2+Q3+Y1+Y3
      Y9=B10*(YH+B11*PH*XDOT)
      Y5=Y1+Q1-YH/3.0
      Y6=-Y3-Q3+YH/3.0
      Y7=Y5*(T1-T2)/(T0-T1+(T2-T1)*RHO(Y5))
      Y8=Y6*(T3-T2)/(T0-T3+(T3-T2)*PSI(Y6))
      Y11=WPL*(T14+TINF)+Y12
      Y12=WPL*(T13-T14)* PSI(WPL)
      Y13=WR*(T15+TINF)+Y14
      Y14=WR*(T43-T15)*PSI(WR)
      Y15=WLP*(T15+TINF)+Y15A
      Y15A=WLP*(TLP-T15)*PSI(WLP)
      Y16=-WHP*(T15+TINF)+Y16A
      Y16A=-WHP*(THP-T15)*RHO(WHP)
```

FIGURE O-2. (Continued)

```
Y16B=-WLS*(T23+TINF)+Y16C
Y16C=-WLS*(T15-T23)*PSI(WLS)
WLS=K20*(PC-P23)
F14T19=C20*(T14-T19)*(L+X)
F14T15=C19*(T14-T15)
F13T14=C19*(T13-T14)
Q14=-B8*(F14T19+F14T15-F13T14)
F15T16=C18*(T15-T16)
F15T20=C20*(T15-T20)
Q15=-B8*(F15T16+F15T20-F14T15)
YC=Y11+Y13+Y15+Y16+Y16B+Q14+Q15
Y19=B1*(YC-B2*PC*XDOT)
Y17=Y11+Q14-YC/3.0
Y18=Y17*(T15-T14)/(T14+TINF+(T15-T14)*RHO(Y17))
F5=C15*WPL*(T5-T3)*PSI(WPL)
TCUBE1=(T0-T5)**3*(L-X)*C7
F5T6=TCUBE1*(T6-T5)
F5T7=TCUBE1*(T7-T5)
F5T8=TCUBE1*(T8-T5)
F4T5=C8*(T0-T5)**3*(T5-T4)
TCUBE2=C7*(T0-T4)**3*(L-X)
F4T6=C4*(T6-T4)/(L-X)+TCUBE2*(T6-T4)
F6T7=C5*(T7-T6)/(L-X)+C6*(T7-T6)*XDOT
F4T7=TCUBE2*(T7-T4)
F7T8=C5*(T8-T7)/(L-X)+C9*(T8-T7)*XDOT
F4T8=TCUBE2*(T8-T4)
F8T9=(C10+C11*XDOT)*(T9-T8)/(L-X+LP)
F9T11=C14*(T11-T9)
F9T10=(C5+C17*XDOT)*(T10-T9)
F10T12=C14*(T12-T10)
F10T17=(C5+C17*XDOT)*(T0-TINF-T10)-C5*T17-C17*XDOT*T18
RTRM1=C15*WPL*(1.0-2.0*RHO(WPL))
F5T11=(C12+RTRM1)*(T11-T5)
F11T12=(C13+RTRM1)*(T12-T11)
F12T18=(C13+RTRM1)*(T0-TINF-T12-T18)
F13=-WPL*C15*(T14-T13)*RHO(WPL)
F13T18=(C12+RTRM1)*(T13-T18)
F13T21=C24*(T13-T21)
F16T26=C25*(T16-T26)
F16T20=C21*(T16-T20)/(L+X)
F17T18=C16*(T17-T18)
F17T19=(C21+C31*XDOT)*(T17-T19)/(L+X+0.666667*LP)
F19T20=(C22/(L+X)+C23*XDOT)*(T19-T20)
F21T22=C24*(T21-T22)
F22T23=C26*(T22-T23)/(LRPC-X)
F23T26=(C28*(LRPC-X)+C26/(LRPC-X))*(T23-T26)
F22T24=C26*(T22-T24)/(LRPC+X)
F24T25=(C28*(LRPC+X)+C26/(LRPC+X))*(T24-T25)
Q23=-B8*(F22T23-F23T26)
Q24=-B8*(F22T24-F24T25)
Y20=W1*(T23+TINF)+Y21
Y21=W1*(THP-T23)*PSI(W1)
Y22=-WUL*(T23+TINF)+Y23
Y23=-WUL*(T24-T23)*RHO(WUL)
Y23A=WUL*(T23-T24)*PSI(WUL)
Y24=-W2*(T23+TINF)+Y25
Y25=-W2*(TLP-T23)*RHO(W2)
Y26=W3*(T24+TINF)+Y27
Y27=W3*(THP-T24)*PSI(W3)
```

FIGURE O-2. (Continued)

```
      Y28=-W4*(T24+TINF)+Y29
      Y29=-W4*(TLP-T24)*RHO(W4)
      YU=Y20+Y22+Y24+Y16B+Q23
      Y30=B20*(YU+B21*P23*XDOT)
      YL=Y26+Y28+Y22+Q24
      Y31=B20*(YL-B25*P24*XDOT)
      F22T25=C27*(T22-T25)
      F22T26=C27*(T22-T26)
      F25T26=(C29+C30*XDOT)*(T25-T26)
      GAMMA1=GAMMA(X,A)
      GAMMA2=K5/SQRT(ABS(X-A)+K6)
      GAMMA3=K5/SQRT(ABS(X+A)+K6)
      GAMMA4=K7/SQRT(K8-X)
      GAMMA5=K7/SQRT(K8+X)
*
*     REGENERATOR EQUATIONS
*
      T34=INTGRL(ICT34,-G12*(KR*(T34-T36)+REGR*(T34-T33)))
      T36=INTGRL(ICT36,-G12*(KR*(2.0*T36-T34-T38)+REGR*(T36-T35)))
      T38=INTGRL(ICT38,-G12*(KR*(2.0*T38-T36+T40-T0+TINF)                ...
                                +REGR*(T38-T37)))
      T40=INTGRL(ICT40,G12*(KR*(T0-T38+T42+TINF-2.0*(T40+TINF))          ...
                                +REGR*(T39-T40)))
      T42=INTGRL(ICT42,G12*(KR*(T40-T42)+REGR*(T41-T42)))
      T33=INTGRL(ICT33,-G13*(T0-T33)/PH*(REGRG*(T33-T34)                 ...
                                +WRG*WR*(T33+T35-2.0*T32)))
      T35=INTGRL(ICT35,-G13*(T0-T35)/PH*(REGRG*(T35-T36)                 ...
                                +WRG*WR*(T37-T33)))
      T37=INTGRL(ICT37,-G13*(T0-T37)/PH*(REGRG*(T37-T38)                 ...
                                +WRG*WR*(T0-T35-T39-TINF)))
      T39=INTGRL(ICT39,G13*(T39+TINF)/PH*(REGRG*(T40-T39)                ...
                                +WRG*WR*(T0-T37-T41-TINF)))
      T41=INTGRL(ICT41,G13*(T41+TINF)/PH*(REGRG*(T42-T41)                ...
                                +WRG*WR*(T39+T41-2.0*T43)))
      T43=(1.5*T41-0.5*T39)*PSI(WR)+T15*RHO(WR)
      WR=(ICPH-ICPC+DPH-DPC)*PH/((T0-T29)/G14+(T0-T33)/G15               ...
                                +(T0-T37)/G16+(T41+TINF)/G17)
*
*     HEATER EQUATIONS
*
      T31=INTGRL(ICT31,-G10*(HTRHS*(T31-TS)+HTRH*(3.0*T31-T29-T29-T30)))
      T29=INTGRL(ICT29,-G11*((T0-T29)/PH*(HTRHG*(T29-T31)                ...
                                -WHG*WR*(2.0*T27-T28-T29))))
      T28=INTGRL(ICT28,-G11*((T0-T28)/PH*(HTRHG*(T28-T31)                ...
                                -WHG*WR*(T28-T30))))
      T30=INTGRL(ICT30,-G11*((T0-T30)/PH*(HTRHG*(T30-T31)                ...
                                -WHG*WR*(T30+T29-2.0*T32))))
      T27=T1*PSI(WR)+(1.5*T28-0.5*T29)*RHO(WR)
      T32=(1.5*T30-0.5*T29)*PSI(WR)+LAMBDA*QH+(1.5*T33-0.5*T35)*RHO(WR)
      QH=INTGRL(ICQH,WR*CPG*(T27-T32)+LAMBDA*QOUT)
      QOUT=INTGRL(ICQOUT, WHP*CPG*(T15-TLP)-CPG*(THP-TLP)*(W1+W2))
*
*     HIGH AND LOW PRESSURE RESERVOIRS
*
      WHP=G18*PC/(T15+TINF)*(PL-PHP)*(PSI(PC-PHP-U1)*PSI(PC-PHP)         ...
                                +RHO(PHP-PC-U2)*RHO(PC-PHP))
      WLP=G18*PC/(TLP+TINF)*(PLP-PC)*(PSI(PLP-PC-U1)*PSI(PLP-PC)         ...
                                +RHO(PC-PLP-U2)*RHO(PLP-PC))
      PHP=PHPBAR+PHI*ETAL(TIME,TBEAT)
```

```
      PLP=PLPBAR+PHI*ETA2(TIME,TBEAT)
END
CONTIN
CONTRL FINTIM=0.0600
END
CONTIN
CONTRL FINTIM=0.0900
END
CONTIN
CONTRL FINTIM=0.1200
END
STOP
$IBFTC TIME.   M94,XR7,NOLIST
      SUBROUTINE TIME1(X)
      RETURN
      ENTRY TIME2(X)
      RETURN
      END
$IBFTC SPEC.   M94,XR7,NOLIST
      FUNCTION SPEC(X,A)
C
C     SPECIAL FUNCTIONS FOR DSL-9C IMPLANTABLE POWER SUPPLY SIMULATION
C
      ENTRY RHO(A)
      IF(A) 102,101,101
C
      ENTRY PSI(A)
      IF(A) 101,102,102
C
      ENTRY GAMMA(A)
      IF(A) 100,100,102
C
      ENTRY ALPHA1(X,A)
      IF(X.GT.A) GO TO 103
      IF(X.LT.-A) GO TO 101
      GO TO 102
C
      ENTRY BETA(X,A)
      IF(X.GT.-A .AND. X.LT.A) GO TO 102
      GO TO 101
C
  100 SPEC=-1.0
      GO TO 110
  101 SPEC=0.0
      GO TO 110
  102 SPEC=1.0
      GO TO 110
  103 SPEC=2.0
      GO TO 110
C
      ENTRY ETA1(X,T)
      C=1.0
  200 TV=X-FLOAT(IFIX(X/T))*T
      IF(TV.LT.T/3.0) GO TO 210
      SPEC=C*(5.0*T-2.0)
      GO TO 110
  210 SPEC=C*(1.0-10.0*T)
      GO TO 110
C
```

FIGURE O-2. (Continued)

```
      ENTRY ETA2(X,T)
      C=-1.0
      GO TO 200
C
  110 RETURN
      END
```

TABLE 0-1

NOMENCLATURE

Symbol	Definition
A	Cross sectional or surface area
C	Flow coefficient
C_p	Specific heat at constant pressure
F	Radiation shape factor
F_f	Sliding friction force
h	Convective heat transfer coefficient
k	Thermal conductivity
L	Length
m	Mass
N	Number of nodes
P	Pressure
f	Heat flow
R	Gas constant
T	Gas temperature
T_W	Wall temperature
V	Volume
w	Flow rate
W	Accumulated flow
X	Piston displacement
θ	Time
ρ	Density
σ	Stephan-Boltzmann constant
FORTRAN	
A	Distance of reversing chamber ports from midstroke
ADP	Displacer piston cross-sectional area
AFCV	Check valve free flow area at full open
AFH	Heater free flow area
AFP	Regenerator piping free flow area
AFR	Regenerator free flow area
AH	Heater wall cross-sectional area

Table 1 - Continued

Symbol	Definition
AHG	Heater gas cross-sectional area
ALS	Labryinth seal length
AR	Regenerator matrix cross-sectional area
ARG	Regenerator gas cross-sectional area
AROD	Connecting rod cross-sectional area
ARP	Reversing piston cross-sectional area
AT	Cross-sectional area of reversing piston tubing
CPDP	Displacer piston specific heat
CPG	Gas specific heat at constant pressure
CPH	Heater wall specific heat
CPHG	Heater gas specific heat at constant pressure
CPR	Regenerator matrix specific heat
CPRG	Regenerator gas specific heat
CPROD	Connecting rod specific heat
CPRP	Reversing piston specific heat
CPRPC	Reversing piston chamber wall specific heat
CPW	Displacer piston chamber wall specific heat
DC	Displacer piston chamber diameter
DDP	Displacer piston diameter
DECV	Equivalent hydraulic diameter of check valve
DEH	Equivalent hydraulic diameter of heater
DELRP	Reversing piston radial clearance
DELTP	Displacer piston radial clearance
DENS	Gas density
DEP	Equivalent hydraulic diameter of regenerator piping
DER	Equivalent hydraulic diameter of regenerator
DROD	Connecting rod diameter
DRP	Reversing piston diameter
DRPC	Reversing piston chamber diameter
F	Piston sliding friction force
FF	Forcing function
G	Gravitational acceleration
GG	Piston aerodynamic drag coefficient

(Table 1 - continued)

Symbol	Definition
GAM	Gas psecific heat ratio
HHI	Source to heater heat transfer coefficient
HHG	Heater to gas heat transfer coefficient
HRG	Regenerator to gas heat transfer coefficient
ICxxx	Initial condition of the parameter xxx
JAY	Conversion factor 9336 in-lb/Btu
K20	Labryinth seal leakage flow coefficient
KDP	Displacer piston thermal conductivity
KG	Gas thermal conductivity
KLS	Labryinth seal material thermal conductivity
KR	Regenerator matrix thermal conductivity
KROD	Connecting rod thermal conductivity
KP	Displacer piston thermal conductivity
L	Displacer piston chamber length from midstroke
LAMBDA	Dummy constant equal to zero
LECV	Check valve equivalent length
LEH	Heater equivalent length
LEPC	Regenerator to cold chamber pipe equivalent length
LEPH	Regenerator to heater pipe equivalent length
LER	Regenerator equivalent length
LH	Heater length exposed to source
LHG	Heater length exposed to gas
LLS	Labryinth seal length
LP	Displacer piston length
LR	Regenerator matrix length
LRG	Regenerator gas length
LROD	Connecting rod length
LRP	Reversing piston length
LRPC	Reversing piston chamber length from midstroke
LT	Reversing piston tubing length
MPRP	Mass of piston assembly
OMEGA	Cycle time of forcing function
Pn, n = 1,2 ...	Pressure of node
PC	Cold chamber pressure

(Table 1- continued)

Symbol	Definition
PERH	Heater perimeter exposed to the source
PH	Hot chamber pressure
PHG	Heater gas wetted perimeter
PHI	Gas reservoir pressure excursion value
PHPBAR	Average high pressure reservoir pressure
PLPBAR	Average low pressure reservoir pressure
PRG	Regenerator gas wetted perimeter
QH	Heat flow from heater to gas
QOUT	Available gross output power
R	Gas constant
RHODP	Displacer piston material density
RHOH	Heater wall material density
RHOR	Regenerator matrix material density
RHOKOD	Connecting rod material density
RHORP	Reversing piston material density
RHORPC	Reversing piston chamber material density
RHOW	Displacer piston chamber wall material density
RO	Reversing chamber part diameter
SH5T2	Radiation shape factor from node 5 to 2
SH5T4	Radiation shape factor from node 5 to 4
SIGMA	Stephan-Boltzmann radiation constant
T_n, n = 1,2....	Temperature of node n
TBEAT	Cycle time of pumping chamber
TCYB	Thickness of displacer piston chamber base
TDPH	Thickness of displacer piston head
TDPW	Thickness of displacer piston wall
THP	High pressure reservoir gas temperature
TIME	Time
TINF	Lower reference temperature
TLP	Low pressure reservoir gas temperature
TO	Upper reference temperature
TRPC	Thickness of reversing piston chamber wall

(Table 1 - continued)

Symbol	Definition
TS	Temperature of the heat source
TWALL	Thickness of displacer piston chamber wall
U1	Pressure differential required to open check valve
U2	Pressure differential required to close check valve
VIS	Gas viscosity
W1	Flow into upper reversing chamber
W2	Flow out of upper reversing chamber
W3	Flow into lower reversing chamber
W4	Flow out of lower reversing chamber
WLS	Labryinth seal leakage
WPL	Displacer piston leakage
X	Piston displacement from midstroke
XDOT	Piston velocity

APPENDIX P

ESTIMATE OF STEAM ENGINE PERFORMANCE

A. GENERAL

The steam Rankine cycle consists of an isentropic compression of feed water to boiler pressure, constant pressure heating (vaporization) in the boiler, isentropic expansion of the vapor, and constant pressure cooling (condensation) in a condenser. This ideal cycle is illustrated in Figure P-1, where the dotted sections of the T-S and P-V diagrams correspond to a superheat cycle. Although superheat complicates the radioisotope boiler design, it increases the cycle efficiency somewhat and is highly desirable to minimize expander thermodynamic losses and erosion caused by moisture formation in turbine expanders.

The Rankine cycle is generally applicable to both reciprocating engines and rotating expanders although the requirements of a particular application may dictate the use of one or the other. Turbine efficiency decreases rapidly at low power levels due to the effect of low exhaust volumetric flow rates, and the limitations on turbine fabrication techniques and rotational speed. Reciprocating steam engines have considerably higher expander efficiencies in low power application and, providing that the engine can ultilize steam at conditions comparable to modern turbine usage, higher overall thermodynamic efficiencies can be achieved. Figure P-2 shows an estimate of turbine and steam engine efficiency as a function of power output[1]. Although such a comparison depends on specific steam conditions, it is clear that a higher efficiency can be achieved from a reciprocating steam engine at the few-watt power output.

---

(1) H. R. Kroeger and J. Grey, "A Steam-Cycle Power Plant for High-Power Communications Satellites", Advanced Energy Conversion, 4, 51 (1964).

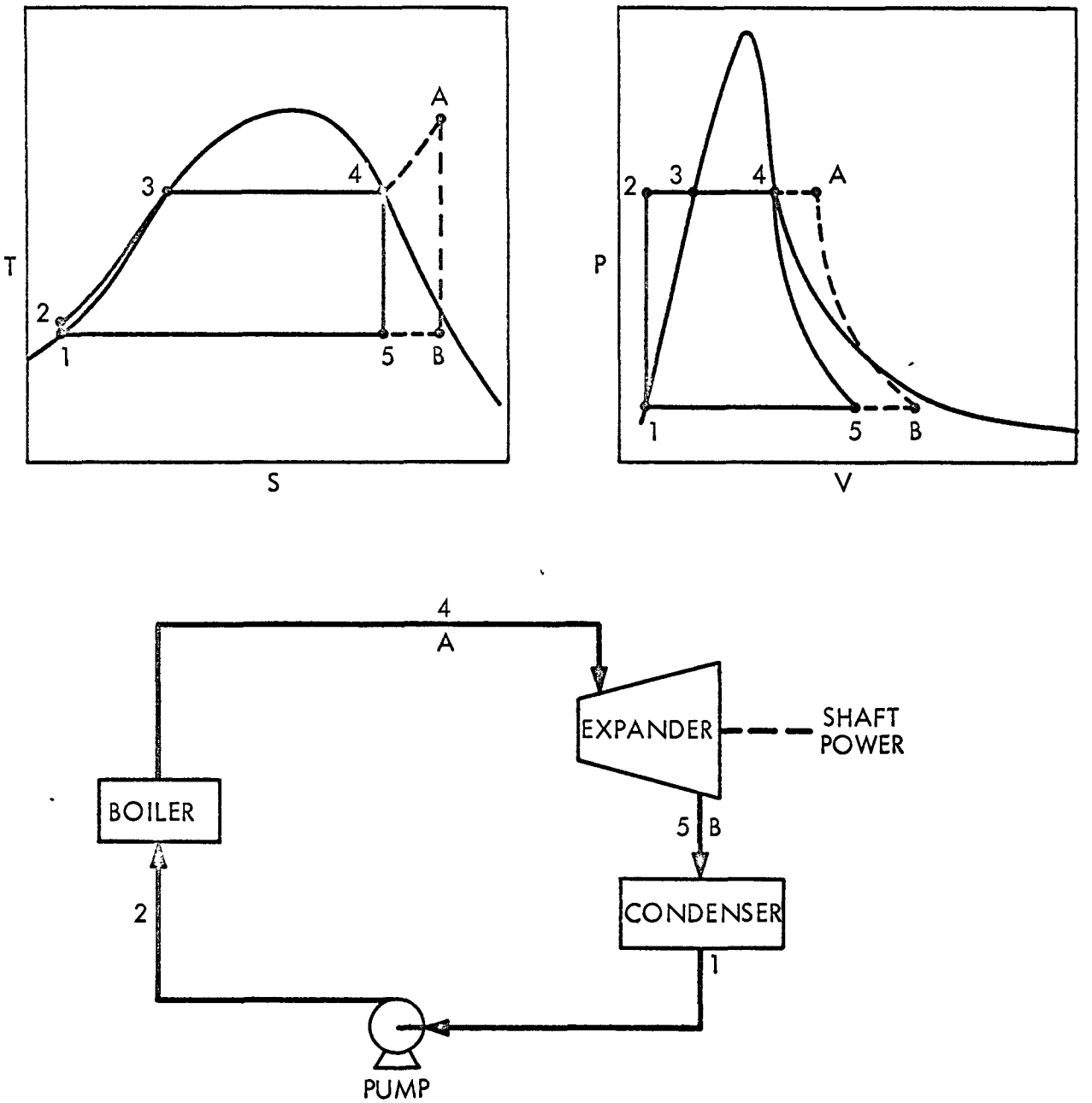

FIGURE P-1. RANKINE CYCLE

3.01-68-054

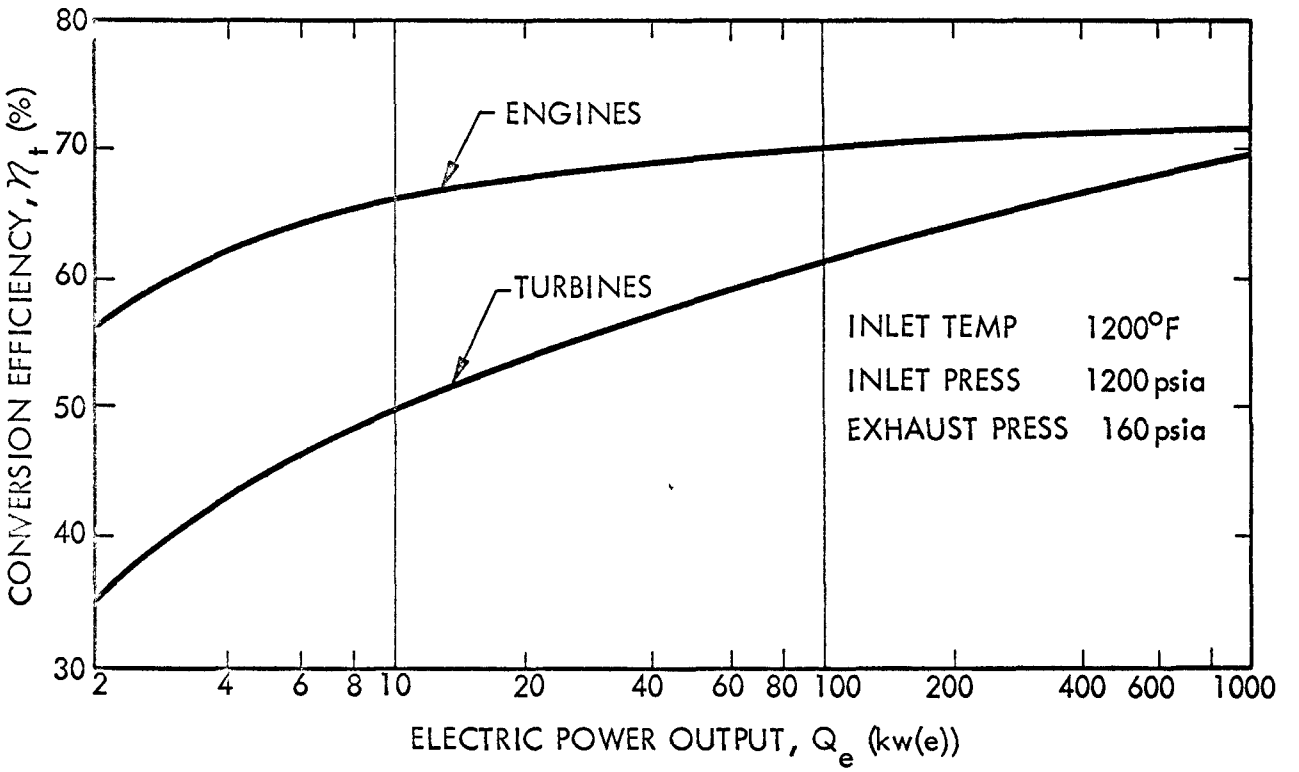

FIGURE P-2. ESTIMATED STEAM TURBINE AND RECIPROCATING ENGINE EXPANDER EFFICIENCIES AS A FUNCTION OF POWER LEVEL

3.01-60-035

level required for the implantable power source application.

B. STEAM ENGINE EFFICIENCY LOSS MECHANISMS

Analyses were performed to determine the magnitude of the thermodynamic inefficiencies of a reciprocating steam engine suitable for use as an implantable power source for circulatory support systems. The results of these analyses serves as a basis for direct comparison with the modified Stirling engine design. Major thermodynamic losses due to clearance volume, recompression, initial condensation, and thermal conduction were calculated, and additional mechanical and thermodynamic losses were estimated to obtain an approximate value for the overall steam engine efficiency.

Figure P-3 is a pressure-volume diagram showing the various steam engine processes and sources of major thermodynamic losses. The area C-1-f-2-b represents the ideal work per stroke. The clearance volume loss, CVL, is defined as:

$$CVL = \frac{\text{AREA a-b-c-d}}{\text{AREA c-1-f-2-b}}$$

The compression loss, CL, is defined as:

$$CL = \frac{\text{AREA 3-a-4}}{\text{AREA c-1-f-2-b}}$$

The cylinder walls and other steam containment surfaces assume a mean temperature somewhere between the steam inlet temperature and the exhaust temperature due to the alternating flow of cold and hot steam over these surfaces. Steam which is admitted to the cylinder at throttle conditions transfers heat to the walls and is cooled or may be partially condensed depending on the initial state. This cooling process continues until the steam has expanded to the point where steam and wall temperature are equal (Process 1-e, Figure P-3). Expansion beyond this point causes a further decrease in steam temperature and heat is transferred from the walls to the steam (Process e-2", Figure P-3). The heat transfered to the walls is recovered at a lower temperature and, as a consequence, there is a net loss of energy availability (increase in entropy). Also, heat transferred to the steam during the exhaust stroke is lost. This loss mechanism involves only heat transfer from

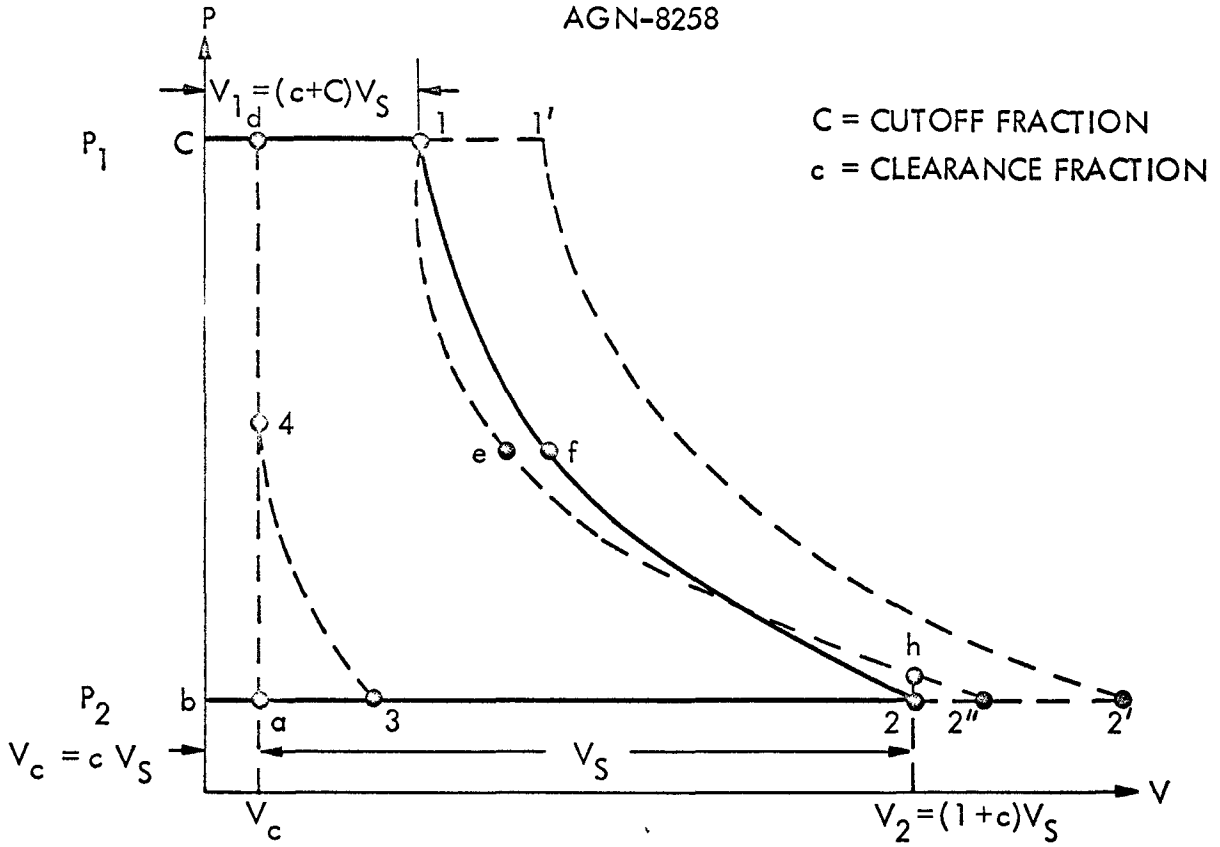

FIGURE P-3. P-V PROCESSES FOR STEAM ENGINE

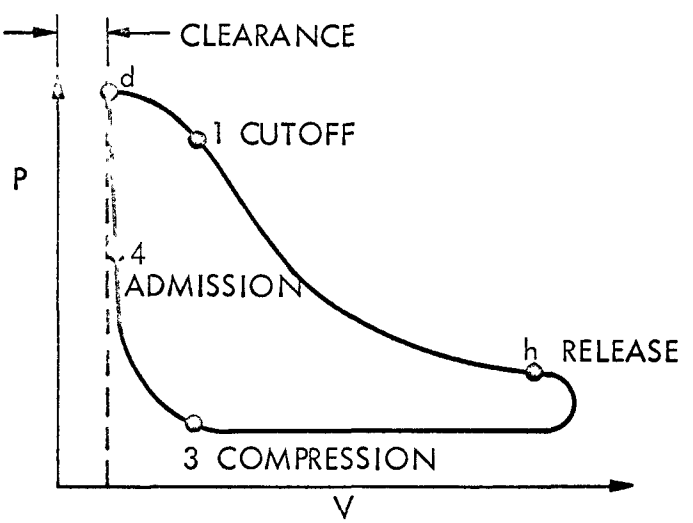

3.01-60-056

FIGURE P-4. P-V INDICATOR DIAGRAM FOR INCOMPLETE-EXPANSION ENGINE

the steam to the cylinder wall and back so external steam jackets or thermal insulation are ineffective in reducing the loss. The initial condensation loss, ICL, is defined as:

$$ICL = \frac{\text{AREA } 1\text{-}1'\text{-}2'\text{-}2\text{-}h\text{-}e}{\text{AREA } c\text{-}1'\text{-}2'\text{-}b}$$

An example of an indicator diagram for an incomplete-expansion engine shown in Figure P-4 illustrates the effect of throttling losses during intake and release. The intake ceases at 1, the point of cutoff, and expansion occurs from 1 to h. At h, the point of release, the exhaust valve opens. Point 3 is the point of compression, where the exhaust valve closes, and the trapped or cushion steam is compressed, with all valves closed, to 4, the point of admission. The intake valve opens at 4 just before the piston has reached the end of the stroke and the pressure increases rapidly to throttle pressure.

The following summarizes the losses previously described and additional losses which must be accounted for to obtain the overall engine efficiency:

1. Clearance volume
2. Recompression
3. Initial condensation and exhaust heat loss
4. Thermal conduction to surroundings
5. Mechanical friction (piston ring, bearing, valve mechanism)
6. Fluid friction - throttling
7. Steam leakage (valves, piston)

C. ENGINE THERMODYNAMIC LOSSES

Steam engine design characteristics and operating conditions used in the analysis of thermodynamic losses are summarized in Table P-1. The clearance fraction, c, is defined as the ratio of clearance volume to swept volume, or

$$c = \frac{V_c}{V_s} = \frac{0.009}{1.4775} = 0.0061$$

The cutoff fraction, c, is defined as

$$c = \frac{V_1 - V_c}{V_s} = \frac{0.0225 - 0.009}{1.4775} = 0.0091$$

That is, the percentage of the stroke at which the intake valve closes.

1. Clearance Volume Loss

Referring to Figure P-3, the clearance volume loss is

$$CVL = \frac{(P_1 - P_2)V_c}{P_1V_1 + \int_1^2 PdV - P_2V_2}$$

Making the proper substitutions, and using the approximation $P\,V^{1.0}$ = constant for the expansion process* from 1 to 2, CVL reduces to

$$CVL = \frac{C\left(\frac{1}{c+C} - \frac{1}{1+c}\right)}{\ln\left(\frac{1+c}{c+C}\right)} = 9.4\%$$

2. Recompression Loss

Referring to Figure P-3, the recompression loss is:

$$CL = \frac{\int_4^3 PdV - P_2\,(V_3 - V_a)}{P_1V_1 + \int_1^2 PdV - P_2V_2}$$

Again taking PV = constant, and letting the fraction of the exhaust stroke at which compression starts be:

$$\frac{V_3}{V_s} = x$$

the recompression loss is then:

$$CL = \frac{(c+x)\ 1\left(\frac{c+x}{c}\right) - x}{(1+c)\ \ln\ \left(\frac{1+c}{c+C}\right)}$$

* V. M. Faires, Applied Thermodynamics, P. 311, The MacMillian Company, New York, 1949.

TABLE P-1 - STEAM ENGINE DESIGN PARAMETERS

Cylinder bore (B), in.	0.75
Stroke (2R), in.	1.4775
Crank throw (R), in.	0.739
Connecting rod length (L), in.	2.5
Speed (N), rpm	600
Swept volume (V_s), in^3	0.652
Clearance length*, in	0.009
Steam inlet pressure, psia	400
Steam inlet temperatue, ^oF	900
Exhaust pressure, psia	3
Release pressure, psia	6
Expansion ratio	66.7
Cutoff point (V_1)**, in.	0.0225

* Includes actual piston clearance length plus clearance length based on bore diameter, which is equivalent to valve clearance volume.

** Measured from cylinder head

assuming that the compression point has the same location as the cutoff point, 0.0225 in. from cylinder head, x = 0.0152, and the recompression loss is 0.26%.

3. Heat Transfer Losses

Heat transfer losses include those due to heat interchange between the steam and containment surfaces (initial condensation and exhaust loss) and thermal conduction losses to the environment through the piston connecting rod and cylinder walls. An exact determination of the instantaneous cylinder wall energy change is difficult because steam temperature, wall temperature, and heat transfer area are all time dependent, and the heat transfer mechanism in the cylinder is quite complex.

The relation between crank angle, θ, and piston displacement from top dead center, y, for a reciprocating engine is given by:

$$y = R - R \cos \theta + \frac{R^2}{2L} \sin^2 \theta$$

and the total cylinder volume, V (including the clearance volume V_c), is then:

$$V = V_c + \frac{\pi B^2}{4} \left[R - R \cos \theta + \frac{R^2}{2L} \sin^2 \theta\right]$$

The steam containment heat transfer surface area, A, is related to crank angle by:

$$A = A_h + A_p + \pi B \left[R - R \cos \theta + \frac{R^2}{2L} \sin^2 \theta\right]$$

where A_h = cylinder head area

A_p = piston face area

The steam pressure can be related to the crank angle dependent volume by $PV^{1.0}$ = constant, and the associated steam temperature then determined from steam tables. Total volume, heat transfer surface area, and steam temperature are shown as a function of time, t, for a full cycle in Figure P-5 based on the relation $\theta = Nt$, where N = 600 rpm.

The mean cylinder wall and piston face temperature, $\bar{T}_w$, is assumed to be equal to the time (or crank angle) average steam temperature, T_g,

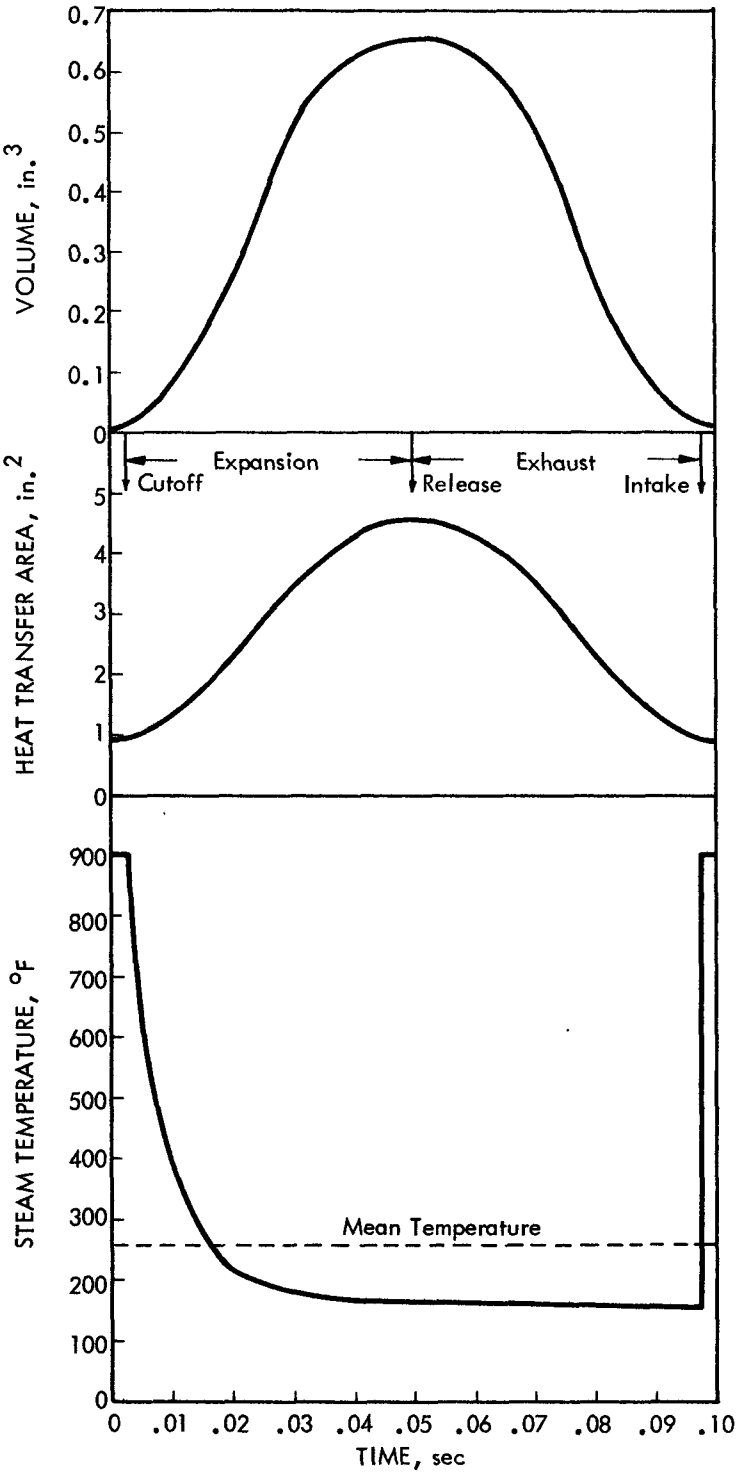

FIGURE P-5. TIME DEPENDENT STEAM ENGINE OPERATING VARIABLES

3.01-68-058

$$T_w = \frac{1}{2\pi} \int_0^{2\pi} T_g d\theta \simeq 250^\circ F$$

Although the steam temperature varies over a wide range during each cycle, the wall surface temperature oscillates only a small amount around its mean value (because of the finite film heat transfer coefficient) and can be assumed to be constant. The amplitude reduction for T_w as compared with T_g is:*

$$T_{w_{max}} - T_{w_{min}} = \frac{T_{g_{max}} - T_{g_{min}}}{\left[1 + 2(\pi k^2/\alpha \tau_o h^2)\right]^{1/2} + 2(\pi k^2/\alpha \tau_o h^2)^{1/2}}$$

For $T_{g_{max}} - T_{g_{min}}$ of 750°F and an engine speed of 600 rpm,

the period of one oscillation $\tau_o = \frac{1}{3.6 \times 10^4}$ hr.

Since the wall thermal diffusivity, α, = 0.163 ft^3/hr, the wall thermal conductivity, k, = 10 Btu/hr-ft-°F, the film heat transfer coefficient, h, = 100 Btu/hr-ft^2-°F, and the amplitude reduction factor is 0.0084, and the wall surface temperature only fluctuates 6.3°F, which is quite negligible. As will be seen later, the calculated heat transfer coefficient is less than the value assumed for this sample calculation, and the wall temperature fluctuation is even less than 6.3°F. The depth of penetration, x_p, of this temperature oscillation into the walls is obtained from*,

$$x_p = 1.6 \sqrt{\pi \alpha \tau_o}$$

The practical depth of penetration is therefore 0.073 in. Since the cylinder wall thickness required to withstand the 400 psia maximum internal pressure and allow for wear and corrosion is about 0.015 in., the cylinder wall sees the full temperature fluctuation, but may be assumed to be at essentially constant temperature for the purpose of estimating heat interchange with steam.

Heat is transferred from the steam to the walls during the time that the steam temperature exceeds 250°F (see Figure P-5), and is returned to

---

* E. R. G. Eckert and R. M. Drake, Jr., Heat and Mass Transfer, p. 106, McGraw-Hill, New York, 1959.

the steam when the steam temperature decreases to less than the 250°F mean wall temperature. The maximum heat transfer coefficient for transport from the superheated steam occurs during intake when the high temperature steam rushes into the small cylinder volume existing between admission and cutoff (See Figure P-6). The thickness, y, of the cylindrical steam volume varies from 0.009 in. at top dead center to 0.0225 in. at cutoff. An average, $\bar{y}$, of 0.016 in. is assumed for intake to calculate a steam film heat transfer coefficient. The steam enters through the 0.25 in. diameter valve port and flows radially outward to fill the cylinder volume. The flow area, A_f, is then:

$$A_f = 2\pi r\bar{y}$$

and the wetted perimeter, P, is

$$P = 4\pi r$$

The hydraulic equivalent diameter, D_e, is then:

$$D_e = \frac{4(2\pi r\bar{y})}{4\pi r} = 2\bar{y} = 0.032 \text{ in.}$$

The average steam mass flow rate, w, during intake, based on steam conditions of 400 psia and 900°F at cutoff, is 1.94 lb/hr. The mass velocity, G, as a function of radius is then:

$$G = \frac{w}{A_f} = \frac{232}{r}$$

The film heat transfer coefficient, h, for superheated steam during intake is calculated from the equation:

$$\frac{hD_e}{k} = 0.023 \left(\frac{GD_e}{\mu}\right)^{0.8} \left(\frac{C_p\mu}{k}\right)^{0.4}$$

where, k, C_p, and μ are the steam properties (thermal conductivity, specific heat, and viscosity, respectively). Substituting appropriate values for these properties at intake conditions and for G and D_e, the radially dependent heat transfer coefficient is:

$$h(r) = 1.53\ r^{-.8} \text{ Btu/hr-ft}^2\text{-}^\circ\text{F}$$

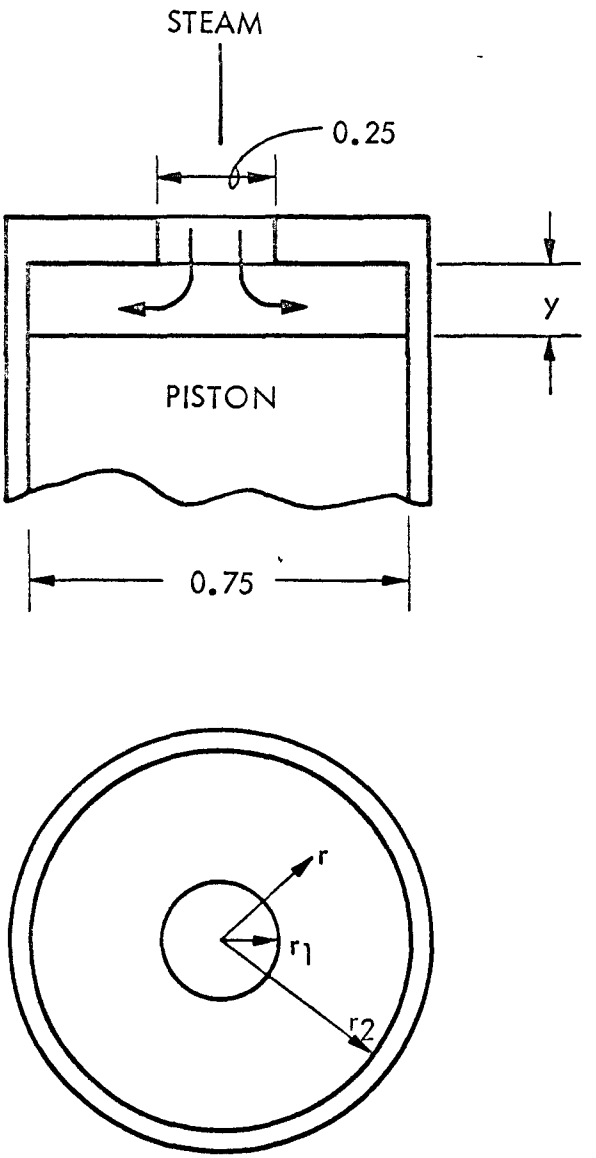

FIGURE P-6. HEAT TRANSFER MODEL DURING INTAKE

3.01-68-058

The average heat transfer coefficient weighted by the heat transfer surface area is:

$$\bar{h} = \frac{\int_{N_1}^{N_2} h \, dA_h}{\int_{r_1}^{r_2} dA_h} = \frac{\int_{r_1}^{r_2} (1.53r^{-.8})4\pi r dr}{\int_{r_1}^{r_2} 4\pi r dr}$$

$$\bar{h} = 33.5 \text{ Btu/hr-ft}^2\text{-}^\circ\text{F}$$

The film heat transfer coefficient was also calculated assuming sonic steam velocity out of the valve port nozzle during the initial intake period when the exit to inlet pressure ratio exceeds the critical value defined by:

$$\left(\frac{P_2}{P_1}\right)_c = \left(\frac{2}{\gamma+1}\right)^{\gamma/\gamma-1} = 0.546$$

where the specific heat ratio, γ, for steam is 1.29. Although the heat transfer coefficient during this short interval is 2100 Btu/hr-ft^2-$^\circ$F, the average value over the full intake period is still approximately the same as that developed in the previous calculation.

Using the calculated value of 34 Btu/hr-ft^2-$^\circ$F for the average heat transfer coefficient during intake, and assuming that this value decreases to 20 Btu/hr-ft^2-$^\circ$F during the expansion phase, the instantaneous amount of heat removed from the steam and transferred to the walls is shown in Figure P-7 for a complete cycle.

The estimated heat loss by conduction through the connecting rod and cylinder wall to the condenser, and from the surrounding thermal insulation is also shown in Figure P-7. The conduction heat transfer temperature differential is 250-140 = 110°F. Taking a connecting rod diameter of 0.125 in. and 2.5 in. length, its loss during one cycle is 1 x 10^{-5} Btu. For a cylinder I.D. of 0.75 in., 0.015 in. wall thickness, and 2.5 in. equivalent conduction length, its loss during one cycle is 3 x 10^{-5} Btu. Assuming 0.5 in. thick, highly effective vacuum-type thermal insulation (Super Linde or equivalent) with an effective thermal conductivity of 2 x 10^{-4} Btu/hr-ft-$^\circ$F, the insulation loss is only 0.2 x 10^{-5} Btu in one cycle. The total conduction

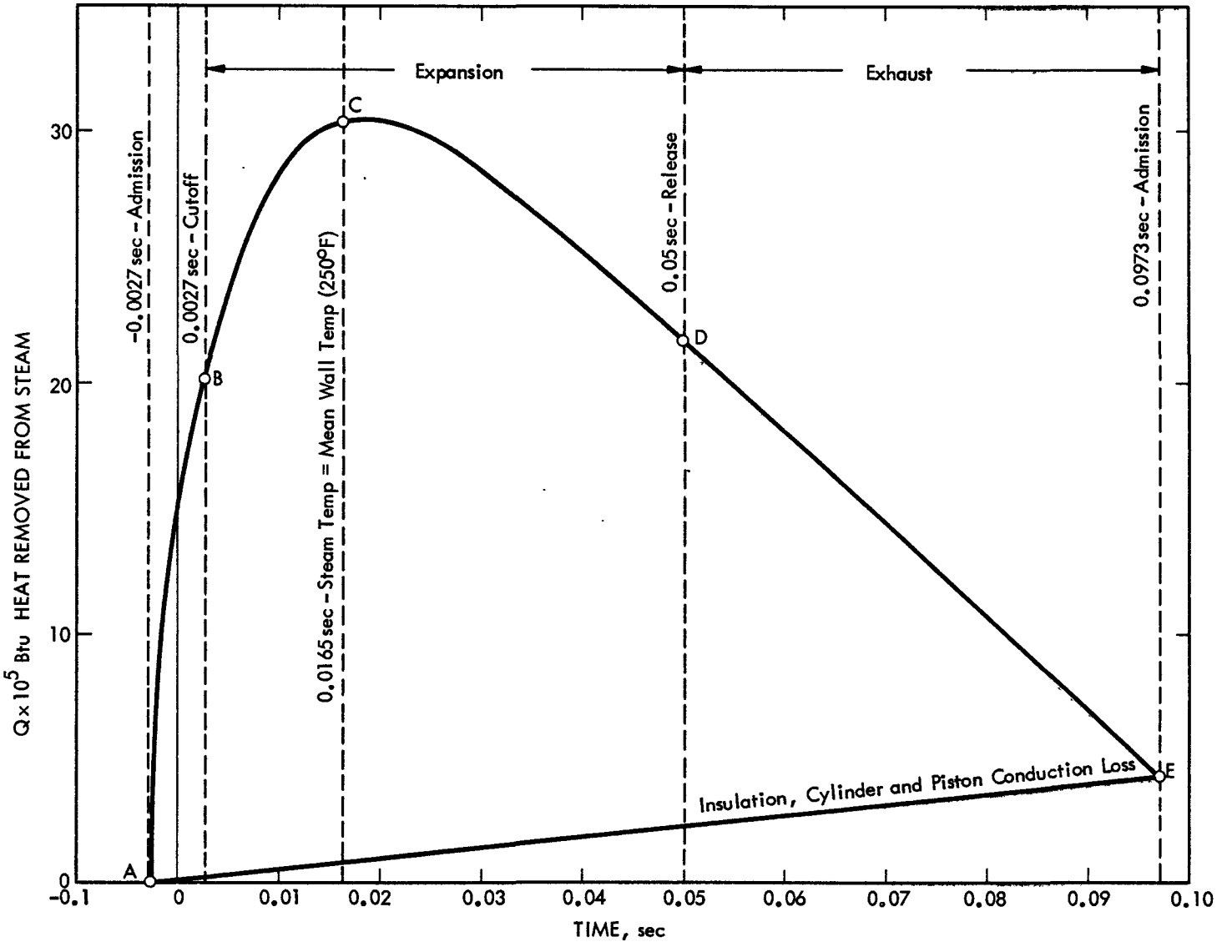

FIGURE P-7. HEAT TRANSFER DURING ONE COMPLETE CYCLE

loss is therefore 4.2×10^{-5} Btu per cycle.

Referring to Figure P-7, during the intake phase 20×10^{-5} Btu are transferred from the steam to the walls (Point B). Heat transfer to the walls continues during the expansion, reaching a peak of 30.2×10^{-5} Btu at 0.0165 sec (Point C) when the steam and wall temperatures are equal. As the steam temperature continues to decrease to a value less than the wall temperature, heat is returned to the steam during the remaining expansion (Point D). All of the remaining heat that was initially transfered to the walls, is returned to the steam during the exhaust stroke with the exception of the parasitic conduction losses (Point E).

The processes that occur are shown on the cycle T-S diagram in Figure P-8, where the ideal isentropic expansion (A-G) is adjusted to account for the differential heat transfer losses. The heat loss prior to cutoff (A-B) occurs essentially at constant pressure, neglecting throttling losses. The heat transfered between D-E at 6 psia is wastefully exhausted; and the steam is then throttled (E-F) to 2.89 psia condenser pressure (140°F). After the steam is condensed and subcooled to 120°F, it is pumped to 400 psia and returned to the boiler. The pump work, W_p, assuming a 30% pump efficiency is,

$$W_p = \nu\Delta P = \left(0.0162 \frac{ft^3}{lb}\right)\left(400\text{-}2 \frac{lb}{in^2}\right)\left(\frac{144}{778}\right)\left(\frac{1}{0.30}\right) = 4.0 \text{ Btu/lb}$$

The ideal Rankine cycle efficiency (neglecting pump work), η_i, is

$$\eta_i = \frac{\text{ideal work}}{\text{heat input}} = \frac{1469\text{-}1023}{1469\text{-}88} = 32.3\%$$

The ideal work is 446 Btu/lb; however, accounting for the noted heat transfer losses, the actual expansion work is only 1400-1043 = 357 Btu/lb. The thermal losses are therefore 20% of the ideal work.

4. Cycle Efficiency

If we assume that all other unaccounted for losses (fluid and mechanical friction, and steam leakage) are equal to the thermal losses, viz. 20%, then the total steam engine losses are:

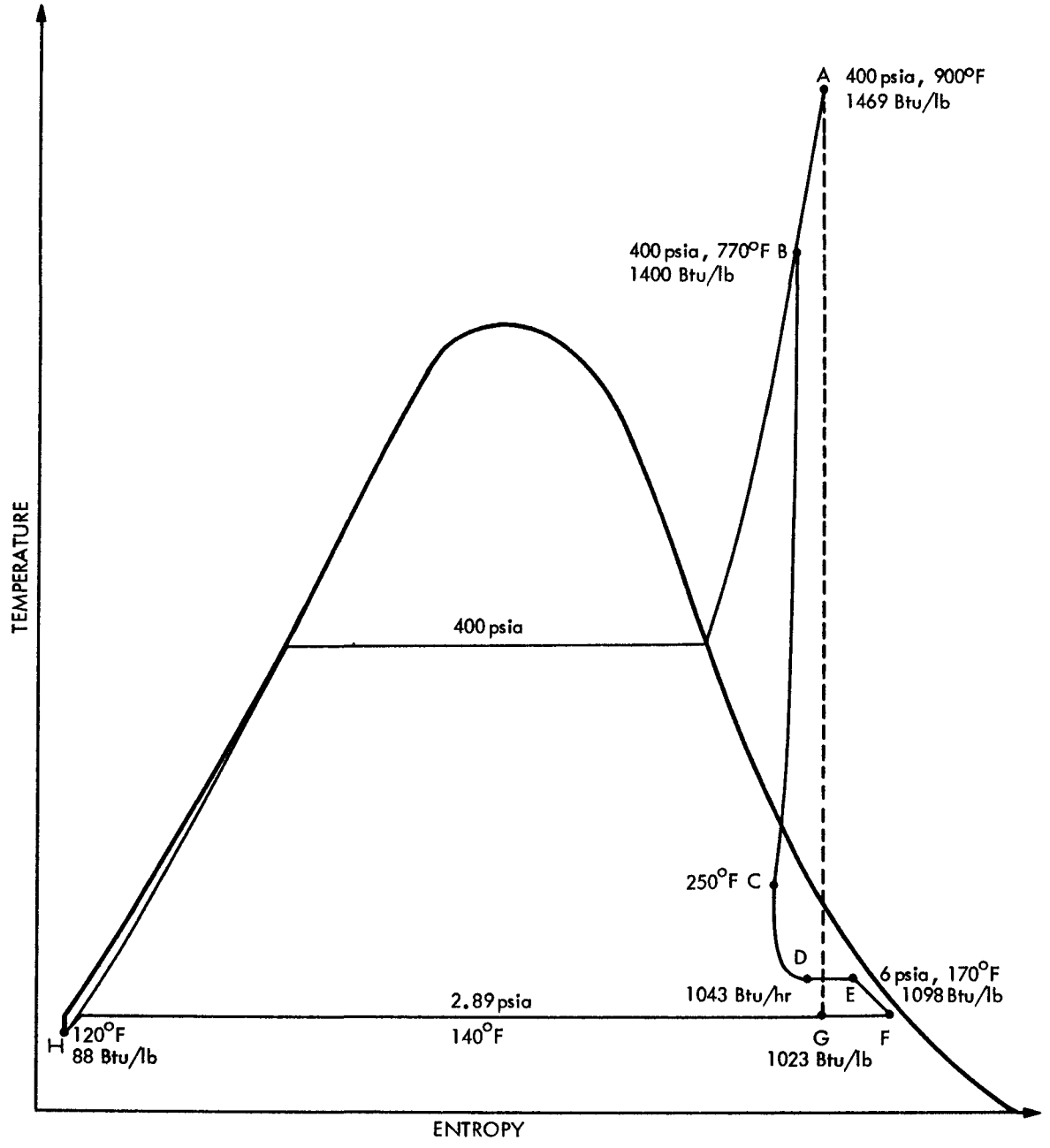

FIGURE P-8. T-S DIAGRAM SHOWING HEAT TRANSFER LOSSES IN STEAM ENGINE

301-68-060

	Engine loss, %
Clearance volume	9.4
Recompression	0.3
Thermal	20
Other	20
Total	50

which results in an estimated 50% engine efficiency.

The overall steam cycle efficiency, η_c, accounting for pump work is then

$$\eta_c = \frac{(.50)(446)-4}{1469-80} = 15.8\%$$

It is probable that the unaccounted for losses would be larger than the 20% assumed due to the extremely low power density of such a small engine (large cylinder surface area-to-power output ratio), which would result in a large frictional loss due to the ring bearing pressure required to limit steam leakage to a tolerable value. The throttling loss during intake would also be abnormally large for an engine whose intake poppet valve is automatically actuated by an exhaust valve located on the piston face, since the available actuator travel is only 0.0135 in.

Referring to Figure P-8, the calculated expansion to the mean wall temperature (B-C) ends below the steam saturation line showing some condensation. The effect of this on heat transfer to the walls was neglected, since, in the actual engine, throttling at the intake valve would shift the expansion toward an increased entropy value and prevent initial condensation. However, if condensation occurs during the end of the expansion and is not dried during the exhaust stroke prior to admission of a fresh steam charge, the wetted walls can have a much larger heat transfer coefficient during intake. In this case, if the heat loss prior to cutoff were larger than the calculated amount, then some initial condensation would occur and the thermal loss due to steam-wall interchange would be substantially larger than estimated. Condensing film heat transfer coefficients are 10 to 50 times larger than the value used, so condensation over only a small portion of the

cycle can have a significant effect.

It is felt that the calculated thermal losses are probably overly optimistic considering the marginal situation on initial condensation. A higher superheat temperature or smaller expansion ratio would help to minimize this most troublesome of steam engine loss mechanisms.

Although the estimated overall engine efficiency based on calculated values for some of the major thermodynamic losses was 50%, it is highly unlikely that a performance better than 30 to 40% could be achieved in an actual engine based on the design parameters indicated in this analysis. In this case, the overall cycle thermal efficiency would be 10 to 13%.

5. Comparison of Steam Engine Performance

It was shown in Figure P-2 that engine efficiencies as high as 70% can be achieved in large steam engines operating over a reasonable expansion ratio of about 8 to 10, and that the efficiency decreases rapidly below about 10 to 15 hp. The Besler Corporation has been particularly successful in developing high performance steam engines. Early experience was gained in the design, construction and operation of a successfully flown steam-powered airplane in 1933. Table P-2 shows the characteristics of several Besler engines which range in efficiency from 69 to 76 percent*, and are representative of the best performance achieved to date. Several other steam engines ranging to lower power outputs are described in Table P-3.

The high Skoda Works engine efficiency was obtained by exhausting superheated steam to minimize initial condensation losses; and operating over a low expansion ratio which, of course, results in a low brake thermal efficiency. The low efficiencies for the NRDC-Ricardo and Poppet-valve solar engines are largely due to the low power density (significant frictional losses), and initial condensation loss, especially for the solar engine since the intake steam is saturated. Steam engine performance as a function of power output is compared in Figure P-9.

---

* W. J. Besler and J. L. Boyen, Steam Power System for a Landing Craft, Contract Nonr 2159(oo), 30 Sept. 1957.

TABLE P-2 - BESLER STEAM ENGINE CHARACTERISTICS

	Airplane Engine	Commuter Train Engine	Landing Craft Engine*
Power rating, hp	150	350	775
Engine efficiency, %	69	72	76
Brake thermal efficiency, %	21.4	22	22.8
Initial steam pressure, psig	1250	1500	1200
Initial steam temperature, ^{o}F	795	750	750
Engine exhaust pressure, psig	2	2	2
Cutoff ratio, %	40	-	-
Speed, rpm	1650	-	2200
High pressure cylinder, in.	3.0	6.5	3.25
Low pressure cylinder, in.	5.25	11.0	5.50
Stroke, in.	3.0	9.0	5.00

* Estimate of performance for proposed landing craft engine to Navy.

TABLE P-3 - COMPARISON OF LOW POWER STEAM ENGINES

	Skoda Works Engine (1)	NRDC-Ricardo Engine (2)	Poppet-Valve Solar Engine (3)
Power rating, hp	440	2½	~ 1
Engine efficiency, %	77	50	27
Brake thermal efficiency, %	12.4	6.9	4.5
Initial steam pressure, psig	600	150	120
Initial steam temperature, °F	715	420	340 (sat.)
Exhaust pressure, psig	85-110	atm.	atm.
Speed, rpm	750	1250	-

(1) H. Frank and J. Rais, "High Speed Steam Engine Without Lubrication", The Engineer's Digest, 2, 516 (1945)

(2) "The N.R.D.C. - Ricardo Power Plant", The Steam Engineer, p. 48, November 1954.

(3) S. T. Hsu and B. S. Lee, "A Simple Reaction Turbine as a Solar Engine", Solar Energy, July-October 7 (1958).

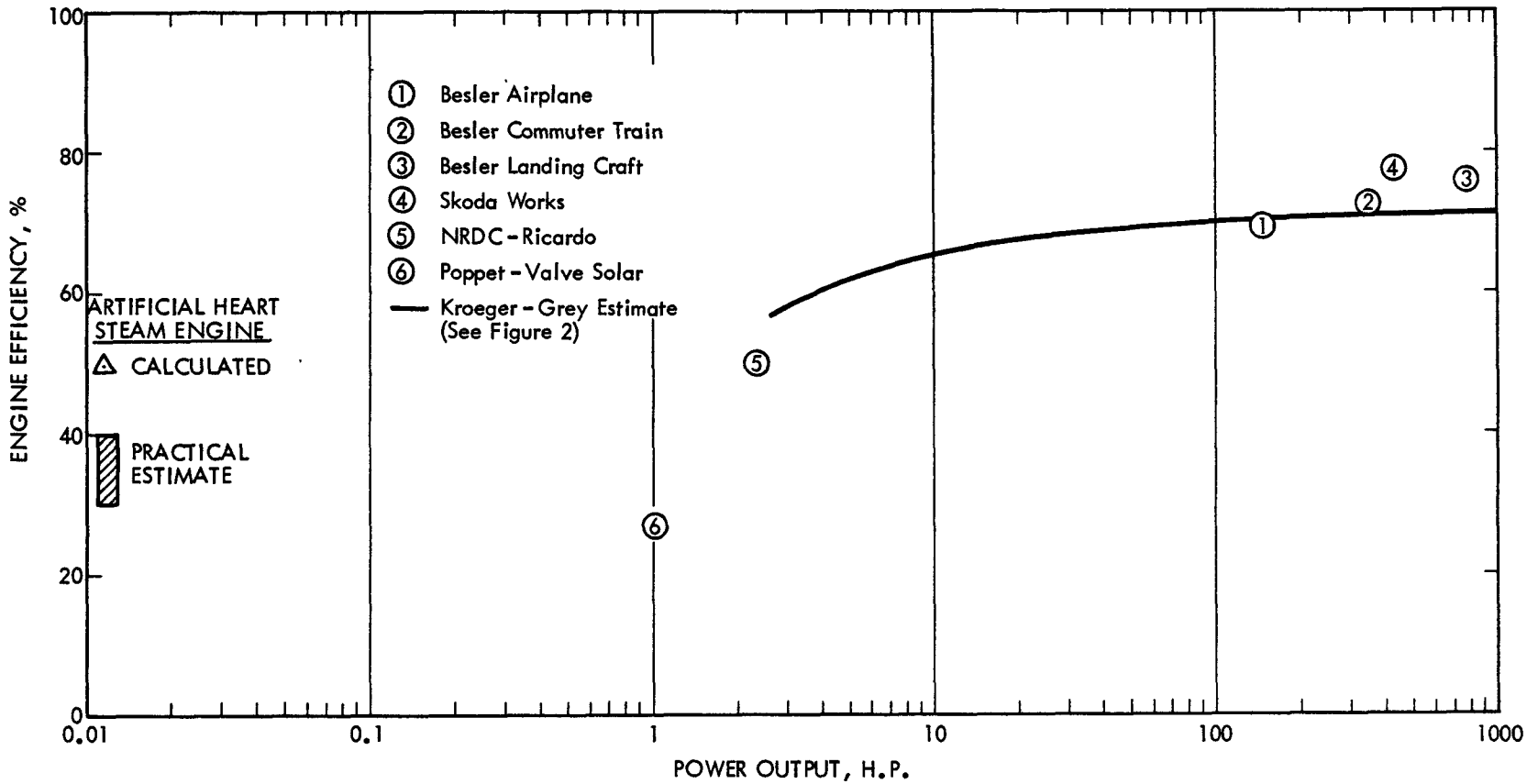

FIGURE P-9. STEAM ENGINE PERFORMANCE COMPARISON

APPENDIX Q
ESTIMATE OF REQUIRED RESOURCES

I. INTRODUCTION

Several different basic approaches to program planning for an implantable power source are possible, and each has certain merits. If one takes the approach which has become basic in the defense/space/nuclear project area, the end goals are defined first, together with the criteria and boundary conditions to be satisfied by each subsystem. The program is then developed in terms of the optimum path to that goal, within the constraints of funding and system integration. If this approach can be applied to a problem, it will usually result in minimum overall development cost and risk.

There are, however, conditions under which this approach to program planning may be inapplicable. If the requirements for each program element cannot be defined, but must evolve in the course of interaction with other developing and changing program elements, a different planning approach may be more appropriate. For this sort of exploratory, open-definition development effort, the optimum approach may consist of a series of iterations of design/build/test, redesign, etc. At each cycle, the program elements interact, inevitable interface and criteria problems arise, and, in the process, the requirements become better defined for the subsequent design iteration. Compared with the first approach, there is more experience at each point in time, and a more complete set of system hardware is in existence; however, the risk of early failure is greater, and final system development costs are probably greater.

The choice between these program plan approaches cannot be made by the power subsystem developer in the artificial heart development program, but must be made at the overall system management and planning level. Accordingly,

Aerojet-General is submitting two alternative plans for the resources required in the development of an implantable radioisotope power source. Plan A is based on good aerospace project planning practices. Plan B, which may better fit the realities of the artificial heart program, is based on an iterative development with successively evolving criteria and interface definitions.

In the remainder of this Appendix, estimates are presented for the resources and time required to carry the conceptual design through a preliminary detailed design to the achievement of a workable prototype model under both of the planning approaches discussed above. It should be emphasized that although the time and funds which are shown for Plan A are greater than those for Plan B, the resulting Plan A prototype is fully-engineered, both as an engine and as an element in the overall artificial heart system, and will differ in only minor ways from the final production units. Conversely, the prototype engine resulting from the next phase of Plan B should more properly be called a "first prototype", and will undoubtedly be followed by later generations of prototypes. This first prototype will not be based on a design which fully incorporates the learning resulting from the component and breadboard tests; it will, however, provide early experience with the entire system. It should be borne in mind that the two plans are not to be compared in detail, and that the choice between them must be based on the approach considerations discussed above.

II. PLAN A

A. OVERALL DEVELOPMENT PROGRAM

The goal of the overall development program for the implantable power source is the preparation of production drawings and process specifications for an engine which has been optimized and tested with the complete circulatory support system, both *in vitro* and *in vivo*. This design will be supported by qualification test results, cost and safety analyses, and as much reliability data as can be generated within the scope of the program.

The task interrelationships for an orderly development effort are indicated in Figure Q-1. The program is divided into four phases: conceptual (I), development (II), engineering (III), and qualification (IV). The conceptual phase has been substantially completed at this time; phases II and III complete the preliminary design and the fabrication of a prototype are discussed in more detail in the next sections.

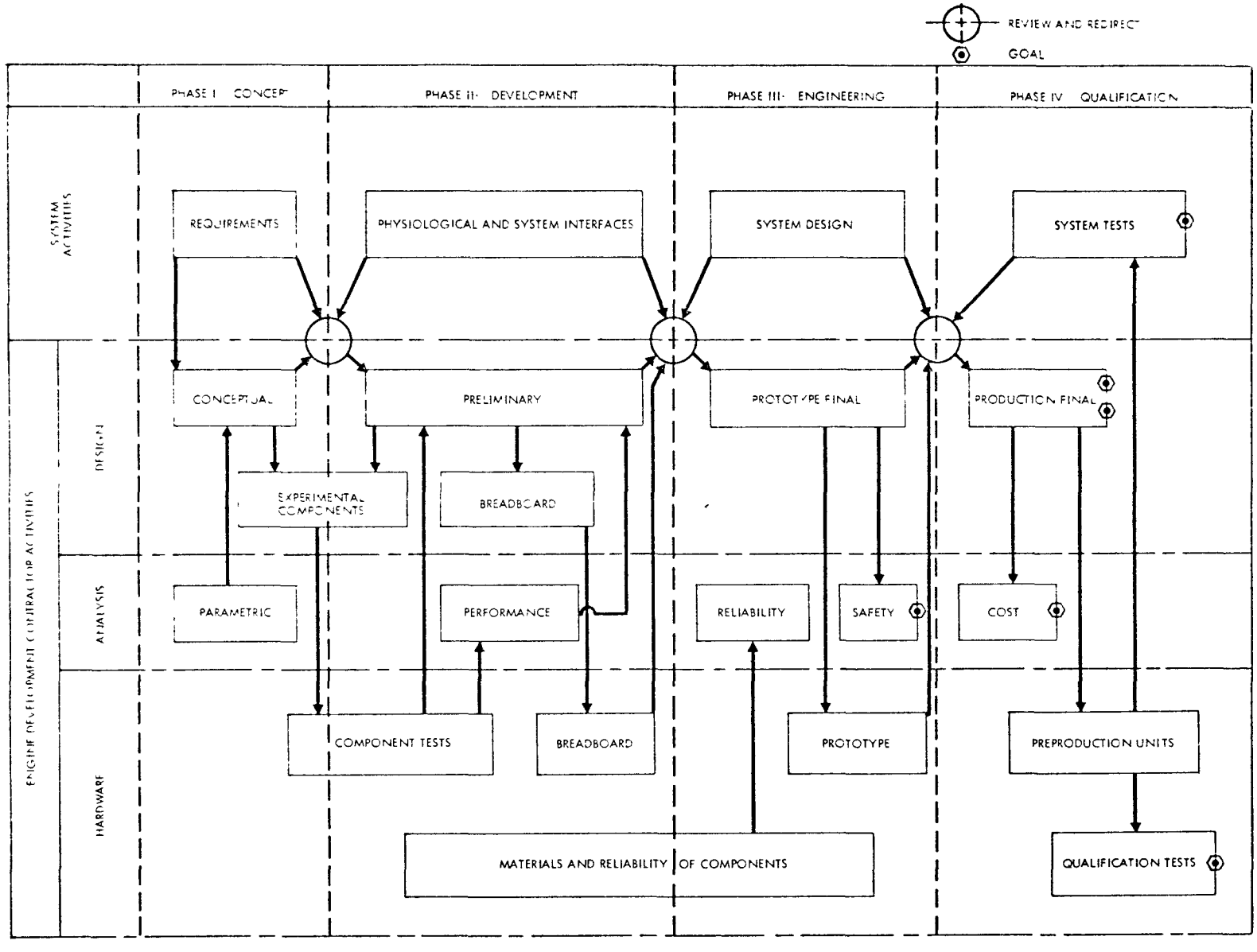

FIGURE Q-1. IMPLANTABLE POWER SOURCE DEVELOPMENT PROGRAM (PLAN A)

The most demanding aspect of the engine development program is the management of the very sensitive interfaces with other system elements that are under concurrent development. The physiological areas of material compatibility with blood and with tissue, and of intracorporeal heat rejection, are major concerns. Even more complex is the relationship of engine control and power transmission with the development of the heart pump which the engine drives. This interface is strongly influenced by the physiological requirements of the vascular system, which are being investigated concurrently. The results of these situations are: very careful liaison will be required with other elements of system research and development; informed projections of physiological limitations must be developed in the absence of adequate data; and broad design options must be maintained to accommodate changes in the interface requirements.

B. PHASE II PROGRAM

The next phase of the engine development program logically consists of a full preliminary design, to serve as the basis for subsequent design, fabrication and test of a breadboard power source. The breadboard would be based as closely as possible on the preliminary design of a prototype, but would not be in prototype configuration. The discrepancies would permit electrical heating, extensive instrumentation, variation of operating parameters and replacement of components with alternates. The preliminary design, plus the experience and data gained from the breadboard, would constitute a sound basis for program decisions and for the succeeding phases.

A suggested schedule for this phase, shown in Figure Q-2 indicates, in addition to the above discussed design and breadboard activities, a significant effort devoted to component performance and reliability testing. The performance information is an important input to the preliminary design; the reliability tests are largely for the benefit of later phases, but must be started as early as possible.

C. PHASE III PROGRAM

This phase incorporates all of the component and breadboard fabrication and test experience into a prototype final design. A prototype unit is fabricated, tested, and then made available for integration with the complete system.

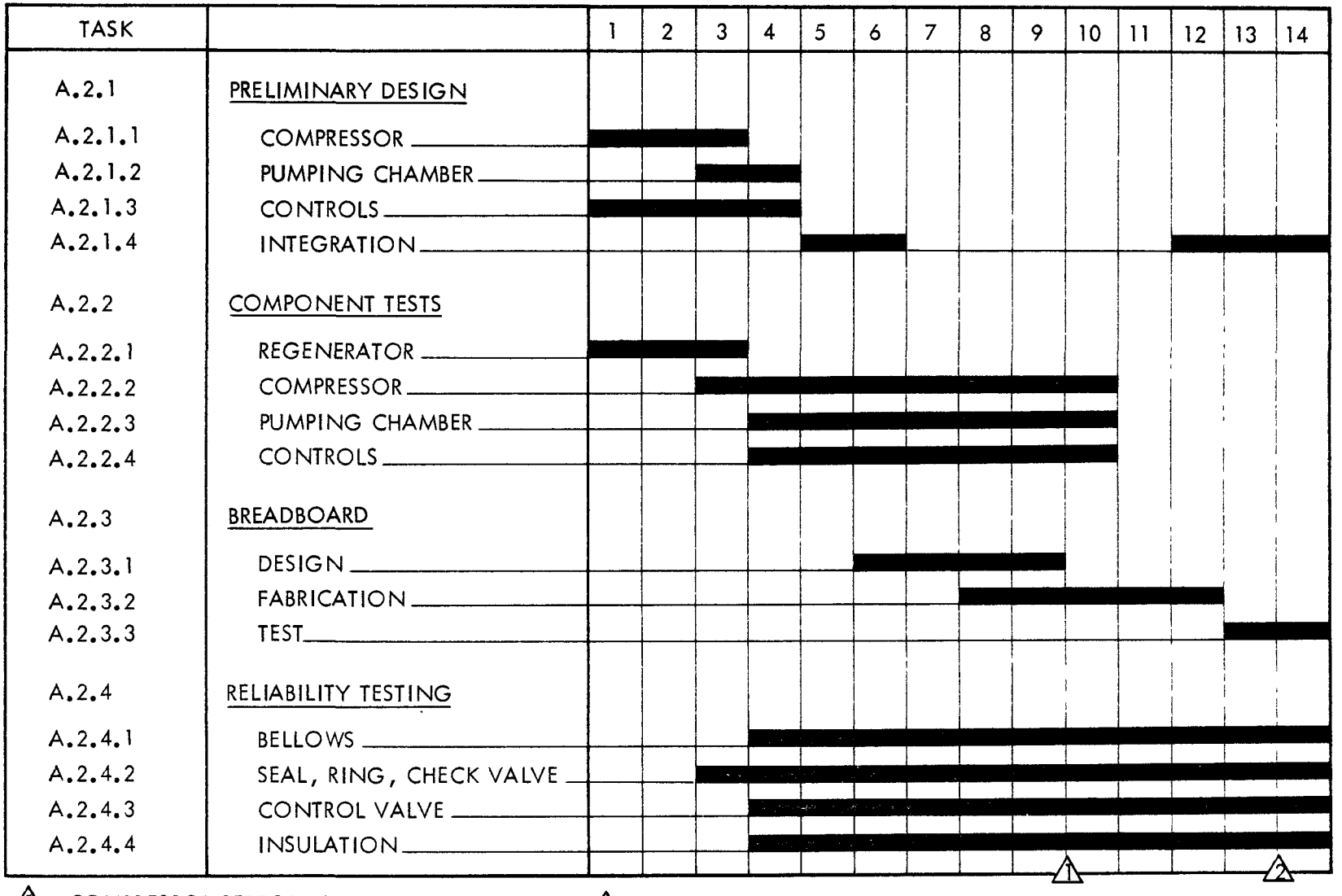

FIGURE Q-2. IMPLANTABLE POWER SOURCE DEVELOPMENT PROGRAM (PLAN A, PHASE II)

Figure Q-3, a suggested schedule for this phase, also indicates reliability and safety analyses, and component reliability and material testing.

D. RESOURCES REQUIRED

Estimates have been prepared of the engineering and supporting personnel manpower loading and of the materials and equipment costs required to perform Plan A, Phases II and III, as shown in Figures Q-2 and Q-3. These data are presented in Table Q-1 and Q-2 by task and by program month. Supporting personnel include draftsmen and test and instrument technicians. All shop fabrication costs are shown as material and equipment, as are computer charges and subcontract costs. Certain general costs, such as travel and consultants, are included in the program management tasks (A-2-0 and A-3-0). The other task numbers correspond with those shown on the schedules.

III. PLAN B

A. OVERALL DEVELOPMENT PROGRAM

The goal of Plan B is to produce a first prototype power source at an early date so that system tests in vitro and in vivo can commence as soon as possible. The penalties paid for this approach, as compared with Plan A are:

a) Unforseen development difficulties or supplier delays will have a greater effect on the entire system schedule.

b) The engine under test will not be as nearly optimum as that resulting later from Plan A, with the concommitant possibility of having unnecessarily discouraging early results.

c) Reliability and lifetime data will be minimal.

d) More thorough liaison with other program elements will be required and broad design options will not be possible.

The task interrelationships for Plan B are shown in Figure Q-4. The content and extent of Phase III cannot be defined until completion of Phase II. These subsequent phases will consist essentially of redefinition, redesign, and fabrication of prototypes of later generations, eventually evolving into the final system.

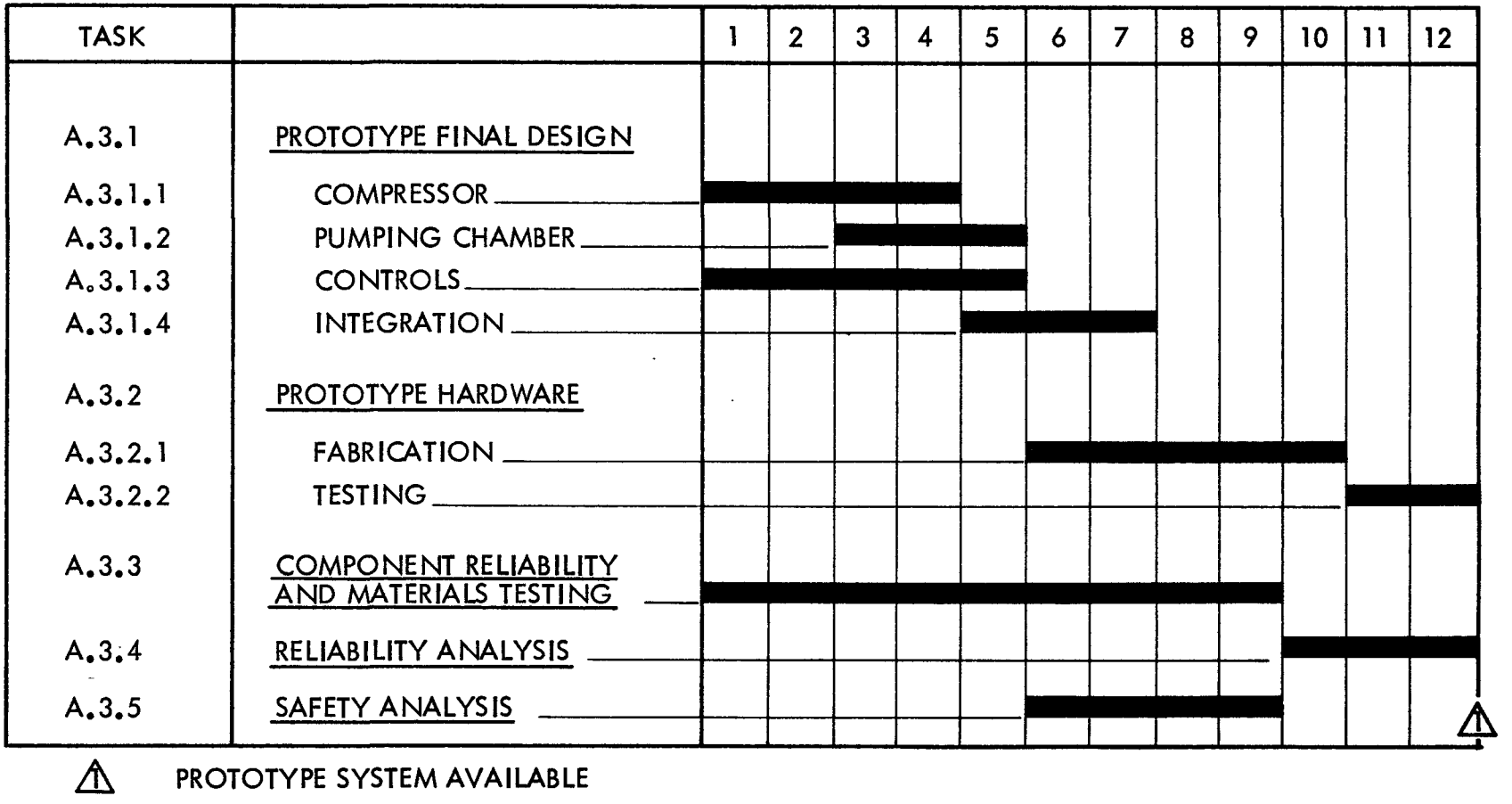

FIGURE Q-3. IMPLANTABLE POWER SOURCE DEVELOPMENT PROGRAM (PLAN A, PHASE III)

TABLE Q-1 - RESOURCES REQUIRED, PLAN A PHASE II

Task	Item*	Program Month 1	2	3	4	5	6	7	8	9	10	11	12	13	14	Total
A-2-0	1	1	1	1	1	1	1	1	1	1	1	1	1	1	2	15
	2	1						1			1			1	2	7
	3	1	1	1	1	1	1	1	1	1	1	1	1	1	2	15
A-2-1	1	6	6	6	4	4	5									31
	2		1	2	2	2	3									10
	3	4	8	10	7	5	5									39
A-2-2	1	1	1	2	4	4	1	1	2	2	2					20
	2	1	1	2	2	2	2	2	2	3	3					20
	3	2	2	2	7	7	16	16	13	6						71
A-2-3	1						1	2	2	2	1	1	1	2	2	14
	2							1	2	3	1	1	1	3	3	15
	3									8	9	7	6			30
A-2-4	1			1	1	1		1							1	5
	2				1	2	1	1		1		1		1	1	9
	3				5	10	5	2	1	1	1	1	1	1	1	29
TOTAL:	1	8	8	10	10	10	8	5	5	5	4	2	2	3	5	85
	2	2	2	4	6	6	6	5	4	7	5	2	1	5	6	61
	3	7	11	13	20	23	27	19	15	16	11	9	8	2	3	184

*1 Engineering man-months (@ $2960/mo including all overheads)

2 Support personnel man-months (@ $1900/mo including all overheads)

3 Materials and equipment K$

Total Estimated Funding Requirements = $616,800.

TABLE Q-2 - RESOURCES REQUIRED, PLAN A PHASE III

Task	Item*	Program Month 1	2	3	4	5	6	7	8	9	10	11	12	Total
A-3-0	1	1	1	1	1	1	1	1	1	1	1	1	2	13
	2	1			1			1			1		2	6
	3	1	1	1	1	1	1	1	1	1	1	1	2	13
A-3-1	1	6	6	8	8	7	4	3						42
	2		2	6	8	7	3	4						30
	3	4	6	8	8	6	4	4						40
A-3-2	1						2	2	2	2	2	2	2	14
	2						2	2	2	2	2	4	4	18
	3						10	12	15	20	15			72
A-3-3	1	1	1	1		1		1		1				5
	2	1	1	1	1	1	1	1	1	1				9
	3	3	2	2	2	2	2	2	2	2				19
A-3-4	1										2	2	3	7
	2												1	1
	3										1	2	2	5
A-3-5	1						2	2	3	2				9
	2								1	1				2
	3						2	3	4	3				12
TOTAL:	1	8	8	9	9	9	9	9	6	6	5	5	7	90
	2	2	3	7	10	8	6	8	4	4	3	4	7	66
	3	8	9	11	11	9	19	22	22	26	17	3	4	161

*1 Engineering man-months (@ $2960/mo including all overheads)
2 Support personnel man-months (@ $1900/mo including all overheads)
3 Material and equipment K$

Total Estimated Funding Requirements = $617,000.

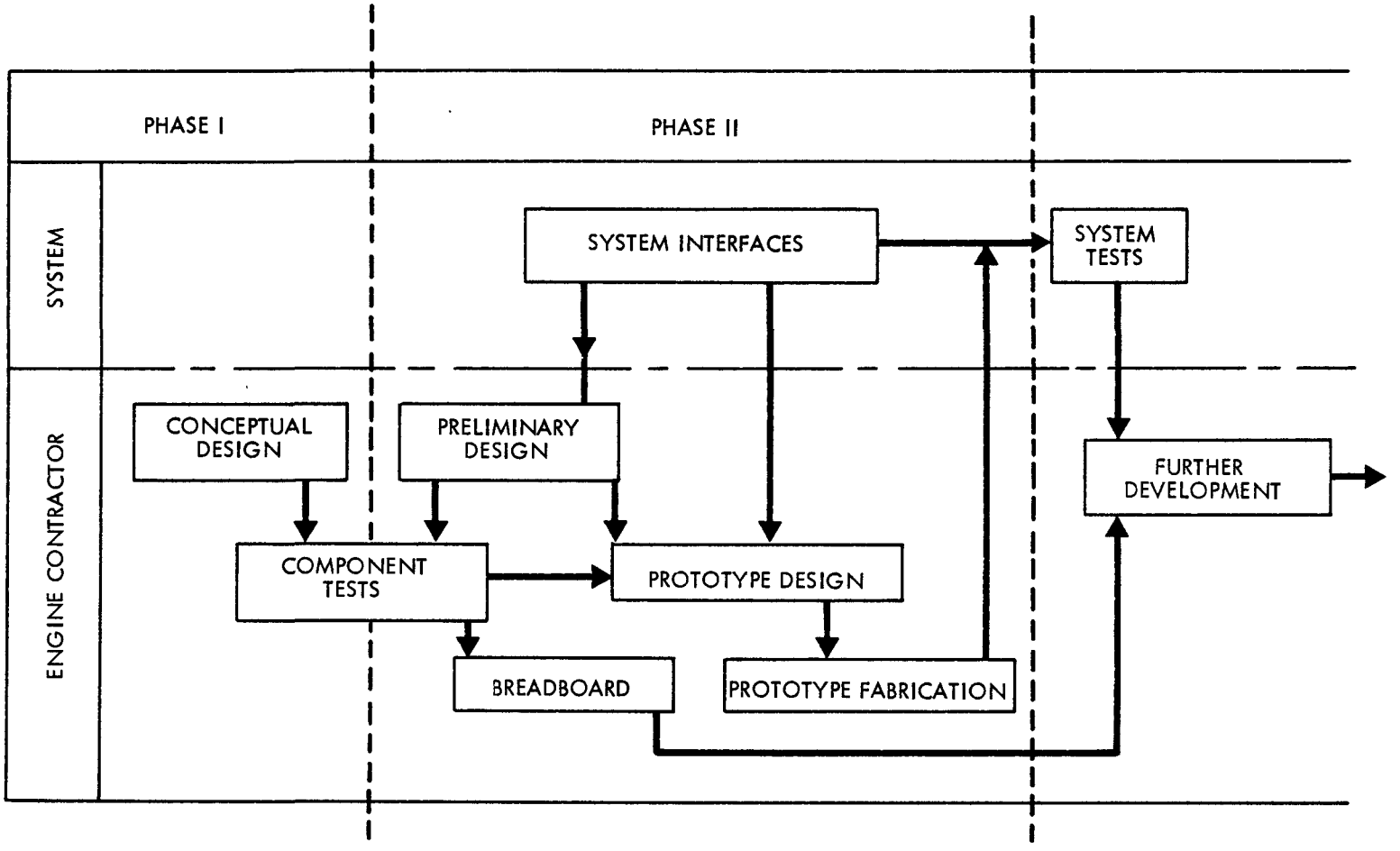

FIGURE Q-4. IMPLANTABLE POWER SOURCE DEVELOPMENT PROGRAM (PLAN B)

B. PHASE II PROGRAM

As in Plan A, the Phase II program consists of preliminary design and componet testing leading to a breadboard power source assembly. However, as shown in Figure Q-5, a prototype design is based directly on the preliminary design, influenced only to a minor extent by component testing and to a lesser extent by breadboard engine tests. Reliability and materials testing are, generally, postponed to later phases.

C. RESOURCES REQUIRED

Table Q-3 shows the resources estimated to be required for Plan B in the format used for Plan A.

3.01-67-1104

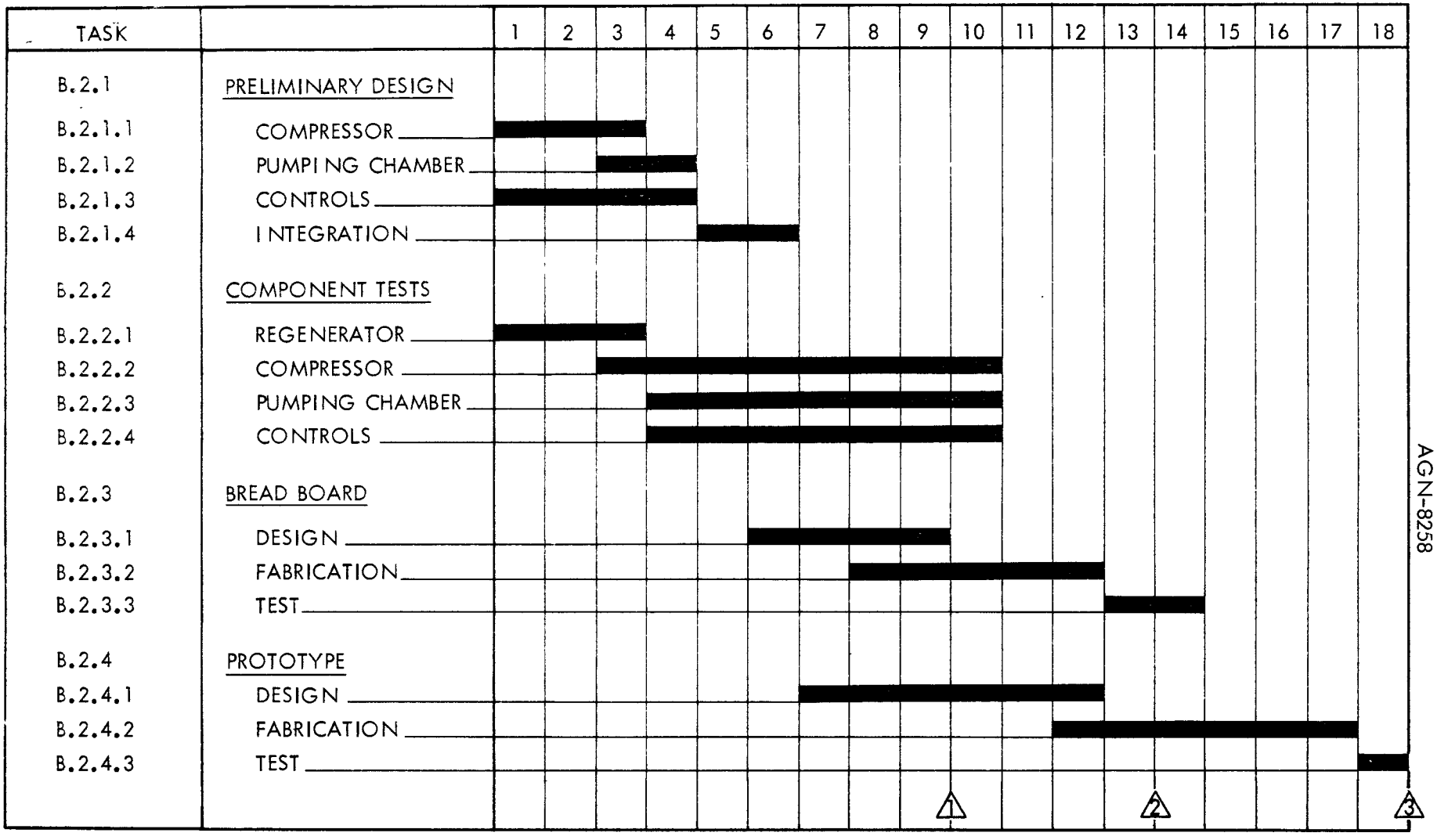

1 COMPRESSOR PERFORMANCE DEMONSTRATED

2 SYSTEM PERFORMANCE DEMONSTRATED

3 PROTOTYPE SYSTEM AVAILABLE

FIGURE Q-5. IMPLANTABLE POWER SOURCE DEVELOPMENT PROGRAM (PLAN B PHASE II)

AGN-8258

TABLE Q-3 - RESOURCES REQUIRED, PLAN B PHASE II

Task	Item*	Program Month 1	2	3	4	5	6	7	8	9	10	11	12	13	14	15	16	17	18	Total
B-2-0	1	1	1	1	1	1	1	1	1	1	1	1	1	1	1	1	1	2	2	20
	2	1			1			1			1			1			1		3	9
	3	1	1	1	1	1	1	1	1	1	1	1	1	1	1	1	1	1	3	20
B-2-1	1	6	6	7	5	5	5													34
	2		1	2	2	2	3													10
	3	4	8	10	7	5	5													39
B-2-2	1	1	1	2	4	4	1	1	2	2	2									20
	2	1	1	2	2	2	2	2	2	3	3									20
	3	2	2	2	7	7	16	16	13	6										71
B 2-3	1						1	2	2	2	1	1	1	2	1	1	2			16
	2							1	2	3	1	1	1	3	2	2	2			18
	3									8	9	7	6	3	2	2	2			30
B-2-4	1							2	2	3	3	4	4	1	1	1	1	2	3	27
	2								1	1	3	3	3	1	1	1	1	2	4	21
	3												5	10	12	12	15	10		64
TOTAL:	1	8	8	10	10	10	8	6	7	8	7	6	6	4	3	3	4	4	5	117
	2	2	2	4	5	4	5	4	5	7	8	4	4	5	3	3	4	2	7	78
	3	7	11	13	15	13	22	17	14	15	10	8	12	11	13	13	16	11	3	224

*1 Engineering man-months (@ $2960/mo including all overheads)

2 Support personnel man-months (@ $1900/mo including all overheads)

3 Materials and equipment K$

Total Estimated Funding Requirements = $802,700

APPENDIX R

EXPERIMENTAL INVESTIGATIONS

A. GENERAL

Aerojet is deeply interested in the development of an implantable power supply and, as a part of this involvement, has undertaken Company-sponsored work to verify experimentally certain features of the Aerojet engine concept. It is planned that several of the novel characteristics of the engine, including the operation of the Stirling engine as a compressor, the linear engine concept with pneumatic reversing system, and the direct coupling of a compressor and pumping chamber, will be evaluated experimentally to support the contract effort. The tests can be conducted more quickly, with better control over test parameters and with a higher probability of success, if the various features are tested separately. As a consequence, three separate tests were planned to investigate the three areas cited above.

B. COMPRESSOR TEST

The compressor operation test was essentially completed during the contract period under discussion; the conduct of the other tests is planned over the next several months. Most of the experimental data for the compressor test have been compiled but the data have not yet been fully reduced. The purpose of this test is to evaluate the operation of the regenerator, heater, check valves, and labyrinth seal, as well as overall system performance.

1. Test Apparatus

Figure R-1 is a photograph of the overall test apparatus. No attempt was made to minimize the size of the drive mechanism or the reservoirs since this experiment was designed to test only the compressor function. The assembly drawing of the engine tested is shown in Figure R-2.

2. Results

The instrumentation used for data collection is shown on Figure R-3.

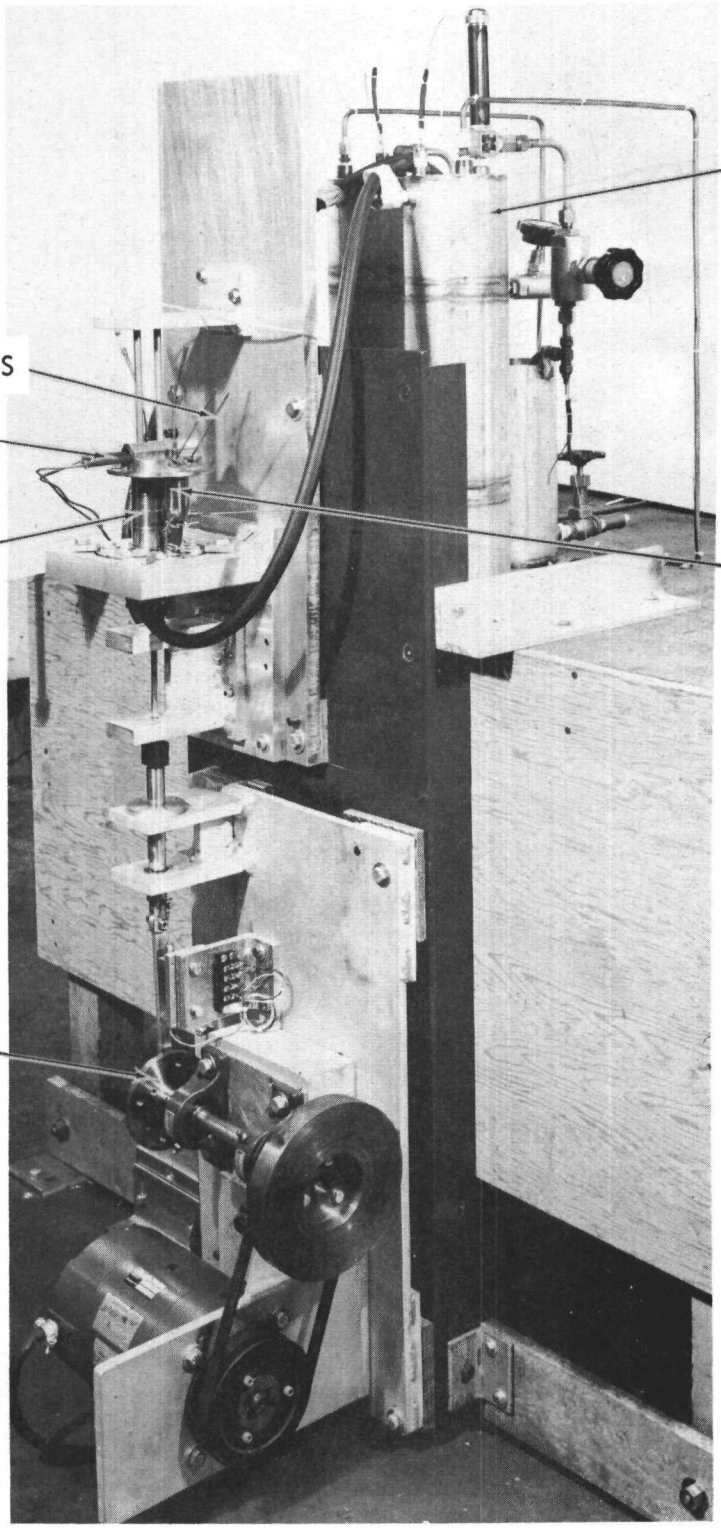

301-67-993

FIGURE R-1. COMPRESSOR TEST APPARATUS

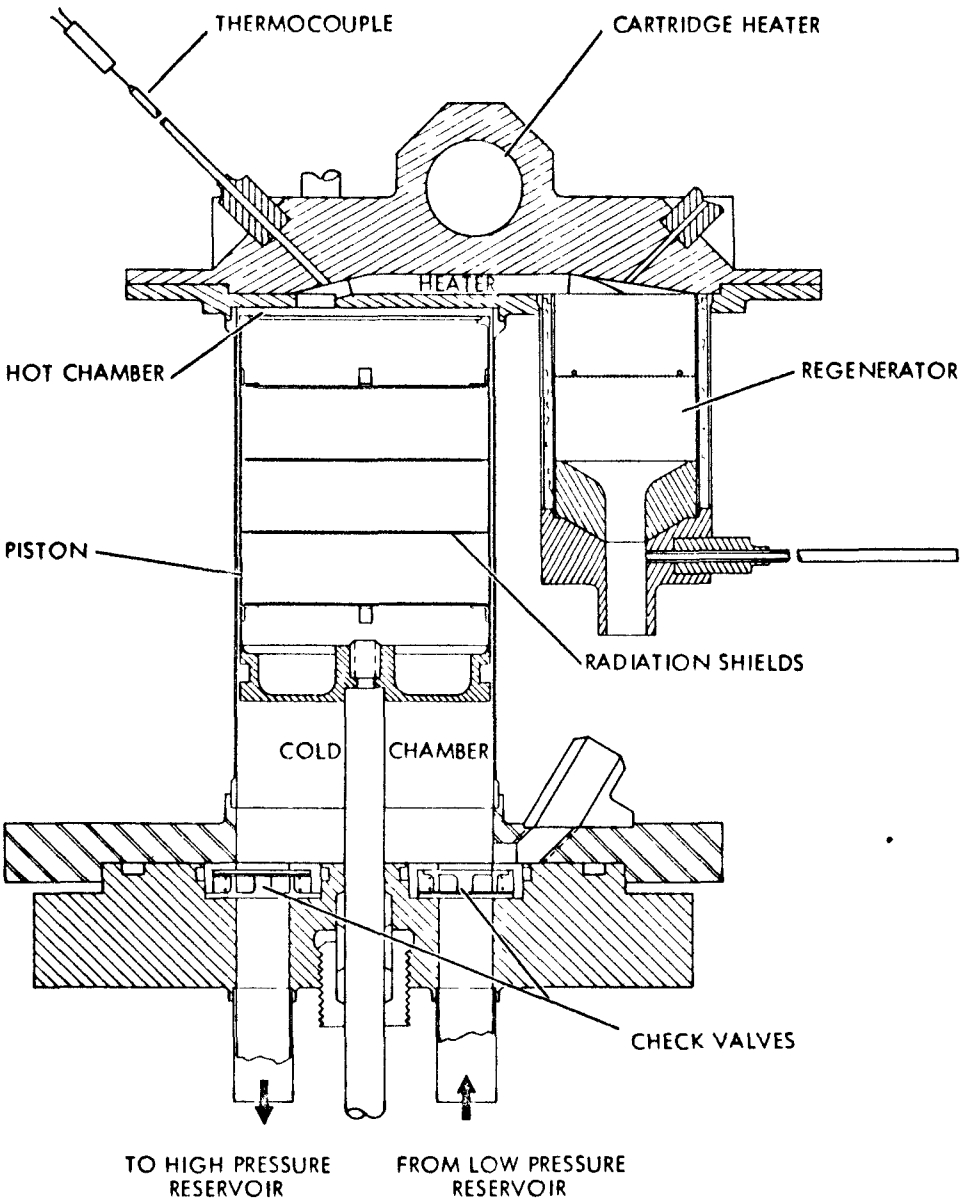

FIGURE R-2. TEST ENGINE ASSEMBLY

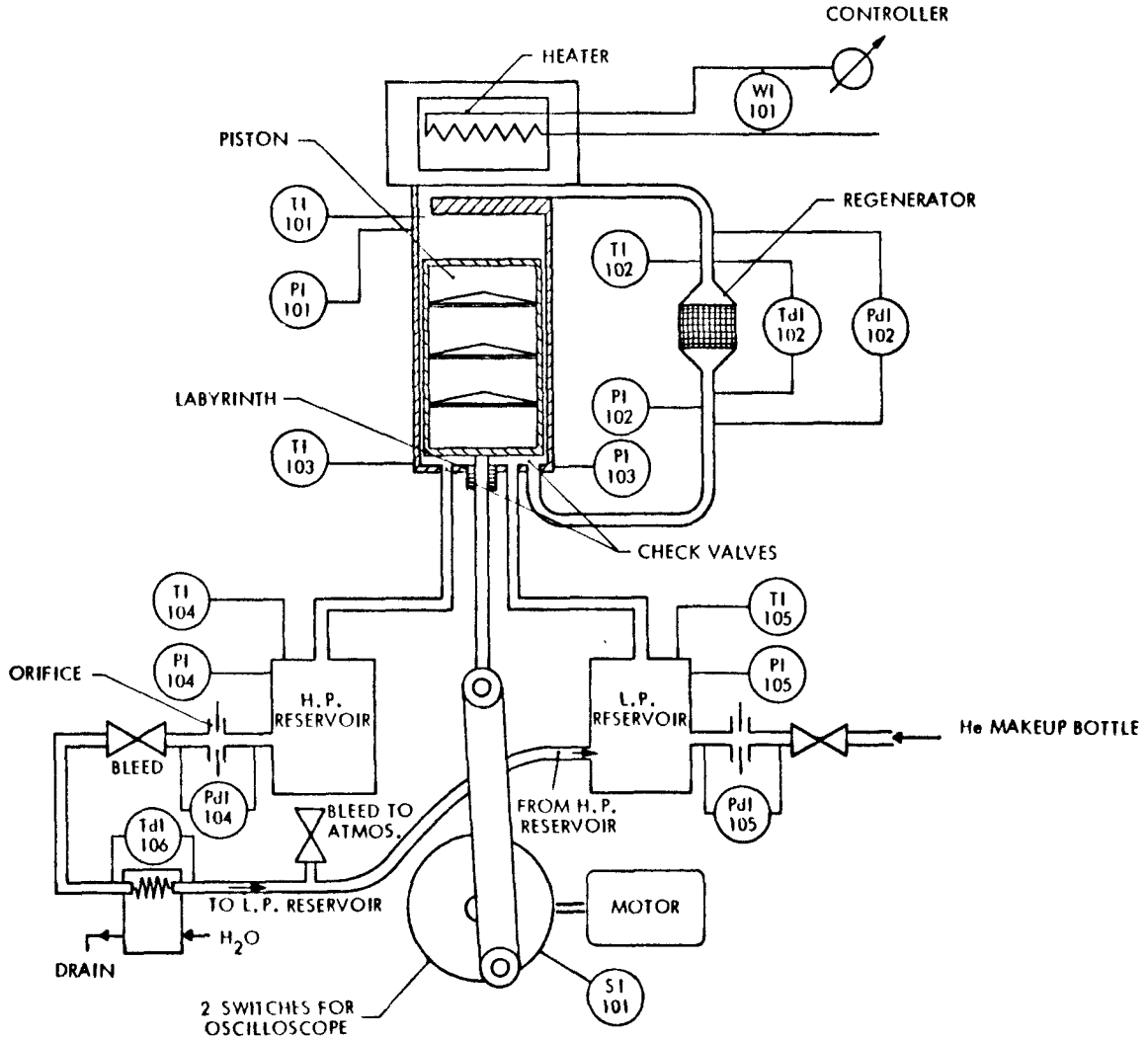

FIGURE R-3. TEST ENGINE P&I DIAGRAM

3.01-67-995

Close correlation was observed between the engine pressure profile predicted from theoretical analysis and that achieved in the test. The principal difference between the theoretical and observed profiles was the result of oscillations of the check valve disks.

Dynamic response of the thermocouples used in this test was not good enough to measure the heater and regenerator performance in detail. The general performance of these components was as anticipated except that the initial regenerator core geometry proved to be inadequate. The regenerator core consisted of a random packing of one mil Nichrome wire. The poor performance was apparently due to an insufficient amount of wire, non-uniform behavior of the packing and compaction of the wire during operation. Subsequent runs with more densely packed wire in the regenerator yielded satisfactory results. Characteristics of the two regenerators tested are as follows:

	Matrix No. 1	Matrix No. 2
Total wire length, ft	800	2400
Unswept volume, $in.^3$	0.75	1.00
Calculated effectiveness, %	82	97

The check valves and piston seal performed as expected. However, leakage through the shaft seal was much higher than expected due to an excessive amount of clearance provided for differential thermal expansion. This loss can be easily eliminated in future engines so the data reported here has been corrected for seal leakage.

Figure R-4 shows the engine output flow and gross power output as a function of pressure ratio for different engine speeds and maximum gas temperatures. The comparison between these data and similar data calculated using the simplified analytical technique reveals very good agreement; the deviation is only about 10%.

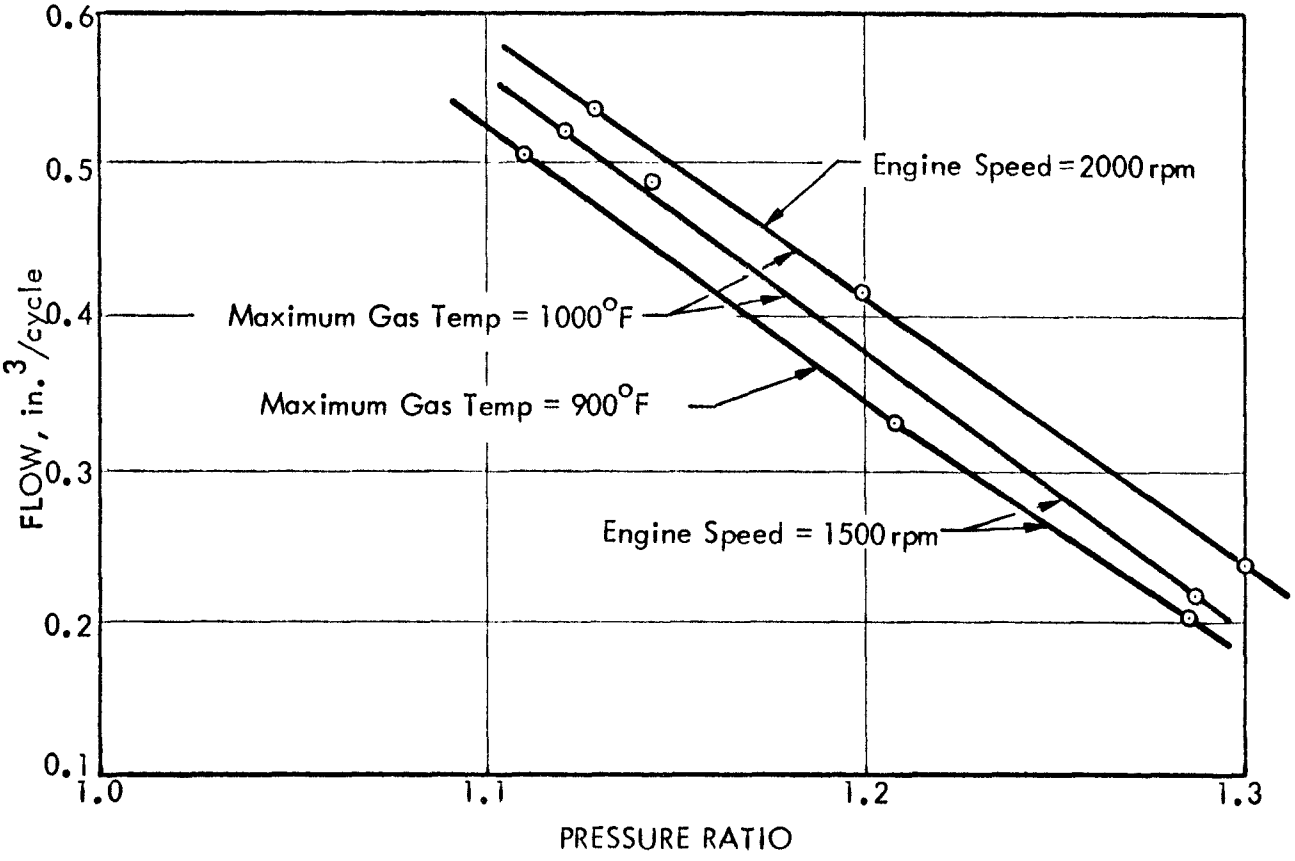

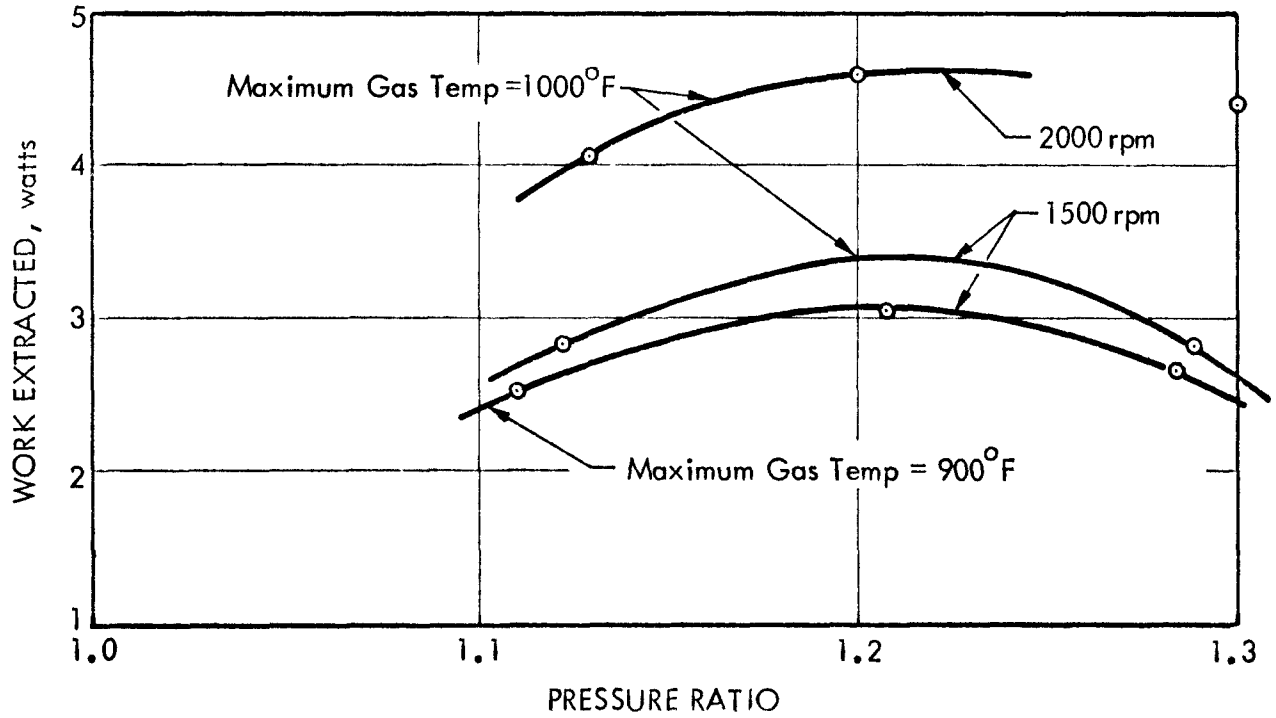

3.01-68-063

FIGURE R-4. EXPERIMENTAL DATA